WITHAFERIN A: A NOVEL THERAPEUTIC APPROACH FOR MALIGANT BRAIN
TUMORS

By

Patrick Thomas Grogan

Submitted to the graduate degree program in Pharmacology, Toxicology, and Therapeutics and
to the Graduate Faculty of the University of Kansas Medical Center in partial fulfillment of the
requirements for the degree of Doctor of Philosophy.

_____

Committee Chair: Thomas Pazdernik, Ph.D.

_____

Mentor: Mark Cohen, M.D., F.A.C.S.

_____

Qi Chen, Ph.D.

_____

Partha Kasturi, Ph.D.

_____

Timothy Fields, M.D., Ph.D.

Date defended: May 19, 2014

The Dissertation Committee for Patrick Thomas Grogan certifies that this is the approved version of the following dissertation:

WITHAFERIN A: A NOVEL THERAPEUTIC APPROACH FOR MALIGANT BRAIN TUMORS

_____
Committee Chair: Thomas Pazdernik, Ph.D.

Date approved: May 19, 2014

Abstract

High-grade gliomas, including the astrocytoma glioblastoma multiforme (GBM), are the most common adult primary malignant brain tumor. The mean post-diagnosis survival time of patients with GBM is approximately 14 months and has improved only minimally over the last several decades given a lack of novel and effective therapeutic strategies or interventions. Similar issues persist for other forms of brain cancer, notably medulloblastomas (MB) in the pediatric patient population. Given our inability to extend survival and enhance quality of life adequately in these brain tumor patients, there is a critical need for novel chemotherapeutic agents in the treatment of GBM and MB that may work as monotherapy agents or in synergistic combinations with current interventions.

In this work, the role of the natural product withaferin A (WA), a steroidal lactone with intriguing cytotoxic properties, was studied alone or in combination with currently approved anti-cancer agents (temozolomide, radiation therapy, and proteosome inhibitors) against GBM and MB brain tumors. It was shown that WA could produce G2/M cell cycle arrest and apoptosis with inhibitory modulation of the Akt/mammalian target of rapamycin (mTOR) pathway in GBM. Similarly, WA inhibited Wnt/β-catenin signaling through degradation of transcription factor (TCF)/lymphoid enhancer-binding factor (LEF) family members in MB. Overall, exposure to WA was associated with generalized N-acetyl-L-cysteine-repressible cellular oxidation, thiol reactivity, and alterations in the heat shock protein (HSP) 90 chaperone axis. WA failed to alter intrinsic HSP90 activity but reduced the association between HSP90 and co-chaperone Cdc37. These findings were expanded to demonstrate WA-mediated potentiation of cytotoxicity with concurrent proteasomal inhibition through an accumulation of aberrant proteins. WA also increased tumor cell radiosensitivity through disruption of normal DNA damage recognition and

repair. While WA failed to significantly enhance the cytotoxicity of temozolomide (TMZ), it demonstrated the ability to re-sensitize TMZ-resistant GBM through reduction in O^6-methylguanine-DNA methyltransferase (MGMT).

This study identifies novel utility for the cytotoxic steroid lactone WA in the treatment of the malignant brain tumors GBM and MB through its alterations of oncogenic cellular signaling pathways, protein homeostasis, and the DNA-damage response mechanism. As such, WA represents a promising experimental therapeutic that warrants further translational exploration.

Dedication

In memory of John R. Ohlfest, Ph.D.:

Dr. Ohlfest was my friend and a truly great mentor at the University of Minnesota and was taken at far too young an age by the very disease he was working to cure. His drive and passion to develop novel and innovative ideas to better the prognosis of cancer patients still serves as a source of inspiration for me, and his underlying desire to help people at their most vulnerable time will always be provide me with the motivation to keep trying.

John, you are missed.

Acknowledgements

To my mentor, Dr. Mark Cohen, I am sincerely grateful for your support and the opportunity that you have provided me over the last five years. Your research program is one of the main reasons I came to KUMC and then moved to the University of Michigan. I thank you for the trust that you have provided me to develop into an independent researcher and learn through both my successes and failures and your willingness to allow me to continue with you at the time of your move. You have been a wonderful example of a physician-scientist for me to follow and from whom I could learn. I appreciate all of your help and advice as I develop as a researcher and hopefully an eventual physician.

To my committee chairperson, Dr. Thomas Pazdernik, I am indebted to you for your willingness to first participate on my committee and then take over as chairperson upon Dr. Cohen's transition to the University of Michigan. Your input as a committee member and both a graduate and medical teacher have proven to be invaluable in my development and progression. Your medical school lectures undoubtedly improved and advanced my clinical comprehension and certainly that of many of my peers and was a key foundation for my graduate work. I thank you as well for the time you've invested walking me through the administrative steps of graduate school to ensure that I maintained course.

To my committee member and MD/PhD Program director, Dr. Timothy Fields, I sincerely thank you for the opportunities and guidance that you have provided me to at KUMC. You were also one of the primary reasons that I chose to attend KUMC and am very fortunate that you allowed

me that chance. I appreciate all of our discussions on science and life and truly take something from each.

To my present committee members, Dr. Qi Chen and Dr. Partha Kasturi, and my past member, Dr. Bao-Ting Zhu, your input and support allowed me to get to where I am. I am grateful for the significant efforts that you have put into mentoring me and helping me move forward. I would also like to thank Drs. Kenneth McCarson and Bruno Hagenbuch for their willingness to serve on my comprehensive examination committee.

To current and former members of the Cohen laboratory or other individuals working within the physical laboratory, including Dr. Chitra Subramanian, Mr. Joseph Bazzill, Dr. Ridhwi Mukerji, Dr. Abbas Samadi, Mr. Piero Protti, Ms. Eileen Brandes, Dr. Michael Sim, Dr. Roy Lirov, Dr. Stephanie Cohen, Dr. Erica Person, Mrs. Jennifer Buseman, and Dr. Xuan Zhang, I thank you for all of your help – especially with the small, unappreciated help and tasks – that made for a fun and productive environment that I enjoyed coming to every day. I am especially grateful to Dr. Chitra Subramanian for her kindness and mentorship within the laboratory, taking the time to teach me new techniques and working together as a great team on a number of projects.

To the past and present administration of the MD/PhD program, Mrs. Janice Fletcher, Dr. Joseph Bast, and Dr. Brenda Rongish, I sincerely appreciate your support during my graduate phase progression. I'd like to especially state my gratitude for Mrs. Fletcher who has put in countless extra hours to make sure that I stay in good standing with my location change. I would be

completely lost without all of your assistance and guidance on a myriad of too many items to list. You have been such a valuable asset to both me and the program as a whole.

To the administration of the graduate program in the Department of Pharmacology, Toxicology, and Therapeutics, namely Dr. Bruno Hagenbuch and Mr. Cody Tully, I appreciate your assistance and guidance, especially in light of my location change.

To now-Dr. Shane Stecklein, I thank you for your help, advice, and guidance with elements of the radiation sensitization chapter of this work.

To Dr. Barbara Timmermann and her lab members Huaping Zhang and Robert Gallagher, I thank you for providing purified withanolides and extracts to evaluate.

To Dr. Yoichi Osawa, Dr. Yoshihiro Morishima, and Dr. William Pratt, I thank you for your advice and help with elements of the HSP90 experimentation.

To my previous mentors (who still remain mentors to this day), Dr. Jann Sarkaria, Dr. John Ohlfest, and Dr. Michael Olin, the opportunities that you provided me and the trust you had in me have helped to shape who I am today. Your passion is admirable, and I thank you for the examples you have provided.

To my parents, Thomas and Debra Grogan, and my brother, Michael Grogan, thank you for your love and support. I would not be to this point without your guidance, advice, assistance, and

motivation. To my girlfriend and best friend, Sarah Kay VanOosten, thank you for taking this journey with me and all the patience that you have shown. I cannot thank you enough for your love and support. I am proud of all that you have and will accomplish on your own path. To the VanOosten family, especially Ann and Jim VanOosten, I am forever grateful for your kindness, support, and understanding. To my feathered buddy Astro (named after the presumed normal cell of origin for GBM), thanks for always being full of energy and happy to see me. I love you all.

To my other best friend, Paul Schwingler, thanks for always being there and even spending time rotating through the lab. You are truly dependable and one-of-a-kind.

To my friends in the MD/PhD Program and medical school, thank you being there. And to members of other labs at the University of Michigan for general advice, assistance, and friendship, notably Joe Nguyen, Lukasz Ochyl, Molly Kozminsky, and Dr. Luis Villa Diaz, I thank you.

To anyone else who I have inevitably forgotten or could not mention, thank you for your contribution, small or large.

Table of Contents

Chapter 1

Background and Introduction

<u>Chapter 2</u>

Cytotoxicity of withaferin A in glioblastomas involves induction of an oxidative stress-mediated

heat shock response while altering Akt/mTOR and MAPK signaling pathways

Chapter 3

Oxidative cytotoxic agent withaferin A resensitizes temozolomide-resistant glioblastomas via
MGMT depletion and induces apoptosis through Akt/mTOR pathway inhibitory modulation

Chapter 4

Withaferin A is a novel inhibitor of the Wnt/β-catenin signaling pathway in medulloblasoma

through proteasome-mediated degradation of TCF/LEF

Chapter 5

Withaferin A promotes global proteasome-mediated protein degradation through oxidation and inhibition of the HSP90 chaperone axis and is cytotoxically potentiated by inhibition of the proteasome

Chapter 6

Withaferin A disrupts the cellular DNA-damage response to promote radiosensitization

Chapter 7

Summary, Significance, and Future Directions

List of Abbreviations

17-AAG	17-N-allylamino-17-demethoxygeldanamycin
5-FU	5-fluorouracil
AA	Ascorbic acid
AMPK	5' AMP-activated protein kinase
AP-1	Activator protein 1
APC	Adenomatous polyposis coli protein
ATM	Ataxia telangiectasia mutated
ATP	Adenosine triphosphate
ATR	ATM and Rad3-related
ATCC	American Type Culture Collection
BCR-ABL	Breakpoint cluster region protein-Abelson murine leukemia viral oncogene (product of Philadelphia chromosome)
BCNU	Carmustine
BRCA1	Breast cancer type 1 susceptibility protein
BRCA2	Breast cancer type 2 susceptibility protein
BSO	DL-buthionine-(S,R)-sulfoximine
C	Celsius (degrees)
c-Met	Hepatocyte growth factor receptor
Cdc37	Cell division cycle protein 37
Cdk4	Cyclin-dependent kinase 4
Cdk6	Cyclin-dependent kinase 6
cDNA	Complementary DNA
Chk1	Checkpoint kinase 1
Chk2	Checkpoint kinase 2
CLL	Chronic lymphocytic leukemia
CNS	Central nervous system
co-IP	Co-immunoprecipitation
CO_2	Carbon dioxide
CtBP	C-terminal binding protein
CYP450	Cytochrome P450
DAPI	4',6-diamidino-2-phenylindole
DDR	DNA-damage response
DMEM	Dulbecco's modified Eagle's medium
DMSO	Dimethylsulfoxide
DNA	Deoxyribonucleic acid
DNA-PKcs	DNA-dependent protein kinase, catalytic subunit (DNA-PK)
DSB	Double-strand DNA break

dsDNA	Double-strand DNA
DTT	Dithiothreitol
EDTA	Ethylenediaminetetraacetic acid
EGFR	Epidermal growth factor receptor
EGTA	Ethylene glycol tetraacetic acid
ER	Estrogen receptor
ERK	Mitogen-activated protein kinase 1/extracellular signal-regulated kinase
FBS	Fetal bovine serum
FDA	U.S. Food and Drug Administration
FiGR	Mouse monoclonal antibody to glucocorticoid receptor
FITC	Fluorescein isothiocyanate
FLAG	FLAG-tag DYKDDDDK octapeptide
G0/G1	Gap 0/Gap 1
G2/M	Gap 2/mitosis
GAPDH	Glyceraldehyde 3-phosphate dehydrogenase
GBM	Glioblastoma multiforme
GFP	Green fluorescent protein
GR	Glucocorticoid receptor
Grp94	Heat shock protein 90kDa beta member 1
GSH	Glutathione
GSK-3β	Glycogen synthase kinase-3β
Gy	Gray
h	hour
H2A.X	H2A histone family, member X
H_2O_2	Hydrogen peroxide
H^3	Tritium
HA	Hemagglutinin
HDAC	Histone deacetylase
HEPES	4-(2-hydroxyethyl)-1-piperazineethanesulfonic acid
Her2/neu/ERBB2	Human epidermal growth factor receptor 2
Hop	Hsp70-Hsp90 Organizing Protein
HPLC	High-performance liquid chromatography
HR	Homologous recombination
HRP	Horseradish peroxidase
HSF1	Heat shock factor 1
HSP27	Heat shock protein 27
HSP32	Heat shock protein 32/heme oxygenase 1
HSP40	Heat shock protein 40
HSP70	Heat shock protein 70

HSP90	Heat shock protein 90
IC_{50}	Half maximal inhibitory concentration
ICC	Immunocytochemistry
IP	Immunoprecipitation
IR	Ionizing radiation
JAK	Janus kinase
JNK	c-Jun N-terminal kinase
Ku70	X-ray repair cross-complementing 6 (XRCC6)
Ku80	X-ray repair cross-complementing 5 (XRCC5)
LC3B	Microtubule-associated proteins 1A/1B light chain 3B
LEF1	Lymphoid enhancer-binding factor 1
m	minute
MAPK	Mitogen-activated protein kinase
MB	Medulloblastoma
MEK	Mitogen-activated protein kinase kinase
MEM	Minimum essential medium
MGMT	O^6-methylguanine-DNA methyltransferase
MLH1	MutL homolog 1
MMR	Mismatch repair
MRN complex	Mre11, Rad50, p95/NBS1
mRNA	Messenger RNA
MSH2	MutS homolog 2
MSH6	MutS homolog 6
mTOR	Mammalian target of rapamycin
MTS	3-(4,5-dimethylthiazol-2-yl)-5-(3-carboxymethoxyphenyl)-2-(4-sulfophenyl)-2H-tetrazolium
Na_3VO_4	Sodium orthovanadate
NAC	N-acetyl-L-cysteine
NFκB	Nuclear factor kappa-light-chain-enhancer of activated B cells
NHEJ	Non-homologous end-joining
OTSA101-DTPA-90Y	Yttrium90-labeled Frizzled-10 monoclonal antibody OTSA101
p21/cip1	Cyclin-dependent kinase inhibitor 1
p23	Prostaglandin E synthase 3
p27/kip1	Cyclin-dependent kinase inhibitor 1B
p70 S6K	p70 S6 kinase
p95/NBS1	Nibrin/Nijmegen breakage syndrome 1
PARP	Poly(ADP-ribose) polymerase
PBS	Phosphate-buffered saline
PI	Propidium iodide
PI3K	PI3 kinase

PMSF	Phenylmethylsulfonyl fluoride
PTEN	Phosphatase and tensin homolog
Raf-1	RAF proto-oncogene serine/threonine-protein kinase (c-Raf; MAP kinase kinase kinase; rapidly accelerated fibrosarcoma protein)
Ras	Rat sarcoma protein
Rb	Retinoblastoma protein
RIPA	Radioimmunoprecipitation assay
RNA	Ribonucleic acid
ROS	Reactive oxygen species
rpm	Revolutions per minute
RT	Radiation therapy
RT-PCR	Real-time polymerase chain reaction
S	Synthesis
SDS	Sodium dodecyl sulfate
SDS–PAGE	Sodium dodecyl sulfate–polyacrylamide gel electrophoresis
Ser	Serine
SHH	Sonic hedgehog
SOD	Superoxide dismutase
SSB	Single-strand DNA break
ssDNA	Single-strand DNA
STAT	Signal transducer and activator of transcription
TCF1	Transcription factor 1
TCF3	Transcription factor 3
TCF4	Transcription factor 4
Thr	Threonine
TMZ	Temozolomide
Trap1	TNF receptor-associated protein 1
TSC1	Hamartin/Tuberous sclerosis 1
TSC2	Tuberin/Tuberous sclerosis 2
VEGF	Vascular endothelial growth factor
WA	Withaferin A
Wnt	Wingless
WT	Wild-type
XLF	XRCC4-like factor/Non-homologous end-joining factor 1

List of Figures

List of Appendices

Chapter 1

Background and Introduction

1.1 Brain tumors

1.1.1 Glioblastoma mutiforme

According to the National Cancer Institute, there were an estimated 22,070 new cases of primary brain tumors with 12,920 deaths from such tumors in 2009 in the United States. High grade gliomas, such as anaplastic astrocytoma and glioblastoma (GBM), account for approximately 38% of primary brain tumors, and, unfortunately, few definitive observations have been reported for potential environmental, occupational, or genetic causes of these tumors. The cell of origin for GBMs remains poorly defined, but studies have shown the most likely target cells to be astrocytes, neural stem cells, and/or oligodendrocyte precursor cells (Jiang and Uhrbom, 2012). Given the fact that these tumors occur in the central nervous system (CNS), treatment options have remained limited. Following optimal surgical debulking, radiation therapy (RT) is able to increase mean survival time from approximately six months to only one year (Gillingham and Yamashita, 1975; Onoyama et al., 1976; Sheline, 1977). Even ideal utilization of stereotactic radiosurgery known as Gamma Knife has only been shown to improve survival by approximately 2.3 months (Pouratian et al., 2009). Of the few treatment options available and approved for high grade malignant gliomas, surgical debulking followed by radiation therapy and concurrent chemotherapy with the methylating agent temozolomide (TMZ) represents the most effective option but still only yields a two-year survival rate in GBM patients of 26.5% (compared to 10.4% for radiation-only patients, the previous standard) (Stupp et al., 2002; DeAngelis, 2005; Stupp et al., 2005; Taphoorn et al., 2005; Chamberlain et al., 2007).

While TMZ confers survival benefit to the glioma patient population as a whole and was approved for use in 2005 by the U.S. Food and Drug Administration (FDA), its extent of efficacy is largely influenced by the methylation state and expression status of the *MGMT* (O^6-methylguanine-DNA methyltransferase) gene promoter, which occurs in 35-45% of these tumors (Paz et al., 2004; Hegi et al., 2005). In patients whose tumors have an unmethylated promoter, the MGMT protein is expressed and repairs the initial DNA lesions caused by TMZ, essentially eliminating any anti-cancer effects of the drug (Hansen et al., 2007; Kitange et al., 2009). These statistics suggest that well over 55-65% of glioma patients do not display tumor phenotypes favorable for treatment with TMZ, and given the lack of adequate preliminary screening techniques for MGMT status, many of these patients end up receiving a therapy that will ultimately have no or minimally significant impact on disease progression. This clinical reality exposes the critical need for improved diagnostic and therapeutic approaches for patients with gliomas.

Although not typically considered first-line standard of care, the Gliadel wafer represents an FDA-approved localized therapy that combines a biodegradable polymer backbone with the alkylating agent carmustine (BCNU) (Buonerba et al., 2011). Following surgical debulking, the wafer is set into the resection cavity to allow for a maintained release of drug to residual cancer cells at the margin of the resection. Average post-diagnosis survival was shown to be increased by two months with the Gliadel wafer, which, while significant, remains a poor outcome for these patients (Westphal et al., 2003). Lastly, in 2009, the anti-angiogenic agent bevacizumab, a monoclonal antibody against vascular endothelial growth factor (VEGF)-A to prevent the recruitment of additional vasculature to the site of the tumor, was approved by the FDA for use in patients with malignant gliomas (Serwer and James, 2012). This option is typically reserved

for patients with recurrent lesions who have failed or otherwise become resistant to TMZ and RT and has demonstrated the ability to extend progression-free survival in Phase II trials (Desjardins et al., 2008; Friedman et al., 2009; Zhang et al., 2012a); Phase III studies are ongoing (Serwer and James, 2012).

1.1.2 Blood-brain-barrier

Currently, the mean post-diagnosis survival time of patients with GBM and other aggressive high grade brain malignancies is approximately 14 months and has improved only minimally over the last several decades. This low survival duration following treatment is partly due to the lack of long-term efficacy of current treatment and partly a result of the highly infiltrative nature of these tumors, resulting in residual invasive tumor cells after surgical resection, high rates of recurrence, and poor clinical outcomes (Giese et al., 2003). Various groups are attempting to identify novel treatment modalities that better target these infiltrative lesions, including identification of chemotherapeutic agents possessing structures more likely to pass through the blood-brain-barrier (BBB), novel delivery mechanisms that circumvent current limitations, and enhancement of the anti-cancer properties of the immune system through immunotherapy (Alam et al., 2010; Serwer and James, 2012; Hamilton and Sibson, 2013). The brain displays a unique perivascular environment as a result of this selectively permeable BBB that limits the movement of chemicals and endogenous molecules from the blood into the brain parenchyma and thereby acts in a protective nature. However, this same protective mechanism under normal conditions establishes a therapeutic challenge in the case of a primary or metastatic brain lesion. In fact, while many inhibitors of pathways known to be important in the progression

of brain tumor growth already exist, the unimpressive results of their use in clinical trials can almost always be attributed, at least in part, to pharmacokinetic and biodistribution shortcomings (Serwer and James, 2012). While the architecture of the BBB is largely disrupted in advanced cases, such a finding becomes largely irrelevant in the context of the poor prognosis subsequently observed at that point (Zhang et al., 1992). Additionally, treatment of such lesions where the BBB has been compromised, while sometimes locally successful due to disruption of the barrier in this location, often fails due to recurrence from peripheral and/or infiltrative portions of the tumor where the BBB is still intact (Agarwal et al., 2011). A large portion of the success achieved with TMZ in brain tumors is due to its ability to cross the BBB (Patel et al., 2003).

1.1.3 Medulloblastoma

One major challenge faced in the treatment of cancer, particularly brain tumors with CNS-directed chemotherapy and radiotherapy, is the damage known to be caused to normal brain and peripheral tissue, resulting in acute and chronic cognitive impairment known as post-chemotherapy cognitive impairment or "chemobrain" (Butler et al., 2006; Nokia et al., 2012). Consideration of long-term complications is particularly important in the treatment of children who are affected by these diseases. The most common brain tumor in children is medulloblastoma (MB), a high grade lesion that typically arises in the posterior fossa and represents 25-30% of primary brain tumors in children but can arise in individuals of all ages (Khatua et al., 2012). MBs are categorized in several unique molecular subgroups based on tumor genetics, cell histology, growth, and clinical outcome including sonic hedgehog (SHH),

5

Wingless (Wnt), group 3, and group 4 (Northcott et al., 2012). As with glioma, the cell of origin for MB has remained elusive, but studies have suggested that different subgroups may develop from different cancer stem cell precursors including granule neuronal precursor cells in the SHH subgroup and dorsal brainstem precursor cells in the Wnt subgroup (Gilbertson and Ellison, 2008; McCarthy, 2011). Although the overall 5-year survival rate for MBs in both children and adolescents is around 70%, differing somewhat between subgroups, therapeutic challenges remain to simultaneously address both treating the tumor and ensuring a high long-term quality of life in the pediatric patient population (Smoll, 2012). Current standards of care includes surgical resection followed by craniospinal radiation and DNA-damaging chemotherapeutic agents such as vincristine, lomustine, cyclophosphamide, carboplatin, and cisplatin (Khatua et al., 2012). However, because of significant morbidities associated with these agents, it has been reported that long-term survivors of childhood MB suffer from endocrine, cognitive, and neurological complications with significant deficits in daily psychosocial functioning including driving, employment, independent living, and personal relationships when compared to their age-matched peers (Boman et al., 2009; Frange et al., 2009; Robinson et al., 2012).

1.2 Proposed targets of withaferin A

1.2.1 Oncogenic pathway signaling inhibition

A recent screening of over 200 compounds derived from natural sources with promising anti-cancer potential at the University of Kansas Lawrence identified a 28-carbon steroidal lactone, withaferin A (WA), with intriguing cytotoxic properties (Figure 1-1). Interest in WA has

Figure 1-1.
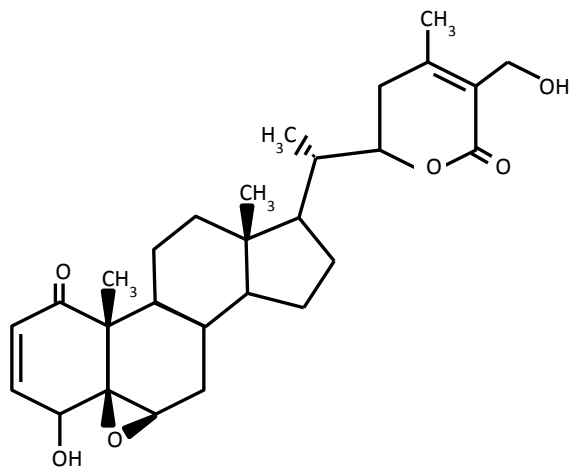
Figure 1-1. Structure of withaferin A.

increased within the last ten years as demonstrated by increased publication on its anti-cancer and anti-inflammatory properties (Vanden Berghe et al., 2012; Vyas and Singh, 2014). In these publications, WA is reported to target or otherwise modulate a plethora of different proteins and signaling pathways including Akt, Notch-1, heat shock protein (HSP) 90, nuclear factor kappa-light-chain-enhancer of activated B cells (NFκB), activator protein 1 (AP-1), estrogen receptor (ER), RET, and p38 among others (Mohan et al., 2004; Singh et al., 2007; Mandal et al., 2008; Oh et al., 2008; Stan et al., 2008; Oh and Kwon, 2009; Shah et al., 2009; Koduru et al., 2010; Samadi et al., 2010a; Yu et al., 2010). Recently, our group and others have demonstrated a pro-oxidant potential of WA in non-brain tumor cells (Malik et al., 2007; Widodo et al., 2010; Hahm et al., 2011; Mayola et al., 2011; Grogan et al., 2013) and its ability to bind to certain thiol residues (Yu et al., 2010; Thaiparambil et al., 2011; Santagata et al., 2012). Despite these findings, the specific mechanism of WA's diverse and widespread effects remained elusive, especially in brain tumors where work has been largely absent. Regardless of the ultimate mechanism, development of WA as an anti-cancer agent has been suggested to provide a potentially unique approach compared to most standard therapies because, in contrast to disrupting a single molecular pathway or interaction like the integrity of DNA as with TMZ, WA demonstrates the ability to modulate several oncogenic pathways simultaneously (Vanden Berghe et al., 2012; Vyas and Singh, 2014). Many cancers, including GBM and MB, often display overactivation and/or dysregulation of multiple oncogenic signaling cascades, including the mitogen-activated protein kinase (MAPK) and PI3 kinase (PI3K)/Akt/mammalian target of rapamycin (mTOR) pathways, establishing therapeutic challenges given the heterogeneity of the activation and the great level of proliferative signaling (Gilbertson et al., 2006; Wen and Kesari, 2008; Mohan et al., 2012).

9

1.2.1a Mitogen-activated protein kinase pathway

The MAPK/ERK signaling pathway involves a chain of proteins in the cell that communicates a signal from a receptor on the cell surface to the nucleus where promotion of growth and proliferation occurs through selective transcription (Figure 1-2A and 1-2B) (Chang and Karin, 2001). The generation of an activated membrane receptor complex activates rat sarcoma protein (Ras), which subsequently promotes the protein kinase activity of rapidly accelerated fibrosarcoma protein (Raf). Raf kinase phosphorylates and activates MEK (MAPKK), which subsequently activates a MAPK, frequently extracellular signal-regulated kinase (ERK1/2) (Avruch et al., 2001). c-Jun N-terminal kinase (JNK) and p38 MAPKs are more responsive to stress signals. Disruption of this pathway at any point can lead to a failure of signal transduction and a slowing of cell growth. Inversely, various cancers often demonstrate activating mutations of proteins in the cascade like Ras and Raf or elevated activation of a surface receptor that promotes pathway signal transduction (Dhillon et al., 2007; Krakstad and Chekenya, 2010). GBMs predominately favor the latter, with 40-60% of cases demonstrating amplification of the tyrosine kinase epidermal growth factor receptor (EGFR) and 40% of those displaying activating EGFR mutations (Krakstad and Chekenya, 2010). Indeed, targeted therapeutics against EGFR are currently in clinical trials for GBM, but, despite some promise, they have not been approved as standard therapeutic agents (Krakstad and Chekenya, 2010). Trials in pediatric CNS tumors patients have also been ongoing but little has been published to date (MacDonald et al., 2014). These studies suggest that inhibition of MAPK signaling in brain tumors may yield improved therapeutic benefits. WA has been shown to affect this signaling

Figure 1-2.

A
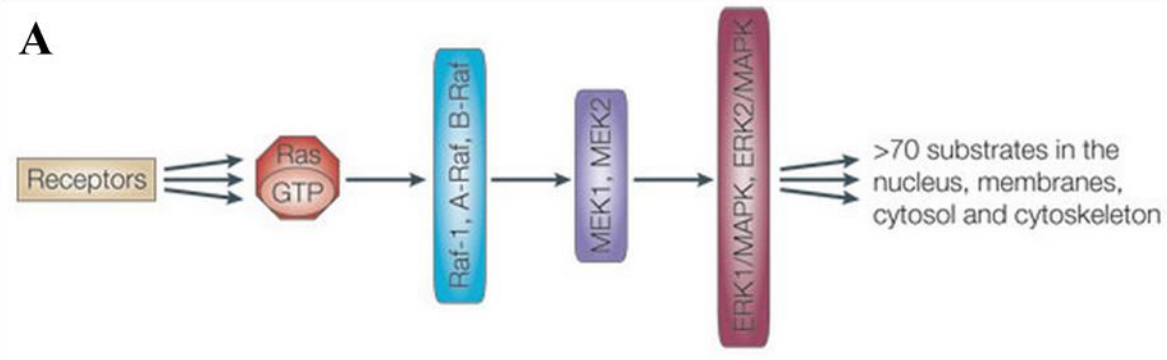
B
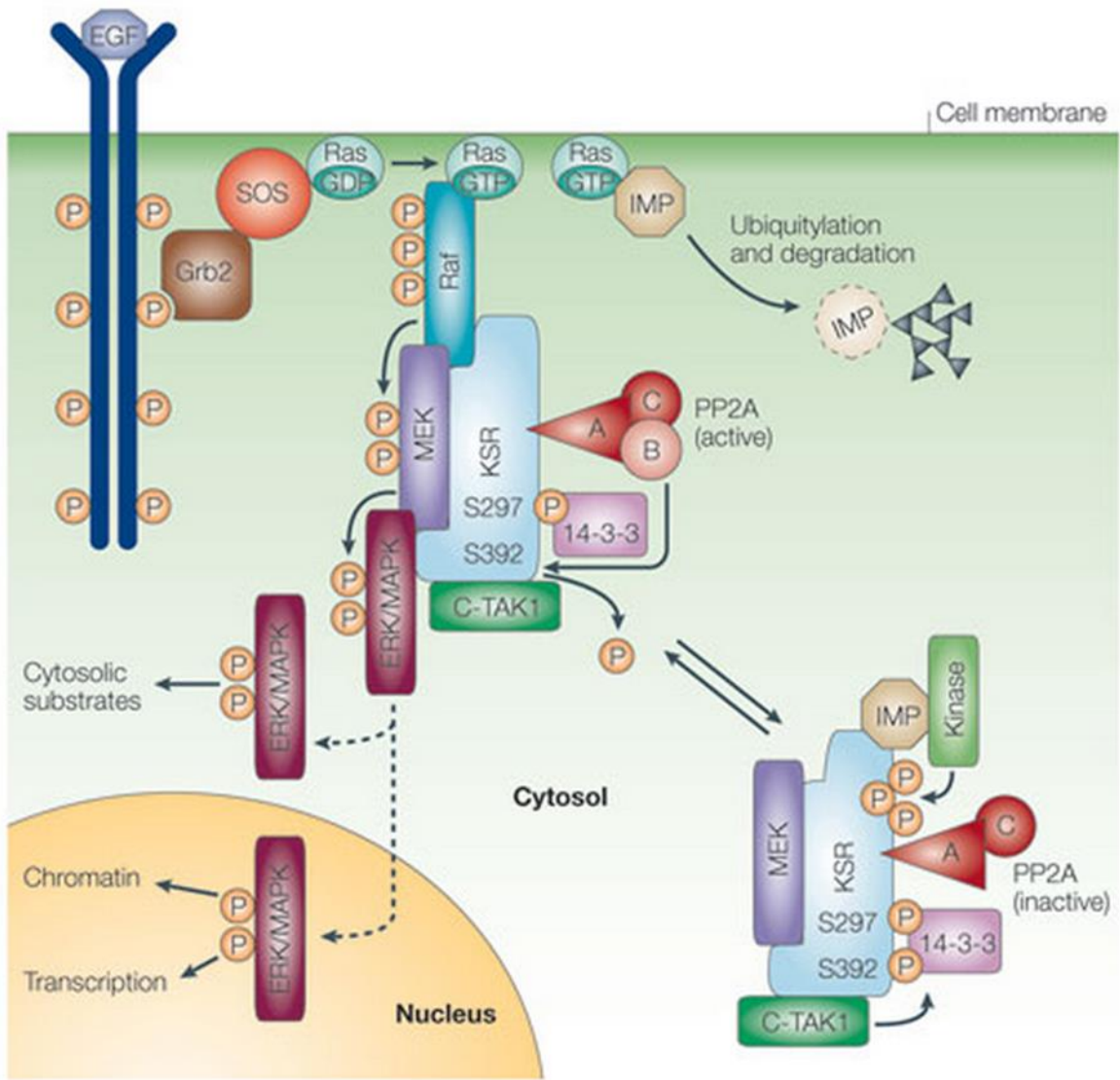
Figure 1-2. A) Simplified schematic of the MAPK/ERK signaling pathway. Activation of a cell surface receptor through ligand binding induces the downstream activation of a Ras GTPase. Ras recruits Raf to the membrane and promotes its protein kinase activity. Raf kinase phosphorylates and activates MEK, which subsequently activates a MAPK, frequently ERK1/2, the main effector protein of the pathway with over 70 identified substrates. Ultimately, this pathway promotes cellular growth and proliferation occurs often through selective transcription of target genes. B) Detailed schematic demonstrating the complexities of the MAPK/ERF signaling pathway including the involvement of numerous adaptor, scaffolding, and regulator proteins.

Reprinted by permission from Macmillan Publishers Ltd: Nature Reviews Molecular Cell Biology (http://www.nature.com/nrm/index.html). Kolch W. Coordinating ERK/MAPK signalling through scaffolds and inhibitors, 2005.

pathway in non-brain tumor models. In leukemic cells and squamous cell carcinoma, WA was shown to deplete total levels of Raf-1 but induce phosphorylation of ERK1/2 and the isoforms p38 and JNK (Mandal et al., 2008; Samadi et al., 2010b), with activation of p38 associated with induction of apoptosis (Mandal et al., 2008).

1.2.1b PI3 kinase/Akt/mammalian target of rapamycin (mTOR) pathway

Similar to the MAPK pathway, the PI3K/Akt/mTOR pathway can be activated by external signaling through tyrosine kinase receptors like EGFR. This leads to a signal cascade through PI3K, Akt, and finally mTOR, with numerous additional proteins playing supporting roles (Figure 1-3) (Krakstad and Chekenya, 2010). Because the tumor suppressor phosphatase and tensin homolog (PTEN), which counteracts PI3K, is inactivated by genetic alterations in approximately 60% of GBMs and mutations have been noted in MBs (Hartmann et al., 2006; Lee et al., 2011) that lead to constitutive activation of Akt and mTOR, this pathway is likely to be highly clinically relevant in the treatment of malignant brain tumors (Koul, 2008; Lino and Merlo, 2011). Hyperactivated Akt has been shown to result in uncontrolled cell cycle progression and protection from apoptosis (Nogueira et al., 2008). Inhibition of Akt, mTOR, and downstream p70 S6 kinase (S6K) represent potential targets for prevention of the pathway's proliferative effects. In the presence of cellular stress, 5' AMP-activated protein kinase (AMPK) suppresses mTOR through phosphorylation of the tumor suppressor tuberin/TSC2 or the mTOR subunit Raptor (Mihaylova and Shaw, 2011). It has previously been shown that AMPK activation contributes to apoptosis in GBM cells (Zhang et al., 2010). Therapeutic activation of either the AMPK complex or tuberin/TSC2 represents a more indirect route to inhibit this

Figure 1-3.
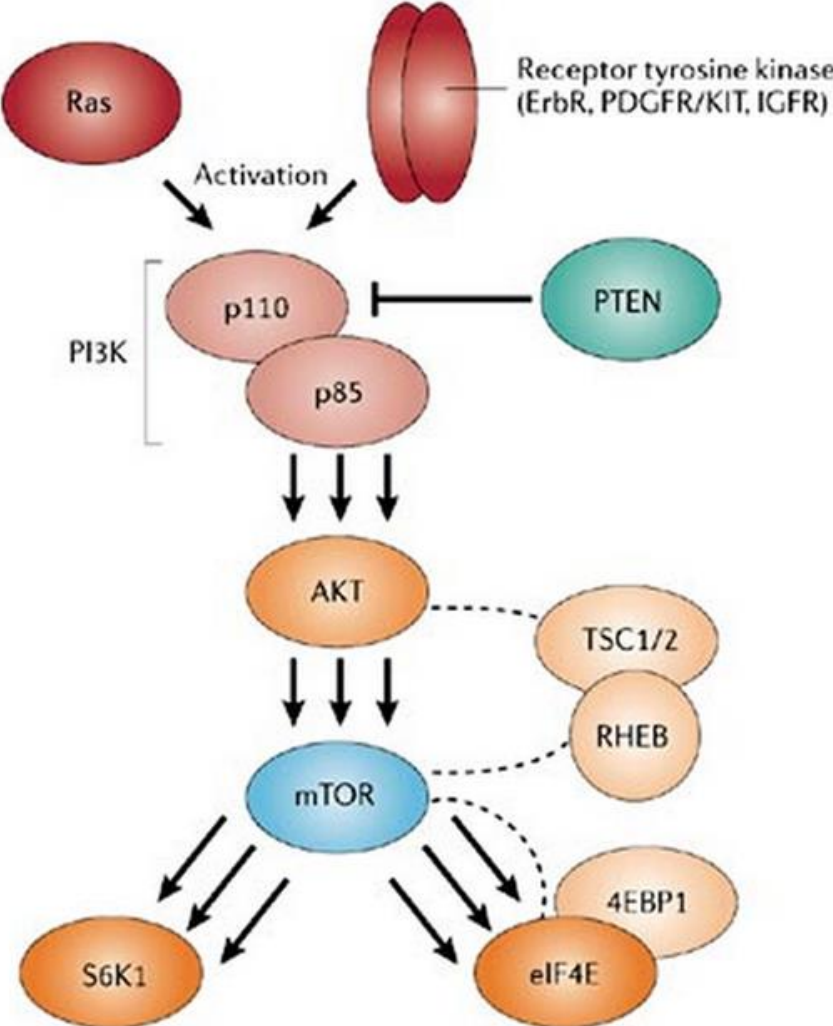
Figure 1-3. Schematic of the PI3K/Akt/mTOR signaling pathway. PI3K is primarily activated by extracellular signaling through tyrosine kinase receptors at the cell surface but can also associated with Ras. PI3K activity is negatively regulated by PTEN. PI3K ultimately activates a signaling cascade including Akt and mTOR with signaling through phosphorylation. mTOR increases protein synthesis and cell proliferation through inhibitory phosphorylation of translational repressor 4E-BP1 and activating phosphorylation of p70 S6K. Reduction of pathway activity is mediated by stress indicator AMPK and tumor suppressors TSC1/2.

Reprinted and adapted by permission from Macmillan Publishers Ltd: Nature Reviews Drug Discovery (http://www.nature.com/nrd/index.html). Faivre S, et al. Current development of mTOR inhibitors as anticancer agents, 2006.

pathway. Current early phase clinical trials in GBM are utilizing agents to inhibit the function of

EGFR, Akt, PI3K, and mTOR in this pathway (Krakstad and Chekenya, 2010). Although

multiple groups have demonstrated decreased levels of total and phosphorylated Akt in response

to WA treatment in several non-brain tumor cancer models (Oh et al., 2008; Oh and Kwon,

2009; Samadi et al., 2010a; Samadi et al., 2010b), no previous reports described its effects on

other proteins in the PI3K/Akt/mTOR signaling pathway despite this early promise.

1.2.1c Wnt/β-catenin signaling pathway

MBs are categorized in several unique molecular subgroups including SHH, Wnt, group

3, and group 4 based on a number of unique tumor traits (Northcott et al., 2012). The Wnt

subgroup of MB patients is defined by overactivation of the canonical Wnt/β-catenin signaling

pathway, often through overexpression of β-catenin or inactivating mutations of adenomatous

polyposis coli protein (APC) and Axin1/2 thereby acting independently of extracellular signaling

of Wnt through the frizzled surface receptor and downstream disheveled protein (Figure 1-4)

(Kim et al., 2011). This leads to excessive nuclear accumulation of β-catenin, which associates

with transcription factors of the transcription factor (TCF)/lymphoid enhancer-binding factor

(LEF) family to promote cell migratory and proliferative activity of the pathway at the

transcriptional level (Taylor et al., 2012). As a result, this pathway has been suggested as a

potential therapeutic target in MB. Only poly(ADP-ribose) polymerase (PARP) inhibition,

described to destabilize β-catenin through Axin, is under trial for MB (Waaler et al., 2012).

The Akt/mTOR pathway establishes cross-talk with the Wnt/β-catenin pathway through

glycogen synthase kinase-3β (GSK-3β) such that activation of Akt produces inhibitory

Figure 1-4.
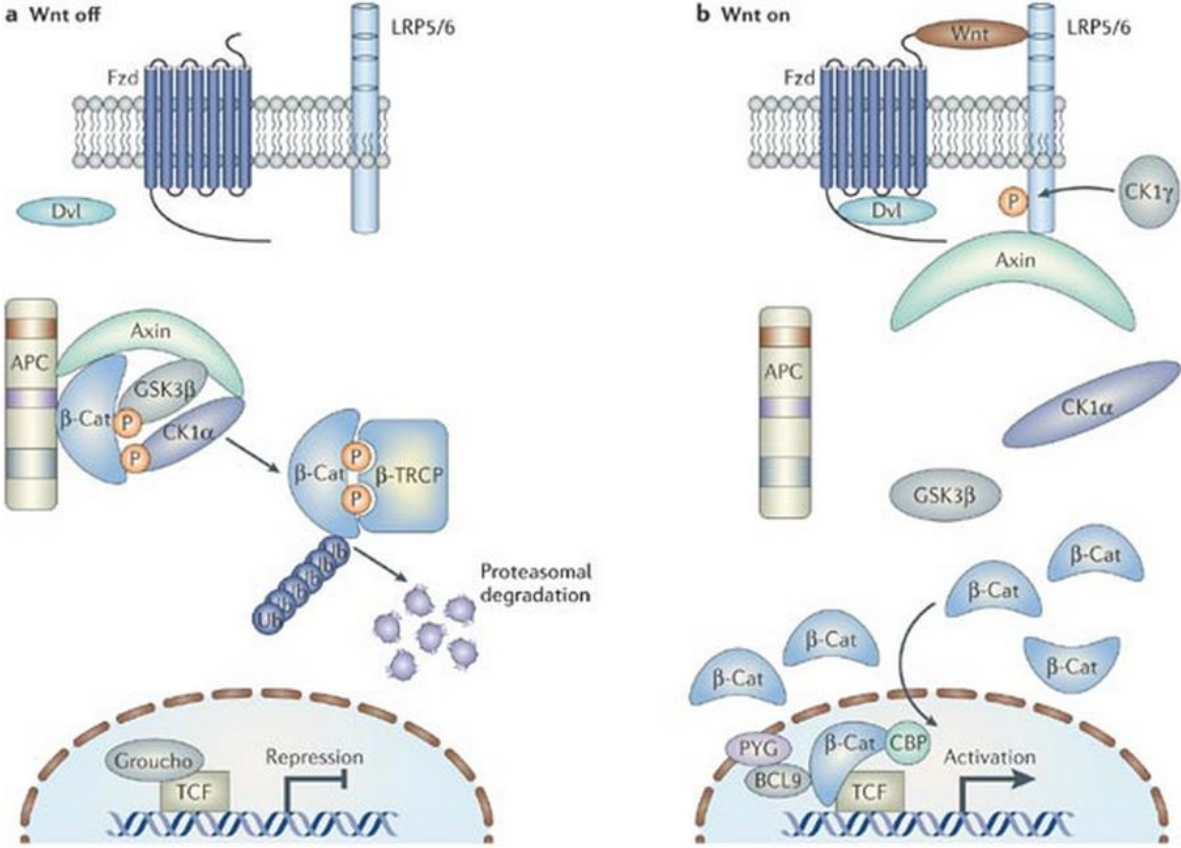
Figure 1-4. Schematic representation of the Wnt signaling pathway in (a) the absence of Wnt ligand and (b) the presence of Wnt ligand. Without Wnt ligand, β-catenin is sequestered by a complex that includes GSK-3β, Axin, and APC which targets it for proteasomal degradation. TCF/LEF transcription factors in the nucleus remain associated with repressor proteins Groucho to prevent target protein transcription. In the presence of Wnt ligand binding a receptor complex that includes Frizzled and low-density lipoprotein receptor-related protein (LRP), the functions of dishevelled and CK1 ultimately lead to diminished GSK-3β and a failure to form the destruction complex. This leads to accumulation of β-catenin with its eventual translocation into the nucleus where it associates with TCF/LEF members to activate gene transcription. Activity of GSK-3β can also be reduced with cross-talk from the Akt/mTOR pathway in which Akt phosphorylates GSK-3β at Ser9 to inactivate it.

Reprinted by permission from Macmillan Publishers Ltd: Nature Reviews Drug Discovery (http://www.nature.com/nrd/index.html). Barker N and Clevers H. Mining the Wnt pathway for cancer therapeutics, 2006.

phosphorylation of GSK-3β, a reduction in the phosphorylation of β-catenin, and enhanced stability of β-catenin. As such, inhibition of PI3K/Akt signaling has been shown to inhibit the Wnt/β-catenin pathway in MB (Baryawno et al., 2010). Given the previously described alterations in Akt induced by WA exposure, it was hypothesized that WA could act as a novel inhibitor of the Wnt pathway in MB by a similar mechanism. Until this study, WA had not previously been explored as a Wnt/β-catenin signaling inhibitor nor examined against MB.

1.2.2 Proteotoxicity

Malignant transformation to cancer often results in deregulation of normal homeostatic processes that is subsequently associated with increased cellular stress, including oxidative, replicative, metabolic, genomic, and proteotoxic stress (Luo et al., 2009). Cancer cell adaptation to these stressors is therefore necessary for survival, resulting in dependence on non-oncogene proteins and mechanisms that would otherwise play a less vital role in a non-malignant cell. Pharmacological induction of oxidative stress has emerged as an intriguing means by which to mount an anti-cancer effect. It is shown that pro-oxidant intervention can alter the redox homeostasis of cancer cells, already stressed by exposure to constitutively high levels of reactive oxygen species (ROS) not observed in normal cells, by shifting the balance to a state of cytotoxicity (Laurent et al., 2005; Cabello et al., 2007). In fact, several investigational chemotherapeutics with redox potential have recently been explored in preclinical and clinical settings (Wondrak, 2009; Tew and Townsend, 2011). Such an oxidative stress mechanism has also been demonstrated to effectively induce the proteotoxic stress of protein unfolding/misfolding, resulting in a downstream secondary cytotoxicity that likely preferentially

affects these already susceptible cancer cells (Xu et al., 2011; Qiao et al., 2012). Previous reports of others have demonstrated the pro-oxidant potential of WA in multiple cancer models (Malik et al., 2007; Widodo et al., 2010; Hahm et al., 2011; Mayola et al., 2011; Grogan et al., 2013). While this has largely remained a general finding, mechanistic evaluation demonstrated that overexpression of Cu,Zn-superoxide dismutase (SOD) resulted in a partial protective effect against WA treatment in breast cancer cells (Hahm et al., 2011). The same study suggested that WA-mediated ROS generation and toxicity was a result of mitochondrial respiration inhibition.

While the WA exhibits both thiol reactivity and the ability to induce ROS, it has been suggested that the nature of such activity occurs with some protein specificity. It has been described that WA is capable of binding to the C-terminus of the chaperone protein HSP90 and altering its activity (Yu et al., 2010), although evidence of the latter is largely indirect and downstream. HSP90 is an well-conserved protein, making up ~1-3% of total cellular protein in any given cell, directly responsible for interacting with and maintaining the stability and function of over 400 key cellular proteins (Barrott and Haystead, 2013). Inhibition of HSP90 results in the depletion of client proteins critical to the proliferation and ultimate survival of cancer cells such as pro-growth signaling proteins, tyrosine kinases, cell cycle regulators, and steroid receptors (Zhang and Burrows, 2004; Powers and Workman, 2006; Sidera and Patsavoudi, 2014). Inhibition of this activity is cytotoxic. Cancer cells demonstrate enhanced responsiveness to HSP90 inhibition compared to normal tissue, and this has been suggested to be a result of enhanced reliance on HSP90 for stabilization of oncoproteins, localization in stressful microenvironments, and selective accumulation of inhibitors in cancer cells (Sidera and Patsavoudi, 2014). To date, 17 HSP90 inhibitors, all N-terminal inhibitors of ATPase activity such as 17-allylamino-17-demethoxygeldanamycin (17-AAG) (Workman, 2003), have been

brought to clinical trial, and while some have shown therapeutic promise despite formulation challenges, none have been approved for standard use against any cancer (Heath et al., 2005; Heath et al., 2008; Solit et al., 2008; Pacey et al., 2012). It has been noted that WA may function to indirectly modulate the HSP90 chaperone axis through disruption of the HSP90/ cell division cycle protein 37 (Cdc37) interaction (Yu et al., 2010; Grover et al., 2011; Gu et al., 2014). Cdc37 functions as a co-chaperone to HSP90 and plays a vital role in localizing target kinases of the kinome with HSP90 for folding (Karnitz and Felts, 2007).

It has been long-noted that oxidative and other stressor damage to proteins triggers their subsequent degradation (Stadtman, 1986). The major chaperones involved in protein quality control decisions are HSP70 and HSP90, which act together in a multi-chaperone complex to regulate the function, trafficking, and turnover of a wide variety of signaling proteins. However, despite being an oversimplification of the complexities of protein chaperoning, these two components of the machinery play opposite yet essential roles with HSP70 promoting ubiquitination followed by proteosomal degradation and HSP90 stabilizing proteins against degradation and instead promoting their refolding (Figure 1-5) (Pratt et al., 2010). This mechanism is supported by studies demonstrating that treatment with HSP90 inhibitors promotes the degradation of client proteins via the ubiquitin-proteasome pathway (Whitesell et al., 1994; Sepp-Lorenzino et al., 1995), and over-expression of HSP70 decreases the level of dysfunctional or misfolded proteins and improves viability in cellular models of certain neurodegenerative diseases characterized by the aberrant protein accumulation such as Parkinson's disease, Huntington's disease, and spinal and bulbar muscular atrophy (Jana et al., 2000; Bailey et al., 2002; Klucken et al., 2004). Indeed, recent reports showed enhanced protein ubiquitination in the presence of WA (Bargagna-Mohan et al., 2006; Yang et al., 2012) and elevated total levels of

Figure 1-5.
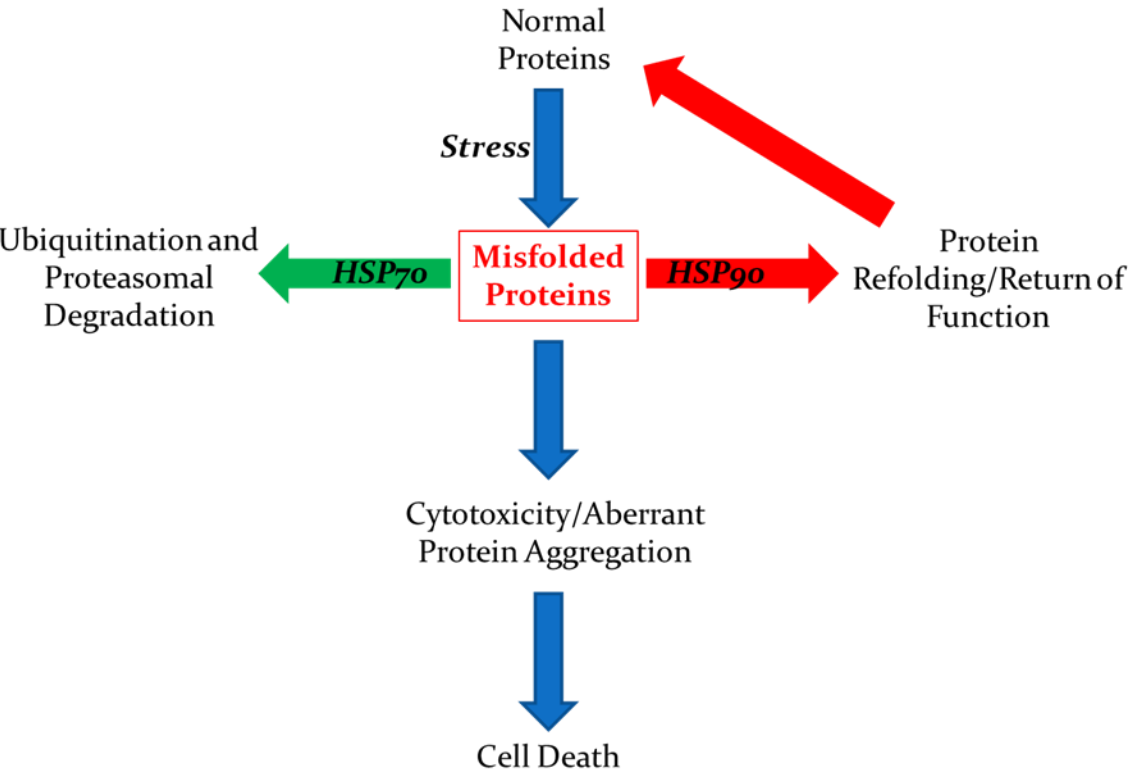
Figure 1-5. In general, chaperone HSP90 promotes protein refolding while HSP70 favors protein degradation to maintain protein homeostasis and prevent the accumulation of aberrant proteins. Various stressors, including oxidation, increases the frequency of protein misfolding. Inhibition of HSP90 shifts protein maintenance toward HSP70-mediated proteasomal degradation and vice versa. Simultaneous inhibition of the HSP90 and HSP70 axes, especially in the presence of a stressor, promotes cellular cytotoxicity through accumulation of many aberrant proteins, given an elimination of both homeostatic pathways.

HSP70 following treatment (Grogan et al., 2013). While several reports indicate that WA at least partially inhibits the proteasome itself, which can lead to an accumulation of ubiquitinated proteins (Yang et al., 2007; Yang et al., 2012), this finding remains unclear in the context of other data demonstrating that pretreatment with proteasome inhibitor MG132 completely reverses WA-mediated degradation of certain proteins (Zhang et al., 2011b) and that the doses used to achieve the effect were significantly above pharmacologically-relevant levels.

Given reports of WA-mediated alterations in proteins and oncogenic signaling pathways potentially through oxidation and modulation of the HSP90 chaperone axis, ultimately resulting in protein depletion and proteotoxicity, it was hypothesized that combinational therapy with WA and an inhibitor of the proteasome would successfully synergize by eliminating the cytoprotective effect of homeostatic aberrant protein degradation and allowing the accumulation of these dysfunctional molecules. Indeed, inhibition of HSP70 or the proteasome in the presence of traditional N-terminal HSP90 inhibitors promotes a synergistic effect (Minnnaugh et al., 2004; Ma et al., 2014). In this work, we further define WA's role in modulating the HSP90 axis and evaluate its efficacy in combination with a proteasome inhibitor.

1.2.3 DNA-damage response modulation

Maintenance of genomic integrity is an essential process for cell homeostasis. While cancer cells are transformed to malignant status through interruption and manipulation of this integrity, excessive disruption of the genome may lead to lethality. The DNA damage response (DDR) promotes accurate transmission of genomes in dividing cells by reversing the extrinsic and intrinsic DNA damage and is required for cell survival during replication (Harper and

Elledge, 2007). Radiation and genotoxic drugs represent a large proportion of anti-cancer agents used in the clinic for years, but DNA damage repair mechanisms are often associated with chemo- and radio-resistance. These agents promote DNA single- and double-strand breaks (SSBs; DSBs) that induce cellular cytotoxicity when unrepaired. DSBs are regarded as the primary lesion of ionizing radiation and require repair through homologous recombination (HR), which maintains fidelity of the sequence at the break site, or non-homologous end-joining (NHEJ), which simply anneals two broken ends together (Figure 1-6) (Mladenov et al., 2013). The overall response to DNA damage is regarded as an immensely complex coordination of damage recognition and repair with simultaneous signal transduction to halt cell cycling during the repair (Figures 1-7A and 1-7B). If such efforts fail, cells enter a sustained period of senescence or simply die (Lamarche et al., 2010; Baskar et al., 2012).

To increase the efficacy of these DNA-damaging treatments and promote the failure of repair, inhibitors of the major components of the DDR such as ATM (ataxia telangiectasia mutated), ATR (ATM and Rad3-related), DNA-PKcs (DNA-dependent protein kinase, catalytic subunit), Chk1 (checkpoint protein 1), and Chk2 (checkpoint protein 2) among others have been used or have attracted interest in the drug development realm (Furgason and Bahassi, 2012). These inhibitors have demonstrated to sensitize cancer cells to the genotoxic standard therapies. Unfortunately, few of these therapeutic options have emerged in the treatment of brain tumors and limited compounds have been taken to clinical trials largely due to translational challenges including trial funding and poor drug pharmacokinetics.

Given the observation that numerous pathways are altered in response to WA, perhaps in part due to wide-scale oxidation or inhibition of the HSP90 axis, WA's mechanism would be expected to overlap with those involved in the response to other therapeutic agents. Disruption of

Figure 1-6.
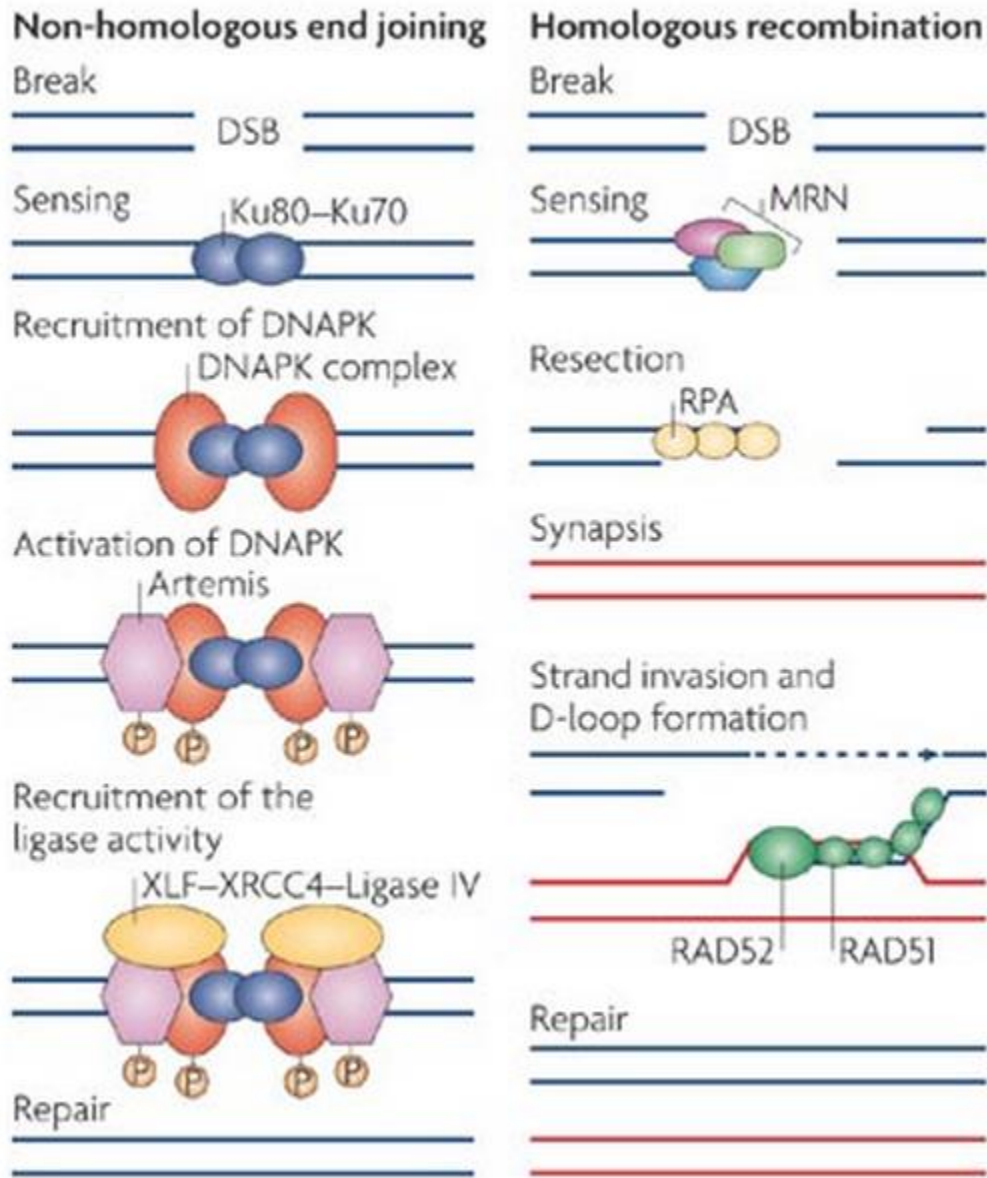
Figure 1-6. Double strand DNA breaks are repaired by either HR or NHEJ. In HR, lesions are detected by the MRN complex which subsequently recruits additional repair proteins that utilize the homologous templeate to copy and restore the original genetic code that was damaged. In NHEJ, lesions are identified by the Ku70/Ku80 heterodimer with a known role of the MRN complex as well which functions to recruit additional proteins to form the DNA-PK complex. This complex promotes the ligation of two broken ends independent of original DNA sequence and is therefore error-prone.

Reprinted by permission from Macmillan Publishers Ltd: Nature Reviews Molecular Cell Biology (http://www.nature.com/nrm/index.html). Misteli T and Soutoglou E. The emerging role of nuclear architecture in DNA repair and genome maintenance, 2009.

Figure 1-7.
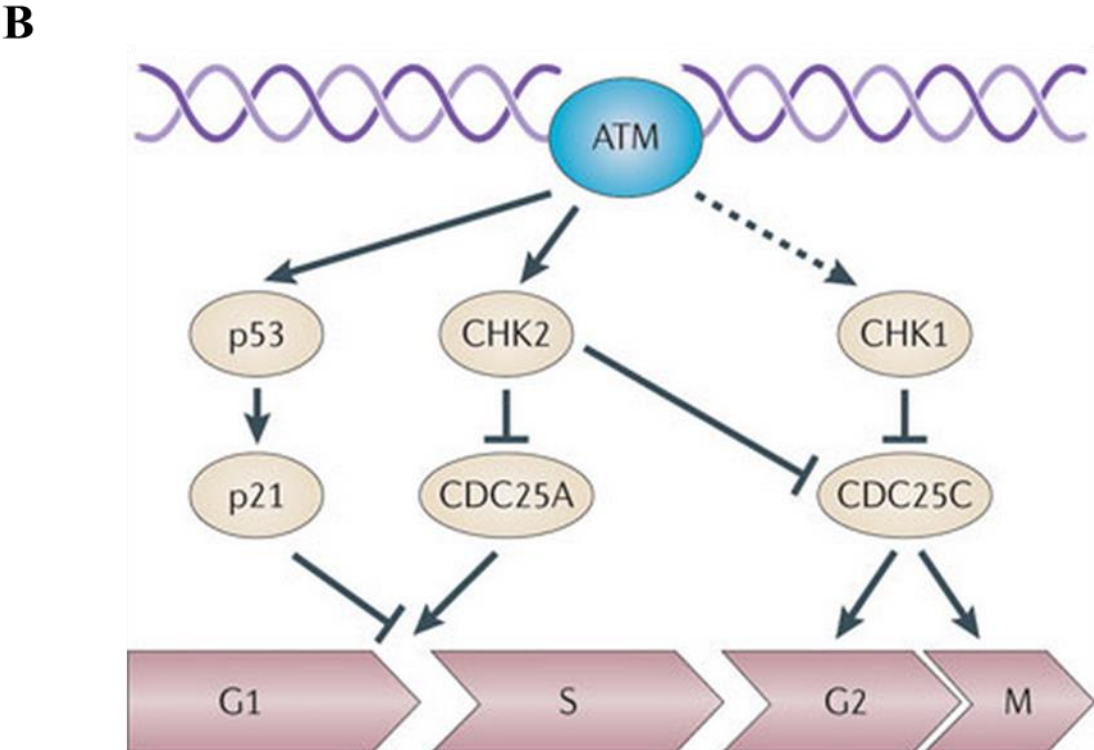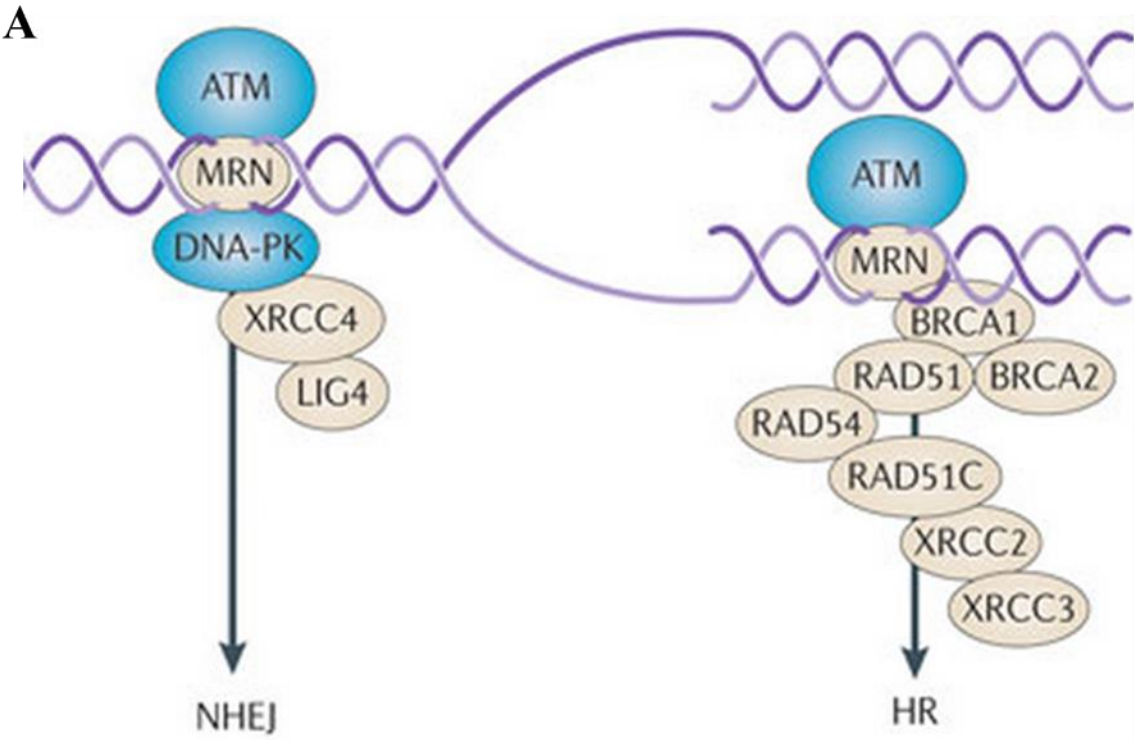
Figure 1-7. A) Simplified schematic of many of the proteins and interactions involved in HR and NHEJ repair responses to double strand DNA breaks induced by radiation or other cytotoxic therapies. Damage is identified by the MRN complex with subsequent recruitment of repair proteins, many of which demonstrate multiple functions. B) Simplified schematic demonstrating ATM phosphorylation-mediated signal transduction cascade in response to double strand DNA breaks. ATM phosphorylates p53, Chk1, and Chk2 in response to DNA damage which ultimately leads to checkpoint arrests of the cell cycle and ultimately cell death if the damage cannot be repaired. Transduction proteins such as p53 are frequently depleted or otherwise mutated in certain cancers.

Reprinted and adapted by permission from Macmillan Publishers Ltd: Nature Reviews Cancer (http://www.nature.com/nrc/index.html). Begg AC, et al. Strategies to improve radiotherapy with targeted drugs, 2011.

proteins important in the recognition and repair of DNA damage would be expected to sensitize glioma cells to the first-line standard therapy of TMZ and RT, both genotoxic agents. Indeed, direct inhibition of HSP90 to destabilize a number of client proteins has previously been shown to act as a radiosensitizer (Dote et al., 2006; Noguchi et al., 2006; Kabakov et al., 2010). Several preliminary studies have suggested that WA functions as a radiosensitizer in multiple cancer models. Utilizing a knockout model to alter the normal function of HR and NHEJ, one study reported that WA may inhibit NHEJ (Devi et al., 2008). Other studies have correlated combination of WA and radiation to enhanced cellular oxidation (Yang et al., 2011b; Yang et al., 2011a), however, the underlying mechanism producing WA-induced sensitization to DNA damage has not been identified. We hypothesized that WA would disrupt the normal DDR and have explored that in this work as a means of radiosensitization and also re-sensitization of GBM cells to TMZ through alterations in MGMT, a protein involved in the removal of TMZ-mediated DNA alkylation.

1.3 Specific Aims

The objective of this study was to evaluate the potential of WA either as a stand-alone chemotherapeutic in the treatment of chemo-sensitive and -resistant brain tumors including GBM and MB, or as an agent whose combination with current standard approaches could be synergized or potentiated. As a single agent therapy, the effects of WA were evaluated on several major proliferative pathways including the MAPK, PI3K/Akt/mTOR, and Wnt/β-catenin signaling pathways as well as its ability to generate intracellular stress through thiol reactivity and the creation of ROS. Further, given the induction of DNA DSBs in tumor cells treated with

TMZ or RT, interference with recognition and/or repair of this damage by the tumor cells indicated a potential broad mechanism through which WA could potentiate the cytotoxicity of DNA-damaging therapy. To this regard, proteins of the DNA damage response mechanism were evaluated in the context of WA treatment and functional manifestations of DNA damage recognition and repair were measured. Additionally, protein levels of repair mechanisms specific to TMZ including MGMT and mismatch repair were explored.

It was hypothesized that WA would act as a potent cytotoxic agent against brain tumors and potentiate the activity of several standard therapies through disruption of homeostatic cellular processes necessary in the response to those agents. The specific aims designed to explore the underlying mechanisms and validate this hypothesis are as follows:

1) Determination of the key anti-cancer mechanistic properties of WA in oncogenic signal transduction pathways in GBM and MB *in vitro.*

   a. Ability of WA to induce cell cycle arrest and apoptosis.

   b. Effects of WA on several major proliferative pathways including the MAPK, PI3K/Akt/mTOR, and Wnt/β-catenin signaling pathways.

   c. Ability of WA to generate intracellular stress through thiol reactivity and the production of ROS and the response of the cell to this stress.

2) Evaluation of the proteotoxic mechanism of WA and its therapeutic implications *in vitro*.

   a. The effects of WA on cellular oxidation and the underlying implications.

   b. WA-mediated modulation of the HSP90/HSP70 protein chaperone.

    c. Therapeutic implications of combination therapy with WA and proteasome inhibitors.

3) Exploration of the effects of WA on the DDR mechanism *in vitro*.

    a. Exploration of WA's effects on the DNA damage recognition and repair responses.

    b. Evaluation of the efficacy of WA in combination with radiation and TMZ.

    c. Determination the ability of WA to alter mechanisms of resistance to provide TMZ resensitization in resistant cell lines.

This research demonstrates several means by which the novel natural compound WA was studied in the context brain tumors to further understand its properties so as to better evaluate its potential as a new treatment for this disease. Completion of these studies, as outlined in the subsequent chapters, provides excellent evidence for the benefit of WA as a novel chemotherapeutic strategy for brain tumors, including GBM and MB with great translational potential both as a monotherapy and in combination with standard agent. Ultimately, the goal of this proposal was to promote progression of novel pharmaceutical development to improve brain tumor patient survival and quality of life.

1.4 Statement of Purpose

The purpose of the conducted research was to identify, define, and utilize the cytotoxic anti-cancer properties and clinical utility of the steroidal lactone WA in high-grade brain tumors

through its alterations of oncogenic cellular signaling pathways, protein homeostasis, and the DNA-damage response mechanism.

Briefly, the following chapters identify and describe key cellular changes in brain tumor cells following exposure to WA. In Chapter 2 (Specific aims 1a-1c), WA was screened as a potential cytotoxic agent against GBM brain tumor cells and was identified to exhibit anti-proliferative activity through induction of G2/M cell cycle arrest and ultimately apoptosis. These findings were associated with modulation of the Akt/mTOR and MAPK pathways and induction of thiol-mediated oxidation. In Chapter 3 (Specific aims 1a-1c and 3b-3c), TMZ-resistant GBM cells were shown to demonstrate enhanced responsiveness to WA as a monotherapy with a similar responsiveness to WA as sensitive cells. This study expanded on the inhibitory nature of the effect on the Akt/mTOR pathway but showed that alterations in the MAPK are a compensatory response to the compound. Additionally, WA pretreatment was shown to deplete MGMT and functionally re-sensitize these cells to TMZ. Chapter 4 (Specific aims 1a-1c) further demonstrates the cytotoxicity of WA in brain tumors with a model of MB. A comparable pattern of general efficacy was observed as in GBM. WA was demonstrated to inhibit Wnt/β-catenin signaling through proteasome-mediated degradation of the TCF/LEF transcription factors without significant alterations in the total levels nor localization of β-catenin. These findings were correlated with TCF/LEF depletion following HSP90 inhibition and WA-mediated alterations in HSP90 co-chaperone association. In Chapter 5 (Specific aims 2a-2c), mechanisms of action for the observed manifestations of WA treatment were explored. Specifically, WA induced reduction of many HSP90 client proteins and disrupted the interaction between HSP90 and Cdc37 as well as Cdc37-dependent proteins without directly inhibiting intrinsic HSP90 activity. Additionally, WA induced an NAC-repressible oxidation that was enhanced with

glutathione depletion. Overall, WA produced protein degradation through the proteasome and cytotoxicity that could be enhanced through the build-up of aberrant proteins with pretreatment of a proteasome inhibitor. Finally, Chapter 6 (Specific aims 3a-3b) demonstrates the radiosensitizing properties of WA through disruption of the DDR mechanisms and enhanced arrest of the cell cycle. WA depleted proteins involved in DNA damage recognition, signaling, and ultimately repair through HR and NHEJ. This was functionally associated with altered phosphorylation of H2A.X and enhanced DSB with combination of WA and RT.

Chapter 2

Cytotoxicity of withaferin A in glioblastomas involves induction of an oxidative stress-mediated heat shock response while altering Akt/mTOR and MAPK signaling pathways

2.1 Abstract

Withaferin A (WA), a steroidal lactone derived from the plant *Vassobia breviflora*, has been reported to have anti-proliferative, pro-apoptotic, and anti-angiogenic properties against cancer growth. In this study, we identified several key underlying mechanisms of anticancer action of WA in glioblastoma cells. WA was found to inhibit proliferation by inducing a dose-dependent G2/M cell cycle arrest and promoting cell death through both intrinsic and extrinsic apoptotic pathways. This was accompanied by an inhibitory shift in the Akt/mTOR signaling pathway which included diminished expression and/or phosphorylation of Akt, mTOR, p70 S6K, and p85 S6K with increased activation of AMPKα and the tumor suppressor tuberin/TSC2. Alterations in proteins of the MAPK pathway and cell surface receptors like EGFR, Her2/ErbB2, and c-Met were also observed. WA induced an N-acetyl-L-cysteine-repressible enhancement in cellular oxidative potential/stress with subsequent induction of a heat shock stress response primarily through HSP70, HSP32, and HSP27 upregulation and HSF1 downregulation. Taken together, we suggest that WA may represent a promising chemotherapeutic candidate in glioblastoma therapy warranting further translational evaluation.

2.2 Introduction

Malignant gliomas, including the grade IV astrocytoma glioblastoma multiforme (GBM), accounting for 60-70% of such lesions, are the most common adult primary malignant brain tumors, representing approximately 14,000 new cancer cases yearly (Wen and Kesari, 2008). The mean post-diagnosis survival time of patients with GBM is approximately 14 months (Wen and Kesari, 2008; Stupp et al., 2009). Most high grade brain tumors are quite infiltrative, resulting in residual invasive tumor cells even after optimal surgical resection. This significantly contributes to the high rate of recurrence and poor clinical outcomes associated with this disease (Giese et al., 2003). Standard-of-care management typically involves surgical debulking followed by treatment with radiation and the methylating agent temozolomide. While this currently represents the most efficacious therapy for prolonging survival, tumors are often quick to develop resistance to this line of therapy (Chamberlain, 2010; Quick et al., 2010). Recent investigational therapies have yielded only modest response rates up to 15% at best without impact on 6-month progression-free survival (Wen and Kesari, 2008; Quick et al., 2010).

Therefore, given a lack of current therapeutic strategies to extend survival in glioma patients, there is a critical need for novel therapeutic agents. We previously screened over 200 natural plant extracts with promising anti-tumor potential and identified a 28-carbon steroidal lactone obtained from the *Vassobia breviflora*, withaferin A (WA), with intriguing cytotoxic properties (Samadi et al., 2010b). WA has been identified as a novel cancer therapy with anti-proliferative, pro-apoptotic, and anti-angiogenic properties as well as a modulator of several key cell-survival and regulatory pathways including those involving Akt, Notch-1, heat shock protein

37

(HSP) 90, NFkappaB, AP-1, estrogen receptor, RET, and p38 among others (Mohan et al., 2004; Singh et al., 2007; Mandal et al., 2008; Oh et al., 2008; Stan et al., 2008; Oh and Kwon, 2009; Shah et al., 2009; Koduru et al., 2010; Samadi et al., 2010a; Yu et al., 2010). Additionally, WA has shown promising anti-tumor activity in several murine xenograft and/or orthograft models including prostate, breast, medullary thyroid, melanoma, uveal melanoma, ovarian, cervical, and brain cancers (Vyas and Singh, 2014).

We have recently demonstrated the anti-proliferative effects of WA in malignant glioma (Grogan et al., 2010; Grogan et al., 2011), and this finding was subsequently confirmed demonstrating the thiol-reactivity of WA and its ability to induce a heat shock response via a reporter assay (Santagata et al., 2012). Several additional reports have identified the pro-oxidant potential of WA (Malik et al., 2007; Widodo et al., 2010; Hahm et al., 2011; Mayola et al., 2011), however, the mechanism of WA's diverse and widespread effects, especially in glioma cells, is largely unknown. Here, we expand on previous findings to further delineate the nature of WA's anti-cancer effects in glioblastoma and examine the molecular response by the cell.

2.3 Materials and methods

2.3.1 Cell culture and general reagents

Two human glioblastoma multiforme cell lines, U87 and U251, were generously provided by Dr. Jann Sarkaria (Mayo Clinic, Rochester, MN), and one murine GBM cell line, GL26, was graciously donated by Dr. John Ohlfest (University of Minnesota, Minneapolis, MN). All cell lines were grown in Dulbecco's modified Eagle's media (DMEM #6429; Sigma-Aldrich,

St. Louis, MO) supplemented with 10% fetal bovine serum (FBS; Sigma-Aldrich, St. Louis, MO) and 1% penicillin/streptomycin (Sigma-Aldrich, St. Louis, MO) at a 37 °C humidified atmosphere of 5% CO_2 in air. WA was extracted and isolated as previously described with a purity of 99% by HPLC and stored as a stock solution, adjusted for impurities, at 20 mM in DMSO at -80 °C (Samadi et al., 2010b). Propidium iodide (PI), RNase, and N-acetyl-L-cysteine (NAC) were acquired from Sigma-Aldrich (St. Louis, MO), and Annexin V-FITC was obtained from BD Biosciences (San Diego, CA).

2.3.2 Cell proliferation and viability assays

Cells were seeded in 96-well plates at 2,500 cells/well. Following a 6 h incubation period, WA-containing media in various concentrations was added to each well, and the cells were incubated for an additional 72 h. The number of viable cells was quantified by the colorometric CellTiter96 Aqueous MTS assay (Promega, Fitchburg, WI) at 490 nm on a BioTek Synergy 2 plate reader (BioTek, Winooski, VT) as per the manufacturer's instructions.

Because of the non-enzymatic, auto-reductive potential of NAC, the MTS assay was unable to be utilized for evaluating WA/NAC co-treatment studies given the nature of the assay mechanism, as described by the manufacturer. As such, the CellTiter-Glo luminescent assay (Promega, Fitchburg, WI) was utilized instead to measure cell viability by ATP levels. Cells were plated in 96-well plates followed by treatment with NAC after 6 h and WA 1 h later. After 72 h, assay reagent was prepared as per the instructions, and 50 uL was added to each well. The luminescent signal was given 10-20 minutes to equilibrate and quantified by the BioTek Synergy 2 plate reader.

2.3.3 Cell cycle analysis

Cells were plated at an amount previously determined, based on the growth characteristics of individual cells, to have a high enough yield without achieving complete confluency upon harvest and were allowed to grow overnight. Cells were treated with appropriate concentrations of WA and, where indicated, pre-treated with 5 mM NAC. Upon the completion of treatment, cells were trypsinized, collected, resuspended in 0.43 mL of 4 °C 1x PBS followed by 1mL of -20 °C ethanol for a 70% ethanol fixative solution, and stored at -20 °C. To analyze, stored cells were collected by centrifugation, resuspended in 1x PBS containing 40 µg/mL PI and 100 µg/mL RNase, and incubated at -37 °C for 30 minutes before being analyzed by flow cytometry (BD LSRII; Becton Dickinson, San Diego, CA). Analysis of these results examined only viable cells without DNA fragmentation to establish the distribution of the true cell cycle in living cells.

2.3.4 Analysis of cell death

Staining phosphatidylserine on the outer leaflet of the cell membranes on apoptotic cells and DNA staining by PI in necrotic and late apoptotic cells was performed to assess WA-induced cell death. Cells were plated and treated as indicated for cell cycle analysis. Upon the completion of treatment, cells were trypsinized, collected, and washed once in Annexin binding buffer (150 mM NaCl, 5 mM KCl,1 mM $MgCl_2.6H_2O$, 1.8 mM $CaCl_2.2H_2O$, 10 mM HEPES, and 2% (v/v) FBS). Cells were stained with Annexin V-FITC and PI according to the manufacturer's

instructions (BD Biosciences, San Diego, CA) for 20 minutes at 4 °C before being washed twice and resuspended in binding buffer. Cells were immediately analyzed by flow cytometry on a BD LSRII.

2.3.5 Western blotting

Cells were plated and treated in the manner outlined for cell cycle analysis. Proteins were collected, quantified, separated by sodium dodecyl sulfate–polyacrylamide gel electrophoresis (SDS–PAGE), and electrotransfered onto a Hybond nitrocellulose membrane as previously described in Samadi, et al. (Samadi et al., 2011). Actin levels were assessed to ensure equal loading and transfer of proteins. All studies were repeated for accuracy.

Primary rabbit antibodies against poly(ADP-ribose) polymerase (PARP; #9542; 1:1000), caspase 3 (#9665; 1:1000), caspase 7 (#9492; 1:1000), caspase 9 (#9502; 1:1000), cyclin B_1 (#4138; 1:2000), p-ERK1/2 (Thr202/Tyr204; #4377; 1:1000), Akt (#9272; 1:1000), p-Akt (Ser473; #4058; 1:1000), c-Met (#4560; 1:500), p-c-Met (Tyr1234/1235; #3077; 1:500), epidermal growth factor receptor (EGFR; #4267; 1:1000), p70 S6 kinase (#2708; 1:500), p-p70 S6 kinase (Thr389; #9234; 1:1000), mTOR (#2972; 1:1000), p-mTOR (Ser2448; #2971; 1:1000), Her2/ErbB2 (#2165; 1:1000), 4E-BP1 (#9644; 1:1000); p-4E-BP1 (Thr37/46; #2855; 1:1000), tuberin/TSC2 (#4308; 1:1000), p-tuberin/TSC2 (Thr1462; #3617; 1:1000), AMPKα (#2603; 1:1000), and p-AMPKα (Thr172; #2535; 1:1000) and primary mouse antibodies against HSP27 (#2402; 1:2000), caspase 8 (#9746; 1:1000), and p-EGFR (Tyr1068; #2236; 1:1000) were acquired from Cell Signaling Technology (Beverly, MA). Total- and phospho-antibodies against p70 S6 kinase were used to detect p85 S6 kinase (phospho-Thr412) given the known cross-

reactivity of the antibodies. Rabbit antibodies against HSP90 (SPA-836; 1:1000), HSP32/heme oxygenase 1 (SPA-894; 1:1000), and heat shock factor 1 (HSF1; ADI-SPA-901; 1:1000) were acquired from Enzo Life Sciences (Farmingdale, NY) or its affiliates along with the rat antibody for Grp94 (SPA-850; 1:1000) and the mouse antibody for HSP70 (ADI-SPA-810; 1:1000). The mouse antibody Trap1 (MA1-010; 1:1000) was purchased from Affinity Bioreagents (Pierce Biotechnology, Rockford, IL). A mouse total actin antibody (MAB1501; 1:50,000) to be used as a control was acquired from EMD Millipore (Billerica, MA). A mouse antibody against Raf-1 (sc-7267; 1:250), a goat antibody against p-Raf-1 (Ser338; sc-12358; 1:250), and a rabbit antibody against ERK1/2 (sc-154; 1:5000) were obtained from Santa Cruz Biotechnology (Santa Cruz, CA). Donkey anti-rabbit IgG HRP (sc-2313; 1:5000), goat anti-mouse IgG HRP (sc-2005; 1:5000), and goat anti-rat IgG HRP (sc-2032; 1:5000) secondary antibodies were also purchased from Santa Cruz Biotechnology. Given primary antibody species specificity, Western analysis was completed in the human U87 and U251 cells lines.

2.3.6 Detection of ROS

The accumulation of intracellular ROS, particularly peroxides like H_2O_2, was determined using CM-H_2DCFDA (Molecular Probes, Grand Island, NY), a general oxidative stress indicator that fluoresces upon oxidation. Cells were preloaded with 20 μM CM-H_2DCFDA in 1x dPBS at 37 °C for 1 h, washed once with phenol red-free DMEM containing 10% FBS and 1% penicillin/streptomycin, and plated in 96-well plates in phenol red-free media at 40,000 cells/well for GL26 and 20,000 cells/well for U87. After 30 minutes, cells were treated with WA, NAC, or

both. Measurements were taken on a BioTek Synergy 2 plate reader at 4 h with excitation and emission filters of 485 nm and 528 nm, respectively.

Detection of mitochondrial superoxide present at a given timepoint was examined by MitoSOX Red (Molecular Probes, Grand Island, NY), an indicator reagent that fluoresces upon oxidation by superoxide radicals. Cells were plated and allowed to attach and grow overnight. Pre-treatment with 5mM NAC occurred 1 h before treatment with 5 μM WA. Cells were harvested 4 h after WA addition, washed once with 1x dPBS, and stained with 5 μM MitoSOX Red in 1x dPBS for 30 minutes at 37 °C. Cells were washed twice with 1x dPBS and run on a BD LSRII flow cytometer (Becton Dickinson, San Diego, CA) with excitation and emission filters of 488 nm and 580 nm, respectively, to assess mean fluorescence intensity.

2.3.7 Statistical analysis

GraphPad (GraphPad Inc., San Diego, CA) was used to generate best-fit sigmoidal dose response curves for IC_{50} determination. Comparisons of differences between two or more means were determined by Student's unpaired t-test (2 means) via a standard statistical analysis software package (SPSS version 17.0; SPSS Inc, Chicago, IL). The level of significance was set at $p < 0.05$. Data are presented as mean values with error bars denoting standard deviation. All studies were minimally performed in triplicate unless otherwise noted.

2.4 Results

2.4.1 Withaferin A reduces cell proliferation and viability in GBM cells

To investigate the general biological effect of WA in GBM cells, three cell lines (U87, U251, and GL26) were incubated with increasing concentrations of WA or a DMSO control for 72 h. Cell number and viability were subsequently determined by using the MTS assay (Figure 2-1). WA dose escalation reduced cell proliferation and viability. By GraphPad analysis, the IC_{50} values of WA were determined to be 1.07 ± 0.071 μM, 0.69 ± 0.041 μM, and 0.23 ± 0.015 μM for U87, U251, and GL26 cells, respectively.

2.4.2 Withaferin A induces G2/M cell cycle arrest in GBM cells in a dose-dependent manner

In order to establish the nature of the anti-proliferative response to WA, distribution of the cell cycle phases of glioblastoma cells was assessed by flow cytometry at 24 h. WA induced a dose-dependent shift in cell cycle arrest from the G0/G1 checkpoint to G2/M arrest. Maximal shift to G2/M arrest above baseline was observed at 0.75 μM in U87 cells (12.0% G2/M in controls increasing to 63.4% with treatment), 1.5 μM in U251 cells (19.1% baseline to 49.7% with treatment), and 0.5 μM in GL26 cells (21.7% baseline to 58.7% with treatment (Figure 2-2A). Doses above these optimal levels showed a somewhat diminished G2/M cell cycle shift. The shift to G2/M cell cycle arrest is accompanied by a depletion of cells in the G0/G1 phase and a relative increase in S phase as observed in the U87 (11%) and GL26 (14%), whereas the S phase proportion in U251 cells was largely unchanged (Figure 2-2A).

To confirm these findings, the G2/M-specific protein cyclin B_1, which is elevated during G2/M cell cycle arrest, was evaluated by Western blot analysis for increases in expression with

Figure 2-1.
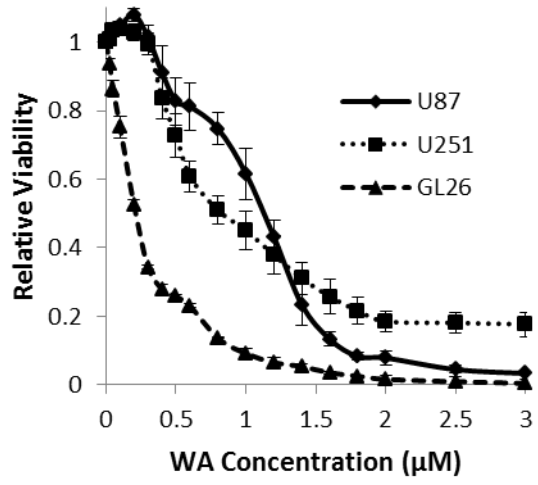
Figure 2-1. U87, U251, and GL26 cells were incubated with increasing concentrations of WA or a DMSO control for 72 h and then assessed by MTS assay. WA dose escalation reduced cell proliferation and viability with IC_{50} values of 1.07 ± 0.071 µM, 0.69 ± 0.041 µM, and 0.23 ± 0.015 µM for U87, U251, and GL26 cells, respectively.

Figure 2-2.
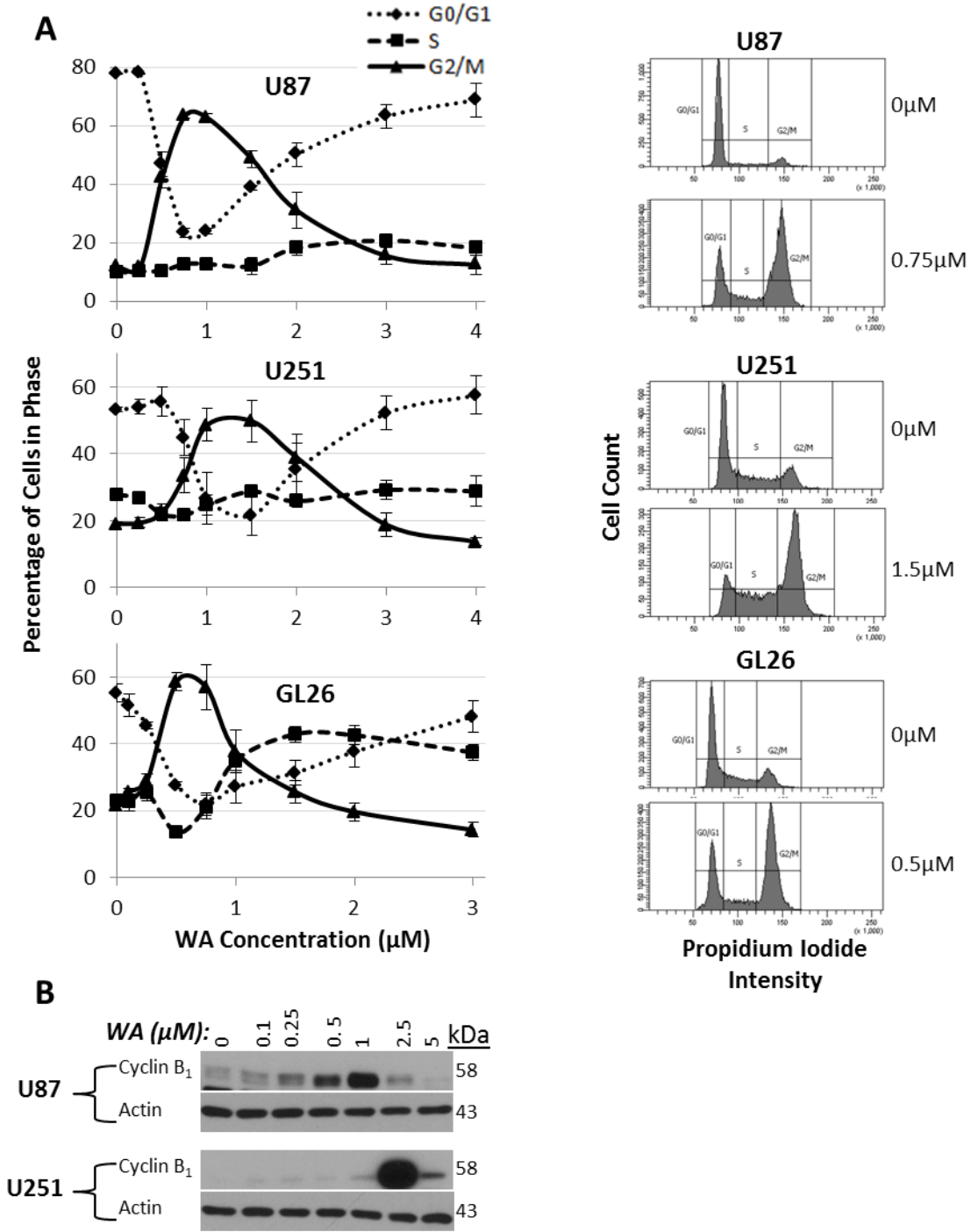
Figure 2-2. A) Cells stained with propidium iodide and analyzed by flow cytometry revealed that WA induces a dose-dependent G2/M cell cycle arrest with an optimal range of such a response at 24 h. Maximal induction of arrest above baseline was observed at 0.75 µM, 1.5 µM, and 0.5 µM for U87, U251, and GL26 cells, respectively. Adjacent histograms display representative examples of these peak values in each cell line. B) G2/M arrest was confirmed by Western blotting for cyclin B_1. At 24 h, U87 and U251 cells demonstrated dose-dependent induction of cyclin B_1 with highest levels at 1 µM and 2.5 µM, respectively.

WA treatment. At 24 h, both U87 and U251 cells demonstrated a dose-dependent induction of cyclin B_1 expression with maximal expression levels observed at 1 μM and 2.5 μM WA, respectively (Figure 2-2B). Flow cytometry identified sustained G2/M cell cycle arrest at both 48 h and 72 h with Western analysis up to 48 h supporting those findings (data not shown).

2.4.3 Withaferin A induces GBM cell death

To further characterize the anti-proliferative effects of WA, annexin V and propidium iodide (PI) dual staining on flow cytometry was used to evaluate the ability of WA to induce cell death through apoptotic and necrotic mechanisms. Figure 2-3A illustrates that increases in WA concentration corresponded with enhanced cell death in U87, U251, and GL26 cells at 24h. While all cell lines demonstrated evidence of an apoptotic response indicated by annexin V staining, U87 cells appear to also exhibit increased levels of necrosis with treatment as indicated by staining with PI only. From baseline measurements of 3.9-5.9%, total cell death at 3 μM WA treatment was 51.4% for U87 cells (9.0% early apoptosis; 18.4% late apoptosis; 24.0% necrosis), 24.4% for U251 cells (12.0% early apoptosis; 9.9% late apoptosis; 2.5% necrosis), and 31.7% for GL26 cells (4.4% early apoptosis; 22.2% late apoptosis; 5.1% necrosis). Upon doubling the concentration to 6 μM, total cell death increased to 86.9% for U87 cells (3.4% early apoptosis; 55.5% late apoptosis; 28.0% necrosis), 47.1% for U251 cells (9.7% early apoptosis; 32.5% late apoptosis; 4.9% necrosis), and 83.1% for GL26 cells (0.6% early apoptosis; 74.1% late apoptosis; 8.4% necrosis). Further induction of apoptosis was observed at 48 h (data not shown).

In order to confirm that these cells were undergoing an apoptotic response, protein levels of mitochondrial/intrinsic procaspase 9, extrinsic procaspase 8, effector procaspases 3 and 7, and

Figure 2-3.
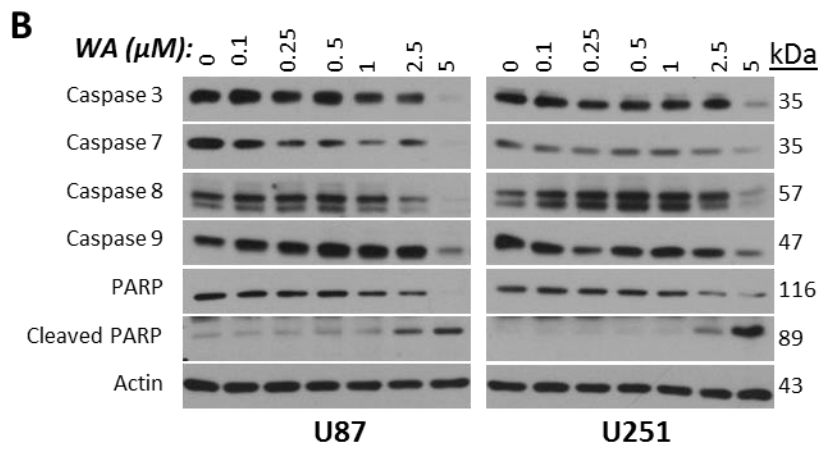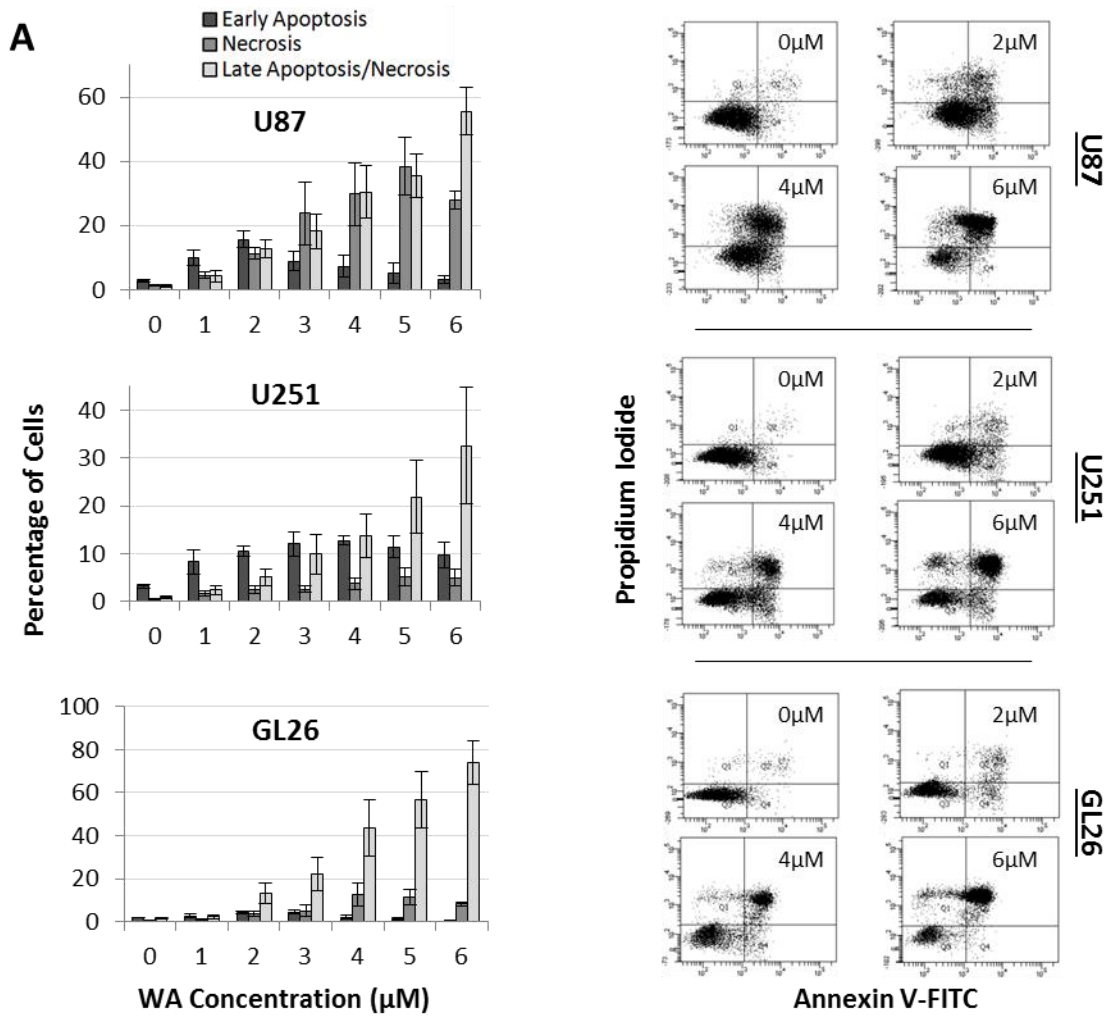
Figure 2-3. A) Cells stained with propidium iodide and annexin V-FITC and analyzed by flow cytometry revealed that increasing WA concentrations correspond with enhanced cell death in U87, U251, and GL26 cells at 24 h. Adjacent dot plots display representative examples of each cell line. B) Induction of apoptosis was confirmed by Western blotting in U87 and U251 cell lines. WA treatment resulted in reduction in the levels of uncleaved initiator caspases 8 and 9 as well as effector caspases 3 and 7. Further, PARP cleavage was observed at 2.5 and 5 µM in both lines.

downstream PARP cleavage were examined by Western blotting (Figure 2-3B). With increasing concentrations of WA, a reduction in the levels of all uncleaved caspases was observed at 5 μM in both U87 and U251 cells at 24 h. Procaspases 3, 7, and 8 demonstrated reduced levels at WA concentrations below 5 μM in U87 cells. Finally, PARP cleavage was observed at both 2.5 and 5 μM WA in both U87 and U251 cell lines. These data confirm that WA-mediated cytotoxicity at concentrations above IC_{50} is in part due to induction of apoptosis in these GBM cells.

2.4.4 Withaferin A alters normal protein expression and activation in the Akt/mTOR and MAPK pathways

Given the inhibition of proliferation and induction of cell death observed with WA treatment, several proteins associated with the Akt/mTOR and mitogen-activated protein kinase (MAPK) growth, proliferation, and survival pathways as well as key surface membrane proteins that signal to each pathway, known to be important in glioma and other cancers (Wen and Kesari, 2008), were screened in U87 and U251 cells for total expression and activation via phosphorylation status at 24 h post-treatment (Figure 2-4). Total levels of Akt and mTOR were reduced with increasing concentrations of WA. Akt and mTOR phosphorylation were dose-dependently diminished in U87 cells, but only p-mTOR was decreased in U251 cells. Total levels of p70 S6K (downstream of mTOR) and its nuclear isoform p85 S6K were largely unchanged in both cell lines with enhanced downregulation only observed in p85 S6K at 5 μM WA in U87 cells. Low-dose WA induced phosphorylation of both proteins, but this was reduced and/or further depleted upon achieving levels of 0.5 μM WA and above. Expression of total levels of the translation-repressor 4E-BP1 (also downstream of mTOR) was markedly

Figure 2-4.
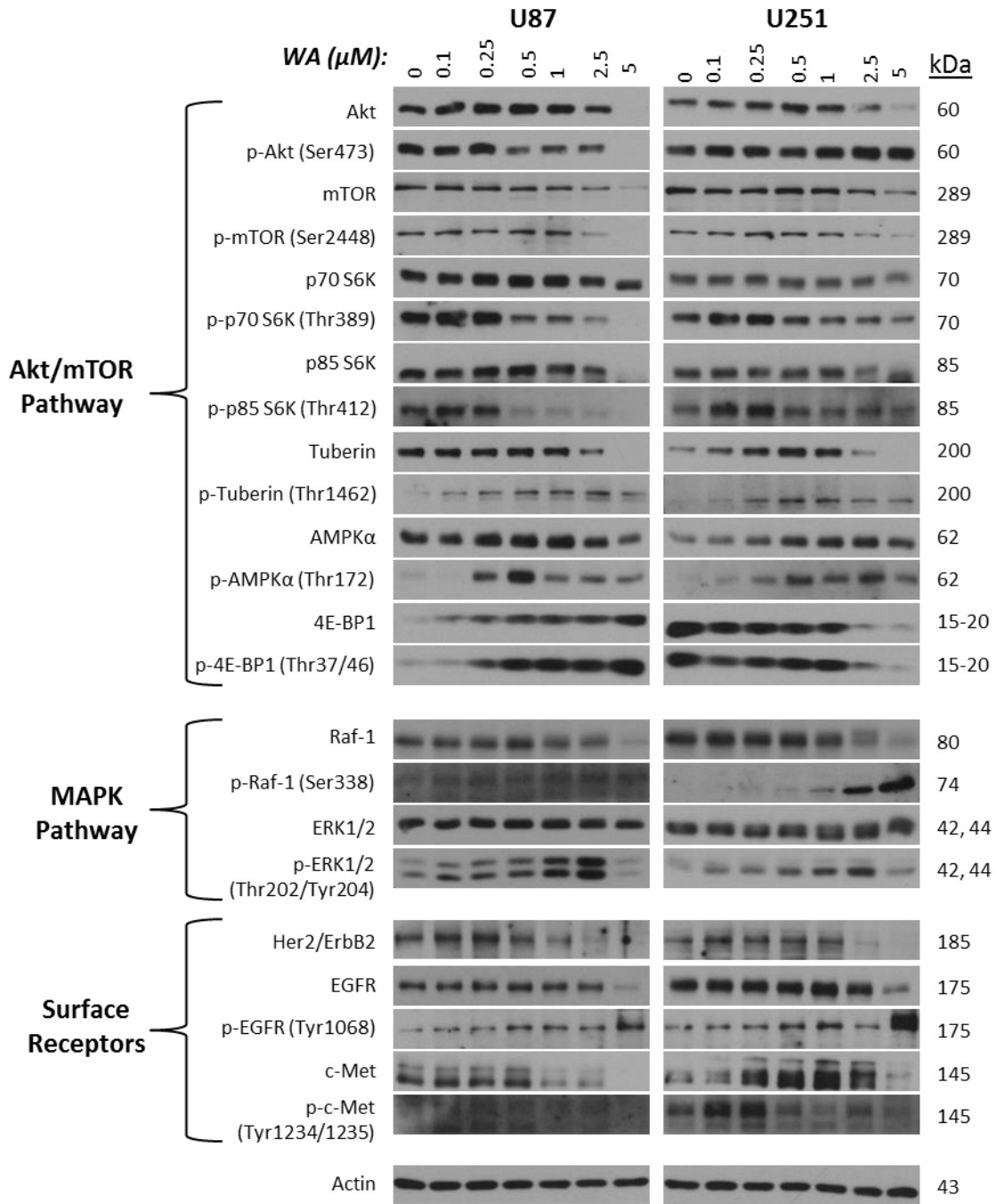
Figure 2-4. Following WA treatment, an array of proteins associated with the Akt/mTOR and MAPK growth, proliferation, and survival pathways as well as surface membrane proteins that signal to each pathway were screened via Western blotting in U87 and U251 cells for total expression and activation via phosphorylation status at 24 h post-exposure in order to help evaluate the molecular changes corresponding with cellular observations. Alterations in expression are observed in both pathways and with the cell surface receptors.

increased in U87 cells with elevated levels of inhibitory phosphorylation upon increasing WA concentration. In contrast, U251 cells exhibited decreased levels of both total and phosphorylated forms of 4E-BP1 with WA treatment suggesting an overall inhibitory alteration to the Akt/mTOR signaling pathway. Negative regulator of the pathway, AMPKα, was sustained or upregulated in total levels at all WA concentrations tested with the exception of 5 µM in U87 cells. Another negative regulator, the tumor suppressor tuberin/TSC2, was sustained in U87 cells and upregulated in U251 cells up to 1 µM WA before diminishing at increased concentrations. However, activation of both tuberin/TSC2 and AMPKα via phosphorylation was observed at WA levels as low as 0.1-0.25 µM and maintained at higher doses. Peak levels were observed between 0.5-2.5 µM in a cell-dependent manner.

Next, the effect of WA on the MAPK cascade was assessed since others have previously implicated WA as an inducer of a MAPK-mediated stress response (Mandal et al., 2008; Samadi et al., 2010b). In the U87 and U251 cells, total levels of ERK1/2 were unchanged with WA treatment over 24 h, but p-ERK1/2 levels were elevated with increasing concentrations of WA up to 2.5 µM and then diminished at 5 µM (Figure 2-4). In contrast to U87 cells, which express both p-ERK1 and p-ERK2 at comparable levels with treatment, p-ERK2 predominates expression with WA treatment of U251 cells. Additionally, total levels of upstream Raf-1 were diminished at 2.5-5 µM WA but activation of this protein by phosphorylation of serine 338 was observed in a dose-dependent manner with increasing WA concentrations.

EGFR, Her2/ErbB2, and c-Met are commonly amplified and/or mutated surface proteins in glioblastoma and signal both the MAPK and Akt/mTOR pathways. As such attempts have, previous attempts have been made to therapeutically target these proteins (Wullich et al., 1993; Potti et al., 2004; Puputti et al., 2006; Guessous et al., 2010; Berezowska and Schlegel, 2011). In

both GBM cell lines, total levels of EGFR, Her2/ErbB2, and c-Met were decreased at 24h with increasing WA levels with the exception of c-Met upregulation from 0.25-2.5 µM WA (Figure 2-4). Phosphorylation of EGFR increased with WA treatment, whereas c-Met phosphorylation was slightly elevated over controls at low WA doses but was downregulated at higher WA concentrations.

2.4.5 Withaferin A elevates pro-oxidant potential in GBM cells and induces a cellular oxidative stress response

WA-induced apoptosis in several cancer types was recently described as being mediated by ROS generation (Malik et al., 2007; Widodo et al., 2010; Hahm et al., 2011; Mayola et al., 2011). Given the role ROS are known to play in a variety of cancer chemotherapeutic agents (Antosiewicz et al., 2008; Wondrak, 2009; Tew and Townsend, 2011), we examined whether the oxidation status of glioblastoma cells was altered by WA. The production of peroxide-type radicals with CM-H$_2$DCFDA and mitochondrial accumulation of superoxide radicals with MitoSOX Red was measured in U87 and GL26 cells at 4 h post-WA exposure. GL26 and U87 cell lines demonstrated elevated oxidation status in response to increasing concentrations of WA. Peroxides rose 29.4% in GL26 cells ($p = 0.01$) and 90.5% in U87 cells ($p = 0.003$) compared to controls (Figure 2-5A) while mitochondrial superoxide increased 10.9% ($p = 0.002$) and 10.8% ($p = 0.03$) above control at 5 µM, respectively (Figure 2-5B). In order to determine the nature of this response, cells were simultaneously incubated with 5 mM of the thiol antioxidant NAC, described as both a redox buffer and ROS scavenger (Deneke, 2000; Mayola et al., 2011). NAC significantly reduced peroxide generation in WA-treated cells and returned levels to near-

Figure 2-5.
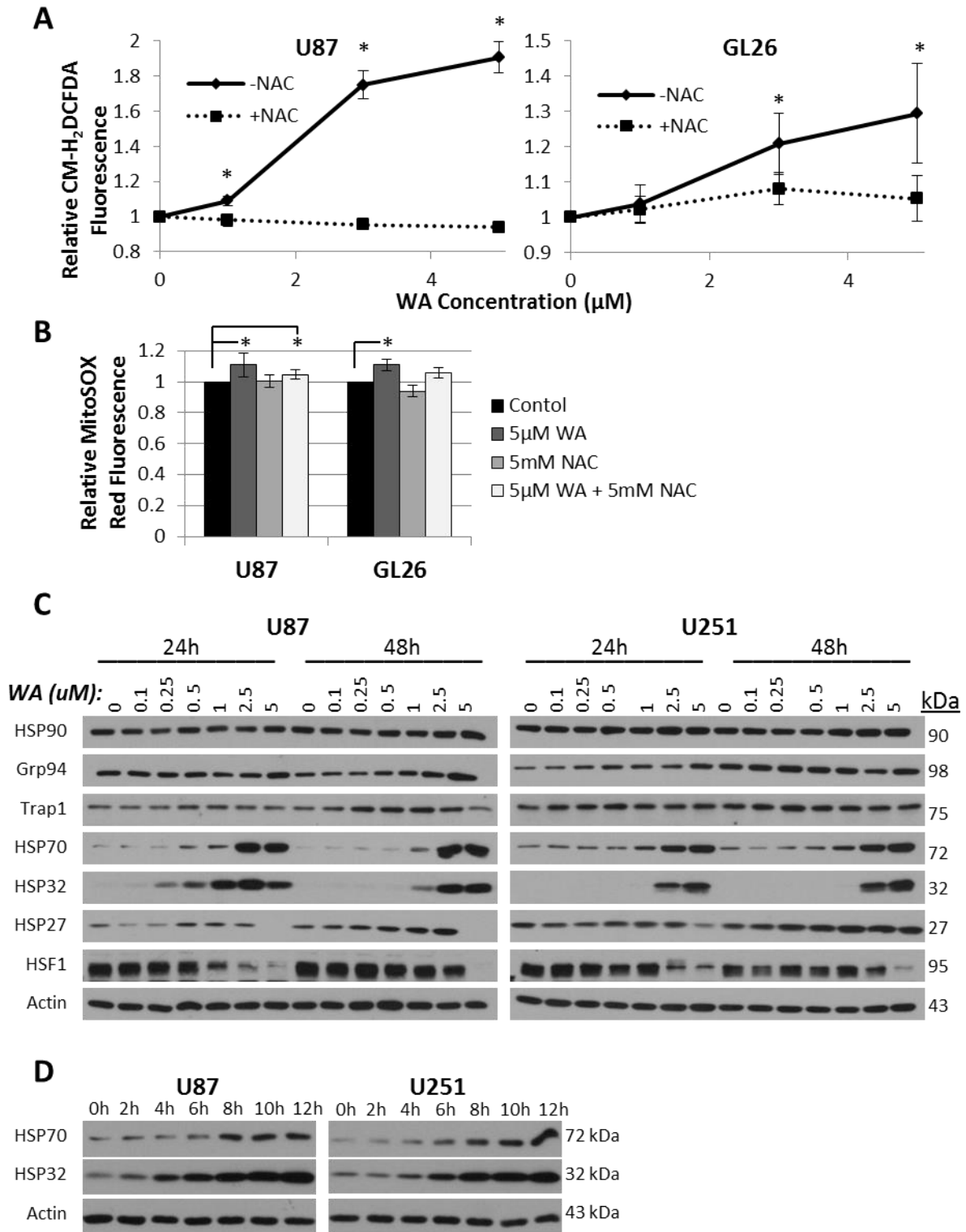
Figure 2-5. A) Generation of peroxide-type radicals like H_2O_2 following exposure to increasing concentrations of WA were quantified with CM-H_2DCFDA staining in U87 and GL26 cells at 4 h. B) Mitochondrial accumulation of superoxide radicals was assessed by flow cytometry with MitoSOX Red staining in U87 and GL26 cells at 4 h post-exposure to 5μM WA. Elevated oxidation status observed in (A) and (B) was reduced or completely eliminated by concurrent treatment with the thiol antioxidant N-acetyl-L-cysteine (5 mM). C) An array of proteins associated with the heat shock stress response were screened via Western blotting in U87 and U251 cells 24 h and 48 h post-treatment of WA. Upregulation was consistently observed with HSP70 and HSP32 in a dose- and time-dependent manner (C and D) with alterations in other proteins displaying a cell-specific response. Expression of the transcription factor HSF1 was decreased across both cell lines. *$p < 0.05$

baseline in both GL26 cells (p = 0.006) and U87 cells (p = 0.001). NAC reduced levels of mitochondrial superoxide radicals but failed to do so within statistical significance, and levels remained significantly elevated in U87 cells, despite being reduced compared to WA alone.

Induction of a heat shock response was also recently described in cells via a luminescence reporter assay following WA exposure (Santagata et al., 2012). Consistent with other models of oxidative stress (Ansari et al., 2011; Qiao et al., 2012), we observed that WA modulates heat shock protein expression levels at both 24 h and 48 h in U87 and U251 cells (Figure 2-5C). While total levels of HSP90 and its isoforms Trap1 and GRP94 were not consistently or significantly altered with changing WA concentration, HSP70 and HSP32 (heme oxygenase 1) were markedly upregulated while HSF-1 was potently downregulated with increasing WA concentration in both a dose-dependent and time-dependent manner (Figures 2-5C and 2-5D). Dose-dependent reduction of HSF1 corresponded with an increase in the higher molecular weight phosphorylated fraction of the total protein remaining. Moderate induction of HSP27 was observed predominantly at 48 h with cell line-dependent diminished expression at 5 µM, the highest concentration examined.

2.4.6 Pre-treatment with a thiol-antioxidant protects GBM cells from the anti-proliferative and cytotoxic effects of withaferin A

To determine if the elevated oxidation state induced by WA is responsible for the apoptotic and anti-proliferative effects observed in vitro, proliferation and apoptosis in the GBM cells were examined in the context of co-treatment with NAC. Consistent with the MTS assay data previously generated, WA was shown to diminish cell viability in a dose dependent manner

with the highest potency being demonstrated in GL26 cells. Pre-treatment with 0.5, 1, and 5 mM NAC enhanced the resulting cell viability, abrogating the anti-proliferative effects of WA such that with 5 mM NAC pretreatment, the anti-proliferative effects of WA were completely eliminated at up to 6 µM doses in the U87, U251, and GL26 cell lines (Figure 2-6A).

Next, the effects of WA on both cell cycle arrest and apoptosis were evaluated by flow cytometry in the context of NAC pretreatment. As previously described, flow cytometry with WA was performed following 1 h pre-treatment with NAC in U87, U251, and GL26 cells. Analysis of the cell cycle data revealed that NAC pretreatment was able to completely prevent cell cycle shift to G2/M arrest following 1 µM WA treatment at 24 h (Figure 2-6B). This was supported by a lack of dose-dependent increases in expression of cyclin B_1 by Western analysis at 24 h when NAC was used in combination with WA (Figure 2-6D). Furthermore, dual staining with PI and Annexin V revealed that NAC pre-treatment completely eliminated all dose-dependent apoptosis and necrosis associated with WA treatment (Figure 2-6C). This observation was then confirmed by a lack of PARP cleavage associated with increasing WA concentration when cells were pre-treated with NAC (Figure 2-6D).

Finally, WA-mediated effects on heat shock response were evaluated following pretreatment with 5 mM NAC. As shown in Figure 2-6D, NAC pre-treatment effectively prevented induction of HSP70 and HSP32 at 24 h post-exposure while limiting depletion of HSF1 following WA treatment.

Figure 2-6.
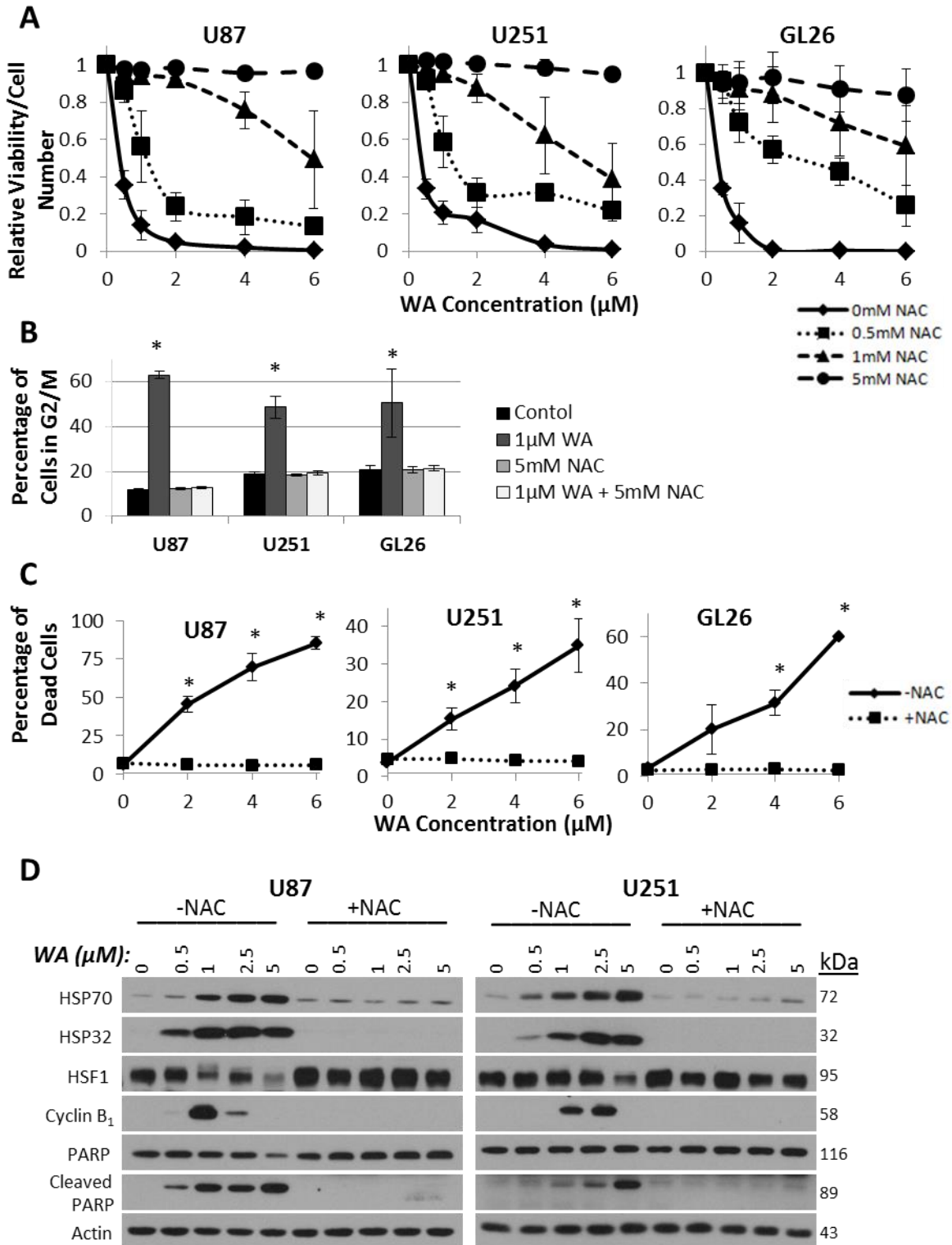
Figure 2-6. N-acetyl-L-cysteine effectively prevented the WA-mediated decrease in viability by the ATP-quantifying CellTiter-Glo assay (A), G2/M cell cycle arrest by propidium iodide staining (B), and cell death by propidium iodide/annexin V-FITC dual staining (C). (D) These findings corresponded with Western analysis for molecular markers of G2/M arrest (cyclin B_1) and apoptosis (PARP cleavage) as well as a complete prevention of the heat shock stress response with 5 mM NAC pretreatment. $*p < 0.05$

2.5 Discussion

Over the past decade, WA has emerged as a promising anti-cancer chemotherapeutic agent. Its effects in cancer cells have been described as anti-proliferative, pro-apoptotic, and anti-angiogenic (Mohan et al., 2004; Singh et al., 2007; Mandal et al., 2008; Oh et al., 2008; Stan et al., 2008; Oh and Kwon, 2009; Shah et al., 2009; Koduru et al., 2010; Samadi et al., 2010a; Yu et al., 2010). To date, however, the detailed mechanism of action of WA in malignant gliomas has not been well-elucidated. The results presented in this study demonstrate for the first time that WA is effectively able to induce a dose-dependent progression of G2/M cell cycle arrest followed by apoptosis-mediated cell death in glioblastoma cells. Reduction in both initiator caspases 8 and 9 suggests that WA can dually activate both extrinsic and intrinsic apoptotic pathways, consistent with previous findings in myeloid leukemia (Malik et al., 2007). Such effects appear to be a result of enhanced cellular oxidative stress generated by these compounds which can be completely abrogated by pretreatment with NAC. This oxidative stress with WA treatment also leads to induction of several heat shock proteins associated with cellular stress as well as alteration of the MAPK and Akt/mTOR growth and proliferation pathways including several of their corresponding surface receptors EGFR, Her2/ErbB2, and c-Met.

Pharmacological induction of oxidative stress has emerged as an intriguing means by which to mount an anti-cancer effect. It is thought that pro-oxidant intervention can alter the redox homeostasis of cancer cells, already stressed by exposure to constitutively high levels of ROS not observed in normal cells, by shifting the balance to a state of cytotoxicity (Laurent et al., 2005; Cabello et al., 2007). In fact, many investigational chemotherapeutics with redox potential have recently been explored in preclinical and clinical settings (Wondrak, 2009; Tew

and Townsend, 2011). Such an oxidative stress mechanism has also been demonstrated to effectively induce the proteotoxic stress of protein unfolding/misfolding, resulting in a downstream secondary cytotoxicity that likely preferentially affects these already susceptible cancer cells that may warrant exploration in the WA model (Xu et al., 2011; Qiao et al., 2012). In our experiments, induction of HSP70, HSP32, and HSP27 with WA treatment follows previous models of oxidative stress (Ansari et al., 2011; Qiao et al., 2012) and lends further credence to the pro-oxidant potential of this drug compound.

HSF1, a transcription factor that plays a major role in the expression of heat shock proteins, has been proposed to be a potentially important target in cancer therapy (Au et al., 2009). While control of HSF1, the major mediator of the observed stress response, has been well-studied, regulation of its stability and turnover remains unclear (Hu and Mivechi, 2011). As such, it remains unknown if WA directly induces HSF1 degradation or if the resulting decrease in expression is due to some cellular feedback mechanism following its role as a transcription factor to induce heat shock protein expression. Here, we demonstrate that WA may represent a pharmacological means by which to downregulate total HSF1 protein levels.

In contrast to studies with other cancer models, superoxide radicals do not appear to be highly elevated in glioblastoma cells upon WA exposure as measured by MitoSOX Red staining, however peroxide-type radicals are elevated in as detected by CM-H$_2$DCFDA (Hahm et al., 2011; Mayola et al., 2011). As noted in Figure 2-5B, it is unclear if the transient but statistically significant elevation in superoxide detected (11% in both cells lines examined) is physiologically relevant. Given that the majority of oxidants measured are known to be potential downstream products of superoxide, it is possible that these GBM cells express elevated levels of enzymes

like superoxide dismutase, either inherently or as a byproduct of maintenance in cell culture (Evans et al., 2004a; Evans et al., 2004b).

Our data indicate that the thiol reactivity and/or enhanced oxidation state associated with WA treatment can be fully sequestered by NAC and is likely the main mechanism responsible for the cytotoxic effects generated by WA, however, it remains unknown whether WA directly releases and/or induces ROS or if its thiol-reactive properties shift the normal balance of oxidation by altering the responsible cellular regulation. While WA has previously been demonstrated to bind directly to thiols of certain proteins including HSP90 (Yu et al., 2010; Santagata et al., 2012), the specificity of such binding has not yet been fully explored. Given the maintained and sometimes elevated levels of certain proteins and signaling pathways evaluated in this study, we hypothesize that some proteins and pathways in gliomas are more susceptible to the effects of WA, whether through direct binding or secondary effects, resulting in dysfunction and degradation.

Although multiple groups, including ours, have demonstrated the ability of WA to downregulate Akt signaling via its total levels and phosphorylation status in several cancer models (Oh et al., 2008; Oh and Kwon, 2009; Samadi et al., 2010a; Samadi et al., 2010b), no reports describe its effects on other proteins in the Akt/mTOR signaling pathway. In this study, WA shifts the balance of such signaling into an inhibitory state, likely representing a plausible means by which the compound limits growth and proliferation in glioma. Because the tumor suppressor phosphatase and tensin homolog (PTEN) is inactivated by genetic alterations in approximately 60% of GBMs, including the cell lines U87 and U251 (Lee et al., 2011), leading to constitutive activation of the Akt/mTOR pathway, the relevance of targeting this pathway is important (Koul, 2008; Lino and Merlo, 2011).. Hyperactivated Akt has been shown to result in

uncontrolled cell cycle progression and protection from apoptosis (Nogueira et al., 2008). Decreases in the total and phosphorylated levels of Akt, mTOR, p70 S6K, and p85 S6K as observed here with WA treatment represent direct prevention of the pathway's proliferative effects. In the presence of cellular stress, AMPK suppresses mTOR through phosphorylation of the tumor suppressor tuberin/TSC2 or the mTOR subunit Raptor (Mihaylova and Shaw, 2011). It has previously been shown that AMPK activation contributes to apoptosis in glioblastoma cells (Zhang et al., 2010). Upon WA exposure, GBM cells exhibit activating phosphorylation of both tuberin/TSC2 and the catalytic alpha subunit of AMPK.

The ability of WA to induce phosphorylation of proteins in the MAPK cascade such as ERK1/2 and the isoforms p38 and JNK has been previously demonstrated in several other cancer models (Mandal et al., 2008; Samadi et al., 2010b). While activation of ERK is generally regarded as a pro-survival attribute and may represent a compensatory mechanism of the cells to stress, it has also been shown as a potential pro-apoptotic signal which may explain its role here. In this study, activation of ERK1/2 with WA treatment was observed in the setting of increasing levels of PARP cleavage and caspase activitation. WA has previously been demonstrated to induce apoptosis through activation of the p38 MAPK (Mandal et al., 2008), so further exploration of ERK's role in WA-induced cell-death in gliomas is warranted.

This study provides new insight into the potent anti-cancer activity of WA against glioblastomas. The findings presented suggest that the underlying mechanism of WA's antiproliferative, pro-apoptotic, and cell-cycle arresting action are mainly due to its induction of oxidative stress and a stress response by the cells leading to alterations in the expression and signaling of several major pathways, especially the Akt/mTOR proliferative pathway. While this drug has great potential to be a novel therapeutic for the treatment of gliomas, future in vivo

studies will determine how these mechanistic effects translate biologically and the role of WA in

clinical applications for patients with glioblastoma multiforme.

Chapter 3

Oxidative cytotoxic agent withaferin A resensitizes temozolomide-resistant glioblastomas via MGMT depletion and induces apoptosis through Akt/mTOR pathway inhibitory modulation

3.1 Abstract

Temozolomide (TMZ) has remained the chemotherapy of choice in patients with glioblastoma multiforme (GBM) primarily due to the lack of more effective drugs. Tumors, however, quickly develop resistance to this line of treatment creating a critical need for alternative approaches and strategies to resensitize the cells. Withaferin A (WA), a steroidal lactone derived from several genera of the *Solanaceae* plant family has previously demonstrated potent anti-cancer activity in multiple tumor models. Here, we examine the effects of WA against TMZ-resistant GBM cells as a monotherapy and in combination with TMZ. WA prevented GBM cell proliferation by dose-dependent G2/M cell cycle arrest and cell death through both intrinsic and extrinsic apoptotic pathways. This effect correlated with depletion of principle proteins of the Akt/mTOR and MAPK survival and proliferation pathways with diminished phosphorylation of Akt, mTOR, and p70 S6K but compensatory activation of ERK1/2. Depletion of tyrosine kinase cell surface receptors c-Met, EGFR, and Her2 was also observed. WA demonstrated induction of N-acetyl-L-cysteine-repressible oxidative stress as measured directly and through a subsequent heat shock response with HSP32 and HSP70 upregulation and decreased HSF1. Finally, pretreatment of TMZ-resistant GBM cells with WA was associated with O6-methylguanine-DNA methyltransferase (MGMT) depletion which potentiated TMZ-mediated MGMT degradation. Combination treatment with both WA and TMZ resulted in resensitization of MGMT-mediated TMZ-resistance but not resistance through mismatch repair mutations. These studies suggest great clinical potential for the utilization of WA in TMZ-resistant GBM as both a monotherapy and a resensitizer in combination with the standard chemotherapeutic agent TMZ.

3.2 Introduction

According to the American Cancer Society, over 23,000 new cases of brain and other nervous system tumors will be diagnosed in 2013 in the United States (ACS, 2013). High grade gliomas, such as anaplastic astrocytoma and glioblastoma multiforme (GBM), account for approximately 38% of primary brain tumors, and to date, treatment options have remained limited. Following optimal surgical debulking, radiation therapy alone has been shown to increase mean survival time of GBM patients from approximately six months to only one year (Gillingham and Yamashita, 1975; Onoyama et al., 1976; Sheline, 1977). Concomitant and adjuvant temozolomide (TMZ) with surgical debulking and radiotherapy represents the most effective approved treatment in GBM patients but still only yields a 2.5 month median survival benefit and two year survival rate of 26.5% (Stupp et al., 2002; DeAngelis, 2005; Stupp et al., 2005; Taphoorn et al., 2005; Chamberlain et al., 2007).

The efficacy of TMZ is most frequently influenced by the methylation status of the *MGMT* (O6-methylguanine-DNA methyltransferase) gene promoter (Paz et al., 2004; Hegi et al., 2005). In patient tumors with an unmethylated promoter, the MGMT protein is expressed and repairs the major O6-methylguanine cytotoxic DNA lesions caused by TMZ, essentially eliminating its anti-cancer efficacy (Hansen et al., 2007; Kitange et al., 2009). Fifty-five to sixty-five percent of glioma patients do not display tumor phenotypes favorable for treatment with TMZ, and those that do often quickly acquire resistance through acquisition of MGMT or mismatch repair (MMR) deficiencies that allow tolerance of the lesion (Chamberlain, 2010; Quick et al., 2010; Zhang et al., 2012c).

To date, experimental targeted therapies against proteins such as epidermal growth factor receptor (EGFR), mammalian target of rapamycin (mTOR), and PI3 kinase have yielded disappointing responses in GBM patients despite promising pre-clinical findings (Wen and Kesari, 2008; Quick et al., 2010). Combined with the limitations of TMZ, this defines a critical need for improved diagnostic and therapeutic approaches for patients with both inherent and acquired TMZ resistance to either promote resensitization of the malignancy to TMZ or exploit unrelated vulnerabilities.

The 28-carbon steroidal lactone withaferin A (WA), extracted from several genera of the *Solanaceae* plant family, has emerged as a promising anti-cancer chemotherapeutic agent with thiol-reactive and oxidative properties that exploit redox alterations in cancer cells (Malik et al., 2007; Widodo et al., 2010; Hahm et al., 2011; Mayola et al., 2011; Santagata et al., 2012; Zhang et al., 2013). As such, it has demonstrated the ability to modulate many pathways involved in promoting cancer progression including specific proteins like heat shock protein (HSP) 90, Akt, NFκB, and the estrogen receptor (ER) (Mohan et al., 2004; Singh et al., 2007; Mandal et al., 2008; Oh et al., 2008; Stan et al., 2008; Oh and Kwon, 2009; Shah et al., 2009; Koduru et al., 2010; Samadi et al., 2010a; Yu et al., 2010; Grogan et al., 2013). Promising anti-tumor efficacy has been observed in prostate, thyroid, breast, melanoma, ovarian, cervical, and brain cancer models (Vyas and Singh, 2014).

Here, we follow-up on our previous findings outlining the efficacy of WA in TMZ-sensitive glioblastoma cells lines to demonstrate its potential role as a novel therapeutic option against resistant tumors as both a single agent therapy and a TMZ-resensitizer through MGMT modulation.

3.3 Materials and methods

3.3.1 Cell culture and general reagents

U87, U251, and T98G GBM cell lines of human origin were grown in Dulbecco's modified Eagle's medium (DMEM #11995-065; Gibco, Grand Island, NY) supplemented with 10% fetal bovine serum (FBS; Sigma-Aldrich, St. Louis, MO) and 1% penicillin/streptomycin (Sigma-Aldrich, St. Louis, MO) in a 37°C humidified atmosphere of 5% CO_2 in air. An additional human GBM cell line, U138, was maintained in equivalent media additionally supplemented with 2% L-glutamine (200 mM; Sigma-Aldrich), 1% MEM-vitamin (100x; Hyclone, Logan, UT), and 1% MEM nonessential amino acids (Sigma Aldrich). The TMZ resistant cells U87TMZ and U251TMZ were derived as previously described via TMZ dose escalation from the parental U87 and U251 cells, respectively (Nadkarni et al., 2012).

TMZ was generously provided by the NCI Developmental Therapeutics Program (Bethesda, MD) and was stored as a 100mM stock solution in DMSO at -80 °C. WA (99% pure by HPLC) was extracted, isolated, and stored as a 20 mM stock solution in DMSO at -80 °C as previously described (Samadi et al., 2010b). Propidium iodide (PI), RNase, N-acetyl-L-cysteine (NAC), protease inhibitor cocktail, and MEK inhibitor PD98059 were acquired from Sigma-Aldrich (St. Louis, MO). Annexin V-FITC was obtained from BD Biosciences (San Diego, CA). Caspase 8 inhibitor Z-IETD-FMK and caspase 9 inhibitor Z-LEHD-FMK were obtained from R&D Systems (Minneapolis, MN).

3.3.2 MTS assay

To determine the IC_{50} values of WA, all cell lines were seeded in 96-well plates at a density of 2,500 cells/well, treated with 0.025-3 μM WA, and incubated for 72 h. Cell number and viability were quantified by the colorometric CellTiter96 Aqueous MTS assay (Promega, Fitchburg, WI) at 490 nm on a BioTek Synergy 2 plate reader (BioTek, Winooski, VT) as per the manufacturer's instructions.

To assess combinational effects of WA and TMZ, cells were plated in 75 cm^2 flasks and allowed to grow overnight. Cells were treated with 0.5-2 μM WA and harvested at 24, 48, and 72 h post-treatment (60-80% confluency) for seeding in 96-well plates at densities of 500-10,000 cells/well. Following a 6 h incubation period, 10-50 μM and 100-500 μM TMZ were added to each well of the TMZ-sensitive and TMZ-resistant cells, respectively. After 48-144 h, cell number and viability were quantified by the MTS assay as described above.

3.3.3 CellTiter-Glo luminescent assay

To circumvent the auto-reductive potential of NAC that interferes with the MTS assay reagent, studies evaluating combination treatment with NAC and WA were completed with the CellTiter-Glo luminescent assay (Promega, Fitchburg, WI) measuring cell viability by adenosine triphosphate (ATP) levels. U251TMZ and U87TMZ cells were seeded at a density of 2,500 cells/well in white-chambered 96-well plates and allowed to incubate for 6 h before treatment with 1-5 mM NAC. After 1 h, 0.5-6 μM WA was added to each well. After 72 h, assay reagent was prepared and added as per the manufacturer's instructions, and the plates were evaluated on the BioTek Synergy 2 plate reader.

73

3.3.4 Cell cycle analysis

U251TMZ and U87TMZ cells were plated and allowed to grow overnight to 30-50% confluency. Cells were treated with 0.125-4 µM WA for 24 h. Cells were then collected, resuspended in 0.43 mL of 4 °C 1x PBS followed by 1 mL of -20 °C ethanol, and maintained at -20 °C for a minimum of 24 h. Finally, cells were then pelleted by centrifugation, resuspended in 1x PBS with 40 µg/mL PI and 100 µg/mL RNase, and incubated at 37 °C for 30 minutes before analysis by flow cytometry (BD LSRII; Becton Dickinson, San Diego, CA). Data analysis included only singlet living cells not displaying DNA fragmentation.

3.3.5 Apoptosis studies

Cells were plated as described for cell cycle analysis, treated with 1-6 µM WA, and pre-treated for 1 h with 5 mM NAC where indicated. After 24 h, cells were collected and washed once with Annexin binding buffer as previously described (Grogan et al., 2013). Staining phosphatidylserine on the outer leaflet of the cell membranes on apoptotic cells with Annexin V-FITC and DNA staining by PI in necrotic and late apoptotic cells was performed to assess WA-induced cell death. Cells were stained with both compounds according to the manufacturer's instructions (BD Biosciences, San Diego, CA) for 15 minutes at 4 °C and washed twice with Annexin binding buffer. Cells were resuspended in buffer and immediately analyzed by flow cytometry on the BD LSRII.

3.3.6 Immunoblotting

Cells were plated in the manner outlined for cell cycle analysis and treated with 0.5-5 µM WA. Where indicated, cells were either pre-treated with 5 mM NAC, 50 µM PD98059, 50 µM Z-IETD-FMK, or 50 µM Z-LEHD-FMK for 1 h or post-treated with 100-300 µM TMZ 24 h after WA. After 24-48 h, proteins were collected in lysis buffer (40 mM HEPES, 2 mM EDTA, 10 mM sodium pyrophosphate decahydrate, 10 mM β-glycerophosphate disodium salt pentahydrate, 1% triton X-100 supplemented with 100 µM phenylmethylsulfonyl fluoride, 1 mM Na_3VO_4, and 2 µL/mL protease inhibitor cocktail), quantified, separated by sodium dodecyl sulfate–polyacrylamide gel electrophoresis (SDS–PAGE), and electrotransfered onto a Hybond nitrocellulose membrane as previously described in Samadi, et al. (Samadi et al., 2011). 10-80 µg of protein sample was utilized per lane. Actin levels were used to ensure equal loading and transfer of proteins. All studies were repeated for accuracy.

Primary rabbit antibodies against MGMT (#2739; 1:1500), MSH2 (#2017; 1:1000), and MSH6 (#3996; 1:1000) and primary mouse antibody against MLH1 (#3515; 1:1000) were acquired from Cell Signaling Technology (Beverly, MA). Primary mouse antibody against p-H2A.X (Ser139; #613401; 1:1000) was purchased from Biolegend (San Diego, CA). Additional primary and secondary antibodies were utilized as previously described at dilutions ranging from 1:250-1:5000 and 1:5000-1:20000, respectively (Grogan et al., 2013).

3.3.7 Evaluation of reactive oxygen species

The accumulation of intracellular peroxide-type reactive oxygen species (ROS) in U251TMZ and U87TMZ cells was determined using the general oxidative stress indicator CM-H_2DCFDA (Molecular Probes, Grand Island, NY) that fluoresces upon oxidation. Cells were incubated at 37 °C in 1x dPBS containing 20µM CM-H_2DCFDA for 1 h to allow for indicator preloading and plated in 96-well plates in phenol red-free DMEM at 20,000 cells/well. After 30 minutes, 1-5 µM WA and/or 5 mM NAC was added to the wells. Fluorescence was assessed on the BioTek Synergy 2 3 h post-treatment with excitation and emission filters of 485 nm and 528 nm, respectively.

3.3.8 Statistical analysis

GraphPad Prism 6 (version 6.02; GraphPad Inc., San Diego, CA) was used to generate best-fit non-linear sigmoidal dose response curves for IC_{50} determination. Comparisons of differences between two or more means/values were determined by Student's unpaired t-test via the statistical functions of GraphPad Prism and Microsoft Excel 2010 software (version 14.0.6129.5000; Microsoft Corporation Redmond, WA). Densitometry, where indicated, was completed using ImageJ software (version 1.46r; Bethesda, MD). Combination studies compared drug efficacy within normalized WA treatment arms. Data are presented as mean values with error bars denoting standard deviation or standard error of the mean where appropriate. Unless otherwise noted, all experiments were performed minimally in triplicate. The level of significance was set at $p < 0.05$.

3.4 Results

3.4.1 Characterization of TMZ-resistant cell lines

U251 and U87 resistant sub-lines (U251TMZ and U87TMZ) were generated by exposing parental lines to increasing concentrations (30-300 µM) of TMZ over an 8-week period, pooling the resulting colonies, and confirming resistance as previously described (Nadkarni et al., 2012). Reduced TMZ effectiveness in established lines T98G and U138 has been previously confirmed (Ryu et al., 2012). Characterization of these cell lines demonstrated the absence of MGMT and the presence of mismatch repair proteins MLH1, MSH2, and MSH6 in parental U251 and U87 cells (Figure 3-1A). MGMT expression was observed in U251TMZ, T98G, and U138 cells but not U87TMZ. Compared to parental U87 cells, U87TMZ displayed lower levels of all three MMR proteins screened, suggesting the mechanism of U87TMZ resistance is due to heterogeneic deletion or mutation of these proteins.

3.4.2 Diminished cell proliferation and viability following withaferin A exposure

To evaluate the general cytotoxic effect of withaferin A, parental and resistant glioblastoma cells were treated with increasing concentrations of WA (0.025-3 µM) for 72 h with resulting cell number and viability determined by MTS assay (Figure 3-1B). WA dose escalation reduced cell proliferation and viability. By GraphPad analysis, the IC_{50} values of TMZ resistant sub-lines U251TMZ and U87TMZ were lower compared to parental lines, demonstrating increased efficacy. IC_{50} values were determined to be 0.766 ± 0.045 µM, $0.357 \pm$
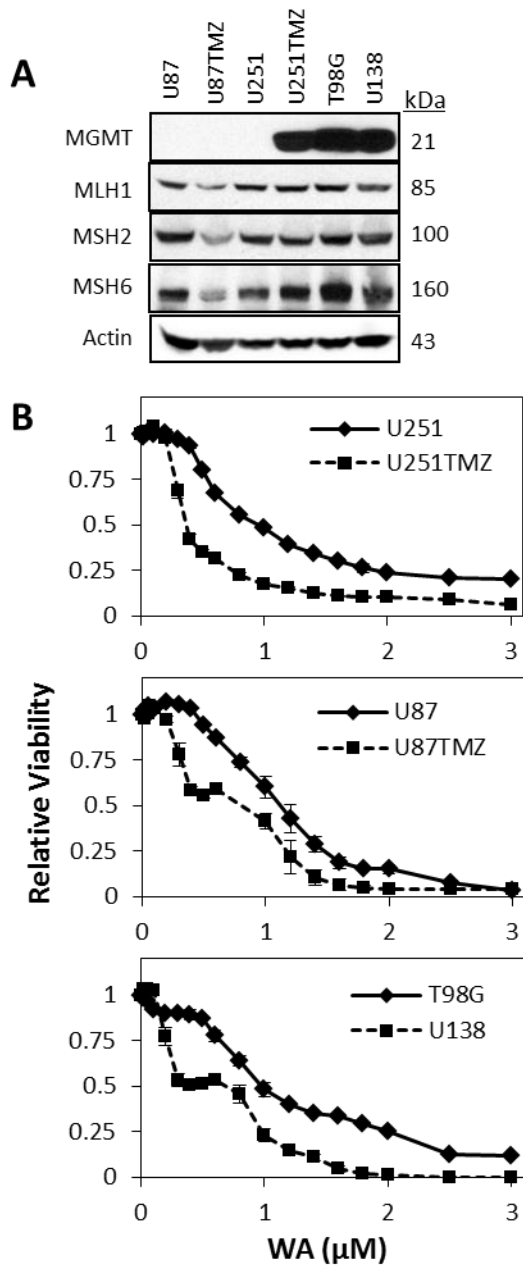
Figure 3-1.

Figure 3-1. A) Characterization of TMZ-resistant cells U251TMZ, U87TMZ, T98G, and U138 compared to parental U251 and U87 cells. U251 and U87 cell lines demonstrated the absence of MGMT and the presence of mismatch repair proteins MLH1, MSH2, and MSH6. MGMT expression was observed in U251TMZ, T98G, and U138 cells but not U87TMZ. U87TMZ displayed lower levels of all three MMR proteins screened compared to parental U87 cells. B) All cell lines were incubated with increasing concentrations of WA for 72 h and then assessed by MTS assay. WA dose escalation reduced cell proliferation and viability with IC_{50} values of 0.766 $\pm$ 0.045 μM, 0.357 $\pm$ 0.019 μM, 1.050 $\pm$ 0.062 μM, 0.657 $\pm$ 0.134 μM, 1.027 $\pm$ 0.105 μM, and 0.610 $\pm$ 0.279 μM for U251, U251TMZ, U87, U87TMZ, T98G, and U138 cells, respectively.

0.019 µM, 1.050 ± 0.062 µM, 0.657 ± 0.134 µM, 1.027 ± 0.105 µM, and 0.610 ± 0.279 µM for U251, U251TMZ, U87, U87TMZ, T98G, and U138 cells, respectively.

3.4.3 Induction of G2/M cell cycle arrest by withaferin A in a dose-dependent manner

Distribution of phases of the cell cycle was assessed by flow cytometry at 24 h. Consistent with the anti-proliferative effects seen in the MTS assays, WA treatment induced G2/M phase accumulation of U251TMZ and U87TMZ cells in a dose-dependent manner, demonstrating a key cellular response to WA exposure. WA induced a dose-dependent shift in cell cycle arrest from the G0/G1 checkpoint to G2/M arrest with minimal change in the percentage of cells in S phase (Figure 3-2A). Maximal shift to G2/M arrest above baseline was observed at 1.5 µM in U87TMZ cells (17.8% G2/M in controls increasing to 42.5% with treatment; p = 0.0001) and 2 µM in U251TMZ cells (43.1% baseline to 72.3% with treatment; p = 0.0001) (Figure 3-2B). Doses above this level demonstrated diminished deviation from control with a return to higher G0/G1 and lower G2/M but also increased DNA fragmentation observed in the sub-G0/G1 region (data not presented).

Additionally, cyclin B_1, a protein that displays G2/M phase-specific elevation, was evaluated by Western blotting to provide molecular confirmation of increases in G2/M cell cycle arrest. At 24 h, dose-dependent induction of cyclin B_1 was observed in both U87TMZ and U251TMZ cells with maximum expression levels observed at 1 µM and 2.5 µM WA, respectively, corresponding with flow cytometry findings (Figure 3-2C). Cyclin B_1 levels displayed similar peak expression levels at 48 h but with a more blunted response.

Figure 3-2.
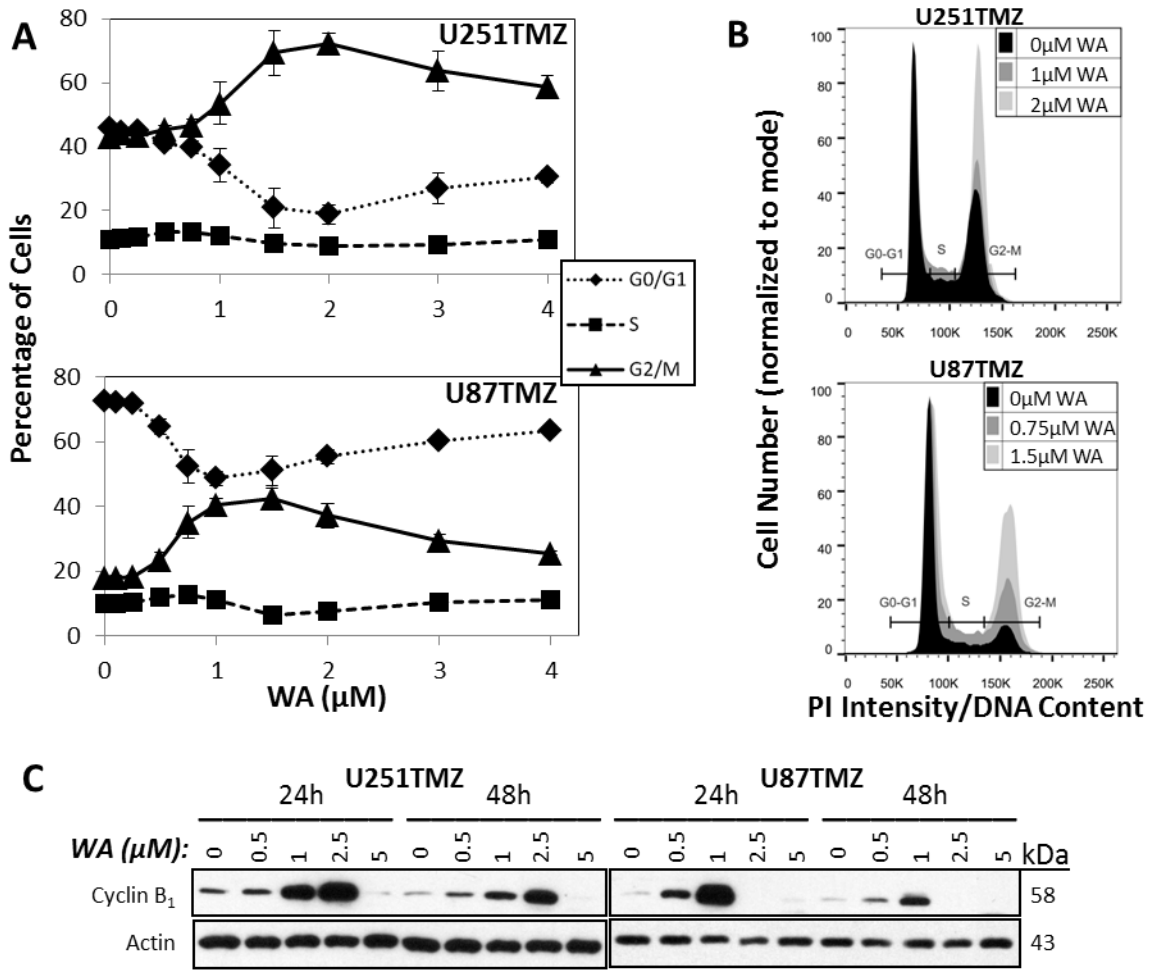
Figure 3-2. A) Ability to induce cell cycle modulation was assessed by flow cytometry at 24 h revealing that WA treatment results in dose-dependent G2/M cell cycle arrest. Maximum arrest was observed at 2 µM and 1.5 µM for U251TMZ and U87TMZ cells, respectively. B) Histograms demonstrate cell cycle distribution for U251TMZ and U87TMZ cells at concentrations up to those yielding maximal arrest. C) Arrest in G2/M phase was molecularly confirmed by immunoblotting for cyclin B_1 at 24-48 h. Highest levels of cyclin B_1 were observed at 2.5 µM and 1 µM WA for U251TMZ and U87TMZ cells, respectively, confirming flow cytometry findings.

3.4.4 Withaferin A induces cell death through both the intrinsic and extrinsic apoptotic pathways

PI and Annexin V-FITC dual staining analysis with flow cytometry was used to further characterize the anti-proliferative effects of WA by assessing levels of apoptosis and necrosis following drug exposure. After 24 h of 1-3 µM WA, U87TMZ and U251TMZ cells demonstrated increases in Annexin V-only staining representative of early apoptotic processes with increases in dual staining representative of late apoptosis present at higher concentrations (2-6 µM) (Figures 3-3A and 3-3B). U87TMZ cells alone appear to also show mild increases in levels of necrosis with WA exposure as demonstrated by staining with PI only. Total positive staining of control U87TMZ and U251TMZ cells was 8.2% and 4.0% but increased to 45.5% (p = 0.01: 14.7% early apoptosis; 23.0% late apoptosis; 7.7% necrosis) and 17.1% (p = 0.0004: 9.1% early apoptosis; 6.9% late apoptosis; 1.0% necrosis) with 2 µM WA, respectively. 6 µM WA elevated total cell death to 80.0% for U87TMZ (p < 0.0001: 4.9% early apoptosis; 62.6% late apoptosis; 12.5% necrosis) and 51.8% for U251TMZ cells (p < 0.0001: 4.0% early apoptosis; 44.6% late apoptosis; 3.1% necrosis).

Molecular confirmation of an apoptotic response was conducted by Western blotting for cleaved and/or total levels of the following proteins: extrinsic procaspase 8, mitochondrial/intrinsic procaspase 9, effector procaspases 3 and 7, and downstream poly(ADP-ribose) polymerase (PARP) cleavage (Figure 3-3C). At 24 h, increasing concentrations of WA resulted in progressively decreased levels of all procaspases and PARP, suggesting both intrinsic and extrinsic routes of apoptotic cell death. Maximum levels of cleaved caspase 8 were observed at 1-2.5 µM WA for U251TMZ and 0.5-1 µM WA for U87TMZ while highest levels for cleaved

83
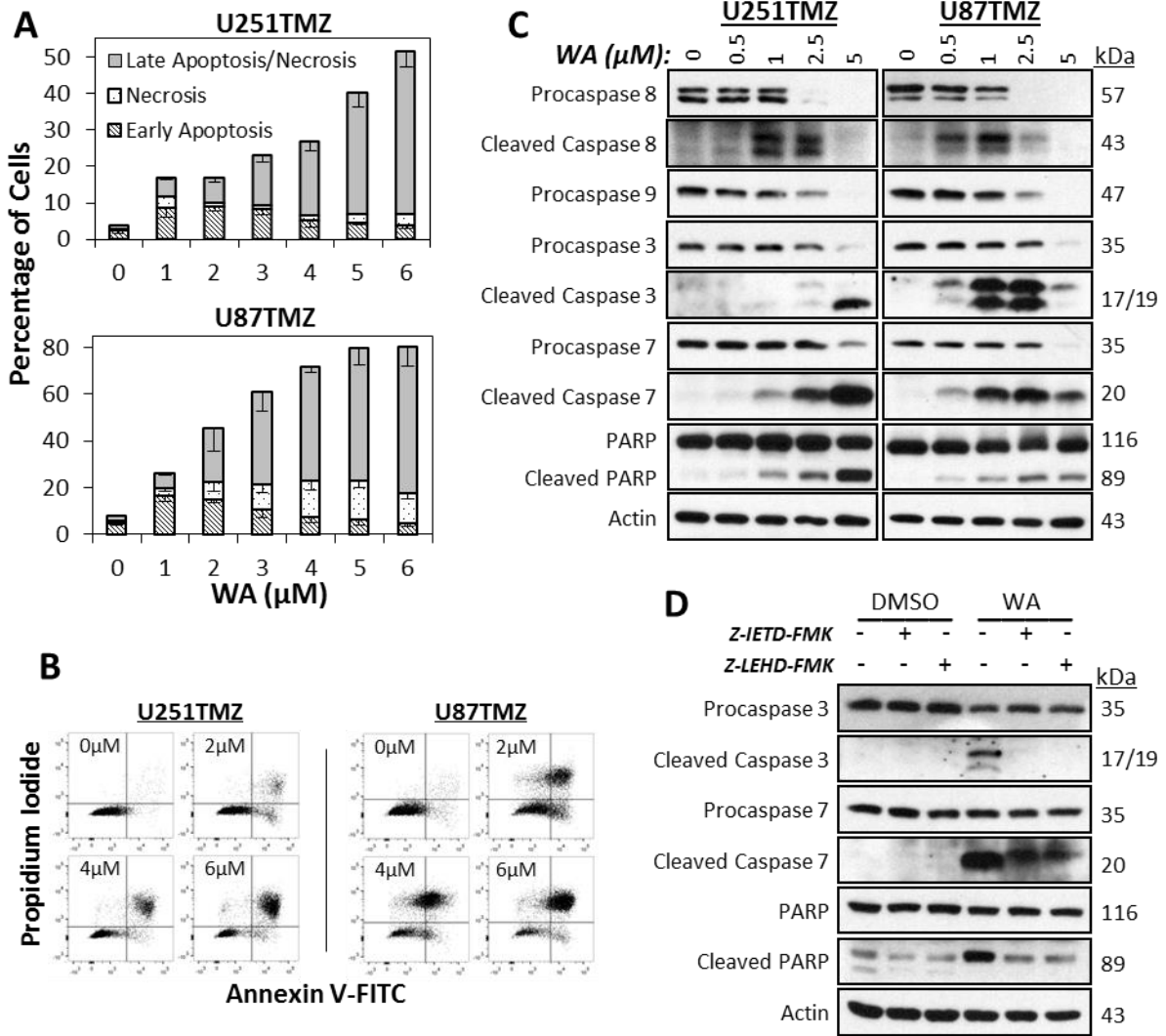
Figure 3-3.

Figure 3-3. A) WA treatment induced apoptotic cell death in U251TMZ and U87TMZ cells with increasing concentrations. 1-3 µM WA induced early apoptotic processes with increasing levels of late apoptosis observed at all concentrations examined. Only U87TMZ demonstrated elevated necrosis with treatment. B) Dot plots demonstrating propidium iodide and Annexin V-FITC staining show representative examples from both cell lines utilized. C) An apoptotic mechanism was confirmed by Western blotting for total and cleaved initiator caspases 8 and 9, effector caspases 3 and 7, and downstream PARP. Uncleaved proteins were decreased with increasing WA concentration. U251TMZ and U87TMZ cells demonstrated optimal concentrations for caspase cleavage with highest levels of PARP cleavage observed in both lines at 5 µM WA. D) U251TMZ cells were pretreated with 50 µM of either caspase 8 inhibitor Z-IETD-FMK or caspase 9 inhibitor Z-LEHD-FMK for 1 h followed by 2.5 µM WA for 24 h to determine if WA-driven apoptosis was intrinsically or extrinsically mediated. Inhibition of both caspase 8 and 9 reduced WA-induced cleavage of caspases 3 and 7 as well as PARP.

caspases 3 and 7 were observed at 5 µM WA for U251TMZ and 1-2.5 µM WA for U87TMZ. PARP cleavage increased up to 5 µM in both cell lines, the maximum concentration utilized, and suggests that the absence of cleaved caspases despite depletion of the procaspase form at high WA concentrations can be explained by a time-dependent nature of caspase signaling in which the upstream cleaved caspases are ultimately degraded following their activity.

To further evaluate the nature of the intrinsic and extrinsic apoptotic processing in WA-induced cytotoxicity, U251TMZ cells were pretreated with 50 µM of either caspase 8 inhibitor Z-IETD-FMK or caspase 9 inhibitor Z-LEHD-FMK for 1 h followed by 2.5 µM WA for 24 h. Pretreatment with both inhibitors resulted in a return to baseline for both cleaved caspase 3 and PARP levels and decreased amounts of cleaved caspase 7 compared to WA alone (Figure 3-3D). Inhibitors alone resulted in negligible changes. These data support that cytotoxicity at WA concentrations above IC_{50} involves induction of intrinsically- and extrinsically-mediated apoptosis in the GBM cell lines tested.

3.4.5 Withaferin A modulates the Akt/mTOR and MAPK pathways

Proteins in and related to the Akt/mTOR and mitogen-activated protein kinase (MAPK) pathways are key to proliferation and survival of GBM cells and other cancers (Wen and Kesari, 2008). These proteins were evaluated by Western blotting at 24-48 h post-treatment in U251TMZ and U87TMZ cells in order to evaluate WA activity against total and phosphorylated protein levels as a potential mechanism for the anti-proliferative effects observed (Figure 3-4A). At 24 h, total levels of Akt and mTOR were decreased between ~1-5 µM WA with minimal changes occurring in total p70 S6 kinase (S6K) in both cells lines. However, activation of each

Figure 3-4.
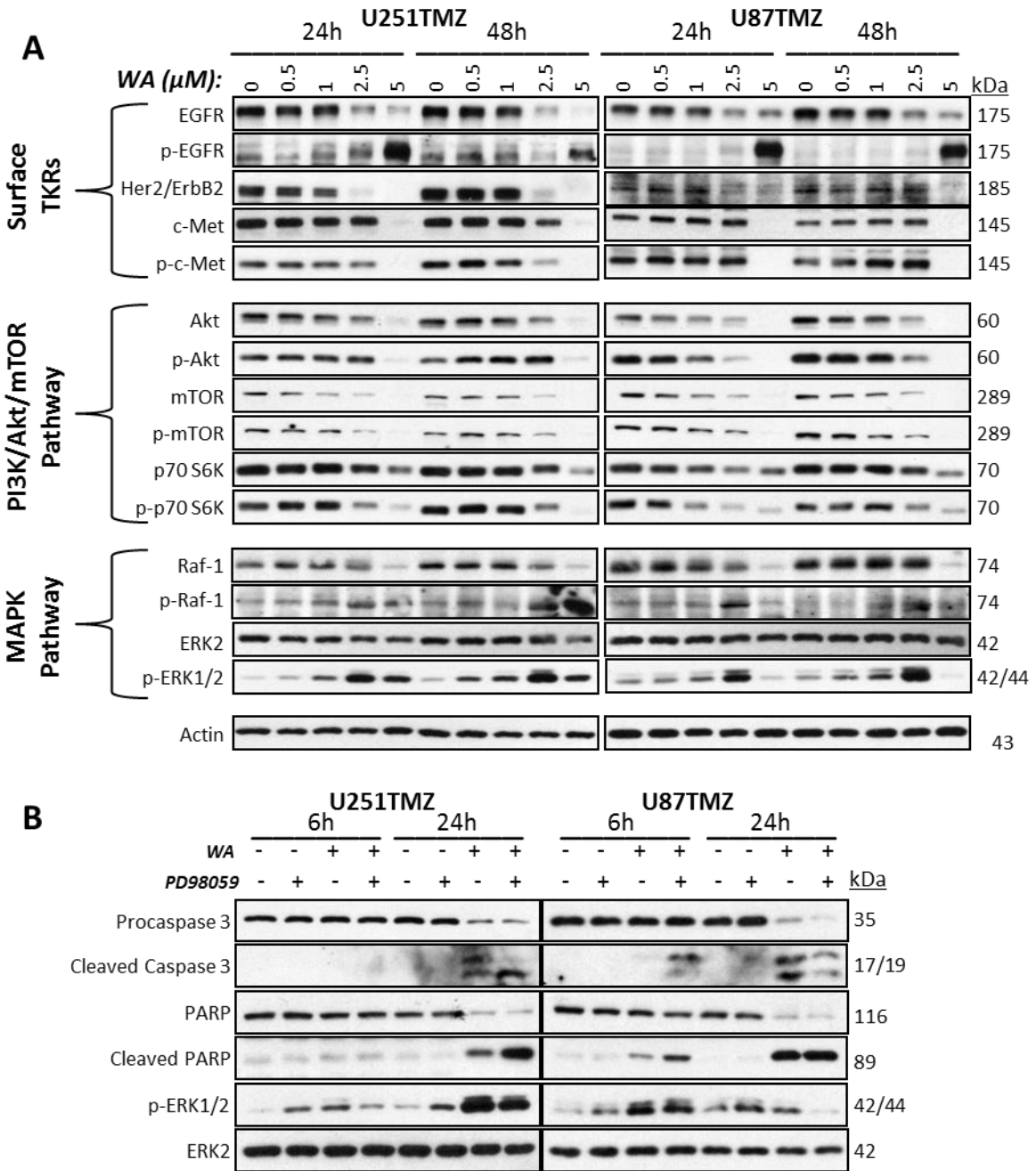
Figure 3-4. A) Key proteins of the survival and proliferation PI3K/Akt/mTOR and MAPK pathways as well as common surface tyrosine kinase receptors were evaluated by immunoblotting for total levels and activation by phosphorylation following treatment with WA at 24-48 h in U251TMZ and U87TMZ cells. Total levels of specific proteins in both pathways were decreased, but reduction of protein activation was only observed in the PI3K/Akt/MAPK pathway whereas phosphorylation of Raf-1 and ERK1/2 was increased. B) To determine the nature of MAPK pathway activation, U251TMZ and U87TMZ cells were pretreated with 50 μM of the MEK inhibitor PD98059 for 1 h followed by 2.5 μM WA for 6 h or 24 h. PD98059 increased ERK1/2 phosphorylation but reduced WA-induced phosphorylation of ERK1/2 in a time-dependent manner. WA alone induced caspase 3 and PARP cleavage in both cell lines in a time-dependent manner that was increased when combined with MEK inhibitor. This demonstrates that MAPK pathway activation with WA was acting in a pro-survival signal rather than contributing to apoptosis.

protein via phosphorylation (p-Akt Ser473, p-mTOR Ser2448, and p-p70 S6K Thr389) was similarly reduced over this range. Phosphorylation at Thr412 of the nuclear isoform of p70 S6K, p85 S6K, was also reduced with increasing WA concentration (data not shown). These effects were observed through the 48 h timepoint and demonstrate an inhibitory effect of WA on the Akt/mTOR growth pathway. Additionally, phosphorylation (Thr172) of AMPKα, the catalytic subunit of a negative regulator of the Akt/mTOR pathway that responds to cellular stressors, was increased with WA treatment, peaking at 1 μM in U251TMZ cells (Supplemental Figure 3-1). Despite depletion of total levels of the downstream tumor suppressor TSC2, phosphorylation at Thr1462 was enhanced or maintained at all WA concentrations tested in U251TMZ cells. In contrast to previous observations in parental U87 cells (Grogan et al., 2013), total and phospho-levels of AMPKα were decreased in U87TMZ cells despite maintenance of p-TSC2 levels (Supplemental Figure 3-1).

The MAPKKK Raf-1 and the MAPK ERK2 were assessed to evaluate the effects of WA on the primary proliferative MAPK pathway (Figure 3-4A). Total Raf-1 levels decreased at ~2.5-5 μM in both U251TMZ and U87TMZ cells, however, activating phosphorylation of the protein at Ser338 increased over the same concentration range. Downstream, minimal changes were observed in total ERK2 levels, but phosphorylation of ERK1/2 (Thr202/Tyr204) was notably increased in a dose-dependent manner in both cell lines with a maximum level achieved at 2.5 μM WA in each at both 24 h and 48 h. Given that phosphorylation of MAPK proteins is typical of a pro-survival response yet WA instead induces apoptosis in GBM cells, the MAPK pathway was further explored to determine if its activation was necessary for the induction of apoptosis or simply a compensatory pro-survival response. U251TMZ and U87TMZ cells were pretreated with 50 μM of the MAPKK MEK inhibitor PD98059 for 1 h followed by 2.5 μM WA for 6h or

24 h. Pretreatment with the inhibitor alone resulted in increased ERK1/2 phosphorylation but limited WA-induced phosphorylation in a time-dependent manner (Figure 3-4B). Alterations in apoptosis were assessed by cleaved caspase 3 and cleaved PARP levels. WA alone induced observable caspase 3 and PARP cleavage at 24 h in both cell lines and PARP cleavage alone at 6h in U87TMZ. However, cleaved caspase 3 and PARP levels were increased when combined with the MEK inhibitor at 24 h in U251TMZ and 6 h in U87TMZ, demonstrating that MAPK pathway activation with WA treatment appears to represent a compensatory response to the apoptotic effects induced by the compound.

Finally, the tyrosine kinase receptors EGFR, Her2/ErbB2, and c-Met, known to signal to both the Akt/mTOR and MAPK pathways, were evaluated due to their status as common amplified, mutated, and/or drug-targeted surface proteins in GBM (Wullich et al., 1993; Potti et al., 2004; Puputti et al., 2006; Guessous et al., 2010; Berezowska and Schlegel, 2011). Total levels of EGFR and Her2/ErbB2 in both U251TMZ and U87TMZ decreased with 2.5-5 µM WA treatment at 24 h and 48 h while total levels of c-Met decreased at 5 µM (Figure 3-4A). Interestingly, increased phosphorylation of Tyr1068 on EGFR was observed at 2.5-5 µM WA depending on the cell line as well as increased phosphorylation of Tyr1234/1235 on c-Met in U87TMZ cells up to 2.5 µM WA at 48 h. Phosphorylation of c-Met was otherwise downregulated with WA treatment in both lines.

3.4.6 Withaferin A elevates oxidative status and induces a heat shock stress response in TMZ-resistant cells

We have previously demonstrated the ability of WA to elevate oxidative potential and ROS-mediated cell death in TMZ-sensitive GBMs (Grogan et al., 2013). TMZ has also been demonstrated to produce ROS that result in inhibitory activation of AMPK (Zhang et al., 2010). We therefore evaluated the nature and ability of WA to continue to induce ROS in TMZ-resistant U87TMZ and U251TMZ cells. Peroxide-type radical production was monitored with CM-H_2DCFDA conversion at 3 h post-WA exposure. Both cell lines showed statistically significant increased detectible CM-H_2DCFDA fluorescence with increasing WA exposure. ROS levels rose 20.9% ($p = 0.001$), 36.6% ($p = 0.002$), and 38.8% ($p = 0.01$) in U251TMZ and 21.3% ($p = 0.003$), 40.6% ($p = 0.004$), 47.3% ($p = 0.001$) in U87TMZ cells at 1, 3, and 5 µM WA compared to control, respectively (Figure 3-5A). The thiol antioxidant and ROS scavenger NAC was added simultaneously with WA and was shown to nearly complete abrogate WA-generated ROS, further demonstrating the nature of the effect.

Various models of oxidative stress are known to be associated with a heat shock response via induction of several HSPs (Ansari et al., 2011; Qiao et al., 2012), and alteration of HSPs were previously reported following WA treatment (Khan et al., 2012; Grogan et al., 2013). Treatment with WA yielded a unique pattern of HSP expression modulation in U251TMZ and U87TMZ cells (Figure 3-5B). Total levels of HSP32/heme oxygenase 1 and HSP70, but not HSP90, were observed to increase with increasing concentrations of WA at 24 h. HSP27 was depleted at 24 h with 5 µM WA in both cell lines but remained largely unchanged in U251TMZ and mildly elevated in U87TMZ with other concentrations at 24 h. The transcription factor heat shock factor 1 (HSF1) showed dose-dependent reduction in expression between 1-5 µM WA. Pretreatment with 5 mM NAC virtually eliminated all modulation of proteins in the heat shock system (Figure 3-5B).

Figure 3-5.
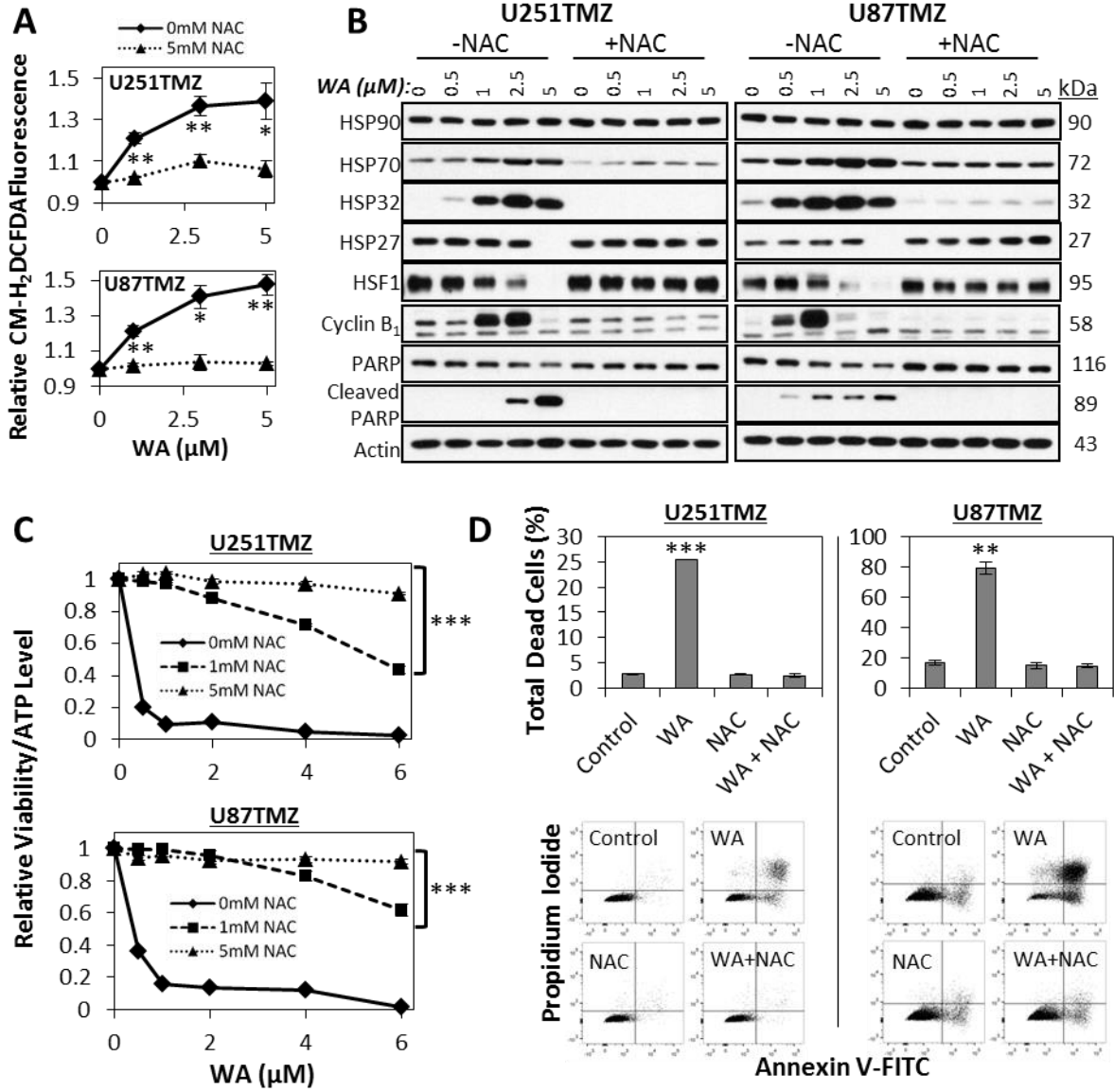
Figure 3-5. A) The peroxide ROS indicator CM-H$_2$DCFDA was preloaded into U251TMZ and U87TMZ cells prior to WA exposure to determine alterations in oxidative potential. Elevations in signal that were observed with increasing concentrations of WA at 3 h were reduced or completely absent with co-treatment of 5mM NAC. B) Treatment with WA resulted in the induction of an NAC-repressible cellular stress heat shock response. Proteins associated with cellular stress and heat shock were evaluated by immunoblotting at 24 h and revealed elevated levels of HSP32 and HSP70, known to be upregulated in response to oxidative stress, but decreased transcription factor HSF1 with increasing WA exposure that could be completely eliminated with 5 mM NAC pretreatment. NAC also prevented induction of cyclin B$_1$ and cleavage of PARP. Functionally, NAC pretreatment reduced the anti-proliferative (C) and pro-cytotoxic (D) effects of WA as assessed by the CellTiter-Glo assay at 72 h and flow cytometry at 24 h, respectively. *p < 0.05, **p < 0.01, ***p < 0.001

Functionally, WA-induced depletion of ATP levels, a marker of reduced cellular viability in the CellTiter-Glo assay, could be reduced or completely eliminated with 1-5 mM NAC pretreatment (p < 0.0001) (Figure 3-5C). Such effects were seen with up to 6 µM WA, the highest concentration examined. Additionally, re-evaluation of cell death by flow cytometry as previously described following pretreatment with 5 mM NAC showed the elimination of death-associated PI and Annexin V staining normally induced by 5 µM WA (p < 0.01) (Figure 3-5D). This was supported by blockage of PARP cleavage via NAC pretreatment (Fig. 3-5B). Additionally, WA-mediated cyclin B_1 induction was blocked by NAC, demonstrating the prevention of G2/M cell cycle arrest seen with WA treatment.

3.4.7 Withaferin A resensitizes TMZ-resistant GBM cells to TMZ through MGMT depletion

Expression of MGMT is associated with TMZ resistance in GBMs and therefore is an attractive target for TMZ resistance resensitization and prevention (Kitange et al., 2009). WA demonstrated the ability to induce depletion of MGMT at 48 h in cell lines (U251TMZ, T98G, and U138) utilizing MGMT as the primary means of TMZ resistance (Figure 3-6A). U251TMZ and U138 cells showed progressive depletion of MGMT from 0.5-10 µM WA with approximately 5-fold and 20-fold less compared to control by 5 µM, respectively. At 5 µM WA treatment, there was a 43% reduction in MGMT in T98G cells with complete elimination by 10 µM. U87TMZ cells, however, failed to express MGMT altogether.

To determine if these findings extended to functional resensitization of resistant cells to WA, two cells lines resistant through MGMT (U251TMZ and T98G) and one cell line displaying MGMT-independent resistance (U87TMZ) were treated with WA for 24 h followed by TMZ and

Figure 3-6.
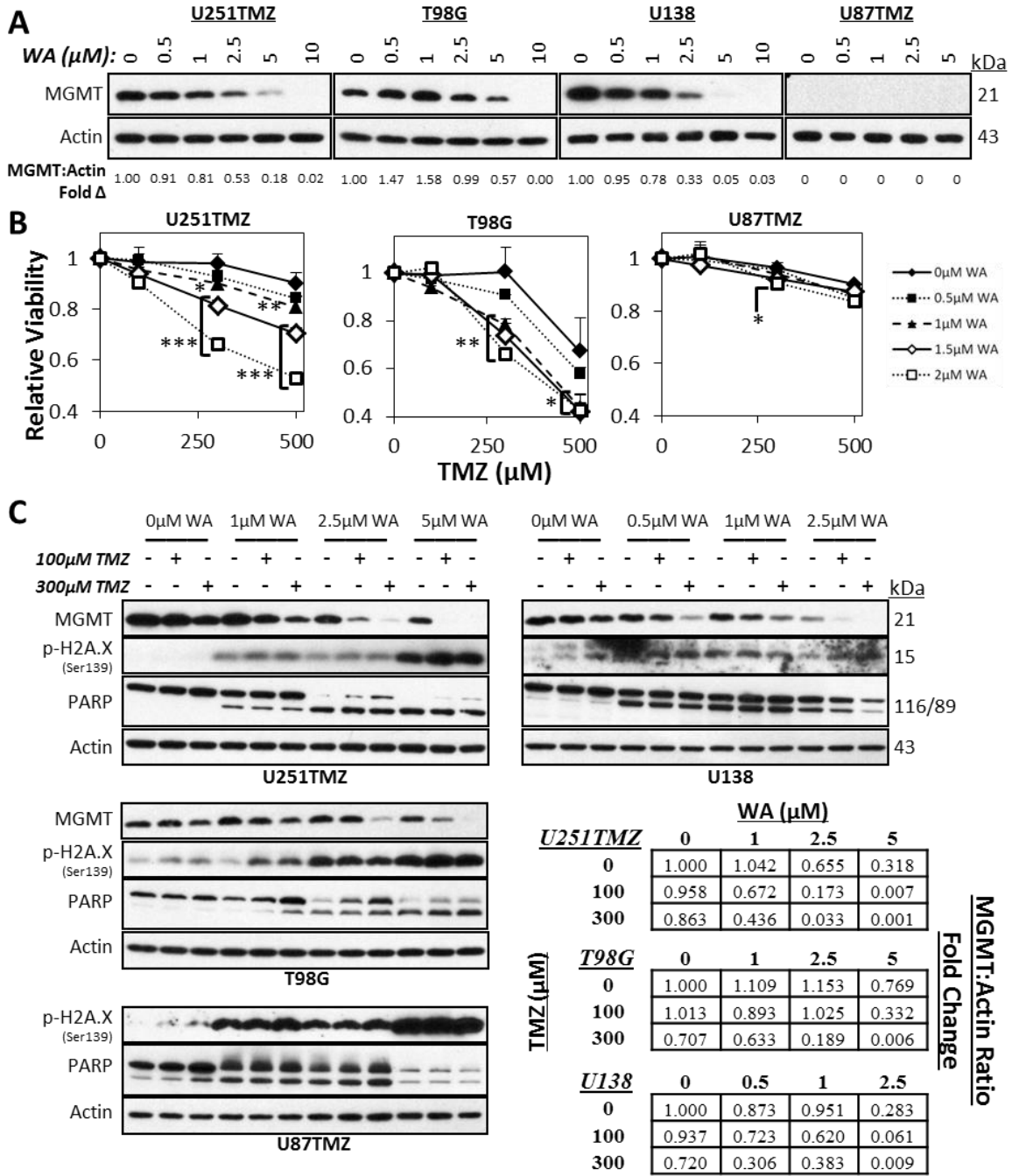
Figure 3-6. A) WA treatment reduced protein levels of MGMT in TMZ-resistant U251TMZ, T98G, and U138 cell lines at 48 h. MGMT was not observed in U87TMZ. B) 24 h pretreatment with WA resensitized MGMT-expressing U251TMZ and T98G cells to TMZ in a dose-dependent manner as assessed by a normalized MTS assay, but no resensitization was observed in MGMT-deficient U87TMZ cells. C) TMZ-resistant cells were treated with WA for 24 h followed by TMZ exposure for an additional 24 h. Pretreatment with WA potentiated and/or synergized with TMZ to induce further depletion of MGMT in MGMT-expressing lines. Increasing WA concentrations yielded higher levels of p-H2A.X and cleaved PARP in all cell lines, but only T98G demonstrated WA-mediated increased levels with TMZ exposure. $*p < 0.05$, $**p < 0.01$, $***p < 0.001$

evaluated with the MTS assay (Figure 3-6B). Both U251TMZ and T98G showed statistically significant decreases in cell viability when 1, 1.5, or 2 µM WA was combined with 300 or 500 µM TMZ. Pretreatment with 2 µM WA followed by 300 µM TMZ yielded a 32% (p < 0.0001) and 34% (p = 0.004) relative decrease in U251TMZ and T98G cell viability compared to TMZ or WA alone, respectively. In contrast, U87TMZ cells only demonstrated a statistically significant enhancement of combination therapy over TMZ alone – only 6% additional reduction in relative viability – with a 2 µM WA and 300 µM TMZ combination (p = 0.02). 48 h pretreatment with WA also demonstrated enhanced effect with significant elimination of the benefit by 72 h pretreatment (data not shown). WA pretreatment did not prevent TMZ efficacy in TMZ sensitive U251 and U87 parental cells (Supplemental Figure 3-2A).

Because TMZ also depletes MGMT (D'Atri et al., 2000), the effect of WA and TMZ combination on MGMT levels was evaluated. Combination therapy demonstrated dose-dependent synergy or potentiation to reduce total levels of MGMT in U251TMZ, T98G, and U138 MGMT-expressing cells (Figure 3-6C). At 1 µM WA in U251TMZ and U138 cells and 2.5 µM WA in T98G cells, minimal decreases and/or increases of MGMT levels were observed. The addition of 300 µM TMZ for 24 h resulted in 43%, 52%, and 34% reduction in MGMT protein levels compared to TMZ alone in U251TMZ, T98G, and U138 cells, respectively.

Phosphorylation of H2A.X as a marker of double strand DNA damage and cleavage of PARP during apoptosis were evaluated to look for molecular evidence of combinational efficacy. Both markers were elevated in the setting of increasing concentrations of WA in U251TMZ, T98G, U138, and U87TMZ cells. However, PARP cleavage was then diminished at the high levels of U87TMZ and U138 cells suggesting non-apoptotic cell death or very late apoptosis at this timepoint. Addition of TMZ was observed to increase p-H2A.X and PARP cleavage in only

T98G, particularly at 1 μM WA. Interestingly, despite similar or increased levels of cleaved PARP within WA treatment groups, levels of uncleaved PARP increased with TMZ treatment in each of the TMZ groups but not control in U251TMZ and T98G cells. Given the reported oxidative effect induced by TMZ (Zhang et al., 2010), markers of oxidative stress including HSP32, HSP70, and p-AMPKα as well as the AMPK-influenced downstream phosphorylation of mTOR were evaluated to determine if combination of WA and TMZ demonstrated enhanced oxidative effect in GBM. While WA increased HSP32 and HSP70 levels in all lines and TMZ enhanced phosphorylation of AMPKα in U138, combination therapy did not result in additional effect and failed to further diminish mTOR activation (Supplemental Figure 3-2B).

3.5 Discussion

While WA has demonstrated effectiveness as a promising new therapeutic agent in a variety of cancer types including TMZ-sensitive GBM, this work is the first to explore its efficacy in a known model of drug-resistance. Here, we show for the first time that WA induces a potent cytotoxic effect against temozolomide resistant GBMs resulting in G2/M arrest and apoptosis from both the intrinsic and extrinsic systems. These findings correspond with the elevation of cellular oxidative potential and inhibitory modulation of the Akt/mTOR pathway but not the MAPK pathway.

Since its approval by the FDA, TMZ remains the standard-of-care chemotherapeutic agent in the treatment of primary GBM. Exposure to this agent results in DNA adducts such as O6-methylation of guanine which, if not removed by MGMT, can mispair with thymine. Cells with intact MMR undergo futile cycles of attempted repair with resultant replication-associated

98

DNA double strand breaks, G2/M arrest, and ultimately apoptosis (Hirose et al., 2003). Targeting mechanisms of DNA damage repair with various inhibitors, such as those of PARP and ataxia telangiectasia mutated (ATM), has provided potentially beneficial strategies in enhancing TMZ effect, but comparatively limited effort has gone into addressing both inherent and acquired resistance to TMZ by MGMT expression or, less frequently, MMR mutation in GBM. Despite about half of patients displaying tumor phenotypes not conducive to TMZ use, it remains a first-line agent, demonstrating the need for better tumor screening techniques. Furthermore, initially responsive tumors are often quick to develop resistance to this line of therapy (Chamberlain, 2010; Quick et al., 2010).

Several experimental agents used to resensitize resistant cancer cells to TMZ or other alkylating agents – such as valproic acid (Sztajnkrycer, 2002; Weller et al., 2011; Ryu et al., 2012), O[6]-benzylguanine (Baer et al., 1993; Kaina et al., 2010), IL-24 (Zheng et al., 2008), and silencing oligonucleotides (Citti et al., 1996; Xie et al., 2011; Kreth et al., 2013) – possess little practical intrinsic anti-cancer cytotoxic properties or clinical applicability, however, some do have the potential for adverse effects in the patient. Alternatively, dose-dense TMZ scheduling, used to deplete MGMT levels quickly to enhance TMZ effects, has yielded disappointing outcomes in several clinical trials (Strik et al., 2012). In this study, WA acted as both an inherently cytotoxic agent and an enhancer of the efficacy of TMZ in MGMT-driven resistant cell lines while maintaining TMZ sensitivity in parental lines. Such data conceptually support the utility of combination therapy WA with TMZ in the first-line treatment of GBM. Such an approach should maximize anti-cancer activity across broad tumor heterogeneity. Importantly, while tumors with resistance due to MMR mutation may not be resensitized to TMZ by WA, the presence of a second cytotoxic chemotherapeutic agent may provide significant benefit in the

context of ineffective TMZ treatment. It remains to be fully explored whether increased levels of p-H2A.X observed with WA treatment are a result of direct DNA damage, perhaps through an oxidative mechanism, or rather a known byproduct observed during cellular apoptosis for DNA fragmentation (Rogakou et al., 2000), however, preliminary results in breast cancer support a caspase-mediated mechanism (data not published). Elevated total PARP with increasing TMZ in the presence of WA in MGMT-expressing lines may indicate the necessity for increased base excision repair (BER) during combination therapy, alluding to induction of DNA damage as a reason for combinational efficacy which will need to be validated by further scientific investigation.

Several studies have implicated the role of WA in the disruption of HSP90 chaperone functions through binding to the C-terminus of HSP90 (Yu et al., 2010; Grover et al., 2011). While direct evidence of such an inhibitory effect has not yet been established, downstream depletion of various HSP90-related client proteins suggests that WA may indeed act at least in part as a novel HSP90 inhibitor. This could explain and support the wide-ranging effects observed in this study, including the depletion in total levels of known HSP90 client proteins such as Akt, mTOR, Raf-1, and EGFR. By depleting these key regulatory client proteins of HSP90, the normal signaling axes of multiple proliferative pathways are simultaneously modulated. MGMT, which is depleted in the presence of WA, has not, however, been reported as a client protein of HSP90. Indeed, current studies demonstrate that total levels of MGMT are not impacted by the widely-utilized HSP90-inhibitor 17-AAG until high concentrations (1-2 µM) are achieved, suggesting that its stability and function are not directly maintained by HSP90 (data not shown). Santagata, et al. demonstrated the thiol reactivity of WA (Santagata et al., 2012), and our results implicate an oxidative mechanism, representing an alternative means by which

MGMT and other non-HSP90 client proteins may be targeted for degradation by WA. Interestingly, valproic acid, which diminishes MGMT levels, has also been shown to cause oxidative stress in glioma cell lines (Fu et al., 2010).

Induction of oxidation has become a promising mechanism by which to target cancer. Alterations in the redox potential of cancer cells due to various molecular turnover and quick replication results in increased cellular stress that can be exploited to shift cells into a state of cytotoxicity (Laurent et al., 2005; Cabello et al., 2007). This approach circumvents traditional therapeutic options such as antigen-targeting and DNA-damaging agents that have received the most attention but are often rendered useless due to rapid development of resistance. In GBM, such traditional agents have been explored in patients but have yielded unimpressive results in clinical trials largely due to the development of tumor mutations that limit the effectiveness and/or relevance of a particular targeted therapeutic (Wen and Kesari, 2008; Quick et al., 2010).

In the present study, thiol-reactivity and oxidation by WA resulted in depletion of proteins in the Akt/mTOR and MAPK pathways including many cell surface receptors either through direct interaction or as a downstream effect of the inhibition of other proteins. As noted previously, other reports have shown additional pathways effected. Such an ability to target multiple pathways simultaneously with a single compound has great potential to generate an enhanced anti-cancer effect while reducing the development of resistance to a particular target. The ability to modulate multiple components of the Akt/mTOR pathway simultaneously provides a novel and important mechanism by which WA can manifest its beneficial effects against GBMs. Because of mutations in proteins like the tumor suppressor phosphatase and tensin homolog (PTEN), this pathway is frequently overactivated in GBM to drive proliferation, as shown in both U251 and U87 cells (Koul, 2008; Lee et al., 2011; Lino and Merlo, 2011).

Interestingly, while we previously showed activation of AMPKα and downstream tumor suppressor TSC2 which act to inhibit mTOR in both U251 and U87 parental cells (Grogan et al., 2013), U87TMZ appears to have lost the ability to act through this pathway which suggests direct inhibition of the Akt/mTOR axis.

WA treatment yields subsequent induction of the MAPK pathway as demonstrated by activating phosphorylation of EGFR, Raf-1, and ERK1/2. Previous studies have shown that reactive oxygen species generated by epoxide-containing compounds in GBM cells are responsible for the phosphorylation of ERK1/2 which then drives apoptosis (Wu et al., 2011). In contrast, inhibition of this pathway prior to WA exposure yields enhanced apoptosis, suggesting that the activation of the MAPK pathway is a compensatory pro-survival response to apoptotic shifts in the cell and may be a therapeutic target that would synergistically enhance the efficacy of WA in future combinational therapy studies.

The studies presented here provide an important framework for the utilization of WA in TMZ-resistant GBM as both a monotherapy and as a resensitizer in combination with the standard chemotherapeutic agent TMZ. WA demonstrates an oxidative mechanism that leads to anti-proliferative and pro-apoptotic effects largely through Akt/mTOR pathway modulation. Simultaneously, depletion of MGMT allows for enhanced activity of TMZ. While future pre-clinical animal studies will be necessary to determine its translational potential in GBMs, evidence is supportive of a future clinical potential for the utilization of WA across the heterogeneic spectrum of glioma patients.

Supplemental Figure 3-1.
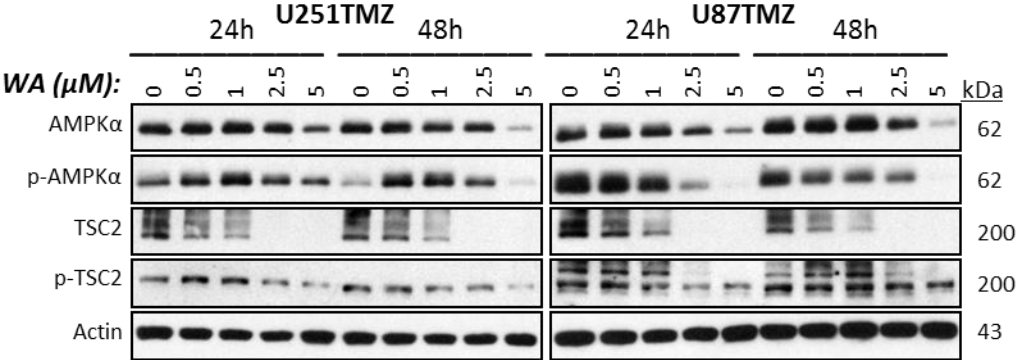
Supplemental Figure 3-1. WA treatment resulted in depletion of total protein levels in both AMPKα and TSC2 at 24-48 h in both U251TMZ and U87TMZ cells. U87TMZ cells also demonstrated reduced phosphorylation of AMPKα in contrast to previous findings in U87 parental cells. U251TMZ cells display dose-dependent activating phosphorylation of AMPKα and downstream TSC2.

Supplemental Figure 3-2.
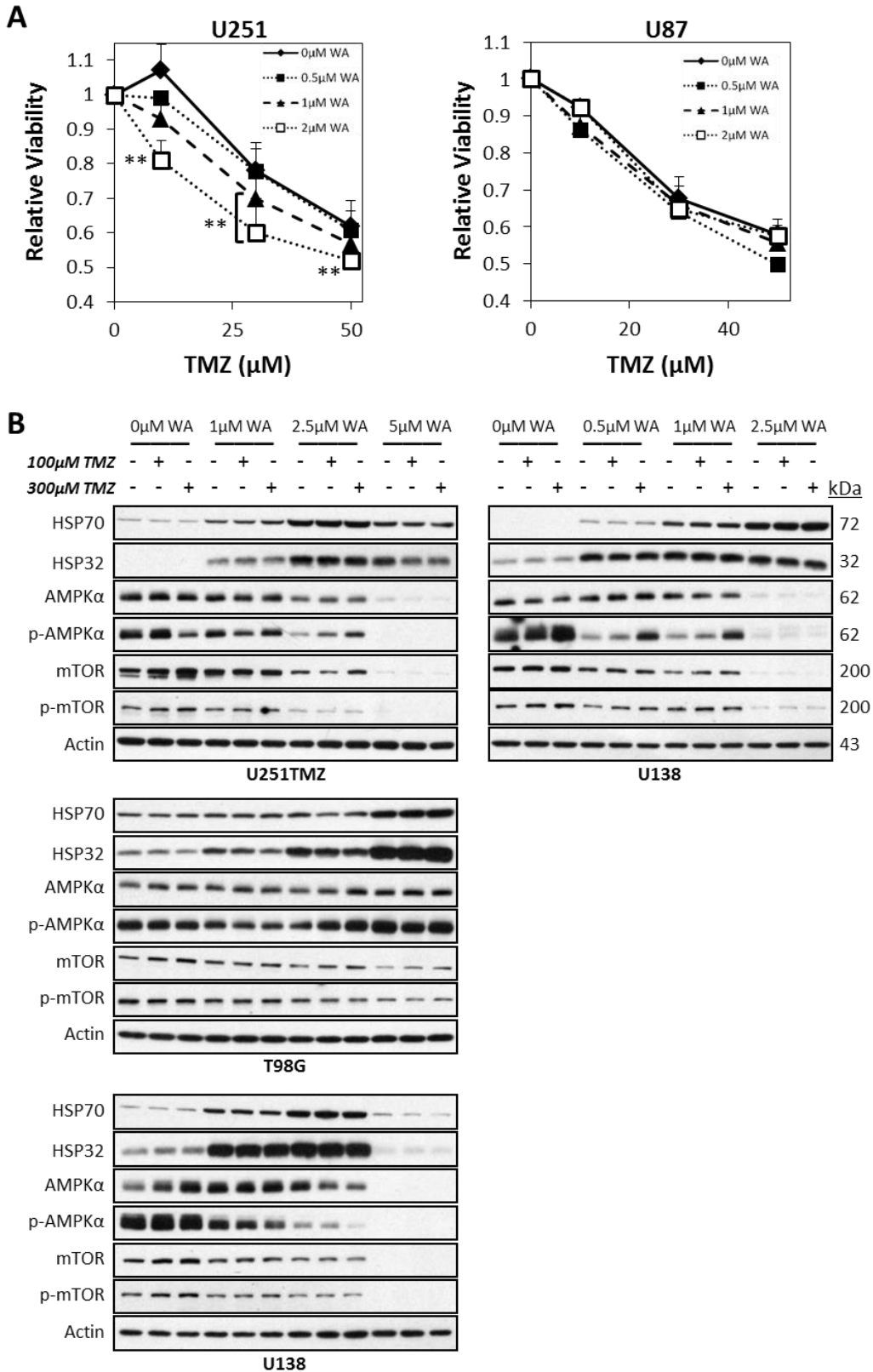
Supplemental Figure 3-2. A) 24 h WA pretreatment did not prevent TMZ efficacy in TMZ-sensitive U251 and U87 parental cells as assessed by a normalized MTS assay, suggesting a lack of inhibition of functional MMR. In U251 cells, WA mildly sensitized cells to TMZ, but no sensitization was observed in U87 cells. B) Given a described oxidative component of TMZ therapy through activation of AMPKα, markers of oxidation were assessed during combination therapy of WA and TMZ in TMZ-resistant cells. HSP32 and HSP70, known to be upregulated in response to oxidative stress, increased with WA treatment to a maximal level but were not further modulated by the presence of TMZ. Treatment with TMZ only resulted in elevated p-AMPKα in only U138 cells, but WA failed to further increase this phosphorylation in combination with TMZ. This was confirmed downstream by failure to further inhibit mTOR activation with combination therapy, suggesting efficacy of such treatment was not due to potentiated or synergized elevation in oxidation status. $**p < 0.01$

Chapter 4

Withaferin A is a novel inhibitor of the Wnt/β-catenin signaling pathway in medulloblasoma through proteasome-mediated degradation of TCF/LEF

4.1 Abstract

Pediatric medulloblastoma (MB) is a challenging tumor to approach therapeutically given significant tumor heterogeneity across patients. While current treatment options have led to an approximately 70% 5-year survival rate in children and adolescents, the off-target toxicity of these agents frequently manifests with chronic quality-of life impairments in these vulnerable patients, identifying a need for novel therapeutic options. Withaferin A (WA) has demonstrated notable anti-cancer efficacy against multiple cancer types through several oncogenic pathways, but its modulation of Wnt/β-catenin signaling, overactive in 10-15% of MB, has not been explored. Here, WA inhibited MB cell proliferation through dose-dependent G2/M cell cycle arrest and induction of apoptosis. Treatment with WA was demonstrated to function as a novel direct inhibitor of Wnt signaling as assessed by TOP FLASH reporter activity. Reduced signaling was mediated through proteasomal degradation the TCF/LEF transcription factors TCF1, TCF3, TCF4, and LEF1 and reduced interaction with β-catenin without significant alterations of β-catenin level or localization. This was associated with a reduction in total and phosphorylated levels of Akt and mTOR but elevations in inhibitory p-GSK-3β which was demonstrated pharmacologically to be independent of remaining Akt activity. Consistent with previous findings in other models, WA treatment resulted in N-acetyl-L-cysteine-repressible cellular oxidation and dissociation of HSP90/Cdc37. While TCF/LEF members were not observed to directly associate with HSP90 or Cdc37, each was decreased following inhibition of HSP90 with N-terminal inhibitor 17-AAG, suggesting an indirect role for HSP90 in their stability. Taken together, these findings show both intriguing translational potential for WA as a

therapeutic agent against MB and other Wnt-driven cancers and a novel role for HSP90 in Wnt signaling, each warranting further exploration.

4.2 Introduction

Central nervous system (CNS) tumors, including the grade IV medulloblastoma (MB) of the posterior fossa, are the most common solid tumors of childhood, accounting for approximately 20% of all pediatric malignancies (Linabery and Ross, 2008). Medulloblastomas represent 25-30% of these primary lesions in children but can arising in individuals of all ages (Khatua et al., 2012). Although the 5-year survival rate for medulloblastomas in both children and adolescents is around 70%, therapeutic challenges remain to simultaneously address both treating the tumor and ensuring a high long-term quality of life in the pediatric patient population (Smoll, 2012). Current standards of care include surgical resection followed by craniospinal radiation and chemotherapeutic agents such as vincristine, lomustine, cyclophosphamide, carboplatin, and cisplatin (Khatua et al., 2012). However, because of significant morbidities associated with these agents, it has been reported that long-term survivors of childhood medulloblastoma suffer from endocrine, cognitive, and neurological complications with significant deficits in daily psychosocial functioning including driving, employment, independent living, and personal relationships (Boman et al., 2009; Frange et al., 2009).

Medulloblastomas are categorized in several unique molecular subgroups based on tumor genetics, cell histology, growth, and clinical outcome including sonic hedgehog (SHH), Wingless (Wnt), group 3, and group 4 (Northcott et al., 2012). SHH and Wnt are named due to upregulation and overactivation of these key signaling pathways. Specifically, the Wnt subgroup

of MB patients is characterized by aberrant overactivation of the canonical Wnt/β-catenin signaling pathway, often through inactivating mutations of the adenomatous polyposis coli (APC) and Axin1/2 proteins or overexpression of β-catenin (Kim et al., 2011). Although the Wnt subgroup represents 10-15% of total MB patients and is characterized by long-term survival rates of 90%, the challenges of conventional therapy persist with current patient morbidity and mortality largely due to the complications of therapy and the development of secondary malignancies rather than recurrence of the MB (Ellison et al., 2011; Kim et al., 2011; Taylor et al., 2012; Remke et al., 2013).

While a number of inhibitors have been identified that alter Wnt signaling at various points in the cascade (Voronkov and Krauss, 2013), only four agents are currently in human clinic trial against any malignacy: olaparib (poly(ADP-ribose) polymerase (PARP)/tankyrase inhibitor), veliparib (PARP/tankyrase inhibitor), LGK974 (porcupine inhibitor), and OTSA101-DTPA-90Y (radiolabeled antibody against frizzled-10) (MacDonald et al., 2014). Only PARP inhibition, described to destabilize β-catenin through Axin (Waaler et al., 2012), is under trial for MB with the latter two therapies failing to target the appropriate location in the signaling cascade given the mutations of MB. Given the heterogeneic nature of the disease supported by multiple subgroup classifications, there is a critical need for novel therapeutics that function to both target this critical aberrant signaling to maximize Wnt subgroup effect while maintaining generalized anti-tumor cytotoxicity in other subgroups lacking these specific signaling alterations.

Withaferin A (WA) is a cytotoxic steroidal lactone identified in several species of the *Solenceae* plant family that has demonstrated the ability to modulate multiple signaling pathways key to cancer proliferation and survival (Vanden Berghe et al., 2012; Vyas and Singh, 2014). Notably, in the brain tumor glioblastoma multiforme (GBM), WA functioned to reduce total and

phosphorylated levels of key oncogenic proteins in the Akt/mammalian target of rapamycin (mTOR) signaling pathway (Grogan et al., 2013; Grogan et al., 2014). The Akt/mTOR pathway establishes cross-talk with the Wnt/β-catenin pathway through glycogen synthase kinase-3β (GSK-3β) such that activation of Akt produces inhibitory phosphorylation of GSK-3β, a reduction in the phosphorylation of β-catenin, and enhanced stability of β-catenin. As such, inhibition of PI3 kinase (PI3K)/Akt signaling has been shown to inhibit the Wnt/β-catenin pathway in MB (Baryawno et al., 2010). We hypothesized that WA could act as a novel inhibitor of the Wnt pathway in MB by a similar mechanism. To date, WA has not been explored as a Wnt/β-catenin signaling inhibitor nor examine against MB.

Studies by our group and others have suggested that modulation of the Akt/mTOR pathway and the other diverse findings associated with WA treatment may be due to two underlying mechanisms which are explored here in MB: enhanced cellular oxidation (Malik et al., 2007; Widodo et al., 2010; Hahm et al., 2011; Mayola et al., 2011; Santagata et al., 2012; Grogan et al., 2013; Grogan et al., 2014) and inhibition of the heat shock protein (HSP) 90 protein chaperone axis including its disruption of its interactions with co-chaperone cell division cycle protein 37 (Cdc37) (Yu et al., 2010; Gu et al., 2014). Previous studies have identified that HSP90 associates with Wnt/β-catenin pathways proteins Axin1, GSK-3β, and β-catenin but that its inhibition only resulted in a cell line-dependent depletion of GSK-3β (Cooper et al., 2011; Liu et al., 2012). p53-regulated HSP90 function was shown to enhance Wnt signaling, but this was likely an indirect effect through phosphorylation of Akt and GSK-3β (Okayama et al., 2014). Direct inhibition of the Wnt/β-catenin pathway through HSP90 inhibition has not been demonstrated previously.

111

In this study, we explored the general cytotoxicity of WA, including evaluation of its described oxidative and HSP90 inhibitory effects, as a potential chemotherapeutic for MB and demonstrate for the first time that it functions in-part as a potent inhibitor of the canonical Wnt signaling pathway. Interestingly, our studies provide evidence that WA induces degradation of the transcription factor (TCF)/lymphoid enhancer-binding factor (LEF) family of transcription factors critical in Wnt signaling to inhibit pathway activity directly rather than through Akt/mTOR pathway cross-talk via GSK-3β. Maintenance of TCF/LEF proteins was shown to be indirectly dependent on HSP90 function with WA inducing disruption of the HSP90/Cdc37 interaction.

4.3 Materials and methods

4.3.1 Cell culture and general reagents

Four human pediatric medulloblastoma cell lines were acquired. DAOY adherent cells were obtained from American Type Culture Collection (ATCC; Manassas, VA). ONS76 adherent cells were generously donated by Dr. Michael D. Taylor (The Hospital for Sick Children, Toronto, Ontario, Canada), and D425(MED) and D283(MED) semi-adherent/suspension cells were kindly provided by Dr. Darell D. Begner (Duke University, Durham, NC). All cells were maintained in Dulbecco's modified Eagle's medium (DMEM #11995-065; Gibco, Grand Island, NY) supplemented with 10% fetal bovine serum (FBS; Sigma-Aldrich, St. Louis, MO), 1% penicillin/streptomycin (Gibco), 2% L-glutamine (200 mM; Gibco), 1% MEM-vitamin (100x; Hyclone, Logan, UT), and 1% MEM nonessential amino acids

(Sigma Aldrich) at a 37 °C humidified atmosphere of 5% CO_2 in air. Cells were utilized in experiments upon achieving exponential growth phase. Withaferin A was isolated as previously described (Samadi et al., 2010b). Propidium iodide (PI), RNase, N-acetyl-L-cysteine (NAC), and puromycin dihydrochloride were acquired from Sigma-Aldrich, Annexin V-FITC was obtained from BD Biosciences (San Diego, CA), and MG132 was purchased from Selleckchem (Houston, TX). 17-*N*-allylamino-17-demethoxygeldanamycin (17-AAG) was obtained from LC Laboratories (Woburn, MA).

4.3.2 MTS assay

Cells were plated at 2,000-4,000 cells/well in 50 µL in a 96-well plate and allowed to adhere and/or settle. After 6 h, cells were treated with various concentrations of WA to bring the total well volume to 100 µL and allowed to incubate for 72 h. Cell viability and proliferation was evaluated with the addition of the colorometric CellTiter96 Aqueous MTS assay reagent as per the manufacturer's instructions (Promega, Fitchburg, WI). Reagent was allowed to incubate with the cells for 1-4 h in a cell line-dependent manner, and absorbance was quantified at 490 nm on a BioTek Synergy 2 plate reader (BioTek, Winooski, VT).

4.3.3 CellTiter Glo assay

The CellTiter-Glo luminescent assay (Promega, Fitchburg, WI) was used to evaluate cell viability and proliferation through assessment of cellular ATP levels in experiments with the NAC pretreatment due to its reducing properties. Cells were plated as outlined in the MTS assay

113

in a white-walled 96-well plate. Where indicated, cells were pretreated with NAC for 1 h followed by WA. After 72 h, assay reagent was added to the wells as per the manufacturer's instructions and gently shaken for 10 minutes in the dark at room temperature. Well luminescence was measured on the BioTek Synergy 2 plate reader.

4.3.4 Cell cycle analysis

Cells were plated to ~50% confluency in the adherent lines or 125,000 cells/mL in the suspension lines and treated with various concentrations of WA for 24 h. At that time, total cells were collected, pelleted, fixed/permeablized, and stained with PI as previously described (Grogan et al., 2013). Cells were analyzed by flow cytometry on a BD LSRII (Becton Dickinson, San Diego, CA). Only living cells without DNA fragmentation were gated.

4.3.5 Apoptosis evaluation

Cells were plated and treated as described for cell cycle analysis. After 24 h, all cells were collected and processed as previously described (Grogan et al., 2013). Briefly, cells were washed once in Annexin binding buffer and subsequently stained with PI and Annexin V-FITV as per the manufacturer's instructions (BD Biosciences, San Diego, CA) for 20 minutes at 4 °C. Stained cells were washed twice with the Annexin binding buffer, resuspended in 400 µL of the buffer, and immediately analyzed by flow cytometry on the BD LSRII.

4.3.6 Immunoblotting

For general Western blotting, cells were plated as previously described for cell cycle analysis before treatment with WA or 17-AAG. Where indicated, cells were pre-treated with 5 mM NAC for 1 h. After 24 h, cells were harvested, and proteins were isolated in lysis buffer (40 mM HEPES, 2 mM EDTA, 10 mM sodium pyrophosphate decahydrate, 10 mM β-glycerophosphate disodium salt pentahydrate, 1% triton X-100 supplemented with 100 μM phenylmethylsulfonyl fluoride (PMSF), 1 mM Na_3VO_4, and 2 μL/mL protease inhibitor cocktail), quantified, separated by sodium dodecyl sulfate–polyacrylamide gel electrophoresis (SDS–PAGE), and transferred onto a Hybond nitrocellulose membrane as previously described (Samadi et al., 2011). 10-50 μg of protein sample was loaded per lane. Equal loading and transfer of sample was confirmed by blotting for actin levels. Studies were repeated for accuracy.

For nuclear and cytoplasmic fractionation of proteins, cells were grown and harvested as described. Washed cells were lysed in harvest buffer (10 mM HEPES pH 7.9, 50 mM NaCl, 0.5 M sucrose, 0.1 mM EDTA, and 0.5% triton X-100), incubated on ice for 5 minutes, and pelleted at 1,000 rpm. The supernatant was collected as the cytoplasmic fraction. The pellet was resuspended for one wash with buffer A (10 mM HEPES pH 7.9, 10 mM KCl, 0.1 mM EDTA, 0.1 mM EGTA) and subsequently repelleted. The supernatant was discarded. The pellet was then resuspended in buffer C (10 mM HEPES pH 7.9, 500 mM NaCl, 0.1 mM EDTA, 0.1 mM EGTA, 0.1% NP-40), vortexed periodically while incubating on ice for 15 minutes, and centrifuged at 14,000 rpm for 10 minutes at 4 °C. The supernatant was collected as the nuclear fraction. Proteins in the two fractions were quantified, prepared, separated, and immunoblotted identically to what was previously described. Histone H4 was used as a nuclear-only control. All buffers were supplemented with 100 μM PMSF, 1 mM Na_3VO_4, and 2 μL/mL protease inhibitor.

Triton X-100 soluble and insoluble fractionation was completed with triton soluble buffer (50 mM Tris-HCl pH 6.8, 150 mM NaCl, 1mM EDTA, 1 mM EGTA, 1% triton X-100) and insoluble buffer (50 mM Tris-HCl pH 6.8, 2% SDS) as previously described (Chen et al., 2008) supplemented with 100 µM PMSF, 1 mM Na_3VO_4, and 2 µL/mL protease inhibitor cocktail. In brief, cells were pre-treated with proteasome inhibitor MG132 for 1 h followed by WA for 24 h. Cells were collected as previously described, lysed with triton soluble buffer, and centrifuged at 14,000 rpm for 20 minutes at 4 °C. The supernatant was collected as the soluble fraction. The pellet was resuspended, washed once with soluble buffer, and repelleted by centrifuged at 14,000 rpm for 10 minutes. The pellet was resuspended in triton insoluble buffer and subsequently ground with a pestle, vortexed, and heated at 100 °C repeatedly for ~15 minutes to promote dissolution of the pellet. Any remaining debris was removed by centrifugation, and the supernatant was collected as the insoluble fraction. Proteins in the two fractions were prepared and evaluated as described above.

Primary rabbit antibodies against β-catenin (#9562; 1:1000), p-β-catenin (Ser33/37/Thr41; #9561; 1:1000), TCF1 (#2203; 1:1000), TCF3 (#2883; 1:1000), TCF4 (#2569; 1:1000), LEF1 (#2230; 1:1000), GSK-3β (#9315; 1:1000), p-GSK-3β (Ser9; #9323; 1:1000), c-myc (#9402; 1:1000), c-Met (#4560; 1:500), and Cdc37 (#4793; 1:1000) and primary mouse antibodies against Cyclin D_1 (#2926; 1:500) and histone H4 (#2935; 1:1000) were acquired from Cell Signaling Technology (Danvers, MA). Primary rabbit antibody for Axin2 (#MA5-15015; 1:1000) was acquired from Pierce Biotechnology (Rockford, IL). Primary mouse antibodies for survivin (sc-17779; 1:100) and FLAG (F1804; 1:1000) were purchased from Santa Cruz Biotechnology (Santa Cruz, CA) and Sigma-Aldrich, respectively. Secondary mouse anti-rabbit conformation specific HRP antibody (#5127; 1:1000) was obtained from Cell Signaling

Biotechnology and used for blotting in appropriate immunoprecipitation blotting. All other primary and secondary antibodies were used as previously described (Grogan et al., 2013).

4.3.7 Reactive oxygen species measurement

WA-mediated production of intracellular reactive oxygen species (ROS), particularly peroxides like H_2O_2, was measured through fluorescent conversion of the general oxidative stress indicator CM-H_2DCFDA (Molecular Probes, Grand Island, NY). All MB cells lines were preloaded with 20 µM CM-H_2DCFDA in 1x PBS at 37 °C for 1 h, washed once with phenol red-free DMEM supplemented with all aforementioned additives, and resuspended in the same medium. Cells were plated at 40,000 cells/well in a 96-well plate and treated with WA ± NAC after 30 minutes. Evaluation of fluorescence was completed on a BioTek Synergy 2 plate reader after 3-4 h with excitation and emission filters of 485 nm and 528 nm, respectively.

4.3.8 TOP/FOP FLASH reporter assay

A luciferase reporter vector for Wnt/β-catenin signaling activity through TCF/LEF DNA binding sites, TOP FLASH, and its negative control, FOP FLASH, along with vectors for wild-type (WT) β-catenin and overactive mutant S33Y-β-catenin (Kolligs et al., 1999) were generously provided by Dr. Eric R. Fearon (University of Michigan, Ann Arbor, MI). DAOY cells were transfected in bulk with reporter construct TOP FLASH or FOP FLASH and a renilla luciferase construct at a ratio of 100:1 along with either β-catenin vector or a pcDNA3 control vector using Lipofectamine 2000 (Life Technologies, Carlsbad, CA) as per the manufacturer's

117

instructions and plated at 7,500 cells/well in a white-walled 96-well plate (50 ng reporter, 0.5 ng renilla, and 400 ng respective β-catenin construct per well in 150 µL). The transfection and gene expression were allowed to occur over 24 h before the cells were treated with WA. Reporter and renilla luciferase activity were quantified after 24 h with the Dual-Luciferase Reporter Assay System (Promega) on a BioTek Syngery NEO plate reader (Winooski, VT). Each reaction was carried out in triplicate, and sample well values were normalized to the renilla signal.

4.3.9 Transfections

DAOY cells were transfected with S33Y-β-catenin-FLAG or a pcDNA3 vector and a puromycin cassette at a 12:1 ratio (6 µg:500 ng in a 6 cm dish) using Lipofectamine 2000 as per the manufacturer's instructions (Life Technologies). The cells were selected with 1.5 ug/mL puromycin, and surviving colonies were pooled. To verify expression of the S33Y-β-catenin, Western blotting for the attached FLAG-tag was carried out. The transfected cells were used as a model of constitutively active Wnt signaling for the outlined assays.

4.3.10 Real-time polymerase chain reaction (RT-PCR)

DAOY Vector or S33Y cells were plated, treated with WA, and harvested as described for cell cycle analysis. RNA was isolated using Qiagen RNeasy Mini Kit as per the manufacturer's instructions (Venlo, Limburg, Netherlands). Quality of the RNA was confirmed using a Nanodrop 2000 spectrophotometer (Thermo Scientific, Waltham, MA), and 400 ng of each RNA was transformed to cDNA with the High Capacity RNA-to-cDNA Kit as per the

manufacturer's instructions (Applied Biosystems, Foster City, CA) using a MyCycler Thermal Cycler (Bio-Rad Laboratories, Hercules, CA). Power SYBR Master Mix (Applied Biosystems) was combined with 10 ng of cDNA according to the manufacturer's directions, and the following primer pairs were used for amplification of mRNA/cDNA for survivin: sense 5'-GGCATGGGTGCCCCGACGTTG-3' and antisense 5'-CAGAGGCCTCAATCCATGGCA-3' (Ikeguchi et al., 2002), cyclin D_1: sense 5'-GCCGCAATGACCCCGCACGATTTC-3' and antisense 5'-TGCCTGGGCCCCTCAGATGTCCACACGT-3' (Seki et al., 2006), and GAPDH: sense 5'-TGATGACATCAAGAAGGTGGTGAAG-3' and antisense 5'-TCCTTGGAGGCCATGTGGGCCAT-3' (Evron et al., 2012) (Invitrogen, Carlsbad, CA). RT-PCR was carried out in a ViiA7 Real-Time PCR System (Applied Biosystems) with the standard SYBR Green amplification settings.

4.3.11 Co-immunoprecipitation (co-IP)

DAOY cells were plated, allowed to adhere overnight, and grown to ~50% confluency before treatment with WA. For co-IP of TCF/LEF proteins from IPed β-catenin, cells were treated with 5 μM WA for 4-8 h before cells were trypsinized, washed twice with 1x PBS, and pelleted. Pelleted cells were lysed in RIPA buffer (50 mM Tris-HCl pH 7.4, 150 mM NaCl, 1% NP-40, 0.5% sodium deoxycholate, and 0.1% SDS) supplemented with 100 μM PMSF, 1 mM Na_3VO_4, and 2 μL/mL protease inhibitor cocktail. Proteins were isolated and quantified as described for immunoblotting. 750 μg of each protein sample was brought to 300 μL in RIPA buffer, and 3 μL of anti-β-catenin antibody (1:100, Pierce Biotechnology #MA1-10056) was added to each tube except for a no-antibody control tube with untreated cell lysate. Tubes were

rocked at 4°C overnight before the addition of 20 µL of protein A/G PLUS-Agarose beads (Santa Cruz Biotechnology) for 2 h. Beads were washed 4x with RIPA buffer, and proteins were eluted with the addition of SDS buffer as used in immunoblotting for 10 minutes at 100 °C. Beads were cleared by centrifugation, and the supernatant was evaluated by immunoblotting.

Co-IP of Cdc37 from HSP90 was similar to this procedure but utilized cells treated for 4 h with varying concentrations of WA collected in a buffer consisting of 20 mM Tris HCl (pH 7.4), 100 mM NaCl, 2 mM DTT, 20 mM sodium molybdate dihydrate, and 0.5% NP-40 supplemented with 100 µM PMSF, 1 mM Na_3VO_4, and 2 µL/mL protease inhibitor cocktail. 2 mg of protein was IPed with 25 uL of anti-HSP90β antibody (1:12; Invitrogen #379400), and IPed proteins were isolated using 25 µL of protein G magnetic bead system as described by the manufacturer (Pierce Biotechnology). Proteins were eluted with the addition of SDS buffer as used in immunoblotting for 15 minutes rocking at room temperature.

4.3.12 Immunocytochemistry (ICC)

DAOY and ONS76 cells were plated to ~50% confluency in 8-well chamber slides (Nalge Nunc International, Penfield, NY) and treated with 1-2.5 µM WA for 24 h. Cells were fixed in 4% PBS-buffered paraformaldehyde at room temperature for 30m and washed three times with 1x PBS. Cell membranes were de-permeablized for 15 minutes in 1x PBS containing 0.3% triton X-100 and subsequently blocked in 5% goat serum (Cell Signaling Technology) in 1x PBS containing 0.15% triton X-100 shaking for 1 h. Cells were exposed to primary antibody in blocking solution overnight at 4 °C. Primary antibodies included TCF1 (1:50; Cell Signaling #2203), LEF1 (1:100; Cell Signaling #2230), and β-catenin (1:200; Pierce Biotechnology #MA1-

10056). After three washes with 1x PBS, secondary antibody (1:1000; anti-rabbit IgG Fab2 Alexa Fluor 555, Cell Signaling #4413; Anti-mouse IgG Fab2 Alexa Fluor 488, Cell Signaling #4408) was added to each well for 1 h at room temperature followed by an additional three washes. Coverslips were mounted on each slide with ProLong Gold Antifade with DAPI (Cell Signaling Technology), allowed to dry, and visualized on a Leica DM IRB microscope (Wetzlar, Germany) with Metamorph Basic software (version 7.7.3.0.; Molecular Devices; Sunnyvale, CA).

4.3.13 Data and statistical analysis

GraphPad Prism 6 (version 6.02; GraphPad Inc., San Diego, CA) was used to generate best-fit non-linear sigmoidal dose response curves for IC_{50} determination. Comparisons of differences between two or more means/values were determined by Student's unpaired t-test via the statistical functions of GraphPad Prism or Microsoft Excel 2010 software (version 14.0.6129.5000; Microsoft Corporation Redmond, WA). Densitometry, where indicated, was completed using ImageJ software (version 1.46r; Bethesda, MD). RT-PCR data was compared via the $\Delta\Delta$Ct method. Data are presented as mean values with error bars denoting standard deviation or standard error of the mean where appropriate. The levels of significance were set at *$p < 0.05$, **$p < 0.01$, and ***$p < 0.001$.

4.4 Results

4.4.1 WA reduces viability and proliferation of MB

General cytotoxicity and anti-proliferative effects induced by WA were evaluated by the MTS assay after 72 h exposure. IC_{50} values were determined to be 168.5 µM ± 7.3, 518.4 µM ± 28.8, 661.7 µM ± 73.9, and 614.4 µM ± 71.1 in DAOY, ONS76, D425, D283 MB cell lines, respectively, representing reduced cell number and viability with sub-micromolar concentrations (Figure 4-1A).

4.4.2 WA prevents cell proliferation through G2/M cell cycle arrest

To examine the nature of the observed anti-proliferative effect of WA in MB, shifts in cell cycle distribution were analyzed by flow cytometry after 24 h (Figure 4-1B and 4-1C). Supporting the general cytotoxicity of the MTS assay, WA demonstrated the ability to induce large elevations in the fraction of MB cells in G2/M, suggesting arrest of the cell cycle. DAOY cells demonstrated a peak G2/M fraction of 77.6% at 0.5 µM compared to a baseline control of 22.2% ($p = 0.004$) and a statistically significant ($p < 0.05$) elevation from 0.5-1 µM. Similarly, ONS76 cells demonstrated a peak G2/M fraction of 59.4% at 1 µM compared to a baseline control of 25.3% ($p = 0.002$) and a statistically significant ($p < 0.05$) elevation from 0.75-2 µM. The fraction of cells in S-phase was slight diminished, but G2/M elevation was shown to be largely at the expense of G0/G1. WA levels above those inducing peak G2/M arrest showed diminishing responses with increasing concentration. These findings were also observed in D425 and D283 cells (Supplemental Figure 4-1A).

Induction of G2/M cell cycle arrest was molecularly confirmed through evaluation of G2/M-specific protein cyclin B_1 (Figure 1D). Both DAOY and ONS76 cells showed WA dose-

Figure 4-1.
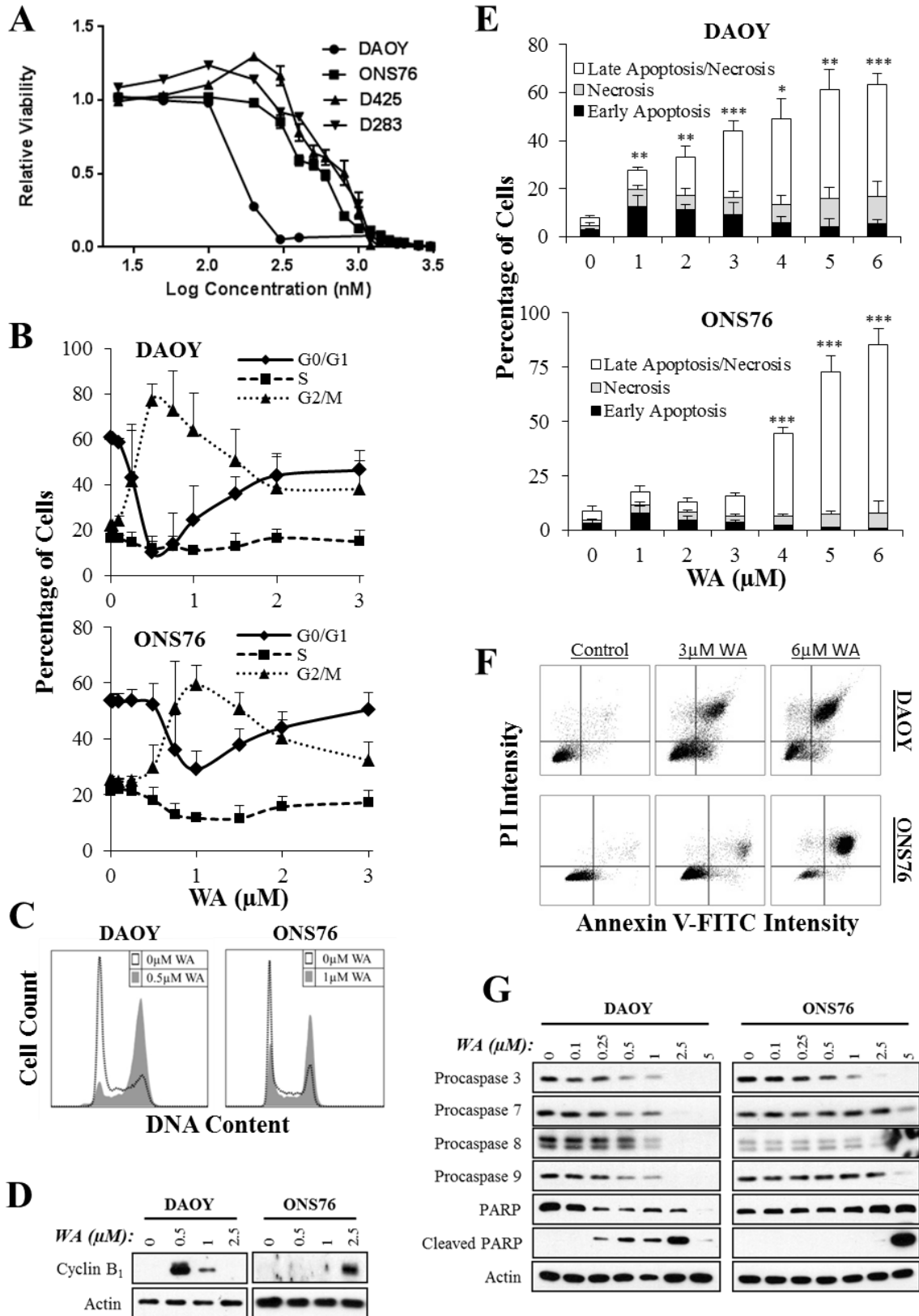
Figure 4-1. A) IC_{50} values were determined by MTS assay to be 168.5 µM ± 7.3, 518.4 µM ± 28.8, 661.7 µM ± 73.9, and 614.4 µM ± 71.1 in DAOY, ONS76, D425, D283 MB cell lines, respectively. B) Cells stained with propidium iodide and analyzed by flow cytometry revealed that WA induces a dose-dependent G2/M cell cycle at 24 h. Maximal induction of arrest above baseline was observed at 0.5 µM in DAOY and 1 µM in ONS76. C) Cell cycle arrest corresponded with induction of G2/M-specific protein cyclin B_1 with highest levels at 0.5 µM and 2.5 µM in DAOY and ONS76, respectively. D) Histograms depict representative examples for the cell cycle distribution of control (white/transparent) and WA-treated (grey) DAOY and ONS76 cells at concentrations inducing a peak effect. E) DAOY and ONS76 cells stained with propidium iodide and annexin V-FITC and analyzed by flow cytometry revealed that WA induced a dose-dependent increase of cell death with a progressive shift from early apoptosis to late apoptosis at 24 h. F) The presence of WA-induced apoptotic processes in DAOY and ONS76 was confirmed by Western blotting that demonstrated dose-dependent reduction in initiator procaspases 8 and 9 and effector procaspases 3 and 7. Downstream cleavage of PARP was observed by 0.25 µM and 2.5 µM in DAOY and ONS76 cells, respectively. G) Dot plots display representative examples of each cell line demonstrating a progressive shift from early to late apoptosis with increasing WA concentration. $*p < 0.05$, $**p < 0.01$, $***p < 0.001$

124

dependent induction of the protein with peak levels observed at 0.5 and 2.5 µM, respectively, supporting the flow cytometry data indicating that G2/M elevation is achieved at lower doses in DAOY. These findings were supported with D425 cells (Supplemental Figure 4-1B).

4.4.3 WA induces dose-dependent cell death through apoptosis

Induction of cellular death through apoptotic and necrotic mechanisms was assessed by flow cytometry with annexin V-FITC/PI staining to further characterize the general cytotoxic effects observed from WA. WA induced dose-dependent cellular death with increasing concentrations in both DAOY and ONS76 cells (Figures 4-1E and 4-1F). Elevation in early apoptosis through annexin V-only staining was notable at low concentrations for DAOY (1-3 µM) at 24 h with increases in dual staining indicative of late apoptosis observed at the higher concentrations evaluated in both DAOY (1-6 µM) and ONS76 (4-6 µM). Each cell line also demonstrated small increases in the PI-only necrotic population with increasing concentrations that did not reach above 11.5% and 7.3% in DAOY and ONS76, respectively. Total cell death staining in control DAOY and ONS76 was 8.0% and 8.7% but elevated to 43.9% ($p < 0.001$; 9.4% early apoptosis, 6.9% necrosis, 27.6% late apoptosis) and 15.9% ($p = 0.100$; 3.7% early apoptosis, 2.9% necrosis, 9.3% late apoptosis) with 3 µM WA, respectively. Cell death was further increased with 6 µM WA to 63.2% ($p < 0.001$; 5.6% early apoptosis, 11.2% necrosis, 46.3% late apoptosis) and 85.5% ($p < 0.001$; 0.8% early apoptosis, 7.3% necrosis, 77.4% late apoptosis), respectively. Consistent with the MTS findings, ONS76 cells required higher WA concentrations than DAOY to achieve cytotoxicity. D425 and D283 cells also exhibited dose-dependent elevations in cell death (Supplemental Figure 4-1C).

The role of apoptotic processes was confirmed molecularly through protein evaluation of procaspase and poly(ADP-ribose) poylmerase biomarkers (Figure 4-1G). Consistent with our previous report that WA-mediated apoptosis in GBM is driven through both the mitochondrial/intrinsic and extrinsic apoptotic pathways, WA treatment of DAOY and ONS76 MB cells resulted in depletion of extrinsic procaspase 8, intrinsic procaspse 9, and effector caspases 3 and 7 upon exposure to approximately 0.5-2.5 µM WA for 24 h with higher concentrations consistently required for ONS76 to achieve the same effect. Downstream cleavage of PARP was observed by 0.25 µM and 2.5 µM in DAOY and ONS76 cells, respectively. Procaspase depletion and PARP cleavage were also observed in D425 and D283, however, PARP cleavage was notably less in D283, consistent with flow cytometry findings suggesting a greater necrotic role (Supplemental Figure 4-1D). Together, these data support the role of apoptosis in the induction of WA-mediated cell death.

4.4.4 WA promotes an NAC-repressible elevation in cellular oxidation

Elevation of the oxidative potential has been a previously described effect in several cancer cell lines following WA treatment and has been suggested to play a partial role in its overall cytotoxicity profile. Therefore, the presence and role of WA-generated oxidative stress was evaluated to determine if it could be functionally extended into a MB model. Peroxide-type reactive oxygen species (ROS) were measured following 3-4 h WA treatment through activating conversion of preloaded CM-H$_2$DCFDA to a fluorescent byproduct (Figure 4-2A). ROS were elevated at 1, 3, and 5 µM WA by 5.3% (p = 0.031), 16.3% (p < 0.001), and 33.8% (p = 0.009) in DAOY and 14.6% (p = 0.037), 37.8% (p = 0.07), and 94.2% (p = 0.048), respectively.

Figure 4-2.
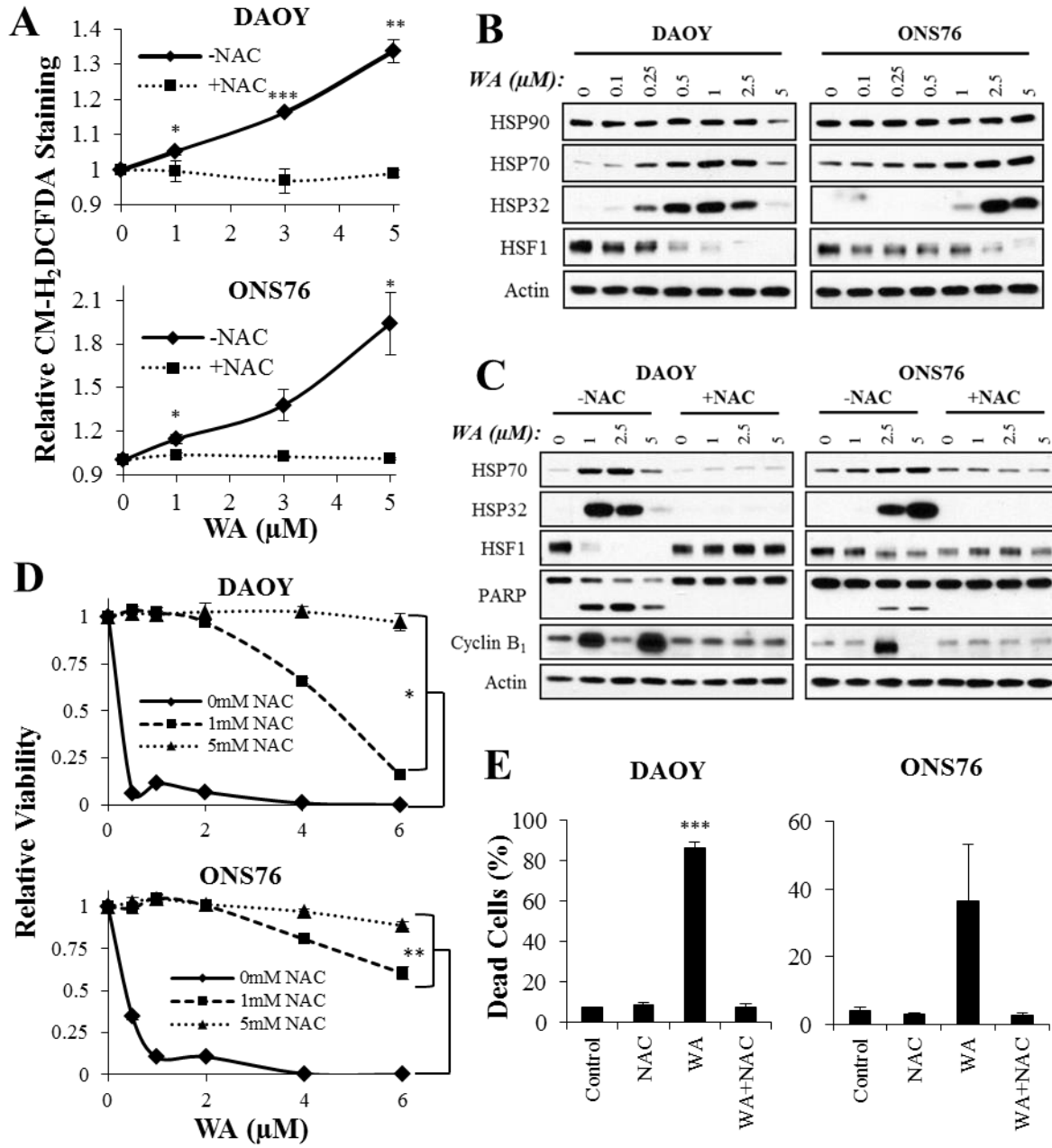
Figure 4-2. A) Increases in the concentration of WA generated peroxide-type radicals like H_2O_2 as quantified by CM-H_2DCFDA fluorescent conversion in DAOY and ONS76 cells at 3-4 h post-treatment. 5 mM NAC thiol antioxidant completely abrogated the elevation in ROS. B) Consistent with a cellular oxidative stress response, HSP32 and HSP70 were induced with increasing WA treatment with corresponding depletion of transcription factor HSF1 in both DAOY and ONS76. Total levels of HSP90 remained largely unchanged in both lines. C) Pretreatment of DAOY and ONS76 cells with 5 mM NAC eliminated WA-induced upregulation of HSP32 and HSP70 and the decrease of HSF1. Similarly, NAC abrogated the cleavage of PARP and induction of cyclin B_1, demonstration reduction in the molecular apoptotic and checkpoint processes. D) DAOY and ONS76 cell viability assessed by ATP levels in the CellTiter Glo assay was increased with NAC pretreatment in the presence of WA. E) WA-mediated induction of overall cell death assessed by flow cytometry of total propidium iodide and annexin V-FITC staining was eliminated with NAC pretreatment. NAC alone had no effect on cell viability. $*p < 0.05$, $**p < 0.01$, $***p < 0.001$

Pretreatment with the thiol antioxidant NAC (5 mM) completely abrogated the elevation of ROS. The pattern of NAC-repressible dose-dependent increases in cellular oxidative potential was also observed in D425 and D283 cells (Supplemental Figure 4-2A).

Elevation in oxidative potential following WA was supported molecularly by the induction of HSPs as has been previously described. Consistent with an oxidative stress-induced heat shock response, DAOY and ONS76 cells displayed dose-dependent increases in HSP70 and HSP32/heme oxygenase 1 with minimal changes in HSP90 levels by 0.1-0.25 μM and 0.5-1 μM WA after 24 h, respectively (Figure 4-2B). Transcription factor heat shock factor 1 (HSF1), a regulator of HSP70 expression, was reduced with an inverse correlation to HSP70 upregulation. Pretreatment with 5 mM NAC completely eliminated induction of the WA-mediated heat shock response (Figure 4-2C). This pattern of altered protein levels was also confirmed to occur in D425 and D283 (Supplemental Figures 4-2B and 4-2C).

WA cytotoxicity in MB was functionally reduced or eliminated following pretreatment with NAC. General cellular cytotoxicity was evaluated at 72 h by the ATP-measuring CellTiter-Glo luminescent assay. Pretreatment with 1 mM NAC showed retention of viability in both DAOY ($p < 0.05$) and ONS76 ($p < 0.01$) up to the highest WA concentration evaluated (6 μM), but reduction in cell viability was completely abrogated with 5mM NAC (DAOY: $p < 0.01$; ONS76: $p < 0.001$) (Figure 4-2D). Similarly, cell death evaluated by annexin V-FITC/PI staining at 24 h revealed that 5 mM NAC pretreatment completely eliminated the effects of 5 μM WA in both DAOY ($p < 0.001$) and ONS76 ($p = 0.070$) (Figure 4-2E). Cells treated with NAC ± WA were not statistically different than control. NAC-mediated reduction of cell death was confirmed in D425 ($p < 0.001$) and D283 ($p < 0.001$) cells (Supplemental Figure 4-2D and 4-2E). Molecularly, diminished apoptosis was supported by the elimination of PARP cleavage with

NAC pretreatment. Similarly, NAC abrogated the cyclin B_1 induction of 24 h WA treatment, suggesting the prevention of G2/M cell cycle arrest (Figure 4-2C; Supplemental Figure 4-2C). Together, these results suggest that WA may manifest its effects in MB through oxidation and thiol reactivity, either directly or indirectly.

4.4.5 WA induces inhibitory phosphorylation of GSK-3β independent of alterations in Akt/mTOR pathway signaling

Previous studies have demonstrated that WA can functionally alter signaling and total proteins levels within the PI3K/Akt/mTOR proliferation pathway (Oh et al., 2008; Oh and Kwon, 2009; Samadi et al., 2010a; Samadi et al., 2010b; Grogan et al., 2013; Grogan et al., 2014). This pathway has been well-described in altering the Wnt/β-catenin signaling pathway, an important and over-active cascade in a subset of MB patients, through inhibition of GSK-3β to prevent proteasomal degradation of β-catenin (Baryawno et al., 2010). As such, the effects of WA on total and phosphorylated protein levels in the Akt/mTOR cascade were evaluated along with the resulting manifestations on GSK-3β and β-catenin.

Akt/mTOR signaling in MB cells lines DAOY, ONS76, D425, and D283 demonstrated variable downstream responses to WA exposure after 24 h (Figure 4-3A). With the exception of unchanged Akt levels in ONS76, total levels of Akt and mTOR were reduced in all cell lines in a dose-dependent manner with complete depletion of Akt occurring at 2.5-5 μM WA. Complete elimination of mTOR was observed at 2.5 μM in DAOY and D425 but was not achieved by 5 μM in ONS76 and D283 despite reduction. Activating phosphorylation of Akt (Ser473) and mTOR (Ser2448) similarly patterned the loss of total protein except for a failure to decrease p-

Figure 4-3.
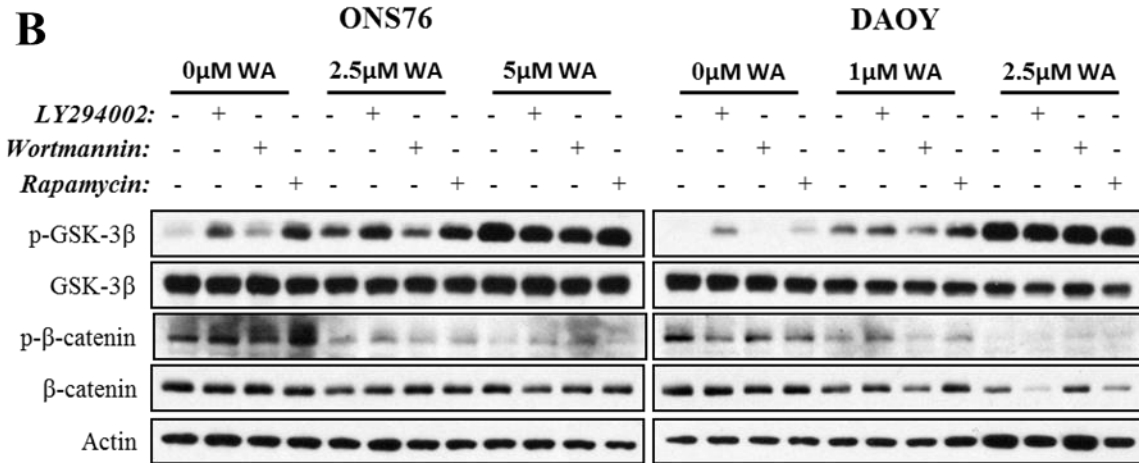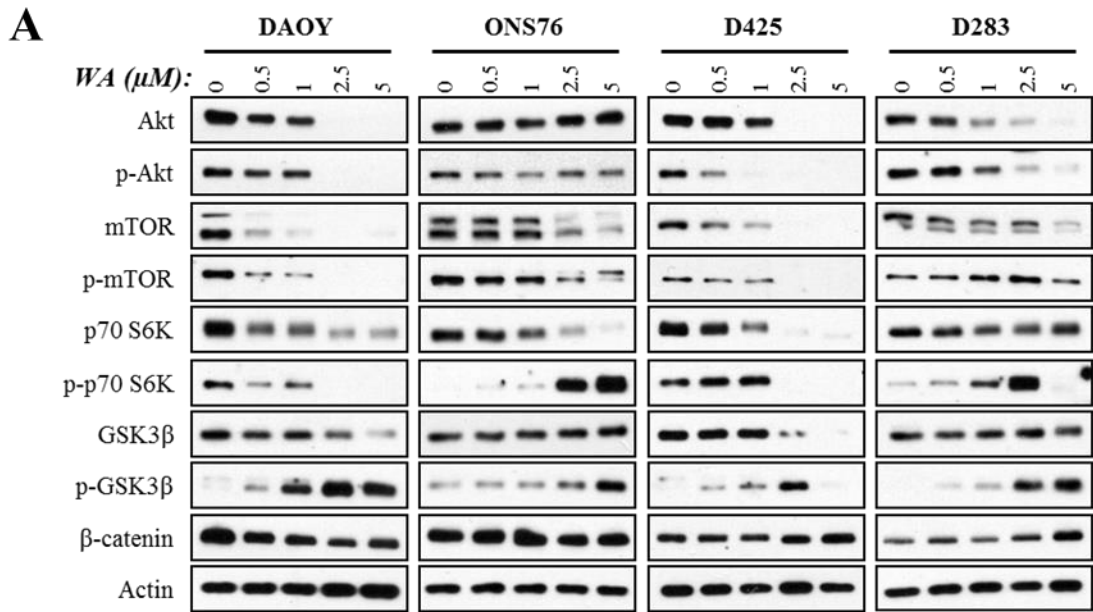
Figure 4-3. A) Akt/mTOR signaling in MB cells lines DAOY, ONS76, D425, and D283 demonstrated variable downstream responses to WA exposure after 24 h. All lines demonstrated reduction or maintenance of total and phosphorylated/active levels of Akt (Ser473) and mTOR (Ser2448) with WA treatment. While total p70 S6K was reduced or sustained in all cell lines, activation of p70 S6K through phosphorylation (Thr389) demonstrated significant variability with DAOY and D425, the cell lines with the highest WA-mediated Akt and mTOR depletion, demonstrating reductionand ONS76 and D283 potently inducing this phosphorylation. Despite diminished p-Akt, phosphorylation of GSK-3β (Ser9) was significantly induced with minimal changes in total β-catenin levels. B) Pharmacological inhibition of PI3K, upstream of Akt, with LY294002 or wortmannin was conducted 1 h prior to WA treatment to evaluate the responsibility of residual p-Akt for phosphorylating GSK-3β. Rapamycin, an inhibitor of mTOR downstream of Akt, was used as a pathway control. All inhibitors failed to prevent WA-induced phosphorylation of GSK-3β, demonstrating that that the observation was independent of Akt signaling.

mTOR in D283 by 5 µM WA. Downstream of mTOR, total p70 S6K was reduced or sustained in all cell lines. However, activation of p70 S6K through phosphorylation (Thr389) demonstrated significant variability. DAOY and D425, the cell lines with the highest WA-mediated Akt and mTOR depletion, displayed consistent reduction of p-p70 S6K initiating at 0.5 µM and 2.5 µM, respectively. In contrast, p-p70 S6K was potently induced through 5 µM WA in ONS76 despite decreases in total protein and through 2.5 µM WA in D283 before reduction at 5 µM in the latter. This suggests either maintained or enhanced activity of Akt/mTOR signaling despite diminished phosphorylation or the presence of alternative and compensatory cell-specific signaling.

Despite decreased or sustained levels of p-Akt in all cell lines with WA treatment, inhibitory phosphorylation of GSK-3β (Ser9), a target of Akt, was induced in all lines by 0.5-1 µM (Figure 4-3A). Total levels of GSK-3β were largely maintained except at high doses in D425 which also resulted in a loss of p-GSK-3β. Consistent with active GSK-3β normally functioning to promote the proteasomal degradation of β-catenin, total levels of β-catenin after 24 h WA treatment remained largely consistent with minimal increases and/or decreases in a cell-dependent manner.

In order to determine if phosphorylation of GSK-3β was a result of residual Akt activity following WA exposure, pharmacological inhibition of PI3K, upstream of Akt, with LY294002 or wortmannin was conducted prior to WA treatment. Rapamycin, an inhibitor of mTOR downstream of Akt, was used as a pathway control. All inhibitors failed to prevent WA-induced phosphorylation of GSK-3β, demonstrating that that the phenomenon was likely independent of Akt signaling (Figure 4-3B). Treatment with the inhibitors alone actually induced mild to moderate phosphorylation of GSK-3β, suggesting compensatory activation of the Wnt pathway through an alternate mechanism. As expected, WA-induced p-GSK-3β correlated with

diminished phosphorylation of β-catenin (Ser33/37/Thr41), a marker for degradation, and maintenance of total protein levels. Interestingly, LY294002 and rapamycin pretreatment before 2.5 µM WA in DAOY cells promoted diminished β-catenin despite not altering its phosphorylation.

4.4.6 WA inhibits the Wnt/β-catenin signaling pathway

To evaluate if inhibition of GSK-3β and maintenance of β-catenin levels following WA treatment led to altered signaling in the Wnt/β-catenin pathway, the TOP/FOP FLASH reporter assay was employed to determine pathway activation and function (Figure 4-4A). DAOY cells were co-transfected with either the TOP FLASH or FOP FLASH reporter and a renilla luciferase control as well as WT-β-catenin, the constitutively active S33Y-β-catenin mutant, or a vector control. After 24 h, cells were treated with 1 µM WA for an additional 24 h and quantified. Negatively control reporter FOP FLASH failed to demonstrate significant signal induction under all conditions. While vector DAOY cells displayed minimal endogenous TOP FLASH reporter activation, the addition of extra WT and S33Y β-catenin increased reporter activation 17.1- and 118.8-fold, respectively. Treatment with WA reduced WT-β-catenin signal by 46.4% (p = 0.073) and S33Y-β-catenin signal by 64.1% (p < 0.001), showing that WA, in part, acts as an inhibitor of the Wnt/β-catenin signaling pathway. This is in contrast to the findings that demonstrate the stabilization of β-catenin following WA treatment and suggests that this retention of β-catenin may be a cellular compensatory attempt to maintain pathway activity despite downstream inhibition.

Figure 4-4.
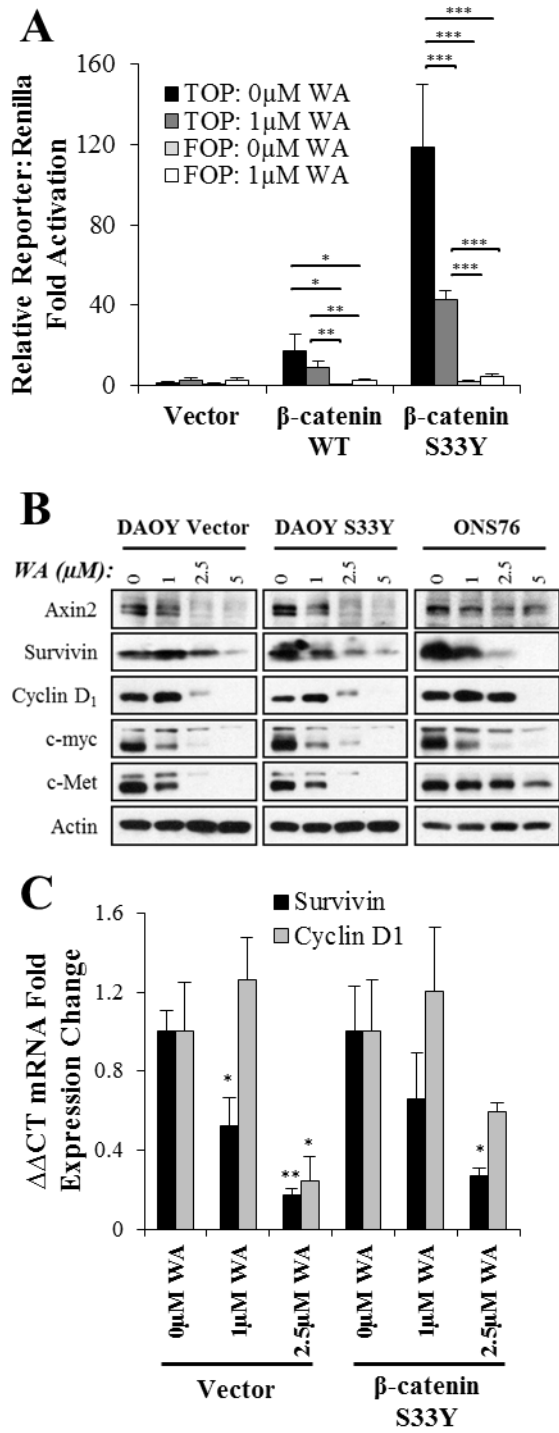
Figure 4-4. A) WA reduced activity of the TOP FLASH luciferase reporter assay for Wnt signaling activity after 24 h when activated with excess WT-β-catenin and constitutively the active S33Y-β-catenin mutant in DAOY cells. Negative control reporter FOP FLASH yielded minimal luminescent signal. All signals were normalize to the renilla control. B) Protein levels of known Wnt signaling target genes (axin2, survivin, cyclin D_1, c-myc, and c-Met) were reduced in DAOY Vector, DAOY S33Y, and ONS76 cells with increasing exposure to WA for 24h. C) mRNA levels of Wnt signaling target genes survivin and cyclin D_1 were evaluated through RT-PCR following 24 h WA treatment in DAOY Vector and DAOY S33Y cells. Consistent with the protein levels, both genes demonstrated a dose-dependent decrease in transcription of mRNA for each gene. $*p < 0.05$, $**p < 0.01$, $***p < 0.001$

Protein levels of known Wnt signaling target genes (Axin2, survivin, cyclin D_1, c-myc, and c-Met) were subsequently assessed to further evaluate and confirm functional manifestations of the inhibition. DAOY cells were stably transfected with S33Y-β-catenin ("DAOY S33Y") or vector ("DAOY Vector") to establish a model of constitutively active Wnt signaling. DAOY Vector, DAOY S33Y, and ONS76 cells were treated with WA for 24 h and evaluated by Western blotting. Each target protein was reduced in a dose-dependent manner with initial efficacy seen between 1-2.5 μM in both DAOY lines and 1-5 μM in ONS76, supporting inhibition of Wnt signaling (Figure 4-4B). Decreases in these proteins were also confirmed in D425 and D283 (Supplemental Figure 4-3A).

To ensure protein decreases were not simply due to WA-induced degradation, transcriptional level evaluation was performed through RT-PCR to quantify mRNA for target genes survivin and cyclin D_1 following WA treatment in DAOY Vector and DAOY S33Y cells (Figure 4-4C). Consistent with the protein levels, 1 μM and 2.5 μM WA decreased mRNA levels of survivin in DAOY Vector by 47.4% (p = 0.012) and 82.5% (p = 0.004), respectively, and in DAOY S33Y by 34.0% (p = 0.162) and 73.0% (p = 0.028), respectively. Also supported by protein reduction, mRNA for cyclin D_1 was decreased only at 2.5 μM WA by 75.5% in DAOY Vector (p = 0.019) and 40.4% in DAOY S33Y (p = 0.105).

4.4.7 WA disrupts Wnt signaling through depletion of TCF/LEF transcription factors and without blocking nuclear translocation of β-catenin

Having established functional inhibition of the Wnt signaling pathway with WA treatment despite the maintenance of total levels of β-catenin, the inhibitory mechanism of WA

on downstream Wnt signaling was evaluated. In addition to decreases of β-catenin levels, Wnt-specific signaling reduction can manifest through failure of β-catenin to translocate to the nucleus or subsequently associated with the necessary transcription factor of the TCF/LEF family.

Changes in nuclear translocation of β-catenin in the presence of WA were assessed by nuclear and cytoplasmic protein fractionation of DAOY Vector and S33Y lines (Figure 4-5A). Consistent with the initial evaluation of β-catenin following WA treatment in DAOY cells, total levels of the endogenous protein were slightly diminished but largely unchanged after 24 h. In both lines, nuclear levels of total β-catenin were decreased at 5µM WA with slight increases in cytoplasmic levels compared to 2.5 µM WA, suggesting possible disruption of translocation at high doses. However, this was associated with slight reduced nuclear histone H4, and it is unclear if the small shift is mechanistically relevant at a high concentration of WA. Similarly, total levels of nuclear S33Y-β-catenin, observed only in the DAOY S33Y line, were reduced only at 5 µM WA, but this was also observed in the cytoplasmic fraction, suggesting a global decrease rather than alterations in translocation. Further, reduced levels of cytoplasmic WT- and S33Y-β-catenin at 1-2.5 µM WA were not matched in the nuclear fraction, demonstrating maintained translocation and localization of remaining β-catenin with WA treatment. ICC of β-catenin with DAPI in DAOY and ONS76 cells confirmed minimal changes in nuclear β-catenin levels up to 2.5µM WA (Figure 4-5B; Supplemental Figure 4-3B).

Upon entering the nucleus, β-catenin is known to function as a co-activator that associates with members of the TCF/LEF transcription factor family to promote transcription of Wnt pathway target genes (Voronkov and Krauss, 2013). Because failure of β-catenin to associate with these factors prevents proper activation of transcription at these target genes, total

Figure 4-5.
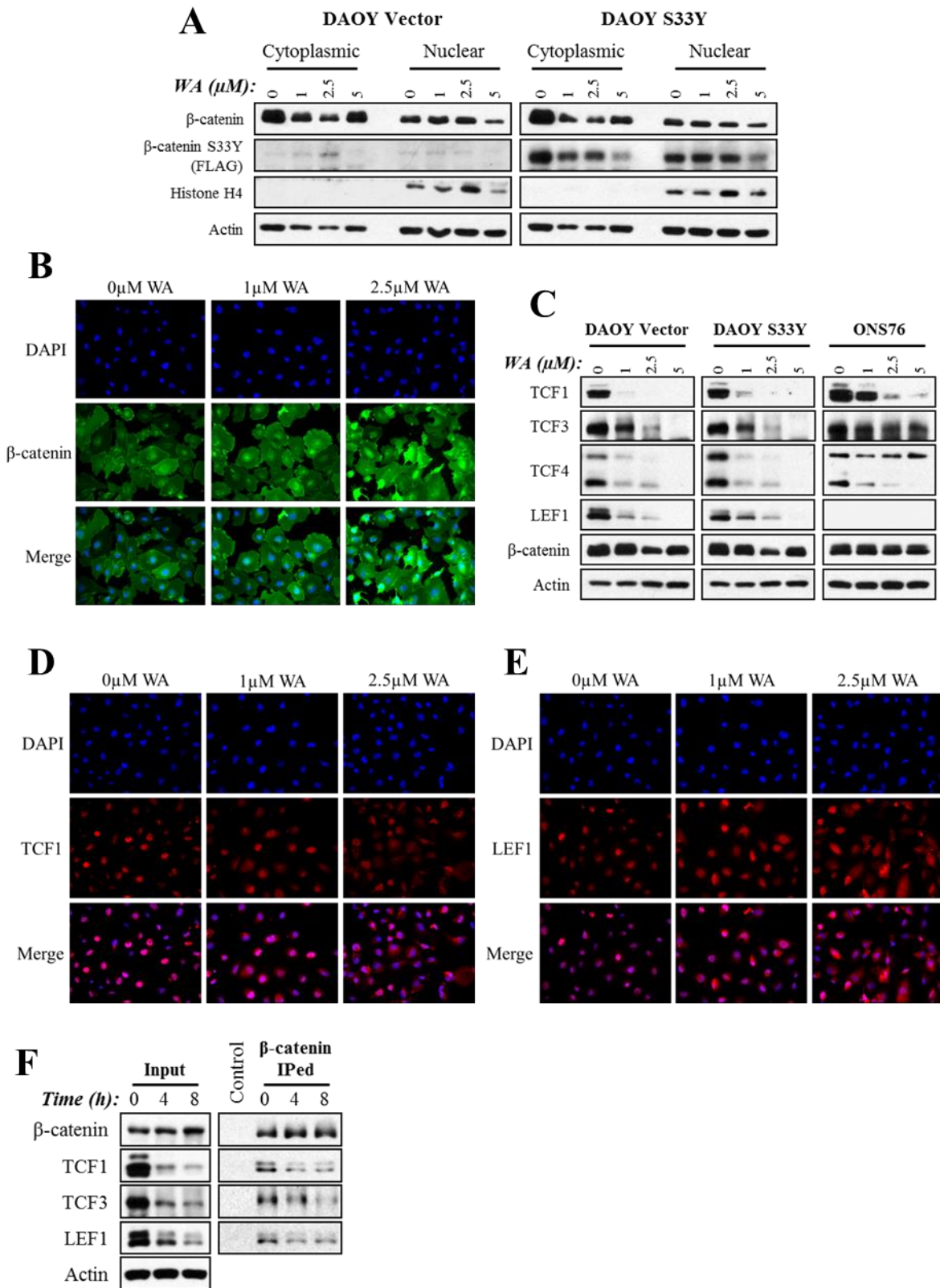
Figure 4-5. A) Changes in nuclear translocation of β-catenin in the presence of WA were assessed by nuclear and cytoplasmic protein fractionation of DAOY Vector and DAOY S33Y lines. Total levels of the endogenous protein were slightly diminished after 24 h. In both lines, nuclear levels of total β-catenin were decreased at 5 µM WA with slight increases in cytoplasmic levels compared to 2.5 µM WA, suggesting possible disruption of translocation at high doses. Similarly, total levels of nuclear S33Y-β-catenin, observed only in the DAOY S33Y line, were reduced only at 5 µM WA in both fractions. B) ICC of β-catenin (green) with DAPI (blue) in DAOY cells confirmed minimal changes in nuclear β-catenin levels. C) Total levels of TCF/LEF transcription factors TCF1, TCF3, TCF4, and LEF1 were assessed in DAOY Vector, DAOY S33Y, and ONS76. In each cell line, all proteins, including both detected isoforms of TCF4, were notable depleted by WA in a dose-dependent manner after 24 h. LEF1 was not detected in ONS76. D and E) ICC of TCF1 and LEF1 (red) in DAOY cells revealed diminished staining intensity and/or a shift from the nucleus to the cytoplasm after 1-2.5 µM WA for 24 h. F) Co-IP experiments revealed decreased β-catenin association with TCF/LEF members after treatment with 5 µM WA for up to 8 h, demonstrating that reductions in total proteins also corresponded with diminished functional interactions.

levels of TCF/LEF family members TCF1, TCF3, TCF4, and LEF1 were assessed in DAOY Vector, DAOY S33Y, and ONS76. In each cell line, all proteins, including both detected isoforms of TCF4, were notable depleted by 1μM WA after 24 h with near-complete elimination by 5 μM except for both TCF3 and the 79kDa TCF4 isoform in ONS76. LEF1 was not detected in ONS76 (Figure 4-5C). Depletion of each protein was confirmed in the additional MB cell lines D425 and D283 (Supplemental Figure 4-3C).

ICC of TCF1 and LEF1 in DAOY cells revealed diminished staining intensity and/or altered cellular localization of the proteins after 1-2.5 μM WA (Figures 4-5D and 4-5E). Control cells showed near-complete overlap of nuclear DAPI staining and both TCF1 and LEF1. Treatment with WA induced diffusion of both proteins into the cytoplasmic region with diminished nuclear staining intensity. While negative for LEF1, ONS76 cells demonstrated the same pattern of TCF1 alteration (Supplemental Figure 4-3D).

Depletion and delocalization of TCF/LEF proteins would be expected to diminish transcription of Wnt signaling target genes given a reduced transcription factors available for β-catenin association upon entering the nucleus. Co-IP was conducted to evaluate β-catenin association with TCF/LEF members after treatment with WA (Figure 4-5F). DAOY cells were treated with 5 μM WA for up to 8 h. At 8 h, total levels of TCF1, TCF3, and LEF1 input were decreased 82.8%, 75.1%, and 71.9% normalized to actin, respectively. Conversely, total β-catenin was elevated by 50.9%. IPed β-catenin showed levels of TCF1, TCF3, and LEF1 that were decreased 70.1%, 58.1%, and 56.1% normalized to β-catenin, respectively. This confirms that total depletion of TCF/LEF proteins also resulted in functional reduction of the association between these transcription factors and β-catenin.

4.4.8 WA-mediated degradation of TCF/LEF proteins is mediated by the proteasome

Triton X-100 fractionation and pretreatment with proteasome inhibitor MG132 were completed to further define WA-mediated alterations in TCF/LEF localization and degradation (Figure 4-6A). Triton soluble proteins are largely regarded as functional, stable molecules, whereas the insoluble fraction contains labile and aggregated proteins. Treatment of DAOY and ONS76 cells with 2.5 µM WA for 24 h resulted in a depletion of triton soluble proteins with variable accumulation in the insoluble fraction. Exploration of these findings suggested that early timepoints (defined relatively in part by dose and cell line sensitivity) following treatment with WA shifted proteins from the soluble to insoluble fractions with later timepoints resulting in absolute depletion in both fractions (data not shown). Consistent with previous reports, MG132 blocked normal protein turnover, inducing cellular stress and a shift of proteins to the insoluble fraction (Kawahara et al., 2008). Cells pretreated with MG132 before WA demonstrated enhanced retention of all TCF/LEF proteins in the insoluble fraction at 24 h, including proteins that were depleted by WA in both the soluble and insoluble fractions and demonstrating the proteasome-dependent manner of WA-mediated TCF/LEF degradation.

4.4.9 TCF/LEF proteins require functional HSP90 for stability and WA disrupts the HSP90/Cdc37 interaction in MB

Previous reports have suggested that WA may disrupt the association between HSP90 and co-chaperone Cdc37, thereby altering normal HSP90 function and resulting in widespread protein misfolding and degradation. We evaluated this finding through co-IP in DAOY cells, and

Figure 4-6.
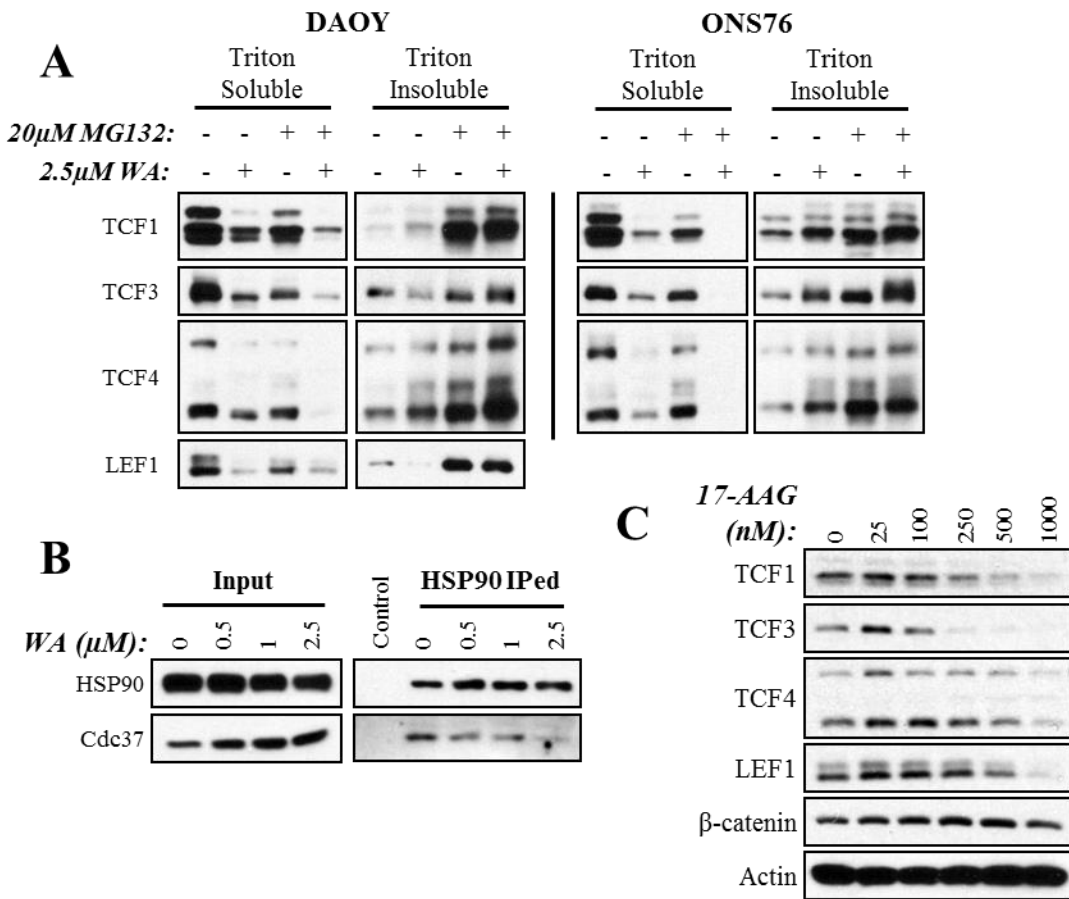
Figure 4-6. A) DAOY and ONS76 cells were pretreated with the proteasome inhibitor MG132 followed by WA for 24 h, and cellular proteins were fractionated by triton X-100 solubility. Treatment with 2.5 μM WA or 20 μM MG132 for 24 h resulted in a depletion of triton soluble TCF/LEF proteins with variable accumulation in the insoluble fraction. Cells pretreated with MG132 before WA demonstrated enhanced retention of all TCF/LEF proteins in the insoluble fraction at 24 h, including proteins that were depleted by WA in both the soluble and insoluble fractions and demonstrating the proteasome-dependent manner of WA-mediated TCF/LEF degradation. B) Co-IP experiments in DAOY cells demonstrated that WA reduced the association between HSP90 and Cdc37 after a 4 h treatment. Total input Cdc37 was not decreased with treatment. C) Treatment of DAOY cells with the N-terminal HSP90 inhibitor 17-AAG demonstrated dose-dependent decreases in total levels of TCF1, TCF3, TCF4, and LEF1 but not β-catenin. TCF1 and TCF3 showed notably enhanced reduction by approximately 250 nM.

indeed, WA reduced the association between HSP90 and Cdc37. After 4 h, 0.5 µM and 2.5 µM WA reduced IPed Cdc37 by 63.7% and 76.2%, respectively, compared to IPed HSP90 (Figure 4-6B). Total input Cdc37 was not decreased with treatment.

To date, members of the TCF/LEF family have not been described as HSP90 client proteins or known to associate with Cdc37. Co-IP for TCF1, TCF3, TCF4, and LEF1 with HSP90 and Cdc37 was unable to identify any direct association between these proteins (data not shown). However, treatment of DAOY cells with the N-terminal HSP90 inhibitor 17-AAG demonstrated dose-dependent decreases in total levels of TCF1, TCF3, TCF4, and LEF1 up to modest doses (1 µM) but not β-catenin (Figure 4-6C). TCF1 and TCF3 showed notable reduction by approximately 250 nM. These findings suggest that while HSP90 and Cdc37 may not directly associate with TCF/LEF members, intact HSP90 function is indirectly necessary for their stability. Combined with the identification that WA works in part through disruption of the HSP90 axis, these findings implicate a potential mechanism involving HSP90 for WA-driven alterations in Wnt/β-catenin signaling.

4.5 Discussion

WA has been demonstrated to be a potent cytotoxic agent in a multitude of cancer models. In this study, we are the first to demonstrate that this efficacy extends to the treatment of MB and is manifested at least in-part through direct inhibition of the oncogenic Wnt/β-catenin signaling pathway resulting in dose-dependent G2/M cell cycle arrest and ultimately apoptosis. Inhibition of this signaling pathway was determined to be a result of proteasome-mediated

145

degradation of transcription factors from the TCF/LEF family. Consistent with previous findings in other models, WA treatment resulted in cellular oxidation and dissociation of HSP90/Cdc37.

WA was demonstrated to function as a novel inhibitor of the Wnt/β-catenin signaling pathway through downstream depletion and altered localization of TCF/LEF resulting in diminished association with transcription activator β-catenin. Significant inhibition of reporter TOP FLASH signaling in a model of constitutively active β-catenin as well as decreased Wnt target mRNA and protein product were observed upon 24 h exposure to 1 μM WA, consistent with levels necessary to decrease TCF/LEF proteins. Concentrations necessary to demonstrate these findings were within the cytotoxically relevant dosing range, supporting that this inhibition was not a high dose off-target drug effect. This study thoroughly evaluated the effects of WA at different levels of the Wnt signaling cascade and demonstrated that this inhibition is not driven by reduced total β-catenin levels or failure of β-catenin to translocate to the nucleus.

While WA also plays a role in altering normal Akt/mTOR signaling in MB, this pathway is not responsible for inhibiting signaling of the Wnt/β-catenin pathway. Pharmacological inhibition of PI3K failed to reduce phosphorylation of GSK-3β or alter levels of β-catenin, suggesting that any remaining Akt activity that was not eliminated with WA treatment was not responsible for this inhibition. It is likely that inhibition of GSK-3β, perhaps through the upstream Wnt signaling protein dishevelled, is a compensatory response to the downstream inhibition of the pathway and an attempt by the cells to overcome this bottleneck. Indeed, GSK-3β phosphorylation was induced at low levels (0.5-1 μM WA) consistent with doses at which TCF/LEF are depleted and suggesting a compensatory effect. Further exploration of the inhibition of GSK-3β is necessary to explain and potentially exploit this finding. On the whole, signaling through the Akt and mTOR proteins was shifted to an inhibitory state with reduced

146

and/or unchanged total and phosphorylated levels. However, in contrast to what has been observed in GBM Akt/mTOR signaling (Grogan et al., 2013; Grogan et al., 2014), downstream signaling to p70 S6K resulted in inconsistent activation/inhibition of the protein compared to GSK-3β inhibition and TCF/LEF depletion, suggesting a greater role of Wnt signaling inhibition in MB.

While a number of inhibitors have been identified that alter Wnt signaling at various points in the cascade (Voronkov and Krauss, 2013), only four agents are currently in human clinic trials not exclusively for MB: olaparib (PARP/tankyrase inhibitor), veliparib (PARP/tankyrase inhibitor), LGK974 (porcupine inhibitor), and OTSA101-DTPA-90Y (radiolabeled antibody against frizzled) (MacDonald et al., 2014). Only PARP inhibition, described to destabilize β-catenin through Axin (Waaler et al., 2012), is under trial for MB with the latter two therapies failing to target the appropriate location in the signaling cascade given the mutations in MB. Such an approach, however, loses utility in presence of significantly overexpressed β-catenin or otherwise mutated β-catenin and/or APC (Voronkov and Krauss, 2013). Of note is the fact that WA alters Wnt signaling at the transcriptional level by targeting the ultimate transcription factors of the pathway. As such, it avoids the potential development of resistance through upstream rerouting or mutations of the Wnt and Akt/mTOR signaling pathways. In this way, WA functions differently than currently available therapeutics and avoids these potential therapeutic pitfalls. Several small molecules have been identified that limit the association of the TCF/LEF members with β-catenin, but to-date, these have not been explored clinically (Voronkov and Krauss, 2013). Similarly, other compounds have been identified that directly disrupt or induce degradation of β-catenin.

Exploration of HSP90 inhibition as a means to disrupt the Wnt pathway therapeutically has not yet been explored. HSP90 was show to interact with Axin1, GSK-3β, and β-catenin but its inhibition resulted in a cell line-dependent depletion of GSK-3β only, indicating that it likely fails to function at that level of the cascade (Cooper et al., 2011; Liu et al., 2012). Further, depletion of GSK-3β would be expected to promote stabilization of β-catenin and subsequent activation of the pathway. The present study supports previous findings that WA disrupts the interaction between HSP90 and Cdc37, a co-chaperone protein necessary for localizing target kinases of the kinome with HSP90 for folding (Karnitz and Felts, 2007), and demonstrates this finding in MB for the first time (Yu et al., 2010). Further alterations of the HSP90 axis beyond this observation have remained unexplored. While direct interaction of HSP90 and Cdc37 with members of TCF/LEF was unable to be demonstrated by co-IP, the importance of functional HSP90 to promote the stability of the TCF/LEF members, likely indirectly, was identified through treatment with the established N-terminal HSP90 inhibitor 17-AAG and subsequent depletion of these transcription factors. TCF/LEF members in the absence of β-catenin have been shown to interact with co-repressors like Groucho, C-terminal binding protein (CtBP), and histone deacetylase (HDAC) with the latter being a known HSP90 modulator (Kekatpure et al., 2009; Voronkov and Krauss, 2013). The role of HSP90 and/or Cdc37, if any, in the stability and function of these proteins remains largely unexplored, especially Cdc37 which is thought to primarily associate with kinome proteins instead. However, if inhibition of HSP90 function results in a failure of the repressor complex or any of the numerous associated proteins to adequately sequester TCF/LEF and result in its delocalization or degradation. Such a hypothesis may explain our findings that TCF/LEF bound to β-catenin is somewhat less readily degraded

compared to total levels. Further exploration of the role of HSP90/Cdc37-mediated stabilization of TCF/LEF directly or indirectly is necessary.

TCF3 is considered to be a repressor of the Wnt signaling transcription and is noted to be less responsive to WA than activator LEF1 as well as context-dependent TCF1 and TCF4 (Arce et al., 2006; Voronkov and Krauss, 2013). TCF3 is more potently decreased by 17-AAG compared to the others. It is hypothesized that differences in currently undefined Cdc37-dependence of the system or non-HSP90 axis effects of WA are likely responsible for this difference and will need to be defined in future studies. However, given the eventual decrease of all TCF/LEF members following WA treatment, it is unclear if this pattern is functionally relevant on the context of general disarray.

Interestingly, ethacrynic acid was previously identified as an inhibitor of Wnt signaling through direct targeting and binding of LEF1 that could be blocked by NAC (Lu et al., 2009). Our findings demonstrate the thiol-reactive and oxidative properties of WA, the latter perhaps a secondary result of the thiol reactivity, which may also play a more direct role in the depletion of the TCF/LEF members. WA was previously shown to induce depletion of O^6-methylguanine-DNA methyltransferase (MGMT), a non-HSP90 client protein with known susceptibility to oxidation (Fu et al., 2010; Ryu et al., 2012; Grogan et al., 2014). Further study is necessary to determine if WA can directly interact with TCF/LEF proteins like ethacrynic acid, but while WA exposure yields numerous alterations and depletions of cellular proteins, previous reports utilizing biotinylated WA for protein pull-down have identified that WA protein-binding is specific to a limited subgroup including HSP90 and vimentin rather than broad-spectrum non-specific associations (Bargagna-Mohan et al., 2007; Yu et al., 2010). Further exploration of the implications of the demonstrated general oxidative effects of WA on TCF/LEF is also necessary

as published reports on the effects of oxidation on TCF/LEF members is lacking. One study utilized hydrogen peroxide treatment to assess oxidative stress on Wnt signaling and demonstrated that it decreased the amount of nuclear β-catenin and resulted in diminished TCF/LEF-mediated transcription (Shin et al., 2004). It did not, however, directly identify any effects on TCF/LEF members. Failure of WA to significantly alter nuclear translocation of β-catenin suggests that oxidation may be a byproduct of a greater mechanism, supporting a direct or HSP90-mediated role for depletion of TCF/LEF by WA.

While the clinical importance of these findings has yet to be evaluated, they predict that WA may be an effective treatment option for MB patients by targeting multiple critical signaling pathways including Wnt/β-catenin which is known to be overactive in a significant subgroup of these patients. Wnt signaling overactivation is most frequently regarded to occur though an increase in total β-catenin, largely through overexpression of β-catenin itself or a failure to properly degrade normal production of the protein through mutations in regulators like APC, including in colorectal cancer as well as MB (Polakis, 2012). However, overexpression of members of the TCF/LEF family like LEF1, which is potently targeted by WA, has also been demonstrated as poor prognostic and disease progression marker in B-cell chronic lymphocytic leukemia (CLL) and a potential option for a targeted therapeutic (Lu et al., 2009; Erdfelder et al., 2010a; Erdfelder et al., 2010b; Wu et al., 2012). Taken together, this suggests potential therapeutic value of WA in Wnt signaling-altered cancers beyond MB. Indeed, previous reports have shown efficacy of WA in colon cancer models despite not evaluating Wnt signaling modulation (Jayaprakasam et al., 2003). Importantly, WA exhibits intrinsic cytotoxicity independent of Wnt signaling. Therefore, while utilization of WA against cancers such as MB or colorectal cancer with frequent overactivation of the Wnt pathway may prove to be beneficial, it

retains potential utility for the population of patients with tumors lacking such characteristics for which it may be challenging to screen prior to the initiation of therapy, including the other MB subgroups representing ~85% of patients.

In this study, we identify the cytotoxic nature of WA against pediatric MB cells for the first time. WA was identified to act as a novel and unique inhibitor of the Wnt/β-catenin signaling pathway, overactivated in one of the MB subgroups, with associated induction of oxidation and modulation of the HSP90/Cdc37 interaction. These findings suggest intriguing clinical potential of the compound in MB and other cancers in which Wnt signaling is known to be overactivated and warrant further translational exploration.

Supplemental Figure 4-1.
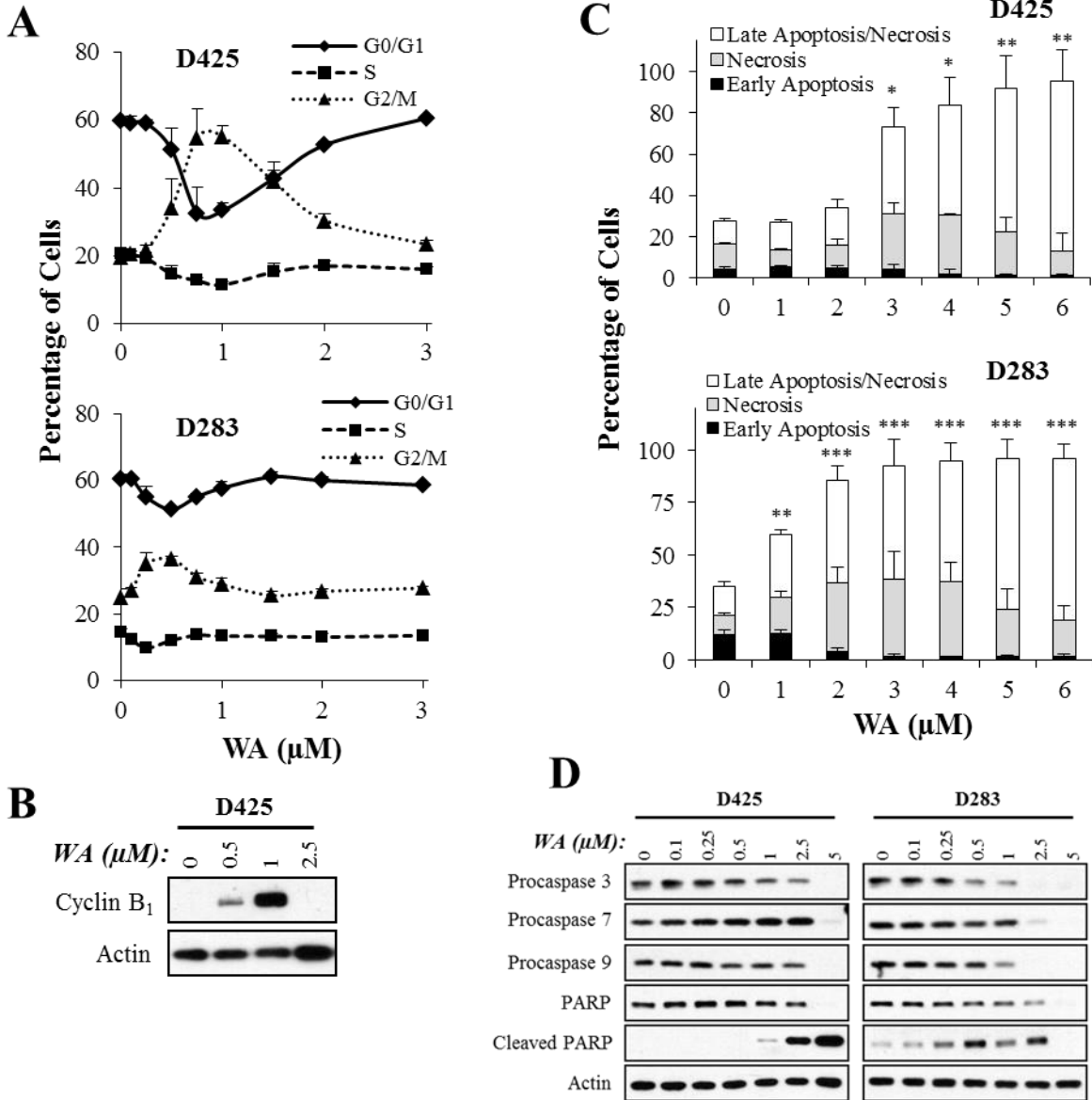
Supplemental Figure 4-1. A) Cells stained with propidium iodide and analyzed by flow cytometry revealed that WA induces a dose-dependent G2/M cell cycle at 24 h. Maximal induction of arrest above baseline was observed at 1 μM in D425 and 0.5 μM in D283. B) Cell cycle arrest corresponded with induction of G2/M-specific protein cyclin B_1 with highest levels at 1 μM in D425 cells. C) D425 and D283 cells stained with propidium iodide and annexin V-FITC and analyzed by flow cytometry revealed that WA induced a dose-dependent increase of cell death with a progressive increase in late apoptotic/necrotic cells 24 h. D) The presence of WA-induced apoptotic processes in D425 and D283 was confirmed by Western blotting that demonstrated dose-dependent reduction in initiator procaspase 9 and effector procaspases 3 and 7. Downstream cleavage of PARP was observed by 1 μM and 0.25 μM in D425 and D283 cells, respectively. Overall PARP cleavage was weaker in D283, consistent with flow cytometry demonstrating a large necrotic response to treatment. $*p < 0.05$, $**p < 0.01$, $***p < 0.001$

Supplemental Figure 4-2.
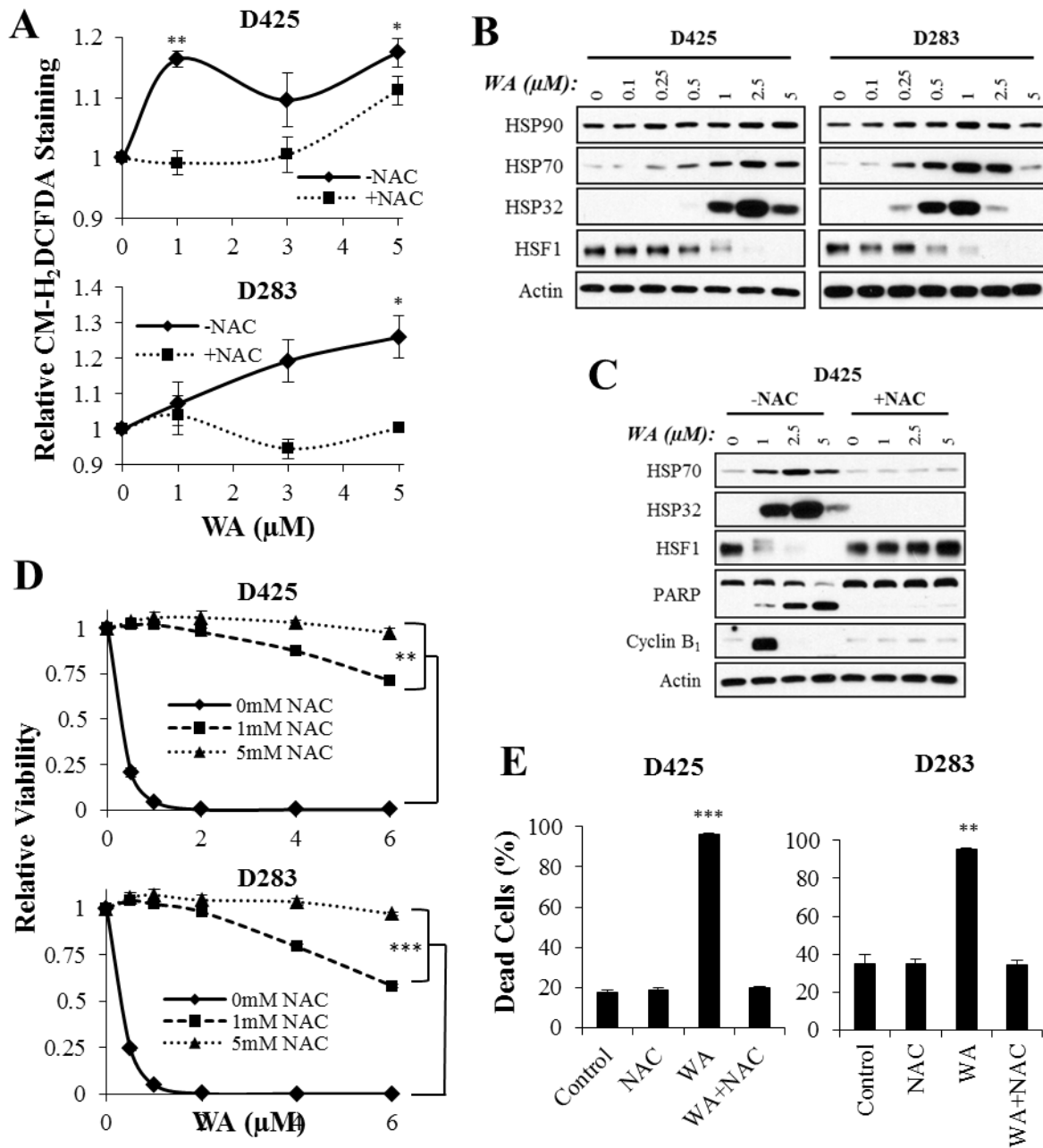
Supplemental Figure 4-2. A) Increases in the concentration of WA generated peroxide-type radicals like H_2O_2 as quantified by CM-H_2DCFDA fluorescent conversion in D425 and D283 cells at 3-4 h post-treatment. Pretreatment 5 mM NAC thiol antioxidant completely abrogated the elevation in ROS. B) Consistent with a cellular oxidative stress response, HSP32 and HSP70 were induced with increasing WA treatment with corresponding depletion of transcription factor HSF1 in both D425 and D283. Total levels of HSP90 remained largely unchanged in both lines. C) Pretreatment of DAOY and ONS76 cells with 5 mM NAC eliminated WA-induced upregulation of HSP32 and HSP70 and the decrease of HSF1 in D425 cells. Similarly, NAC abrogated the cleavage of PARP and induction of cyclin B_1, demonstration reduction in the molecular apoptotic and checkpoint processes. D) D425 and D283 cell viability assessed by ATP levels in the CellTiter Glo assay was increased with NAC pretreatment in the presence of WA. E) WA-mediated induction of overall cell death assessed by flow cytometry of total propidium iodide and annexin V-FITC staining was eliminated with NAC pretreatment. NAC alone had no effect on cell viability. $*p < 0.05$, $**p < 0.01$, $***p < 0.001$

Supplemental Figure 4-3.
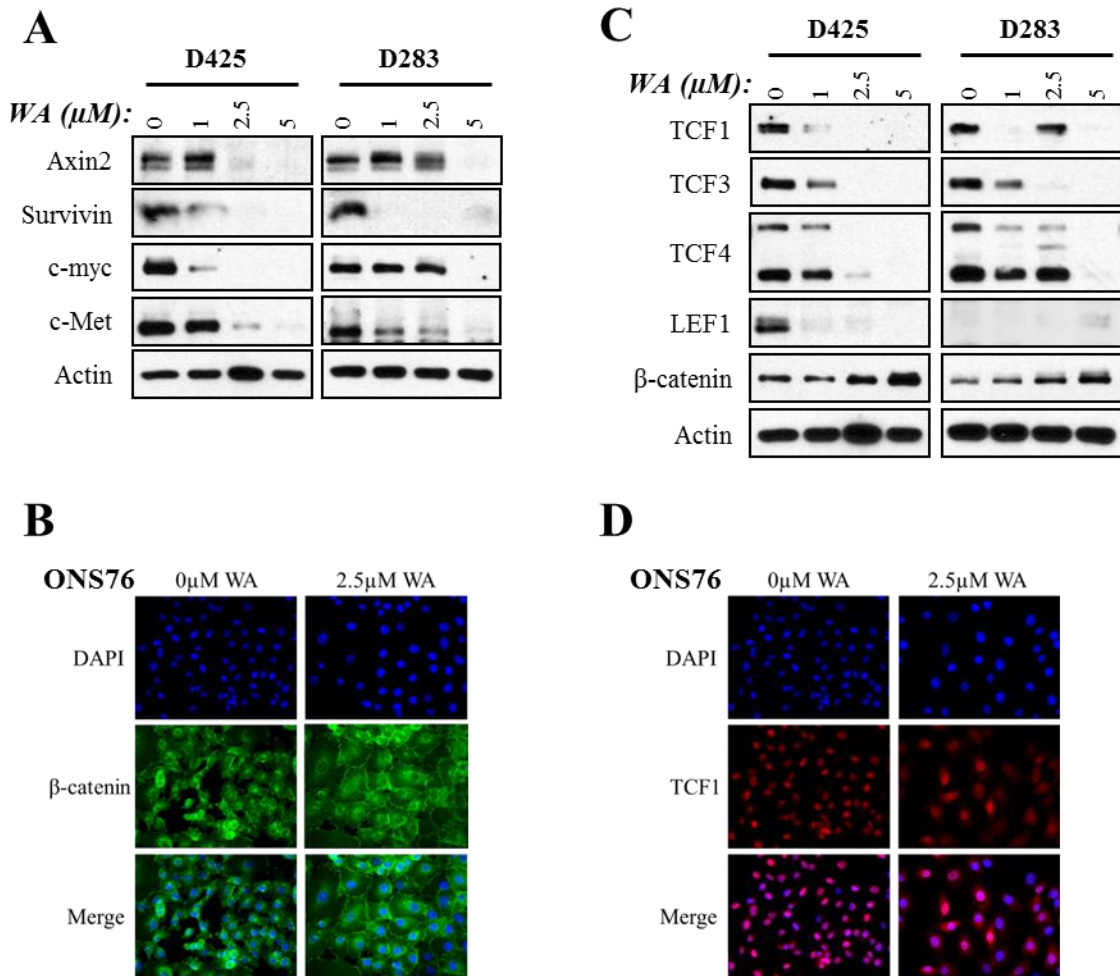
Supplemental Figure 4-3. A) Protein levels of known Wnt signaling target genes (axin2, survivin, c-myc, and c-Met) were reduced in D425 and D283 cells with increasing exposure to WA for 24 h. B) ICC of β-catenin (green) with DAPI (blue) in ONS76 cells demonstrated minimal changes in nuclear β-catenin levels and alterations in protein localization after 24 h of 2.5 μM WA. C) Total levels of TCF/LEF transcription factors TCF1, TCF3, TCF4, and LEF1 were assessed in D425 and D283. In each cell line, all proteins, including both detected isoforms of TCF4, were notable depleted by WA in a dose-dependent manner after 24 h. LEF1 was scarcely detected in D283. D) ICC of TCF1 (red) in ONS76 cells revealed diminished staining intensity anr a shift from the nucleus to the cytoplasm after 2.5 μM WA for 24 h.

Chapter 5

Withaferin A promotes global proteasome-mediated protein degradation through oxidation and inhibition of the HSP90 chaperone axis and is cytotoxically potentiated by inhibition of the proteasome

5.1 Abstract

Withaferin A (WA), a 28-carbon steroidal lactone isolated from members of the *Solenceae* plant family, has previously demonstrated significant anti-cancer efficacy in multiple models through modulation and disruption of numerous oncogenic signaling pathways and cellular events. The underlying mechanism behind these diverse effects, however, has been incompletely explained. In this study, we follow up on previous findings suggesting that WA functions through oxidation and modulation of the HSP90 protein chaperone. WA was demonstrated to shift the HSP90/HSP70 balance with HSP70 upregulation and associated increase in global protein ubiquitination in U87 and HeLa cancer cells. Similarly, WA treatment yielded depletion of known HSP90 client proteins but not non-clients. Interestingly, this was associated with no inhibition of intrinsic HSP90 function as evaluated by HSP90-mediated glucocorticoid receptor (GR) steroid binding, but WA did induce dissociation of co-chaperone Cdc37 from HSP90. This was confirmed by dissociation of Cdc37-dependent Cdk6 but not Cdc37-independent GR from HSP90. Overall, WA promoted elevated cellular oxidation and glutathione (GSH) depletion. Pretreatment with the thiol antioxidant completely eliminated WA-induced oxidation and cytotoxicity, but non-thiol antioxidant ascorbic acid failed to prevent cytotoxicity despite a reduction in general oxidation. Depletion of cellular GSH with γ-glutamylcysteine inhibitor L-buthionine-sulfoximine enhanced the effect of WA. WA shifted depleted proteins to a triton X-100 insoluble fraction with subsequent degradation through the proteasome and, to a lesser extent, the lysosome. Functionally, pretreatment of U87 and HeLa cells with proteasome inhibitor MG132 potentiated the cytotoxicity of WA with a resulting decrease in proliferation, increased apoptosis, and an accumulation of ubiquitinated proteins.

This study further defines the mechanism of WA as a proteotoxic agent through increased oxidation and modulation of the HSP90 axis to produce significant proteasome-mediated protein degradation. Further exploration is warranted to fully explain the inhibitory effect on the HSP90 axis and the translational use of combination WA and MG132.

5.2 Introduction

The effective and sustained treatment of cancer remains an elusive and challenging goal in the scientific community. While great strides have been made in recent decades to understand the biological nature of initiation and progression of the disease at the molecular level, these finds have arguably resulted in comparatively fewer breakthroughs in the management and treatment of such malignancies.

Many current standard therapeutic agents target mechanisms necessary for cellular replication or susceptibilities of cell cycling, often through induction of DNA damage or inhibition of DNA replication (Kamal and Burrows, 2004). While these agents have shown benefits in preventing disease progression and extending survival, they are often restricted by the development of resistance or dose-limiting toxicity, including those affecting neuropsychological and cognitive abilities (Ahles and Saykin, 2001). For example, the platinating agent cisplatin, currently one of the most effective broad-spectrum agents, is frequently used in the management and treatment of many solid tumors including lung, breast, ovarian, cervical, and testicular among many others. However, its administration is associated with significant use-limiting toxicity, most notably nephrotoxicity, and the ultimate development of resistance through a spectrum of complex mechanisms (Stordal and Davey, 2007; Shen et al., 2012; Markman, 2013;

Wensing and Ciarimboli, 2013; Petrelli et al., 2014). Similarly, while the alkylating agent temozolomide (TMZ) in combination with radiation currently represents the most efficacious therapy for glioblastoma multiforme (GBM) patients and demonstrates limited toxicity, its efficacy is often quickly limited by the expression of O^6-methylguanine-DNA methyltransferase (MGMT) (Paz et al., 2004; Hegi et al., 2005).

Advances in targeted therapy through both biological agents and small molecular inhibitors allow for the specific and directed inhibition or modulation of many protein targets and pathways including epidermal growth factor receptor (EGFR), vascular endothelial growth factor (VEGF), BCR-ABL, and Her2/neu, among others (Stebbing et al., 2000; Herbst, 2004; Kamal and Burrows, 2004; Baka et al., 2006; Jakopovic et al., 2014). While this results in comparatively less toxicity due to the specificity of the protein target, it is frequently limited by the development of resistance through tumor mutations or downregulation of the target protein. Additional challenges arise with heterogeneity of target protein expression in the patient population and the individual patient throughout the treatment period (Ellis and Hicklin, 2008; Wheeler et al., 2010; Wong and Lee, 2012; Huang et al., 2014). These considerable challenges demonstrate the need for therapeutic agents that can target multiple oncogenic and resistance pathways simultaneously to circumvent the shortcomings of established therapeutic options.

Heat shock protein (HSP) 90, an evolutionarily well-conserved chaperone protein directly responsible for the stability and/or function of over 400 key cellular proteins, represents an ideal target for this purpose (Barrott and Haystead, 2013). Inhibition of HSP90 results in the depletion of client proteins critical to the proliferation and ultimate survival of cancer cells such as pro-growth signaling proteins, tyrosine kinases, cell cycle regulators, and steroid receptors (Zhang and Burrows, 2004; Powers and Workman, 2006; Sidera and Patsavoudi, 2014). Cancer cells

161

demonstrate enhanced responsiveness to HSP90 inhibition compared to normal tissue due to enhanced reliance on HSP90 for stabilization of oncoproteins, localization in stressful microenvironments, and selective accumulation of inhibitor in cancer cells (Sidera and Patsavoudi, 2014). To date, 17 HSP90 inhibitors, all N-terminal inhibitors of ATPase activity have been brought to clinical trial, and while some have shown therapeutic promise despite formulation challenges, none have been approved for standard use against any cancer. Further development of HSP90 axis modulators, both directly and indirectly through co-chaperones, will be necessary to better target this potential vulnerability of cancer.

Withaferin A (WA), a 28-carbon steroidal lactone isolated from members of the *Solenceae* plant family, has shown promise as an experimental anti-cancer agent by inducing protein degradation and subsequently disrupting numerous signaling pathways including those served by Akt/mammalian target of rapamycin (mTOR), nuclear factor kappa (NFκB), and mitogen-activated protein kinase (MAPK) (Vyas and Singh, 2014). These alterations ultimately result in pro-apoptotic, anti-proliferative, and anti-angiogenic manifestations both *in vitro* and *in vivo* (Vanden Berghe et al., 2012; Vyas and Singh, 2014). While this cytotoxic capacity of WA has been well-defined in a broad spectrum of cancer types, the underlying mechanism responsible for these observations remains incompletely defined. It has been noted that WA may function in part through disruption of the HSP90 chaperone axis either directly or through disruption of the HSP90/Cdc37 interaction (Yu et al., 2010; Grover et al., 2011; Gu et al., 2014). Cdc37 (cell division cycle protein 37) functions as a co-chaperone to HSP90 and plays a vital role in localizing target kinases of the kinome with HSP90 for folding (Karnitz and Felts, 2007). Additionally, WA has demonstrated intrinsic thiol-reactivity and oxidizing properties which have been thought to, in part, play a role in the spectrum of effects observed (Malik et al., 2007;

162

Widodo et al., 2010; Hahm et al., 2011; Mayola et al., 2011; Santagata et al., 2012; Grogan et al., 2013).

In this study, we further define the mechanism of WA responsible for protein depletion through oxidation and modulation of the HSP90 axis and demonstrate its therapeutic utility in combination with an inhibitor of the proteasome.

5.3 Materials and methods

5.3.1 Cell culture and general reagents

The human GBM cell line U87 was generously provided by Dr. Jann N. Sarkaria (Mayo Clinic, Rochester, MN), and the human embryonic kidney cell line 293T was kindly provided by Dr. Roland Kwok (University of Michigan, Ann Arbor, MI). The human cervical cancer line HeLa was obtained through the American Type Culture Collection (ATCC; Manassas, VA). All cell lines were grown in Dulbecco's modified Eagle's medium (DMEM #11995-065; Gibco, Grand Island, NY) supplemented with 10% fetal bovine serum (FBS; Sigma-Aldrich, St. Louis, MO) and 1% penicillin/streptomycin (Gibco), at a 37 °C humidified atmosphere of 5% CO_2 in air. Medium for HeLa cells was further supplemented with 2% L-glutamine (200 mM; Gibco), 1% MEM-vitamin (100x; Hyclone, Logan, UT), and 1% MEM nonessential amino acids (Sigma Aldrich). WA was isolated as previously described (Samadi et al., 2010b). Propidium iodide (PI), DL-buthionine-(S,R)-sulfoximine (BSO), ascorbic acid (AA), N-acetyl-L-cysteine (NAC), monochlorobimane, chloroquine diphosphate salt, and puromycin dihydrochloride were acquired from Sigma-Aldrich, Annexin V-FITC was obtained from BD Biosciences (San Diego, CA), and

163

MG132 was purchased from Selleckchem (Houston, TX). 17-*N*-allylamino-17-demethoxygeldanamycin (17-AAG) was obtained from LC Laboratories (Woburn, MA).

17-AAG resistant HeLa cells were generated through serial escalations in drug exposure to the parental HeLa line. Cells were initially exposed to 250 nM 17-AAG and allowed to recover. All surviving cells remained pooled. Escalation ultimately reached 5 µM and was maintained at this level until the cells were observed to demonstrate minimal change in response to the drug. Resistant cells were not treated with 17-AAG for at least one month before any functional studies.

5.3.2 MTS assay

HeLa and U87 cells were plated at 1,500 and 3,000 cells/well, respectively, in 100 µL in a 96-well plate. After 5-6 h, cells were treated with various concentrations of MG132 for 1 h followed by the addition of WA to bring the total well volume to 200 µL. Similarly, parental and 17-AAG resistant HeLa cells were plated at 1,500 cells/well in 50 µL, allowed to settle for 5-6 h, and treated with varying concentrations of WA or 17-AAG. After a 72 h incubation, viable cell levels were quantified with the addition of the colorometric CellTiter96 Aqueous MTS assay reagent as per the manufacturer's instructions (Promega, Fitchburg, WI). Reagent was allowed to incubate with the cells for 1-2 h, and absorbance was quantified at 490 nm on a BioTek Synergy 2 plate reader (BioTek, Winooski, VT).

5.3.3 CellTiter Glo assay

The CellTiter-Glo luminescent assay (Promega, Fitchburg, WI) was used to evaluate cell viability and proliferation through assessment of cellular ATP levels in assays with the use of reducing agents that would otherwise interfere with the MTS assay mechanism. Cells were plated as outlined in the MTS assay in a white-walled 96-well plate. Where indicated, cells were pretreated with AA or NAC for 1h followed by WA. After 72 h, assay reagent was added to the wells as per the manufacturer's instructions and gently shaken for 10 minutes in the dark at room temperature. Well luminescence was measured on the BioTek Synergy 2 plate reader.

5.3.4 Evaluation of cell death

HeLa and U87 cells were plated and allowed to adhere and grow to ~50% confluency overnight. Cells were then pretreated with MG132 for 1 h followed by WA. DMSO was used as a vehicle control for both agents. After 24 h, all cells were collected and processed as previously described (Grogan et al., 2013). Briefly, cells were washed once in Annexin binding buffer and subsequently stained with PI and Annexin V-FITC as per the manufacturer's instructions (BD Biosciences, San Diego, CA) for 30 minutes at 4 °C. Stained cells were washed twice with the Annexin binding buffer, resuspended in 400 µL of the buffer, and immediately analyzed by flow cytometry on a Beckman Coulter CyAn ADP analyzer (Brea, CA).

5.3.5 Immunoblotting

For general Western blotting, cells were plated as previously described for the evaluation of cell death. Cells were treated with WA or 17-AAG for 24 h and pretreated with 20 µM

MG132, 50 µM chloroquine, or 5 mM NAC for 1 h or 500 µM BSO for 24 h where indicated. After 24 h, cells were harvested, and proteins were isolated in lysis buffer (40 mM HEPES, 2 mM EDTA, 10 mM sodium pyrophosphate decahydrate, 10 mM β-glycerophosphate disodium salt pentahydrate, 1% triton X-100 supplemented with 100 µM phenylmethylsulfonyl fluoride (PMSF), 1 mM Na_3VO_4, and 2 µL/mL protease inhibitor cocktail), quantified, separated by sodium dodecyl sulfate–polyacrylamide gel electrophoresis (SDS–PAGE), and transferred onto a Hybond nitrocellulose membrane as previously described (Samadi et al., 2011). 20-50 µg of protein sample was loaded per lane. Equal loading and transfer of sample was confirmed by blotting for total actin levels. Studies were repeated for accuracy.

Triton X-100 soluble and insoluble fractionation was completed with triton soluble buffer (50 mM Tris-HCl pH 6.8, 150 mM NaCl, 1 mM EDTA, 1 mM EGTA, 1% triton X-100) and insoluble buffer (50 mM Tris-HCl pH 6.8, 2% SDS) as previously described (Chen et al., 2008) supplemented with 100 µM PMSF, 1 mM Na_3VO_4, and 2 µL/mL protease inhibitor cocktail. In brief, cells were pre-treated with proteasome inhibitor MG132 for 1 h where indicated followed by WA for 24 h. Cells were collected as previously described, lysed with triton soluble buffer, and centrifuged at 14,000 rpm for 20 minutes at 4°C. The supernatant was collected as the soluble fraction. The pellet was resuspended and washed once with soluble buffer and repelleted by centrifuged at 14,000 rpm for 10 minutes. The pellet was resuspended in triton insoluble buffer and subsequently ground with a pestle, vortexed, and heated at 100 °C repeatedly for ~15 minutes to promote dissolution of the pellet. Any remaining debris was removed by centrifugation, and the supernatant was collected as the insoluble fraction. Proteins in the two fractions were prepared and evaluated as described above. For electrophoresis under non-reducing conditions, β-mercaptoethanol was not added to the SDS loading buffer.

Primary antibodies against ubiquitin (#3936; 1:2000), glucocorticoid receptor (GR; #12041; 1:500), Akt (#4691; 1:2000), mTOR (#2972; 1:1000), EGFR (#4267; 1:1000), c-myc (#9402; 1:1000), Cdk4 (#2906; 1:2000), Cdk6 (3136; 1:1000), BRCA1 (#9010; 1:500), Chk1 (#2360; 1:1000), GAPDH (#2118; 1:1000), Cdc37 (#4793; 1:1000), PARP (#9542; 1:1000), and caspase 3 (#9665; 1:1000) were acquired from Cell Signaling Technology (Danvers, MA). HSP40 (#ADI-SPA-400; 1:1000), HSP90 (SPA-836; 1:1000), and HSP70 (ADI-SPA-810; 1:1000) antibodies were collectively obtained from Enzo Life Sciences (Farmingdale, NY). Total actin antibody (#MAB1501; 1:50000) was obtained from EMD Millipore (Billerica, MA), and FLAG antibody (F1804; 1:500) was acquired from Sigma-Aldrich. The primary antibodies for ERK2 (sc-154; 1:5000)and Raf-1 (sc-7267; 1:250) and the secondary antibodies donkey anti-rabbit IgG HRP (sc-2313; 1:2500-1:10000) and goat anti-mouse IgG HRP (sc-2005; 1:5000-1:20000) were purchased from Santa Cruz Biotechnology (Santa Cruz, CA).

5.3.6 Immunocytochemistry (ICC)

U87 and HeLa cells were plated to ~50% confluency in 8-well chamber slides (Nalge Nunc International, Penfield, NY) and treated with 1-2 µM WA for 24h. Cells were fixed in 4% PBS-buffered paraformaldehyde at room temperature for 30 minutes and washed 3x with 1x PBS. Cell membranes were de-permeablized for 15 minutes in 1x PBS containing 0.3% triton X-100 and subsequently blocked in 5% goat serum (Cell Signaling Technology) in 1x PBS containing 0.15% triton X-100 shaking for 1 h. Cells were exposed to primary antibody in blocking solution overnight at 4 °C. Primary antibodies included HSP90 (1:100; Cell Signaling #4877), HSP70 (1:250; Enzo Life Sciences #SPA-810), and ubiquitin (1:200; Biolegend

167

#646301; San Diego, CA). After three washes with 1x PBS, secondary antibody (1:1000; anti-rabbit IgG Fab2 Alexa Fluor 555, Cell Signaling #4413; Anti-mouse IgG Fab2 Alexa Fluor 488, Cell Signaling #4408) was added to each well for 1 h at room temperature followed by an additional 3 washes. Coverslips were mounted on each slide with ProLong Gold Antifade with DAPI (Cell Signaling Technology), allowed to dry, and visualized on a Leica DM IRB microscope (Wetzlar, Germany) with Metamorph Basic software (version 7.7.3.0.; Molecular Devices; Sunnyvale, CA).

5.3.7 Steroid-binding assay

The GR steroid binding assay was performed as previously described (Murphy et al., 2011). U87 and HeLa cells were plated to ~50% confluency, treated with WA or 17-AAG, collected after 24 h, washed and pelleted, and snap frozen in liquid nitrogen. Homogenization HEM buffer (10 mM HEPES pH 7.35, 1 mM EDTA, 20 mM sodium molybdate, 1 mM PMSF, 1x protease inhibitor cocktail) was added at 1.5 volumes of the pellet, and the protein was isolated by centrifugation. FiGR antibody producing cells were purchased at American Type Culture Collection (ATCC; Manassas, VA; FiGR ATCC CRL-2173), and ascites was produced at the University of Michigan Hybridoma Core as described (Morishima et al., 2003). 50 µL murine GR from the lysate of overexpressing SF9 cells as previously produced (Morishima et al., 2003) was combined with 178 µL TEG buffer (8 mM TES pH 7.6, 4 mM EDTA, 50 mM NaCl, 10% (v/v) glycerol), 70 µL protein A sepharose (Sigma-Aldrich), and 2 µL FiGR and rotated at 4 °C for 2 h to promote immunoadsoption of the GR. Immunoadsorbed GR was salt-stripped of associated HSP90 complex proteins with 0.625 M NaCl in TEG buffer at 4 °C. After 2 h, the

beads were washed with TEG buffer followed by 10 mM HEPES (pH 7.4) and reconstituted in 50 µL of U87 (185 µg) or HeLa (250 µg) lysate volume-equilibrated amongst treatment samples with 5µL of an ATP-regenerating system (10 mM HEPES pH 7.4, 50 mM ATP, 250 mM creatine phosphate, 20 mM magnesium acetate, and 100 U/mL creatine phosphokinase). Each sample was incubated at 30 °C for 20 minutes with agitation every 2 minutes. After 20 minutes, samples were washed twice with TEGM buffer (TEG buffer with 20 mM sodium molybdate).

To evaluate the steroid binding ability of the immunopellets, each pellet was resuspended in 100 µL of HEM buffer with 100 nM [H^3]dexamethasone (PerkinElmer, Waltham, MA) and incubated overnight at 4 °C. Samples were then washed three times with TEGM buffer and measured by liquid scintillation spectrometry on a Beckman LS 5000CE counter. Steroid binding was identified as counts/minute. Negative and positive controls were control lysate without FiGR and 50 µL reticulocyte lysate, respectively.

5.3.8 Co-immunoprecipitation (co-IP)

HeLa cells were plated, allowed to adhere overnight, and grown to ~50% confluency before treatment with WA. For co-IP of Cdc37, Cdk6, and GR proteins from IPed HSP90, cells were treated with 5µM WA for 1-16 h or 0.5-5 µM WA for 4 h before cells were trypsinized, washed twice with 1x PBS, and pelleted. Pelleted cells were lysed in a buffer consisting of 20 mM Tris HCl (pH 7.4), 100 mM NaCl, 2 mM DTT, 20 mM sodium molybdate dihydrate, and 0.5% NP-40 supplemented with 100 µM PMSF, 1 mM Na_3VO_4, and 2 µL/mL protease inhibitor cocktail. Proteins were isolated and quantified as described for immunoblotting. 2 mg of each protein sample was brought to 300 µL in buffer, and 25 uL of anti-HSP90β antibody (1:12;

Invitrogen #379400) was added to each tube except for a no-antibody control tube with untreated cell lysate. Tubes were rocked at 4 °C overnight before the addition of 25 µL of protein G magnetic bead system as described by the manufacturer (Pierce Biotechnology, Rockford, IL) for 2 h. Beads were washed 4x with buffer, and proteins were eluted with the addition of SDS buffer as used in immunoblotting for 15 minutes rocking at room temperature. Beads were cleared, and the supernatant was evaluated by immunoblotting. For immunoblotting, secondary mouse anti-rabbit conformation specific HRP antibody (#5127; 1:1000) was obtained from Cell Signaling Biotechnology and used for blotting in appropriate to limit heavy-chain interference.

5.3.9 Reactive oxygen species (ROS) measurement

WA-mediated production of intracellular ROS, particularly peroxides like H_2O_2, was measured through fluorescent conversion of the general oxidative stress indicator CM-H_2DCFDA (Molecular Probes, Grand Island, NY). U87 cells were preloaded with 20 µM CM-H_2DCFDA in 1x PBS at 37 °C for 1 h, washed once with phenol red-free DMEM supplemented with 10% FBS and 1% penicillin/streptomycin, and resuspended in the same medium. Cells were plated at 20,000 cells/well in a 96-well plate and treated with WA ± 5 mM NAC or 100 µM AA after 30 minutes. Evaluation of fluorescence was completed on a BioTek Synergy 2 plate reader after 4 h with excitation and emission filters of 485 nm and 528 nm, respectively.

5.3.10 Determination of glutathione (GSH) levels

U87 and HeLa cells were plated at 10,000 cells/well using phenol red-free medium in 50 µL in a 96-well plate and allowed to adhere overnight before treatment with WA in a 50 µL volume. Monoclorobimane, a non-fluorescent compound until reacting with thiols like GSH, was made up in DMSO at a stock concentration of 25 mM and diluted to 200 µM in 1xPBS before immediately before use. After 6 h of WA exposure, 100 µL of the diluted monoclorobimane was added to each well, and plates were incubated at 37 °C for 30 minutes. Evaluation of fluorescence, corresponding with free cellular GSH levels, was then completed on a BioTek Synergy NEO plate reader excitation and emission filters of 390 nm and 478 nm, respectively.

5.3.11 Transfections

c-myc has previously been shown to require amino acid sites T58 and S62 for phosphorylation-directed ubiquitination and subsequent degradation via the proteasome (Gregory and Hann, 2000; Sears et al., 2000; Kamemura et al., 2002). 293T cells were transfected with pcDNA3-c-myc$^{T58A/S62A}$-FLAG, a mutant for both sites, or the pcDNA3 control vector and a puromycin cassette at a 20:1 ratio (4 µg:200 ng in a 6 cm dish) using Lipofectamine 2000 as per the manufacturer's instructions (Life Technologies, Carlsbad, CA). The constructs were previously produced as described (Sundberg et al., 2006). The cells were selected with 1.5 ug/mL puromycin, and surviving colonies were pooled. To verify expression of c-myc$^{T58A/S62A}$, Western blotting for the attached FLAG tag was carried out. The transfected cells were used as a model of altered proteasomal degradation in the present of WA.

5.3.12 Data and statistical analysis

GraphPad Prism 6 (version 6.02; GraphPad Inc., San Diego, CA) was used to generate best-fit non-linear sigmoidal dose response curves for IC_{50} determination. Comparisons of differences between two or more means/values were determined by Student's unpaired t-test via the statistical functions of GraphPad Prism or Microsoft Excel 2010 software (version 14.0.6129.5000; Microsoft Corporation Redmond, WA). Densitometry, where indicated, was completed using ImageJ software (version 1.46r; Bethesda, MD). Data are presented as mean values with error bars denoting standard deviation or standard error of the mean where appropriate. Unless otherwise noted, all experiments were performed minimally in triplicate. The levels of significance were set at $*p < 0.05$, $**p < 0.01$, and $***p < 0.001$.

5.4 Results

5.4.1 Withaferin A alters the HSP90/HSP70 balance to favor HSP70 upregulation and molecular ubiquitination

While HSP90 and HSP70 associate in a heteroprotein chaperone complex, it has been described that each, when favored, provides a contrasting dominant function in response to the presence of misfolded proteins. HSP90 promotes selective protein refolding and function, whereas HSP70 mediates aberrant protein degradation. WA has previously demonstrated the ability to reduce total levels of key proteins in multiple signaling pathways, but the underlying mechanisms remain incompletely defined. In order to determine if changes in the HSP90/HSP70 axis are observed with WA treatment, total levels of HSP90 and HSP70 were evaluated in HeLa

Figure 5-1.
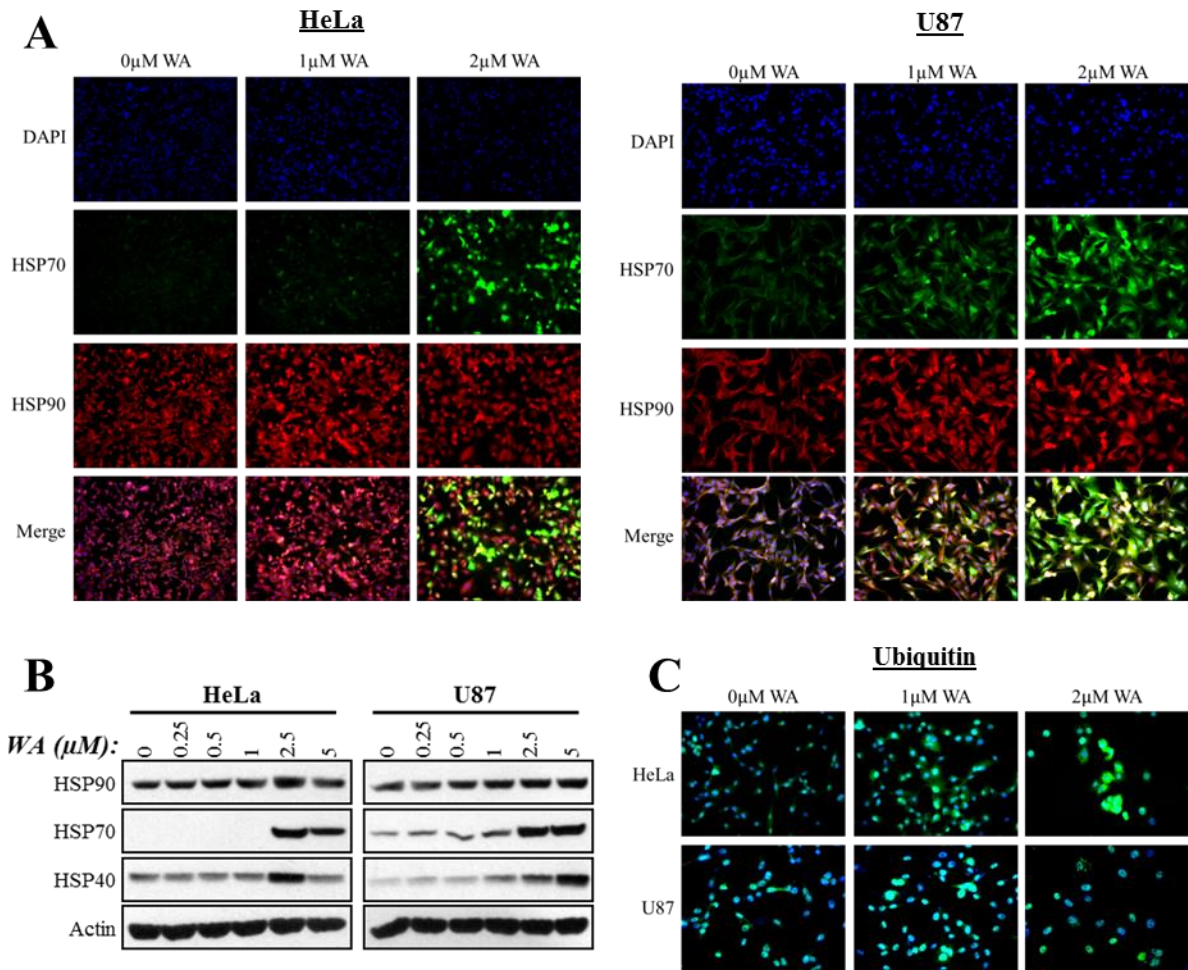
Figure 5-1. A) ICCrevealed dose-dependent increases of HSP70 in both cell lines with visible induction throughout the nucleus and cytoplasm occurring at 2 µM WA in HeLa and elevation at 1 µM in U87 after 24 h. Baseline HSP70 staining was notably higher in U87 compared to HeLa. Total HSP90 levels were largely unchanged in HeLa but slightly elevated in U87 with significant staining observed at baseline in both lines. Merged images revealed the shift in the HSP90/HSP70 balance toward HSP70 with the predominant red HSP90 staining in control cells replaced by the green staining of HSP70 and yellow staining of combined HSP90/HSP70. B) Immunocytochemistry results were confirmed by Western blotting demonstrating minimal changes in total HSP90 levels but dose-dependent increases in HSP70 and HSP40. C) Dose-dependent increases of ubiquitin staining with WA treatment were observed in both HeLa and U87 after 24 h. Notable aggregation of ubiquitinated proteins was visible at 2 µM WA in both lines.

and U87 cells by ICC and Western blotting (Figure 5-1A). ICC revealed dose-dependent increases of HSP70 in both cell lines with visible induction throughout the nucleus and cytoplasm occurring at 2 µM WA in HeLa and elevation at 1 µM in U87. Baseline HSP70 staining was notably higher in U87 compared to HeLa. Total HSP90 levels were largely unchanged in HeLa but slightly elevated in U87 with significant staining observed at baseline in both lines. Merged images revealed the shift in the HSP90/HSP70 balance. Predominant red HSP90 staining in control cells was replaced by the notable green staining of HSP70 and yellow staining of combined HSP90/HSP70.

Western blotting confirmed the ICC observations (Figure 5-1B). Total levels of HSP90 were predominantly unchanged with WA concentrations up to 5 µM with mild increases noted in U87. Consistent with ICC findings, baseline levels of HSP70 were not noted in HeLa cells but were observed in U87. HSP70 was significantly induced at 2.5 µM WA in both HeLa and U87. Levels in U87 cells were moderately increased between 0.25-1 µM WA. Additionally, HSP40, a co-chaperone known to aid in the function of HSP70, was notably elevated from 1-5 µM WA in U87 but only 2.5 µM WA in HeLa, consistent with highest levels of HSP70 upregulation.

Given the WA-mediated shift toward the HSP70 axis which favors proteasome-mediated protein degradation, total cellular ubiquitination, a signaling marker for this degradation, was evaluated by ICC following WA treatment. Staining for ubiquitin was increased in a dose-dependent manner in both HeLa and U87 (Figure 5-1C). By 2 µM, notable aggregates of ubiquitination were seen in both cell lines, suggesting accumulation of normal and/or aberrant proteins targeted for degradation.

5.4.2 Withaferin A inhibits the HSP90 axis through disruption of the HSP90/Cdc37 interaction

Several previous investigations have identified a pattern of protein degradation characteristic of HSP90 inhibition following exposure to WA (Samadi et al., 2009; Yu et al., 2010; Gu et al., 2014). Yu, et al. suggested that WA binds HSP90 and reduces its association with co-chaperone Cdc37 but questioned whether alterations in the stability of HSP90 client proteins were a result of this disruption or rather inhibition of HSP90 (Yu et al., 2010). To evaluate this, the effects of WA were examined in Cdc37-dependent and independent models.

WA was first demonstrated to induce protein depletion of known HSP90 clients Akt, mTOR, Raf-1, EGFR, c-myc, Cdk6, BRCA1, and Chk1 by 2.5 µM in both HeLa and U87 cells (Figure 5-2A). In contrast, WA treatment failed to decrease levels of non-HSP90 client proteins ERK2, GAPDH, and actin. The role of HSP90 in the stability of each protein was confirmed by treating HeLa cells with known HSP90 inhibitor 17-AAG.

The glucocorticoid receptor (GR) has been well-described as requiring an association with HSP90 for its steroid binding activity. In contrast to the androgen receptor, this activity does not require the presence of Cdc37 (Rao et al., 2001). HSP90 function was measured through the ability of purified GR to bind [^{3}H]dexamethasone following re-exposure to cellular lysate containing HSP90 and other co-chaperones as previously described (Murphy et al., 2011) (Figure 5-2B). Lysate was obtained from HeLa and U87 cells treated with vehicle, WA, and 17-AAG for 24 h. Reticulocyte lysate was used as a positive control and confirmed model efficacy (data not shown). WA failed to demonstrate inhibition of HSP90 activity at cytotoxically relevant concentrations 2-5 µM and rather displayed elevated promotion of steroid binding by 4-10% and 49-57% with HeLa and U87 lysates, respectively (p > 0.05 expected 2 µM WA in U87 cells: p = 0.047). At 10 µM WA, steroid binding in U87 was seen to return to baseline but reduced to 45%

Figure 5-2.
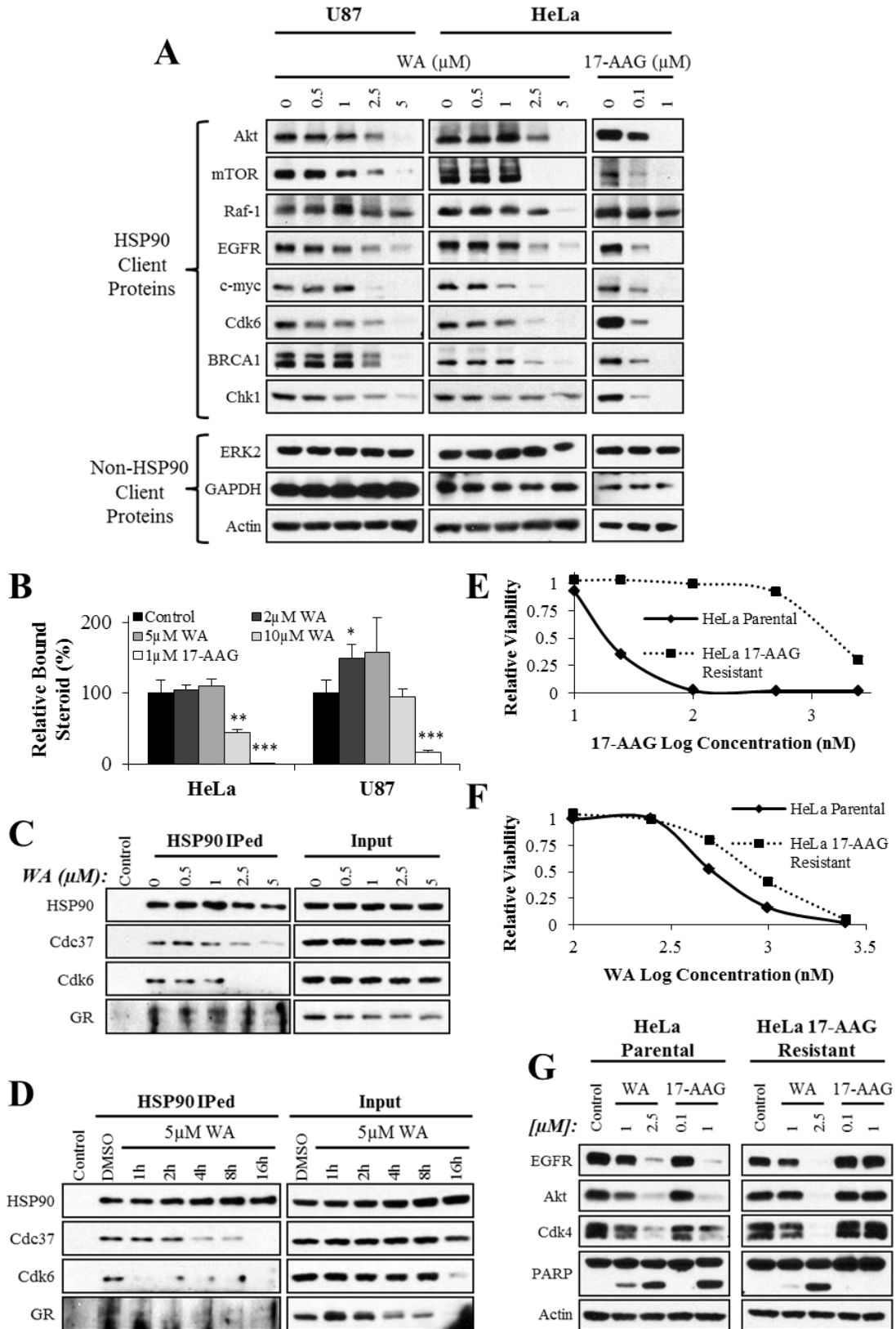
Figure 5-2. A) WA treatment for 24 h in U87 and HeLa caused protein depletion of known HSP90 clients Akt, mTOR, Raf-1, EGFR, c-myc, Cdk6, BRCA1, and Chk1 but failed to decrease levels of non-HSP90 client proteins ERK2, GAPDH, and actin. HSP90-mediated stability of each protein was confirmed by treating HeLa cells with known N-terminal HSP90 inhibitor 17-AAG. B) HSP90 function was measured through the ability of purified GR to bind [^{3}H]dexamethasone following re-exposure to cellular lysate containing HSP90 and other co-chaperones treated with WA or 17-AAG for 24 h. WA failed to demonstrate inhibition of HSP90 activity at cytotoxically relevant concentrations 2-5 μM and rather displayed elevated promotion of steroid binding with HeLa and U87 lysates. At 10 μM WA, steroid binding in U87 was seen to return to baseline but reduced to 45% of baseline in HeLa. In contrast, 1 μM 17-AAG, a positive control for HSP90 inhibition, significantly reduced HSP90-mediated GR steroid binding with HeLa and U87 lysates. C and D) Co-IP experiments in HeLa cells using an HSP90 antibody pull-down demonstrated that WA reduced the association between HSP90 and Cdc37 in a dose-dependent manner after 4 h and in a time-dependent manner when exposed to 5 μM WA. Total input HSP90 and Cdc37 was not decreased with treatment. Similar to Cdc37, the Cdc37-dependent client protein Cdk6 was also shown to dissociate with WA treatment, but Cdc37-independent protein GR did not. Total levels of both Cdk6 and GR were reduced over time. E) A 17-AAG resistant HeLa cell line was developed and shown to have a 72 h IC$_{50}$ to 17-AAG of 1380 nM compared to 21 nM for the parental line, a 66-fold difference. F) In contrast to findings with 17-AAG, WA IC$_{50}$s in the parental and resistant lines were 503 nM and 841 nM, respectively, a different of only 1.7-fold. G) Both WA and 17-AAG decreased total levels of HSP90 client proteins EGFR, Akt, and Cdk4 and increased the apoptotic cleavage of PARP in

parental HeLa cells, but only WA demonstrated these findings in the resistant line, showing its maintained utility. $*p < 0.05$, $**p < 0.01$, $***p < 0.001$

of baseline in HeLa (p = 0.002). In contrast, 1 µM 17-AAG, a positive control for HSP90 inhibition, reduced HSP90-mediated GR steroid binding in HeLa and U87 by 99% and 83%, respectively (p < 0.001). These findings suggest that WA does not directly inhibit HSP90 function.

The ability of WA to alter the association between HSP90 and Cdc37 was confirmed in HeLa cells by co-immunoprecipitation for HSP90 (Figures 5-2C and 5-2D). After 4 h WA treatment, co-IPed Cdc37 was reduced 36.9% with 1 µM up to 67.0% with 5 µM relative to IPed HSP90, demonstrating a dose-dependent effect. Similarly, a time-dependent effect was observed by maintaining WA at 5 µM with diminished association from 1-16 h post-treatment. IPed Cdc37 was reduced 23.8%, 72.7%, 77.2%, and 99.4% after 2 h, 4 h, 8 h, and 16 h relative to IPed HSP90, respectively. Total input HSP90 and Cdc37 remained consistent with WA treatment.

To further define the importance of this co-chaperone disruption, IPed HSP90 was also evaluated for a Cdc37-dependent protein, Cdk6, and a Cdc37-independent protein, GR (Figures 5-2C and 5-2D) (Lamphere et al., 1997; Rao et al., 2001). Treatment with WA in both dose- and time-dependent manners demonstrated a progressive failure of HSP90 to associate with client protein Cdk6. This association was completely eliminated after 4 h with 2.5 µM WA. Similarly, association was nearly completely eliminated with 5µM WA after 1 h and remained consistently reduced at latter timepoints. Total input levels of Cdk6 were constant among samples except for 5 µM WA at 16 h which demonstrated near-complete elimination of the protein. In contrast, co-IPed GR in both the dose- and time-dependence studies was maintained under all conditions. Interestingly, total input GR was decreased with time and concentration in both experiments with near-complete depletion with 5 µM at 16 h, but this did not result in a corresponding decrease in HSP90-GR association, suggesting the retention of HSP90 function independent of Cdc37.

In contrast to 17-AAG, WA has been shown to associate with the C-terminus of HSP90 and did not affect molecular ATPase function (Yu et al., 2010). To demonstrate if WA's unique disruption of the HSP90 axis could be utilized in overcoming inhibition to 17-AAG while still generating a similar effect, a HeLa cell line resistant to 17-AAG was developed through serial escalations in drug exposure. Evaluation of 17-AAG cytotoxicity revealed 72 h IC_{50} values of the parental and resistant lines to be 21 nM and 1380 nM, respectively, for a 66-fold change in response (Figure 5-2E). WA sensitivity, however, was only elevated 1.7-fold from 503 nM in the parental line to 841 nM in the 17-AAG resistant derivative (Figure 5-2F).

Maintained cytotoxicity of WA in the 17-AAG resistant line was confirmed molecularly through evaluation of HSP90 client proteins EGFR, Akt, and Cdk4 as well as cleavage of the apoptotic biomarker PARP (Figure 5-2G). Depletion of the client proteins and increased PARP cleavage observed with 1 µM 17-AAG after 24 h in the parental HeLa line was completely absent in the resistant line, but WA-mediated client degradation remained consistent with near-complete elimination by 2.5 µM. WA also maintained the ability to induce PARP cleavage in the resistant sub-line.

5.4.3 Cytotoxicity of withaferin A is driven by thiol-reactivity and cellular oxidation

Previous studies have identified an oxidative component resulting from treatment with WA (Malik et al., 2007; Widodo et al., 2010; Hahm et al., 2011; Mayola et al., 2011; Santagata et al., 2012; Grogan et al., 2013; Grogan et al., 2014). Given that certain proteins are susceptible to oxidative stress and may become misfolded, the nature of this oxidative component was explored. Treatment of U87 cells with WA resulted in a dose-dependent increase in oxidation as

measured by CM-H$_2$DCFDA conversion to a fluorescent product by 4 h (Figure 5-3A). 5 µM WA increased fluorescence 1.9-fold (p = 0.038). This enhanced oxidative signal was reduced by pretreatment with 100 µM non-thiol antioxidant AA by 17.2% (p = 0.233) and completely returned to baseline with 5 mM thiol antioxidant NAC (p = 0.037), suggesting a greater role of thiol reactivity in the manifestation of WA's effects.

Further evaluation of thiol reactivity and changes in the redox states following WA exposure was accomplished through measurements of GSH levels with monochlorobimane which fluoresces when conjugated to GSH (Figure 5-3B). GSH is a protective component of cells that sequesters thiol reactive agents to prevent cellular damage. After 6 h, 2.5 µM WA reduced total cellular glutathione in both HeLa and U87 cells by 41.1% (p < 0.001) and 31.9% (p = 0.012), respectively, further indicating WA-mediated thiol reactivity and disruption of the redox balance.

Evaluation of anti-oxidant pretreatment was completed with the CellTier-Glo assay to define the functional cytotoxic effects of WA treatment (Figure 5-3C). In the assay, cellular viability was assessed by total ATP levels 72 h after treatment. WA alone exhibited significant (p < 0.001) reduction in the viability of HeLa and U87 cells at the concentrations tested (2.5-5 µM). While 100 µM AA previously reduced WA-mediated oxidation, it was unable to limit cytotoxicity, mirroring the cell viability reduction of WA alone. However, 5 mM NAC completely abrogated WA cytotoxicity, returning cell viability to baseline and demonstrating the predominant thiol reactive mechanism of WA.

Triton X-100 fractionation under non-reducing conditions was completed to define WA-mediated redox alterations in HSP90 localization. While triton soluble proteins are largely regarded as functional, stable molecules, the insoluble fraction is thought to contain labile and

Figure 5-3.
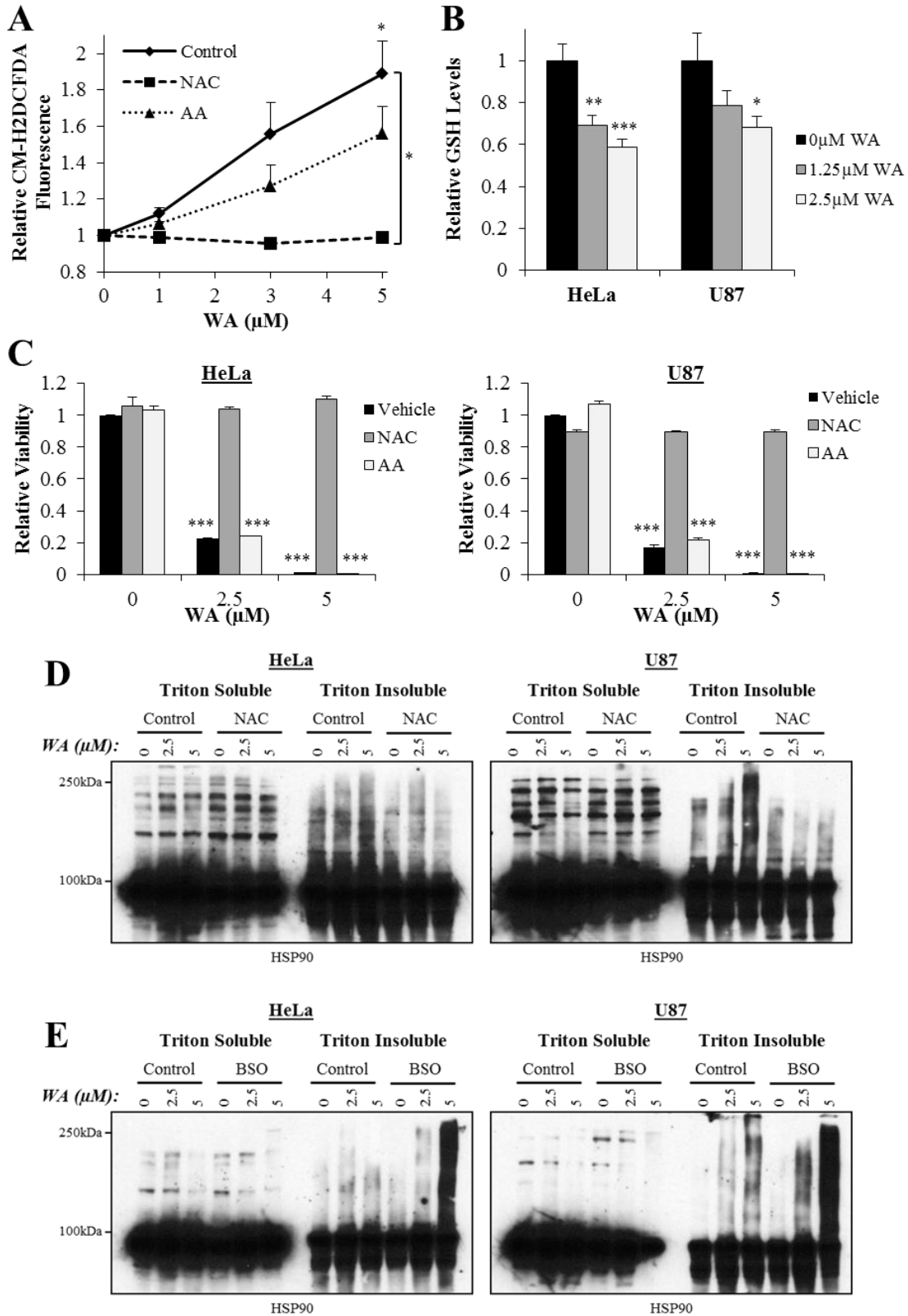
Figure 5-3. A) WA generated peroxide-type radicals like H_2O_2 as quantified by CM-H_2DCFDA fluorescent conversion with increasing concentrations of WA in U87 cells 4 h post-treatment. The thiol antioxidant NAC (5 mM) completely abrogated the elevation in ROS, while 100 μM of the non-thiol antioxidant AA produced a small reduction in overall oxidation. B) GSH levels were measured by monochlorobimane conversion to a fluorescent product in the presence of a thiol. WA treatment was shown to significantly reduce GSH levels in both HeLa and U87 after treatment for 6 h. HeLa (C) and U87 (D) cell viability was assessed by total ATP levels with the CellTiter Glo assay. WA-induced reduction of viability was completely eliminated with NAC but not AA pretreatment. E) Triton X-100 fractionation under non-reducing conditions was completed to define WA-mediated redox alterations in HSP90 localization. Slower migrating proteins aggregates of heterogeneic molecular weight positive for HSP90 were dose-dependently increased by WA in the triton insoluble fraction and was reduced with NAC pretreatment. F) In contrast, triton insoluble HSP90 aggregation was enhanced by reduction in GSH through inhibition of γ-glutamylcysteine synthetase by BSO. $*p < 0.05$, $**p < 0.01$, $***p < 0.001$

aggregated proteins. Additionally, previous reports have demonstrated increased disulfide-bonded HSP90 in the insoluble fraction in response to oxidative stress (Cumming et al., 2004; Chen et al., 2008). Enhanced exposure of Western blots for HSP90 in HeLa and U87 revealed minimal changes to total levels of HSP90 in both the soluble and insoluble fractions 24 h after 2.5-5 μM WA. Slower migrating disulfide-bonded HSP90 was not elevated following WA exposure. However, slower migrating proteins of heterogeneic molecular weight positive for HSP90 were dose-dependently increased by WA in the triton insoluble fraction indicating damaged, aggregated, and delocalized HSP90 protein complexes. Pretreatment with NAC completely eliminated this protein aggregation (Figure 5-3D). In contrast, reduction in GSH through inhibition of γ-glutamylcysteine synthetase by BSO potentiated the total level of WA-induced HSP90 aggregate in the insoluble fraction, demonstrating the thiol-dependent nature of HSP90 disruption (Figure 5-3E). While BSO enhanced WA-induced HSP70 upregulation and NAC prevented HSP70 induction, changes in disulfide-bonded or otherwise aggregated HSP70 was not detected (data not shown).

5.4.4 Withaferin A-mediated protein degradation requires the proteasome

Cellular protein elimination is largely driven through two primary pathways: proteasome- and lysosome-mediated degradation. Given the observation that WA drives upregulation of HSP70 and ubiquitination of proteins globally and that the latter targets proteins to the proteasome, the mechanism of WA-driven protein depletion was evaluated.

Triton X-100 fractionation under reducing conditions was utilized to evaluate WA-altered protein localization and depletion in the presence of proteasome inhibitor MG132 and lysosome

inhibitor chloroquine (Figure 5-4A). As previously described, 20 µM MG132 alone, mimicking

cellular stress and altering normal protein turnover, reduced soluble levels of the proteins

evaluated (Cdk6, Cdk4, mTOR, c-myc, Akt, and EGFR) and promoted elevated levels in the

insoluble fraction (Kawahara et al., 2008). Also, consistent with previous reports (Carter and

Sorkin, 1998), 50 µM chloroquine, an inhibitor of lysosomal protein degradation, blocked

endogenous EGFR turnover driven in part through endocytosis and lysosomal degradation and

enhanced the triton insoluble fraction. WA treatment promoted depletion of soluble proteins with

variable shift to the insoluble fraction. Complete elimination after 24 h WA exposure was

favored in the more sensitive HeLa cells compared to U87. However, extended treatment

duration in U87 cells demonstrated diminished levels of insoluble proteins (data not shown).

Compared to WA alone, the combination of WA and MG132 demonstrated increased retention

of all evaluated proteins in the insoluble fraction, suggesting that WA-mediate protein depletion

occurred at least in part through proteasomal degradation. Protein retention with chloroquine

pretreatment was variable and demonstrated larger effect in the HeLa cells, suggesting a greater

cellular role of WA-induced lysosomal degradation in addition to proteasomal degradation.

Combination of MG132 and chloroquine to rescue WA-induced protein depletion was not shown

to be greater than either compound alone.

HSP90 client protein c-myc has previously been shown to require amino acid sites T58

and S62 for phosphorylation-directed ubiquitination and subsequent degradation via the

proteasome (Gregory and Hann, 2000; Sears et al., 2000; Kamemura et al., 2002). 293T cells

were stably transfected with T58A/S62A FLAG-tagged c-myc (c-myc$^{T58A/S62A}$-FLAG), a variant

with mutations to disrupt the normal c-myc proteasomal degradation, and treated with WA. Both

vector control and mutant transfected cells demonstrated dose-dependent depletion of

Figure 5-4.
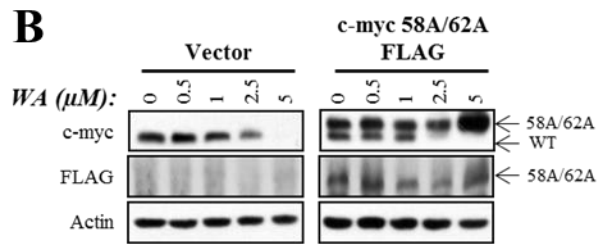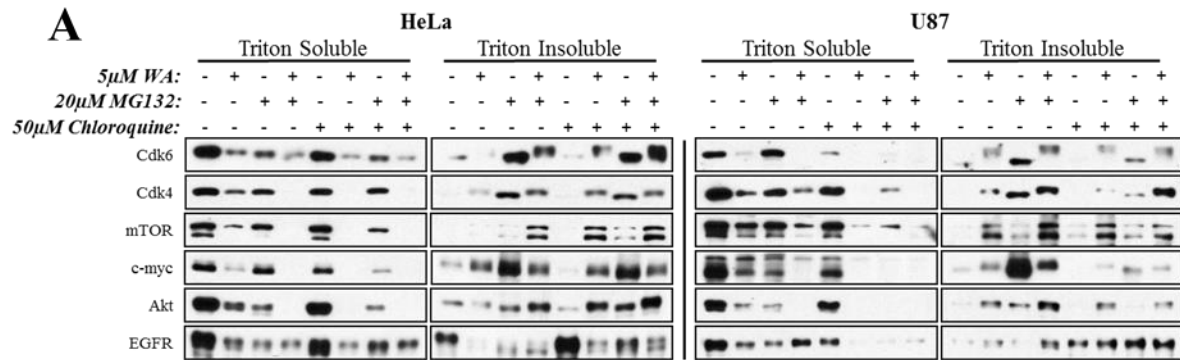
Figure 5-4. A) HeLa and U87 cells were pretreated with the proteasome inhibitor MG132 or the lysosome inhibitor chloroquine for 1 h followed by WA for 24 h, and cellular proteins were fractionated by triton X-100 solubility. Treatment with WA induced a loss of HSP90 client proteins (Cdk6, Cdk4, mTOR, c-myc, Akt, EGFR) in the soluble fraction with a shift to either the insoluble fraction or a depletion in both fractions. MG132 also acted to shift proteins to the insoluble fraction. Combination of WA and MG132 demonstrated increased retention of all evaluated proteins in the insoluble fraction. Protein retention with chloroquine pretreatment followed by WA was variable and demonstrated greater effect in the HeLa cells. Combination of MG132 and chloroquine to rescue WA-induced protein depletion was not shown to be greater than either compound alone. B) 293T cells were transfected with c-myc$^{T58A/S62A}$-FLAG, a variant with mutations to disrupt the normal c-myc proteasomal degradation, and treated with WA. Endogenous wild-type c-myc was depleted by WA in a dose-dependent manner, but the mutant failed to decrease after 24 h.

endogenous wild-type c-myc by 2.5 μM WA. The c-myc$^{T58A/S62A}$ mutant, however, showed no decrease in response to WA treatment, demonstrating the functional requirement for proteasomal-targeting in WA-mediated protein degradation (Figure 5-4B).

5.4.5 Proteasomal inhibition potentiates the cytotoxicity of withaferin A

Given the apparent importance of the HSP70 chaperone axis and the proteasome in regulating protein degradation following WA treatment, simultaneous inhibition of the proteasome with MG132 to prevent degradation of aberrant protein accumulation was evaluated to determine the utility of combination therapy. Cell viability was assessed by MTS assay after 72 h (Figure 5-5A). HeLa and U87 cells displayed no significant decrease in viability with 25-75 nM and 75-125 nM MG132 alone, respectively. However, 1h sub-cytotoxic MG132 pretreatment potentiated the anti-proliferative response to treatment with escalating concentrations of WA. 62.5 nM WA reduced HeLa cell viability by 15.5% after 72 h but was enhanced to 38.2% with 25 nM MG132 (p = 0.010) and 42.2% with 75 nM MG132 (p = 0.043). Comparable enhancement was observed with 125-250 nM WA. In U87, 750 nM WA decreased cell viability by 25.0% but was enhanced to 56.3% with 75 nM MG132 (p = 0.072) and 83.1% with 125 nM MG132 (p = 0.016).

Similarly, evaluation of drug-induced cell death by flow cytometry revealed that pretreatment with MG132 potentiated the cytotoxicity of WA (Figures 5-5B and 5-5C). In HeLa, combination therapy induced 45.8% cell death (25.3% early apoptosis, 7.7% necrosis, 12.9% late apoptosis/necrosis) compared to only 2.4% in control (1.2% early apoptosis, 0.5% necrosis, 0.7% late apoptosis/necrosis; p = 0.015), 2.6% with 125 nM MG132 (0.6% early apoptosis, 1.1%

Figure 5-5.
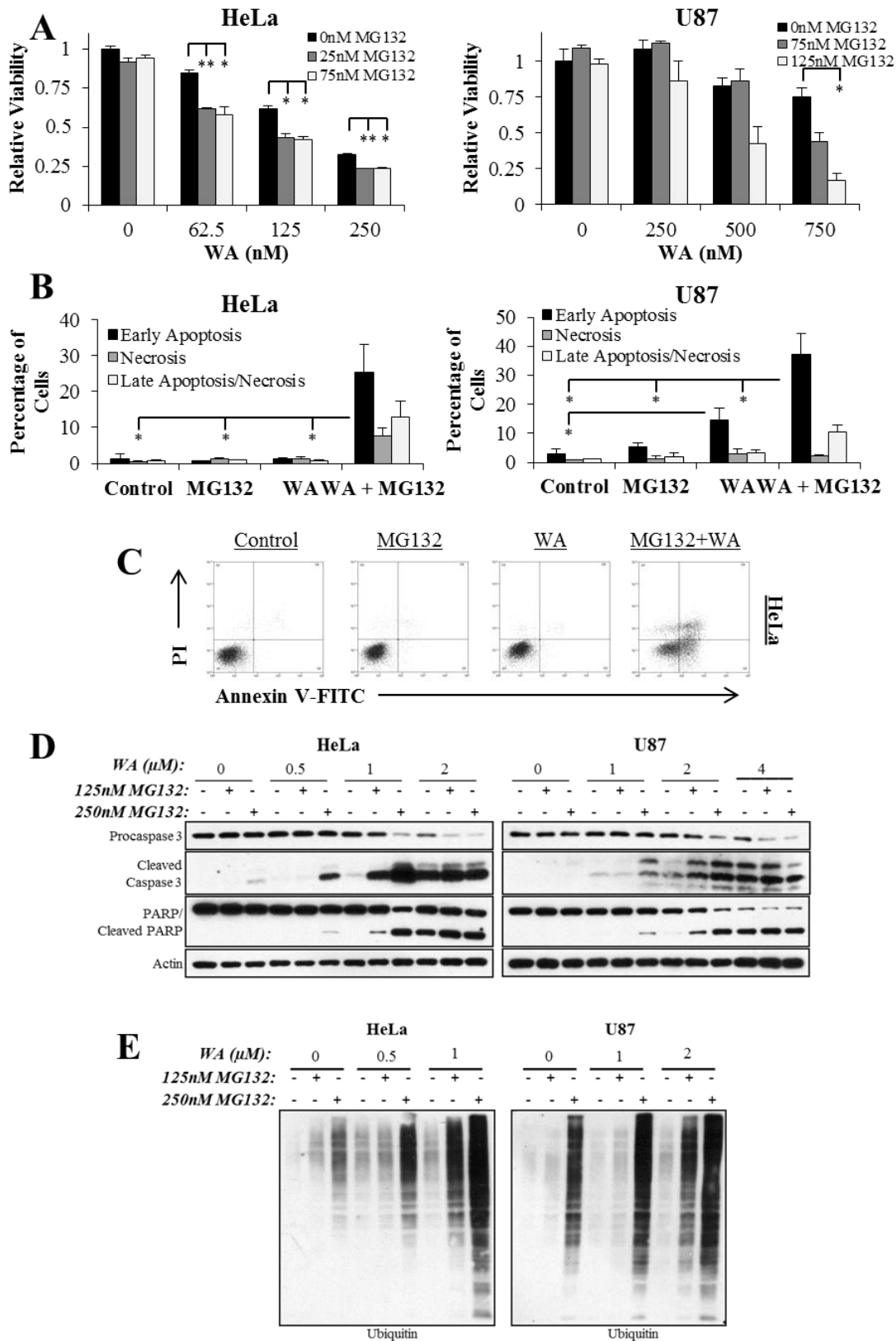
Figure 5-5. A) HeLa and U87 cell viability following combination therapy with proteasome inhibitor MG132 and WA was evaluated by MTS assay after 72 h. HeLa and U87 cells displayed no significant decrease in viability with 25-75 nM and 75-125 nM MG132 alone, respectively. However, MG132 pretreatment at these concentrations potentiated the anti-proliferative response to treatment with escalating concentrations of WA. B) Efficacy of combination MG132 and WA therapy on HeLa and U87 cells after 24 h was further evaluated by flow cytometry with propidium iodide and annexin V-FITC doe cell death. Staining revealed that pretreatment with 125 nM MG132 potentiated the cytotoxicity of 1 μM WA in both lines. MG132 alone had no statistically significant effect compared to control, and only WA demonstrated elevated death in U87 cells, but combined, the cytotoxic effects were significantly elevated. C) A representative example of the flow cytometry results in HeLa cells. D) Flow cytometry data was supported by molecular evaluation of apoptotic markers procaspase 3 and PARP cleavage in both HeLa and U87 cells. After 24 h, treatment with 125-250 nM MG132 in both lines as well as 0.5-1 μM WA in HeLa and 1-2 μM WA in U87 failed to induce significant cleavage of either protein but yielded large increases in the cleaved product when combined. E) Combined treatment with MG132 and WA for 24 h resulted in the accumulation of ubiquitinated proteins at all concentrations evaluated in both HeLa and U87 cells, demonstrating retention of proteins targeted for degradation. $*p < 0.05$, $**p < 0.01$, $***p < 0.001$

necrosis, 0.9% late apoptosis/necrosis; p = 0.016), and 3.2% with 1 µM WA (1.2% early apoptosis, 1.3% necrosis, 0.7% late apoptosis/necrosis; p = 0.016). WA and WA+RT demonstrated no statistically significant difference over control. Similarly, in U87, combination therapy induced 50.2% cell death (37.3% early apoptosis, 2.2% necrosis, 10.6% late apoptosis/necrosis) compared to only 4.7% in control (2.8% early apoptosis, 0.8% necrosis, 1.1% late apoptosis/necrosis; p = 0.013), 8.3% with 125nM MG132 (5.4% early apoptosis, 1.2% necrosis, 1.8% late apoptosis/necrosis; p = 0.024), and 20.9% with 1 µM WA (14.6% early apoptosis, 3.0% necrosis, 3.3% late apoptosis/necrosis; p = 0.015). WA alone also demonstrated a statistically significant cytotoxic advantage over control (p = 0.011). Together, these data demonstrate that sub-cytotoxic pre-exposure to MG132 potentiates minimally or non-lethal WA concentrations.

Flow cytometry data was supported by molecular evaluation of apoptotic markers procaspase 3 and PARP cleavage in both HeLa and U87 cells (Figure 5-5D). After 24 h, treatment with 125-250 nM MG132 in both lines failed to induce significant cleavage of either protein. Similar findings were observed with 0.5-1 µM WA in HeLa and 1-2 µM WA in U87. However, combination of these agents at the noted concentrations revealed large increases in the cleaved product of both procaspase 3 and PARP, demonstrating the advantage of combination therapy.

Consistent with the expectation that combination therapy would result in enhanced cytotoxicity through an accumulation of aberrant proteins generated by WA treatment and unable to be properly degraded via the proteasome due to MG132, dual treatment over 24 h resulted in the accumulation of ubiquitinated proteins at all concentrations evaluated (Figure 5-5E). Potentiation of the effect was particularly notable at modest concentration of each compound that

alone produced minimal yet early indications of ubiquitination. By denisometry, 125 nM MG132 increased ubiquitination 2.2-fold in HeLa and 1.8-fold in U87, while 1 μM and 2 μM WA resulted in 3.0- and 3.3-fold elevations in HeLa and U87, respectively. Combination of MG132 and WA showed further enhanced levels of global protein ubiquination by 11.4-fold in HeLa and 10.7-fold in U87, demonstrating the value of this approach.

5.5 Discussion

WA is a promising naturally-derived anti-cancer compound that has demonstrated efficacy across a spectrum of cancer types both *in vitro* and *in vivo*. Underlying WA's antiproliferative, pro-apoptotic, and anti-angiogenic effects is disruption of various signaling pathways including those utilizing Akt/mTOR, MAPK, Notch, NFκB, JAK/STAT, and more (Vanden Berghe et al., 2012; Vyas and Singh, 2014). However, details of the mechanism driving these diverse effects have remained poorly defined to-date. Previous studies have identified a pro-oxidant effect (Malik et al., 2007; Widodo et al., 2010; Hahm et al., 2011; Mayola et al., 2011; Santagata et al., 2012; Grogan et al., 2013) and suggested that alterations in HSP90 function occurs with WA treatment (Yu et al., 2010; Gu et al., 2014). Here, we further characterized these findings and propose each as the two of the dominant mechanisms by which WA mediates in anti-cancer effects: Induction of cellular oxidation and disruption of the interaction between HSP90 and its co-chaperone Cdc37 independent of direct HSP90 inhibition. These proposed mechanisms explain the numerous descriptions of alterations in oncogenic proteins and signaling pathways that have come to define the cellular response to WA.

HSP90 functions as a chaperone to promote the folding, refolding, and function of a specific set of client proteins (Pearl et al., 2008). This ability is dependent on the association of HSP90 with several co-chaperone proteins that promote this function (Taipale et al., 2010). Although not yet fully understood mechanistically, Cdc37 is thought to act largely as a kinase-specific co-chaperone to promote the folding and maturation of these proteins through localization with HSP90 with enhanced client loading though modulation of HSP90 ATPase activity (Siligardi et al., 2002; Roe et al., 2004). Cdc37 has also demonstrated chaperoning functions independent of HSP90 (MacLean and Picard, 2003). Here, we demonstrate that pharmacological disruption of this interaction between HSP90 and Cdc37 with WA is associated with a failure of HSP90 to associate with Cdc37-dependent protein Cdk6 but not Cdc37-independent protein GR as well as degradation of multiple HSP90 client proteins. Additionally, depletion of HSP90 client proteins known to interact with Cdc37 (Akt, Raf-1, EGFR, Cdk4, Cdk6, and Chk1) was observed. Intrinsic HSP90 chaperone function, assessed by supporting GR steroid binding, was not impaired at relevant concentrations of WA, although several HSP90 client proteins not previously described as Cdc37-dependent (BRCA1, c-myc, GR) were also depleted suggesting an alternate mechanism of protein modulation and/or a previously undescribed requirement for Cdc37. These findings, if not mediated through an alternative mechanism, suggest that WA may still maintain a direct role in the inhibition of HSP90's folding mechanism independent of its GR support. Cdc37 has been primarily reported to facilitate folding of newly translated proteins (MacLean and Picard, 2003; Karnitz and Felts, 2007), but its importance has been demonstrated in the stability of existing proteins (Jinwal et al., 2011). Further studies are necessary to determine if either situation represents the predominant inhibitory effect of WA.

Interestingly, a recent study demonstrated that mutant Cdc37 lacking the C-terminal/middle HSP90-association domain maintained cellular levels of client proteins and augmented the interaction between HSP90 and client Cdk4 despite diminished client protein interaction itself (Smith et al., 2013). However, this directly contrasts previous reports about the importance of the C-terminal/middle domain for association with HSP90 in maintaining the stability of client proteins like Raf-1 (Grammatikakis et al., 1999; Rao et al., 2001). It is possible that the client proteins evaluated have different co-chaperone requirements for interacting with HSP90 or can be maintained through Cdc37's inherent chaperone activity given that only approximately half of mammalian Cdc37/Cdk4 complexes contain HSP90 (Dai et al., 1996). However, the latter is likely not the case here given the reduced client affinity of the mutant Cdc37 despite maintained client levels (Smith et al., 2013). Cdc37 has also been shown to interact with other co-chaperone proteins, suggesting another way by which it can still join the HSP90 chaperone complex, although its ability to alter HSP90 ATPase activity and otherwise function properly through this indirect association is unknown (Abbas-Terki et al., 2002). Clearly, further study of this system is required to better understand the variations observed. Regardless of the nature of the HSP90/Cdc37 interaction, its disruption and the resulting cytotoxicity by exposure to WA and celastrol, as previously studied, demonstrate pharmacological proof-of-concept of this target (Zhang et al., 2008; Zhang et al., 2009; He et al., 2013).

While computational analysis revealed a potential binding site for WA on Cdc37 to disrupt the HSP90/Cdc37 interaction (Grover et al., 2011), IP studies with biotinylated WA showed that it actually bound to the C-terminus of HSP90 (Yu et al., 2010). The C-terminus of HSP90 is responsible for the association with various co-chaperones (Young et al., 1998; Sidera

and Patsavoudi, 2014), however, WA does not decrease HSP90 association with co-chaperones Hop or p23 but rather Cdc37 which interacts primarily on the N-terminus of HSP90 (Yu et al., 2010; Eckl et al., 2013). This unexpected finding requires further study to explain but may be a result of WA-mediated direct steric hindrance, conformational alterations in HSP90 structure that prevent effective binding of Cdc37 but maintain HSP90 function, or changes in the ability of Cdc37 to associate with C-terminal co-chaperones. Interestingly, celastrol also binds to the C-terminus of HSP90 to disrupt HSP90/Cdc37 interaction but fails to disrupt association with HSP70, Hop, or p23 (Zhang et al., 2009). Novobiocin, also known to associate with the C-terminus, demonstrates completely opposite effects, suggesting specific sites of co-chaperone regulation on HSP90 (Yun et al., 2004).

HSP90 represents an intriguing anti-cancer target given that it is endogenously expressed in all cells, typically accounting for 1-3% of the total cellular protein (Welch and Feramisco, 1982; Workman et al., 2007; Moulick et al., 2011; Barrott and Haystead, 2013). However, most cancer cells demonstrate significantly greater sensitivity to HSP90 inhibitors than non-cancerous cells with sub-toxic doses resulting in anti-tumor efficacy. This is thought to likely be the result of several factors that frequently differ in cancer cells including upregulation of HSP90 protein and mRNA, enhanced basal activation of HSP90 through post-translational modifications and/or enhanced association with various co-chaperones and client proteins, and altered localization to the ectopic portion of the cell (Barrott and Haystead, 2013). These considerations for enhancing inhibitory selectivity of HSP90 alone would appear to translate well to the disruption of co-chaperones such as Cdc37, particularly HSP90 dependency and localization. Further studies are necessary to identify whether WA affinity favors disruption of HSP90 and Cdc37 that are already associated or prevention of the initiation of the association. Treatment with WA in

196

several murine models demonstrates an appropriate therapeutic window against several cancer types with minimal off-target toxicity and shows the translatable promise of this approach (Vyas and Singh, 2014).

WA also demonstrated the ability to induce cellular oxidation. AA was used as a non-thiol antioxidant to evaluate the oxidative effects of WA independent of concerns that NAC may simply sequester WA, preventing the availability of free drug rather than actually directly reducing generated oxidation (Santagata et al., 2012; Vyas and Singh, 2014). AA at a previously-identified effective concentration (100 μM) was capable of reducing total oxidative potential within U87 GBM cells but was unable to completely eliminate the effect like NAC. Similarly, the cytotoxicity of WA was completely blocked by NAC but not AA. These findings suggest that while oxidation does indeed play a part in the mechanism of WA, the generation of free reactive oxygen species likely does not have nearly as significant of an impact in the manifestations of WA as its thiol reactivity and thiol-mediated redox alterations. The observation that WA depletes GSH suggests that the oxidation may be a general effect of an altered redox state. Interestingly, overexpression of Cu,Zn-superoxide dismutase demonstrated a partial protective effect against WA treatment in breast cancer cells (Hahm et al., 2011). The same study suggested that WA-mediated ROS generation and subsequent toxicity was a result of mitochondrial respiration inhibition, although the impact of the mitochondrial alterations on normal intrinsic/mitochondrial apoptotic pathway function, shown to be partially necessary for apoptosis following WA exposure (Grogan et al., 2014), was not evaluated. Taken together, these findings support an important role for oxidation following WA treatment but suggest it may be more critical for cytotoxicity in certain cancer types.

197

We have also previously demonstrated WA-mediated depletion of MGMT, a non-HSP90 client protein with known susceptibility to oxidation (Fu et al., 2010; Ryu et al., 2012; Grogan et al., 2014). Similarly, GR has been shown to be modulated by redox alteration, especially with thiol-modifying agents (Carter and Ragsdale, 2014). Despite not requiring Cdc37 for its function and stability and maintaining association with HSP90, we demonstrated in the present study that GR is eventually depleted with WA treatment, suggesting either an extended role of WA as an HSP90 inhibitor beyond Cdc37 effects or oxidation-mediated proteotoxicity. Utilization of oxidative therapies to induce proteotoxicity has gained interest as an anti-cancer approach given the frequently altered redox states and exposure to increased cellular stress which can be exploited in cancer cells (Laurent et al., 2005; Cabello et al., 2007).

Treatment with WA resulted in the accumulation of aggregated HSP90 of heterogeneic molecular weight in the triton insoluble fraction of the cell, often regarded as the biologically inactive compartment. Previous studies have suggested that chaperone proteins form disulfide bonds in response to oxidative insults (Cumming et al., 2004; Chen et al., 2008), and while the described homodimeric complex of HSP90 was not readily observed in this study, significant aggregation was noted. Further study will be necessary to determine whether this pattern of aggregation was related to dissociation from Cdc37 (showing direct interplay between the two proposed mechanisms of WA), a byproduct of oxidative stress, or misfolding and destabilization guided by direct WA binding. While Cdc37 plays a role in the appropriate client targeting for HSP90 and has been shown to localize in the cell for recruitment of HSP90-mediated refolding (Jinwal et al., 2011), it has not been shown necessary to promote HSP90 complex stability or intrinsic function. While pretreatment with NAC reduced or eliminated the general cytotoxicity of WA, it also prevented this alteration in HSP90 localization. Conversely, depletion of cellular

GSH through inhibition of γ-glutamylcysteine synthetase by BSO greatly enhanced this HSP90 alteration. Together, these findings support an oxidative or thiol-reactive role of WA in promoting insoluble complexation of HSP90. Of note, BSO also enhanced general WA cytotoxicity in several additional cancer models (data not published). Combined with the observation that WA depleted GSH, this suggests that GSH plays a protective role against WA. Future studies are necessary to determine how basal cellular oxidation, GSH levels, and susceptibility to oxidative stress enhance or resist the cytotoxic sequelae of WA exposure.

Several early studies attempting to identify the mechanism of WA suggested that it functions through inhibition of the proteasome (Yang et al., 2007; Khan et al., 2012; Yang et al., 2012). Our data suggests that the proteasome is still functionally intact and necessary for protein degradation at cytotoxically-relevant concentrations of WA. While the findings in these reports are likely accurate, they have consistently utilized concentrations of WA well-above those considered therapeutically relevant – including in cell-free models – to achieve modest proteasomal inhibition, suggesting that these findings may simply be off-target effects that manifest at high concentrations. Interestingly, our studies demonstrate direct inhibition of the HSP90 chaperone heterocomplex independent of Cdc37 in a cell-free system with an IC_{50} of <10μM (data not shown), well above physiologically relevant dosing but still lower than observed in the GR-reactivation cell lysate system. Combined, these findings indicate non-specific targeting by WA at high concentrations and suggest caution is necessary during the interpretation of data at these levels.

While the suggestion that HSP90 promotes protein refolding while HSP70 favors degradation oversimplifies the complex mechanism of the protein chaperone machinery, these generalizations accurately describe the accepted primary roles that these chaperones play in

protein homeostasis (Pratt et al., 2010). In the presence of oxidative stress, proteins are prone to misfold with greater frequency. Simultaneous inhibition of the HSP90 axis, as observed with WA, would suggest the accumulation of many aberrant proteins requiring proper degradation to limit cellular cytotoxicity. Previous studies have identified upregulation of HSP70, as observed in the present study, to be a biomarker of HSP90 inhibition and/or oxidative stress (Zhang et al., 2006; Workman et al., 2007; Ansari et al., 2011; Qiao et al., 2012), acting as a compensatory mechanism for protein dysregulation and promoting this necessary degradation. Indeed, inhibition of HSP70 or the proteasome in the presence of traditional HSP90 inhibitors promotes a synergistic effect (Minnnaugh et al., 2004; Ma et al., 2014). Given the promotion of proteasome-mediated protein degradation induced by WA, the addition of a proteasome inhibitor was a logical progression in the development of a clinical utility for WA. Here, we further demonstrate the efficacy of this approach with WA, an oxidizing inhibitor of the HSP90/Cdc37 association. This suggests a potential clinical utility for combining a co-chaperone disruptor with already established chemotherapeutic agents like the proteasome inhibitor bortezomib. While the value of this combination therapy was demonstrated in highly aggressive solid tumor cervical and brain cancer cell lines, perhaps the greatest early clinically applicability lies in the treatment of multiple myeloma (MM). Proteasome inhibitors have been approved for use as standard agents in the treatment of MM (Chauhan et al., 2005), and an early human trial with combination bortezomib and the HSP90 inhibitor tanespimycin, a promising formulation of 17-AAG with a Cremophor-containing vehicle (Modi et al., 2007; Modi et al., 2011), has shown promise (Richardson et al., 2011). Given the enhanced efficacy of many agents in combination with traditional HSP90 inhibitors, further exploration of combination therapy with WA in alternative models is also warranted (Neckers, 2002).

The studies here provide an important framework for further defining the mechanisms by which WA induces significant protein depletion. We demonstrate that WA acts to produce thiol-mediated oxidation and disrupt the interaction between HSP90 and Cdc37 but fails to inhibit intrinsic HSP90 function assessed by HSP90-mediated GR steroid binding. Ultimately, this shifts the HSP90/HSP70 balance toward HSP70-domination with associated protein degradation that can be cytotoxically potentiated therapeutically with simultaneous inhibition of the proteasome. While further pre-clinical studies will be necessary to fully evaluate the therapeutic potential of WA alone and in combination with proteasome inhibitors, current findings support the translational utility of this approach.

Chapter 6

Withaferin A disrupts the cellular DNA-damage response to promote radiosensitization

6.1 Abstract

Radiation therapy (RT) plays in important role in the treatment of cancer for an estimated 50% of patients, including as a standard therapy for the brain tumor glioblastoma multiforme (GBM). Withaferin A (WA) is a naturally-derived steroidal lactone that has demonstrated significant intrinsic anti-cancer activity. Several preliminary reports have identified WA as a potential radiosensitizer, but the underlying mechanism has remained largely unexplored. In this study, WA potentiated or otherwise enhanced the anti-proliferative activity of RT in both U87 GBM and HeLa cervical cancer cells. These findings were associated with reduction of cells in the DNA-synthesis phase of the cell cycle and increased levels of cell cycle checkpoint inhibitors p21 and p27 with combination therapy through 72 h. Combination therapy failed to enhance PARP cleavage and LC3B conversion, demonstrating that the effect was not mediated through apoptosis or autophagy. Treatment with WA reduced total levels of DNA-damage response (DDR) proteins involved in damage recognition (Mre11, p95/NBS1, Rad50), signaling (ATM, Chk1), and repair through homologous recombination (BRCA1, BRCA2, Rad51), non-homologous end-joining (DNA-PKcs, XLF, Ku70, and Ku80), and mismatch repair (MLH1, MSH2, MSH6) in both U87 and HeLa. This protein depletion was an expansion of that observed with traditional HSP90 inhibitor 17-AAG. WA differentially modulated normal the normal recognition response to RT-mediated DNA damage with U87 and HeLa cells showing a reduction and an increase of p-H2A.X compared to RT alone, respectively, with WA pretreatment. Both lines showed alterations of normal signal transduction through ATM and Chk1. WA pretreatment also enhanced the level of RT-induced double strand DNA damage after 4 h measured by a neutral comet assay and was associated with functional inhibition of

homologous recombination through a DR-GFP reporter. These findings demonstrate that WA-driven radiosensitization is a direct result of an impaired DDR. Given the widespread success of WA as a monotherapy in numerous cancer models and the large therapeutic spectrum for RT, further translational exploration of WA as an adjuvant agent is warranted.

6.2 Introduction

In recent years, significant effort has been invested in the development of more effective therapeutic and diagnostic techniques to better the outcomes of cancer patients. While numerous advances have adjusted the treatment paradigms of various malignancies, the management and treatment of many cancers depends on the use of radiation therapy (RT), including an indication in an estimated 50% of patients (Delaney et al., 2005). Given that survival rates following RT, which in many cases represents a component of the base available approved therapeutic regimen, remain low for certain cancer types like glioblasoma multiforme (GBM), any means by which to elevate RT efficacy would be critical in helping a wide population of patients (Begg et al., 2011).

With the widespread importance and critical role of RT, efforts have been made to maximize its therapeutic potential through adjustments of dose intensity and fractionation as well as addition of chemotherapeutics. Such therapies focus on modulating the DNA damage response (DDR), signal transduction pathways critical for radioresistance, and oxygen levels necessary for generating an effect (Begg et al., 2011). Additionally, several commonly utilized DNA-modifying anticancer agents, including 5-fluorouracil (5-FU) and temozolomide (TMZ), have shown radiosensitization effects with unclear mechanisms. Similar agents like gemcitabine demonstrate off-target inhibition of HR as a mechanism of radiosensitization (Byfield, 1989;

Wachters et al., 2003; Chakravarti et al., 2006; Bobola et al., 2010). Other agents that directly target elements of the cellular DDR, including the recognition and repair of the damage, have generated significant interest as well (Begg et al., 2011).

RT utilizes the energy of ionizing radiation (IR) to induce DNA lesions in targeted cells. Genomic instability through double-strand DNA (dsDNA) breaks (DSBs) is largely recognized as the primary cytotoxic event of IR, but other lesions such as single-strand DNA (ssDNA) breaks (SSBs) and damage to individual bases has been reported. DSBs are repaired by two primary pathways: homologous recombination (HR) and non-homologous end joining (NHEJ). While HR maintains the fidelity of the DNA sequence at the break site, NHEJ simply anneals two ends of DNA without respect to sequence homology and is therefore intrinsically mutagenic.

The cellular response to DNA damage, including that induced by IR, involves an immensely complex network of signaling pathways that recognize and repair the damage with associated arrest of the cell cycle or induction of death (Lamarche et al., 2010; Baskar et al., 2012). Very generally, following DSBs, damage is recognized by the MRN complex (Mre11, Rad50, p95/NBS1) which functions to coordinate signal transduction through ATM to arrest cell growth at specific cell cycle checkpoints. This complex also functions directly and indirectly to mediate dsDNA damage repair through HR and NHEJ (Weterings and Chen, 2008; Krejci et al., 2012). Appropriate coordination of these efforts in normal tissue usually results in either effective DNA damage repair and cell survival or failure to appropriately correct the insult followed by the controlled induction of cellular senescence or death.

Several studies have identified the potential utility of withaferin A (WA), a 28-carbon steroidal lactone identified from genera of the *Solenceae* plant family with intrinsic cytotoxicty, as a potential radiosensitizer (Vanden Berghe et al., 2012; Vyas and Singh, 2014). One study that

utilized a knockout model suggested WA may alter NHEJ (Devi et al., 2008), while another group identified enhanced oxidation and modulation of the mitogen-acitviated protein kinase (MAPK) and Akt pathways as markers of combination therapy efficacy (Yang et al., 2011b; Yang et al., 2011a). However, to date, the underlying mechanism behind this effect has not been explored. Studies from our group and others have identified two key components of WA monotherapy that are hypothesized to lead to the inhibition and modulation of many oncogenic proteins that have been observed: oxidation and inhibition of the HSP90 axis through disruption of the HSP90/Cdc37 association (Malik et al., 2007; Widodo et al., 2010; Yu et al., 2010; Hahm et al., 2011; Mayola et al., 2011; Santagata et al., 2012; Grogan et al., 2013). Indeed, direct inhibition of HSP90 has been previously noted to function in a radiosensitizing role (Dote et al., 2006; Kabakov et al., 2010; Ko et al., 2012; Stecklein et al., 2012), suggesting a potential mechanism by which WA may function and a novel role for disruption of Cdc37.

In this study, we identify WA as a potent radiosensitizer of two highly aggressive cancer cell lines, the GBM U87 and the cervical cancer HeLa with the latter being utilized as a known model of highly competent HR, through depletion of key DDR proteins that prevent the proper recognition and repair of DSBs.

6.3 Materials and methods

6.3.1 Cell culture and reagents

The human GBM cell line U87 was generously provided by Dr. Jann N. Sarkaria (Mayo Clinic, Rochester, MN), and the human cervical cancer line HeLa was obtained through the

American Type Culture Collection (ATCC; Manassas, VA). These cell lines were chosen given their DNA damage repair preferences: HeLa is more competent at HR than GBM cells while the latter favor NHEJ after RT (Kachhap et al., 2001; Golding et al., 2004; Ransburgh et al., 2010; Quiros et al., 2011; Lim et al., 2012; Stecklein et al., 2012). Both cell lines were grown in Dulbecco's modified Eagle's medium (DMEM #11995-065; Gibco, Grand Island, NY) supplemented with 10% fetal bovine serum (FBS; Sigma-Aldrich, St. Louis, MO) and 1% penicillin/streptomycin (Gibco), at a 37 °C humidified atmosphere of 5% CO_2 in air. Medium for HeLa cells was further supplemented with 2% L-glutamine (200 mM; Gibco), 1% MEM-vitamin (100x; Hyclone, Logan, UT), and 1% MEM nonessential amino acids (Sigma Aldrich). Where indicated, cells were irradiated with a Kimtron IC-320 orthovoltage x-ray device (Oxford, CT) at a calibrated dose-rate of 452.23 cGy/minute. WA was isolated as previously described (Samadi et al., 2010b). Propidium iodide (PI), RNase, and puromycin dihydrochloride were acquired from Sigma-Aldrich, and 17-*N*-allylamino-17-demethoxygeldanamycin (17-AAG) was obtained from LC Laboratories (Woburn, MA).

6.3.2 Clonogenic assay

HeLa and U87 cells in exponential growth phase were plated in 6cm dishes at densities expected to yield approximately 20-50 colonies per plate following exposure to WA, RT, or combination therapy based on preliminary studies. After 6 h, plates were changed to WA- or DMSO-containing media and allowed to incubate for 2 h before exposure to 2-4 Gy of radiation. 24 h post-RT, media was changed on each plate to remove WA. Cells were incubated for 10-14 d at which time they were gently washed with 1x phosphate-buffered saline (PBS), stained and

fixed with Coomassie brilliant blue, and quantified. Colonies were considered viable if they consisted of approximately > 50 cells.

6.3.3 Cell cycle analysis

U87 and HeLa cells were plated to ~20-50% confluency depending on the collection timepoint and treated with WA for 2 h followed by 2.5-5 Gy RT. After 24-72 h, cells were collected, pelleted, fixed/permeablized in 70% ice-cold ethanol and stored at -20 °C. Cells were subsequently stained with PI as previously described (Grogan et al., 2013) and analyzed by flow cytometry on a Beckman Coulter CyAn ADP analyzer (Brea, CA). Only living cells without DNA fragmentation were gated for analysis.

6.3.4 Immunoblotting

Cells were plated to appropriate confluencies as outlined for cell cycle analysis and treated with various concentrations of WA or 17-AAG. Where indicated, cells were irradiated with 5-10 Gy 2 h post-WA. After 1-72 h, cells were trypsinized and washed twice with 1x PBS. Proteins were isolated in a HEPES-based lysis buffer, quantified, separated by sodium dodecyl sulfate–polyacrylamide gel electrophoresis (SDS–PAGE), and transferred onto a Hybond nitrocellulose membrane as previously described (Samadi et al., 2011; Grogan et al., 2014). 25-50 µg of protein sample was loaded per lane with equal loading and transfer of sample confirmed by total actin levels. Studies were repeated for accuracy.

Primary antibodies kits were acquired from Cell Signaling Technology (Danvers, MA) and used as per the manufacturer's recommendations: DNA damage (#9947), double stand breaks (DSB) repair (#9653), MRN complex (#8344), mismatch repair (#9786), and Rb (#9969). Additional primary antibodies obtained from Cell Signaling Technology included ATM (#2873; 1:1000), Chk1 (#2360; 1:1000), Chk2 (#2662; 1:1000), Ku70 (#4588; 1:1000), BRCA1 (#9010; 1:500), BRCA2 (#9012; 1:1000), p27 (#2552; 1:1000), cyclin B_1 (#4138; 1:1000), cyclin D_1 (#2926; 1:500), cyclin E_1 (#4129; 1:1000), poly(ADP-ribose) polymerase (PARP; #9542; 1:1000), and LC3B (#3868; 1:1000). Rad51antibody (#ab213; 1:1000) was purchased from Abcam (Cambridge, England). p-H2A.X antibody (Ser139; #613401; 1:1000) was acquired from Biolegend (San Diego, CA). Total actin antibody (#MAB1501; 1:50000) was obtained from EMD Millipore (Billerica, MA). The primary antibody for p21 (#sc-6246; 1:200) and the donkey anti-rabbit IgG HRP (sc-2313; 1:2500-1:10000) and goat anti-mouse IgG HRP (sc-2005; 1:5000-1:20000) secondary antibodies were purchased from Santa Cruz Biotechnology (Santa Cruz, CA).

6.3.5 Immunocytochemistry (ICC)

U87 and HeLa cells were plated to ~50% confluency in 8-well chamber slides (Nalge Nunc International, Penfield, NY) and treated with 2.5 μM WA for 2 h. Slides then received 10 Gy RT. After 1 h, cells were fixed in 4% PBS-buffered paraformaldehyde at room temperature for 30 minutes and washed 3x with 1x PBS. Cell membranes were de-permeablized for 15 minutes in 1x PBS containing 0.3% triton X-100 and subsequently blocked in 5% goat serum (Cell Signaling Technology) in 1x PBS containing 0.15% triton X-100 shaking for 1 h. Cells

were exposed to p-H2A.X (Ser139) primary antibody (1:500; Biolegend #613401) in blocking solution overnight at 4 °C. After three washes with 1x PBS, secondary antibody (1:1000; anti-mouse IgG Fab2 Alexa Fluor 488, Cell Signaling #4408) was added to each well for 1h at room temperature followed by an additional 3 washes. Coverslips were mounted on each slide with ProLong Gold Antifade with DAPI (Cell Signaling Technology), allowed to dry, and visualized on a Leica DM IRB microscope (Wetzlar, Germany) with Metamorph Basic software (version 7.7.3.0.; Molecular Devices; Sunnyvale, CA)

6.3.6 Comet assay

U87 cells were assessed for dsDNA damage by a neutral comet assay. Cells were plated to 50% confluency and treated with WA. After 12 h, cells were irradiated 5 Gy via the orthovoltage device and allowed to incubate for 4 h. Evaluation of DNA damage through migration was conducted according to the manufacturer's instructions (Trevigen, Gaithersburg, MD). Briefly, cells were collected, combined with agar, and plated on slides (~500 cells/slide). Agar was solidified at 4 °C for 10 minutes, and slides were immersed in a lysis buffer solution for 1 h at room temperature. Slides were then washed with neutral electrophoresis buffer and underwent electrophoresis for 45 minutes at 4 °C with the recommended voltage. At room temperature, slides were then immersed in DNA precipitation buffer for 30 minutes followed by 70% ethanol for 30 minutes. Samples were dried at 37 °C for 15 minutes, stained with SYBR Gold (Molecular Probes, Eugene, OR) as outlined in the instructions, and visualized on the Leica DM IRB microscope with Metamorph Basic software. Comets from eight independent visual

fields per sample were quantified with ImageJ software (version 1.46r; Bethesda, MD) using the automated scoring of the OpenComet software macro (version 1.3) (Gyori et al., 2014).

6.3.7 DR-GFP reporter assay

The DR-GFP reporter construct, pCAGGS empty vector, and pCBASce I-SceI vector were generously provided by Dr. Maria Jasin (Memorial Sloan-Kettering Cancer Center, New York, NY). Adenovirus was kindly provided by Dr. Jeffrey Parvin (The Ohio State University, Columbus, OH). The production and titering of HA-tagged I-SceI or empty vector adenovirus was described previously (Stecklein et al., 2012). U87 and HeLa cells were transfected with the DR-GFP and selected with 2-5 µg/mL puromycin. Surviving colonies were collected and expanded under puromycin selection. The empty control vector or HA-I-SceI construct (~1 µg/1x10^5 cells) were introduced into the U87-DR-GFP stable transfectants via electroporation using the Amaxa Cell Line Nucleaofector Kit V according to the manufacturer's instructions (Lonza, Bazel, Switzerland). The vectors were introduced into the HeLa-DR-GFP cells via the adenovirus. Both cells were immediately plated and treated with DMSO or various concentrations of WA. After 72 h, cells were collected, and HR was evaluated visually by microscopy and by determining the number of GFP+ cells on the Beckman Coulter CyAn ADP analyzer. Western blotting for HA was used to confirm that WA had no effect on the expression level of the HA-tagged I-SceI.

6.3.8 Data and statistical analysis

211

Comparisons of differences between two or more means/values were determined by Student's unpaired t-test via the statistical functions of GraphPad Prism 6 (version 6.02; GraphPad Inc., San Diego, CA) or Microsoft Excel 2010 software (version 14.0.6129.5000; Microsoft Corporation Redmond, WA). Densitometry, where indicated, was completed using ImageJ software (version 1.46r; Bethesda, MD). Data are presented as mean values with error bars denoting standard deviation or standard error of the mean where appropriate. The levels of significance were set at $*p < 0.05$, $**p < 0.01$, and $***p < 0.001$.

6.4 Results

6.4.1 WA potentiates the cytotoxicity of radiation therapy

Combinational efficacy of WA and RT was evaluated by the clonogenicity survival assay for single cell colony formation (Figure 6-1). Plated cells of appropriate number were pretreated with WA for 2 h followed by RT at various doses, washed after 24 h, and quantified after a growth period of 10-14 days. WA demonstrated the ability to potentiate or otherwise enhance the anti-proliferative effects of RT in both U87 and HeLa cells at concentrations as low as 125 nM. U87 cells showed no significant changes in cell survival between control and 2 Gy alone groups with a colony growth efficiency reduction of only 1.4% ($p = 0.947$). The addition of 125 nM and 250 nM WA reduced colony formation efficiency by 10.8% ($p = 0.538$) and 74.5% ($p = 0.003$) in U87 cells not treated with RT and 57.3% ($p = 0.010$ compared to RT only; $p < 0.001$ compared to WA only) and 84.8% ($p = 0.002$ compared to RT only; $p = 0.026$ compared to WA only) in 2 Gy treated cells, respectively. 4 Gy RT reduced colony formation efficiency to 29.1%, however,

Figure 6-1.
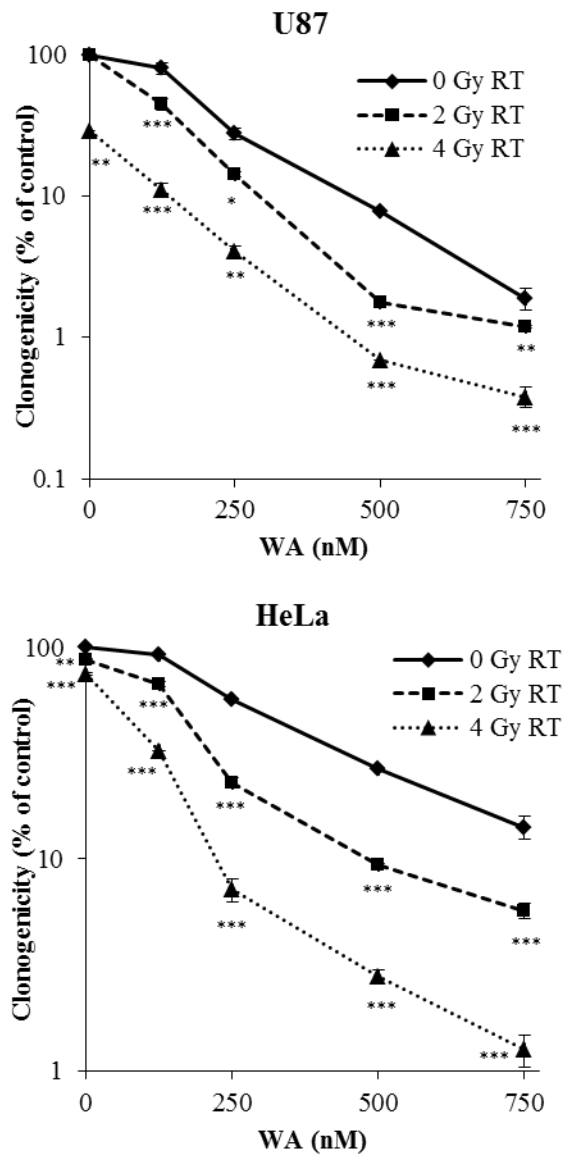
Figure 6-1. U87 and HeLa cells were treated with WA and irradiated 2 h later. After 10-14 d, surviving cells demonstrating growth clonogenicity through the formation of a colony were scored. WA potentiated or otherwise enhanced the anti-proliferative effects of RT in both U87 and HeLa cells at concentrations as low as 125 nM. Notably, no significant decrease in cell survival was observed with 2 Gy RT in U87 and 125 nM WA in HeLa. Addition of the other agent in each line significantly potentiated the anti-proliferative effect. $*p < 0.05$, $**p < 0.01$, $***p < 0.001$ (Statistics indicate significant difference from the WA alone treatment.)

the relative enhancement of treatment efficacy mediated by WA was comparable to that of the 2 Gy treated cells. HeLa cells showed a similar pattern of WA-mediated radiosensitization. 2 Gy and 4 Gy RT reduced colony formation by 13.2% (p = 0.002) and 26.7% (p < 0.001) compared to control, respectively, while 125 nM WA reduced this efficacy by 7.7% (p = 0.126). The combination of 125nM WA with 2 Gy RT reduced colony formation by 35.0% (p < 0.001 compared to control and WA only) and 25.2% relative to 2 Gy alone (p < 0.001). Similarly, The combination of 125 nM WA with 4 Gy RT showed additional efficacy, reducing colony formation efficiency by 67.7% (p < 0.001 compared to control and WA only) and 56.0% relative to 4 Gy alone (p < 0.001). Further extension of these WA sensitizing effects were observed at higher WA concentrations with enhanced combinational efficacy compared both to control and when normalized to individual RT groups.

6.4.2 Combination WA and RT favors reduced cell cycling but not enhanced apoptosis or autophagy

To determine the nature of the reduced clonogenicity following combination WA and RT treatment for 24-72 h, cell cycle evaluation was conducted by PI staining and subsequent flow cytometry to quantify levels of DNA. As demonstrated previously, WA treatment resulted in an increased percentage of cells in the G2/M-phase of the cell cycle with minimal changes in S-phase percentage (Supplemental Figure 6-1) (Grogan et al., 2013). RT-treated U87 and HeLa cells both demonstrated small reductions in S-phase percentage, maximally at 24 h or 48 h, but showed variable shifts with cell predominantly moving to G0/G1 (2N DNA) in U87 and G2/M (4N DNA) in HeLa. Combination of WA and RT produced enhanced depletion of S-phase cells

at 24 h and maintained the depletion at 72 h despite normalizing levels in the RT-only groups in both U87 and HeLa cells (Figure 6-2A). Depletion of S-phase cells was primarily associated with maintained or minimally decreased levels of G0/G1-phase cells compared to WA-only with displacement to G2/M after 24 h. U87 cells demonstrated maintained elevation of G0/G1-phase cells at 24 h only with combination therapy, consistent with a predominant response to RT.

At 24 h, control HeLa cells displayed 22.3% of cells in S-phase. Treatment with 250 nM WA maintained the S-phase fraction at 21.8% ($p = 0.205$), while 5Gy RT reduced S-phase to 19.5% ($p = 0.010$). Combined, the treatment yielded 16.1% of cells in S-phase ($p = 0.006$ vs. control; $p = 0.002$ vs. WA; $p = 0.005$ vs. RT). This efficacy was even more pronounced after 72 h in HeLa cells with respective depletion of the S-phase fraction of WA, RT, and WA+RT to be 1.7% ($p = 0.075$), 4.5% ($p = 0.036$), and 10.6% ($p = 0.019$ vs. control; $p = 0.022$ vs. WA; $p = 0.002$ vs. RT) (Figure 6-2A). Comparable findings were observed in U87 cells, notably at 24 h when the percentage of S-phase cells increased by 0.5% following 500 nM WA ($p = 0.648$ vs. control) but was decreased by 3.5% with 2.5 Gy RT ($p = 0.064$ vs. control) and 6.8% with combination therapy ($p = 0.045$ vs. control; $p = 0.019$ vs. WA; $p = 0.025$ vs. RT) (Figure 6-2A). Reduction in S-phase percentage was maintained at 72 h post-treatment. Complete changes in G0/G1 and G2/M levels are presented in Supplemental Figure 6-1.

Shifts in the cell cycle at different levels were then evaluated molecularly through Western blotting for cyclins B_1 (G2/M transition), D_1 (G1/S transition), E_1 (G1/S transition) and cyclin-dependent kinase inhibitors p21/cip1 (G1/S transition) and p27/kip1 (G1/S transition) (Sgambato et al., 2000; Cazzalini et al., 2010) (Figure 6-2B). Consistent with the induction of G2/M cell cycle arrest, WA treatment in U87 increased levels of cyclin B_1, but this was not observed in HeLa at the moderate concentrations tested. Cyclin B_1 was also mildly induced with

Figure 6-2.
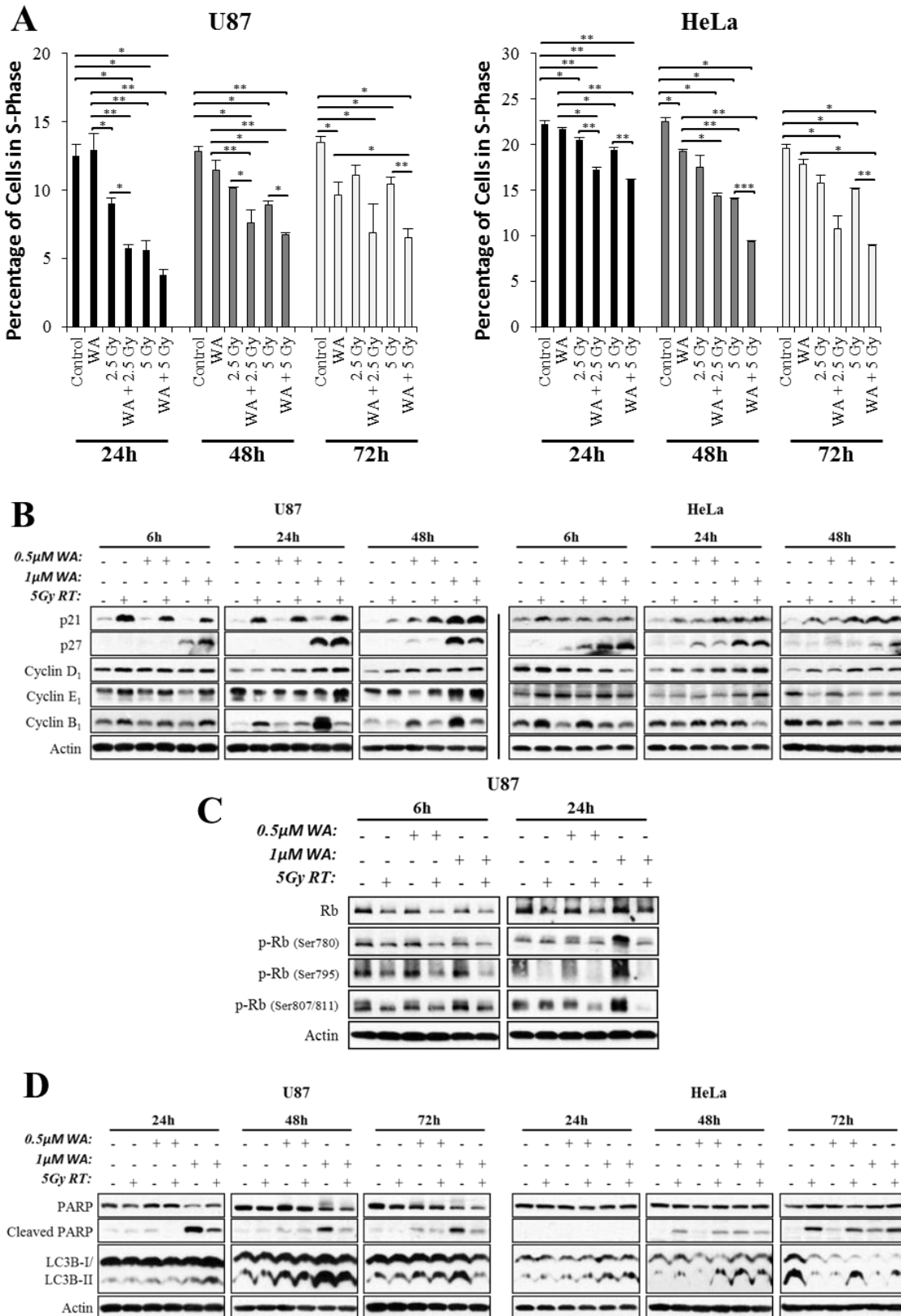
Figure 6-2. A) Cell cycle analysis was conducted by propidium iodide staining and subsequent flow cytometry following combination WA and RT treatment for 24-72 h. RT-treated U87 and HeLa cells both demonstrated small reductions in S-phase percentage, maximally at 24 h or 48 h, but combination of WA and RT produced enhanced depletion of S-phase cells at 24 h and maintained the depletion after 72 h despite normalizing levels in the RT-only groups in both cells. B) Shifts in the cell cycle at different levels were then evaluated molecularly through Western blotting for cyclins B_1 (G2/M transition), D_1 (G1/S transition), E_1 (G1/S transition) and cyclin-dependent kinase inhibitors p21/cip1 (G1/S transition) and p27/kip1 (G1/S transition). Consistent with G2/M arrest, WA alone induced elevated cyclin B_1 in U87 cells but was abrogated with RT. While Cyclin E_1 was largely unchanged, cyclin D_1 was elevated in a WA dose-dependent manner at 24-48 h in both cell lines. At 24 h in both lines, small increases in cyclin D_1 were noted with the addition of RT after WA pretreatment. Negative regulators of the G1/S transition, p21 and p27, demonstrated notable induction with combination WA and RT compared to either agent alone in a time-dependent manner. C) Treatment with RT diminished total levels of total Rb protein and phosphorylation at Ser780, Ser795, and Ser807/811 after 6-24 h. Pretreatment with WA further enhanced this decreased Rb phorphorylation with observable depletion of Ser780 and Ser795 at 6h and Ser807/811 at 24h. D) Combination of WA with RT failed to enhance apoptotic PARP cleavage or the autophagy-mediated conversion of LC3B compared to either agent alone, suggesting the cytotoxic effect of combination therapy was not through these mechanisms. $*p < 0.05$, $**p < 0.01$, $***p < 0.001$

5 Gy RT in U87 through 24h and in HeLa through 6 h. WA-mediated induction of cyclin B_1 in U87 cells was repressed with RT co-treatment. Cyclin E_1 was largely unchanged with small RT-induced elevation at 6 h and 1 μM WA-induced cell-dependent increases at 24-48 h. Cyclin D_1 was elevated in a WA dose-dependent manner at 24-48 h in both cell lines. At 24 h in both lines, small increases in cyclin D_1 were noted with the addition of RT to WA, suggesting a potential block in the G1/S transition and an enhanced attempt to enter S-phase, consistent with the reduced S-phase fraction noted by flow cytometry findings.

Levels of p21 and p27, negative regulators of the G1/S transition which function to block cyclin-Cdk1/2/4/6 activity (Sgambato et al., 2000; Cazzalini et al., 2010), supported this claim, demonstrating notable induction with combination WA and RT compared to either agent alone (Figure 6-2B). p21 was significantly induced by RT in U87 after only 6 h as previously reported (Lee et al., 2011) and mildly increased in HeLa. Induction of p21 by WA alone was not observed until 24 h in HeLa and 48h in U87, and the enhanced combinational effect, particularly distinguishable at 0.5 μM WA, was consistent with these timepoints. p27 induction was driven by WA in a dose-dependent manner in both U87 and HeLa cells. Combination with radiation enhanced this induction at 6 h but failed to show notable benefit at later timepoints except with 1 μM WA in HeLa at 48 h as total induced levels were nearing depletion, suggesting that predominant early combinational effects are mediated by p27 while long-term responses are p21-driven.

The retinoblastoma protein (Rb) prevents progression from G1- to S-phase through inactivation of the transcription factor E2F (Cazzalini et al., 2010). Because cyclin-Cdk1/2/4/6 promotes inactivation of Rb through hyperphosphorylaton and is inhibited by p21 and p27, both of which were elevated with WA+RT therapy, the downstream status of Rb was evaluated in

U87 (Figure 6-2C). Consistent with a previous report demonstrating the activated status of Rb (Orr et al., 1997), treatment with RT paradoxically diminished total levels of the protein. RT also decreased inhibitory phosphorylation of Rb at Ser780, Ser795, and Ser807/811 after 6-24 h. Pretreatment with WA further decreased Rb phorphorylation with observable depletion of Ser780 and Ser795 at 6 h and Ser807/811 at 24 h. Phosphorylation of Ser795 was nearly completely eliminated in all RT treatment groups at 24 h. Notably, 1 µM WA alone increased phosphorylation at all measured sites after 24 h, suggesting a single agent-mediated inverse effect when not used in combination with RT.

To evaluate whether enhanced apoptosis and/or autophagy also played a role in the cytotoxicity of combination therapy, cleavage of PARP (apoptosis marker) and conversion of LC3B-I to LC3B-II (autophagy marker) were examined by Western blotting from 24-72 h (Figure 6-2D). PARP cleavage was noted with increasing concentrations of WA in both cell lines but only in HeLa with RT as previously reported (Eriksson et al., 2009; Lee et al., 2011; Grogan et al., 2013). WA+RT failed to increase PARP cleavage above RT alone in HeLa cells and decreased WA-mediated PARP cleavage in U87 cells. Despite dose-dependent increases with WA alone, conversion of LC3B-I to LC3B-II did not demonstrate a consistent pattern of enhancement with combination therapy. In U87 cells at 48-72 h, 1 µM WA with RT demonstrated reduced levels of LC3B-II compared to WA alone, and by 72 h in HeLa cells, LC3B-II levels were consistently depleted compared to control. These findings suggest that combination of WA and RT favors a mechanism of diminished cellular replication over apoptosis or autophagy in U87 and HeLa cells.

6.4.3 WA induces depletion of key proteins in HR, NHEJ, and MMR

220

The recognition and repair of DNA damage, particularly double-stranded breaks, involves the coordination of numerous proteins in multiple pathways with known overlap. For the purposes of this study, several well-defined proteins necessary for the DSB response were broadly categorized: damage recognition and signal transduction (Mre11, p95/NBS1, Rad50, ATM, Chk1, Chk2), homologous recombination repair (Rad51, Rad52, BRCA1, BRCA2), and non-homologous end-joining (DNA-PKcs, Ku70, Ku80, and XLF). WA demonstrated the ability to deplete key proteins involved in all dsDNA damage response categories as well as mismatch repair (MMR) in HeLa and U87 cells (Figure 6-3). 17-AAG was used as a control HSP90 inhibitor at both timepoints to demonstrate the potential direct or indirect role of HSP90 in the stability of each protein. While most proteins depleted by 17-AAG demonstrated a similar pattern with WA, the reverse was not explicitly observed. HeLa cells expressed basally lower levels of NHEJ proteins DNA-PKcs and XLF while U87 cells exhibited lower expression of the HR protein Rad52, consistent with previous reports that HeLa is more competent at HR than glioma cells while the latter favor NHEJ after RT (Kachhap et al., 2001; Golding et al., 2004; Ransburgh et al., 2010; Quiros et al., 2011; Lim et al., 2012; Stecklein et al., 2012). Each line has demonstrated the ability to complete both HR and NHEJ.

At 24-48 h, dose-dependent decreases in the expression of recognition and transduction proteins Mre11, p95/NBS1, Rad50, ATM, and Chk1 were observed in both cell lines evaluated with depletion of Chk2 in only U87 cells. Similarly, total levels of HR proteins BRCA1, BRCA2, and Rad51 were also decreased following escalated exposure to WA but depletion of Rad52 was limited to HeLa. Notably, reductions of ATM, Chk1, and BRCA1 in both lines occurred at the lower WA concentrations evaluated (1-2.5 µM) after 24 h, suggesting enhanced

Figure 6-3.
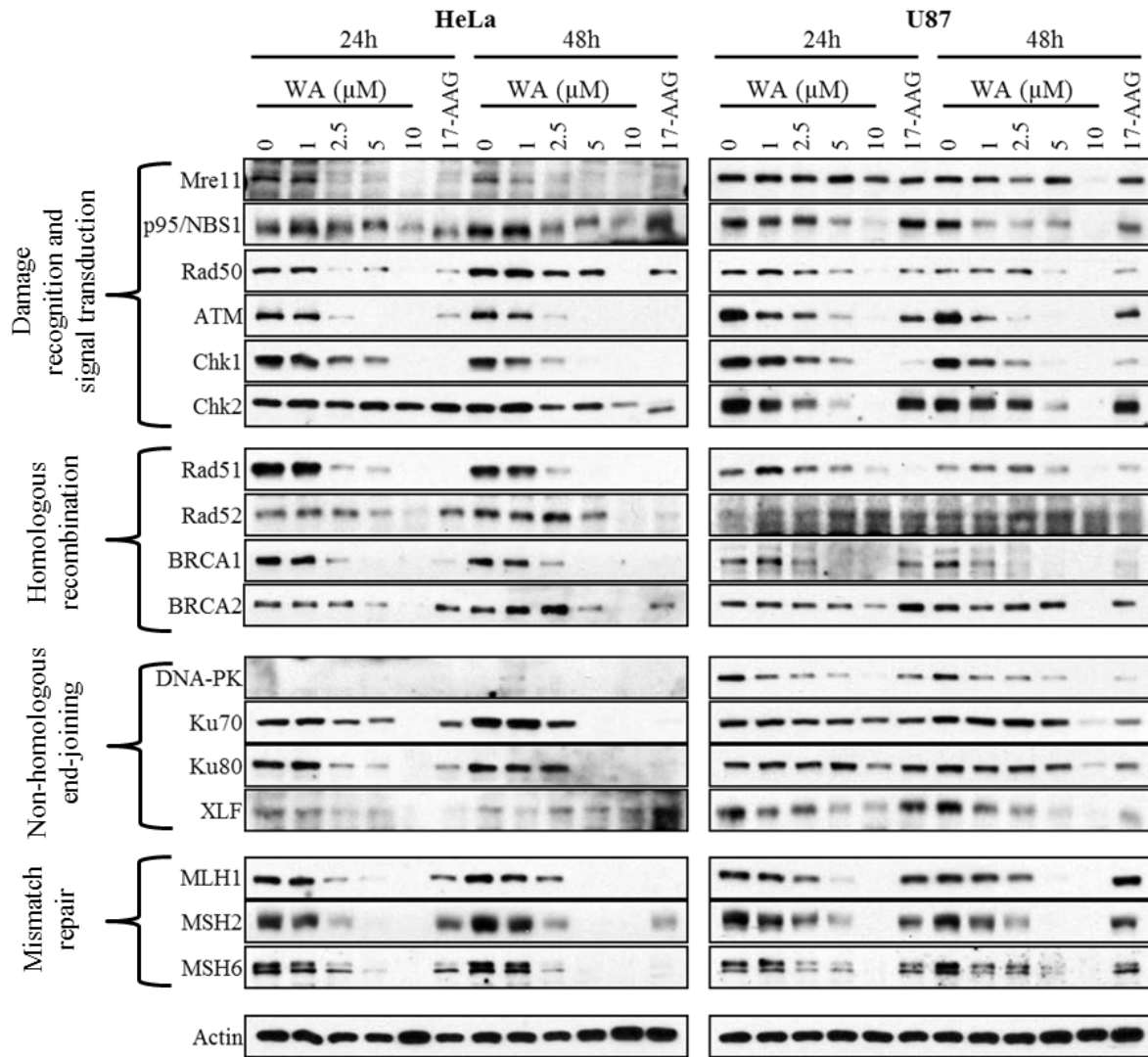
Figure 6-3. Treatment with increasing concentrations of WA for 24-48 h reduced total levels of DNA-damage response (DDR) proteins involved in damage recognition (Mre11, p95/NBS1, Rad50), signaling (ATM, Chk1), and repair through homologous recombination (BRCA1, BRCA2, Rad51), non-homologous end-joining (DNA-PK, XLF, Ku70, and Ku80), and mismatch repair (MLH1, MSH2, MSH6) in both U87 and HeLa. This protein depletion was an expansion of that observed with 1 µM of the traditional HSP90 inhibitor 17-AAG.

and consistent selectivity for these targets. Reduced expression of these three proteins was also observed with 17-AAG. NHEJ proteins XLF, Ku70, Ku80 were depleted with WA dose escalation in both cells lines after 24-48 h, however, the effect in Ku70/80 was observed at 2.5 µM WA in HeLa (lower baseline expression) compared 10µM WA in U87 (higher expression). Higher DNA-PKcs expression was detected in U87 cells and was decreased at 1 µM WA. WA-mediated decreases in NHEJ protein levels corresponded with the effects of 17-AAG treatment. MMR proteins MLH1, MSH2, and MSH6 showed reduction in expression at 2.5 µM WA at 24 h with complete protein ablation by 5-10 µM in both HeLa and U87 cells. Treatment with 17-AAG induced minimal MMR protein reduction after 24 h, however, this effect was more pronounced in HeLa cells after 48 h. Overall, most proteins evaluated demonstrated reduced or absent expression at 10 µM WA, suggesting limited selectivity of effect at high concentrations. HeLa cells also demonstrated enhanced response to 1µM 17-AAG compared to U87 cells which was confirmed by a cell viability assay (data not shown).

6.4.4 WA alters radiation-induced DNA damage recognition

Following the induction of dsDNA damage and recognition by the MRN complex, ATM is recruited to the site of the break where it is phosphorylated and can then phosphorylate Chk1/Chk2 for cell cycle checkpoint activation and H2A.X at the site of damage for recruitment of repair proteins (Lamarche et al., 2010). Normalized phosphorylation of ATM at Ser1981 was measured to evaluate the response to RT-mediated DNA damage following WA pretreatment. Compared to control 1 h post-RT (5 Gy in U87; 10 Gy in HeLa), p-ATM was induced 15.4-fold in U87 and 8.8-fold in HeLa. The presence of 1 µM WA reduced this activation 56.3% and

14.9% in the two lines, respectively (Figure 6-4A). By 6 h, reduction of ATM activation by WA was no longer observed in U87 cells, showing a delayed enhancement of this phosphorylation with combination therapy. In HeLa cells, despite diminished total activation of ATM after 6h (2.2-fold above control) and 24 h (1.89-fold above control), WA 1 μM WA reduced this activation 66.2% and 74.6%, respectively, showing a delayed response to 2 h WA pretreatment. U87 cells demonstrated increased p-ATM with WA exposure after 24 h, but this still demonstrated a 33.6% and 16.9% reduction in the residual p-ATM induced by RT (5.09-fold above control) with 0.5 μM and 1 μM WA, respectively, by despite the increase induced by combination therapy at 6 h.

To further evaluate the downstream effects of altered ATM signaling, normalized phosphorylation of Chk1 at Ser296, an autophosphorylation site requiring previous ATM-mediated signaling, was measured (Okita et al., 2012) (Figure 6-4A). Minimal changes were observed in U87 cells 1 h post-RT with slight elevation of p-Chk1. After 6 h, however, total RT-mediated induction was 2.82-fold compared to control and was reduced by 58.5% with 1μM WA pretreatment, demonstrating a delayed response compared to p-ATM. Despite relative WA-mediated reductions in p-ATM largely manifesting at 6 h in HeLa cells, induction of p-Chk1 by RT at 1 h (2.46-fold above control) was reduced by 40.2% with 1 μM WA pretreatment, suggesting WA-mediated inhibition of signal transduction. Overall, high induction of p-Chk1 at 1 h corresponded with the largest levels of p-ATM 1h post-RT. Induction by RT at 6 h was reduced to 1.74-fold above control and only slightly diminished with WA pretreatment.

Phosphorylation of H2A.X (Ser139) is regarded as a marker of DNA damage for recruitment of repair machinery and is mediated, at least in part, by the activity of ATM (Lamarche et al., 2010). Recognition of DNA damage was evaluated by immunocytochemistry

Figure 6-4.
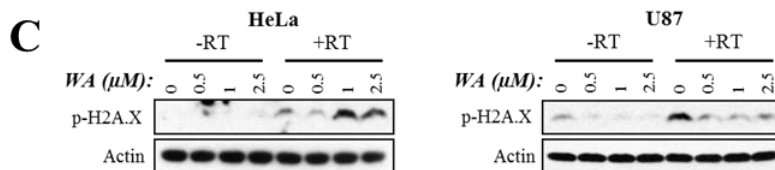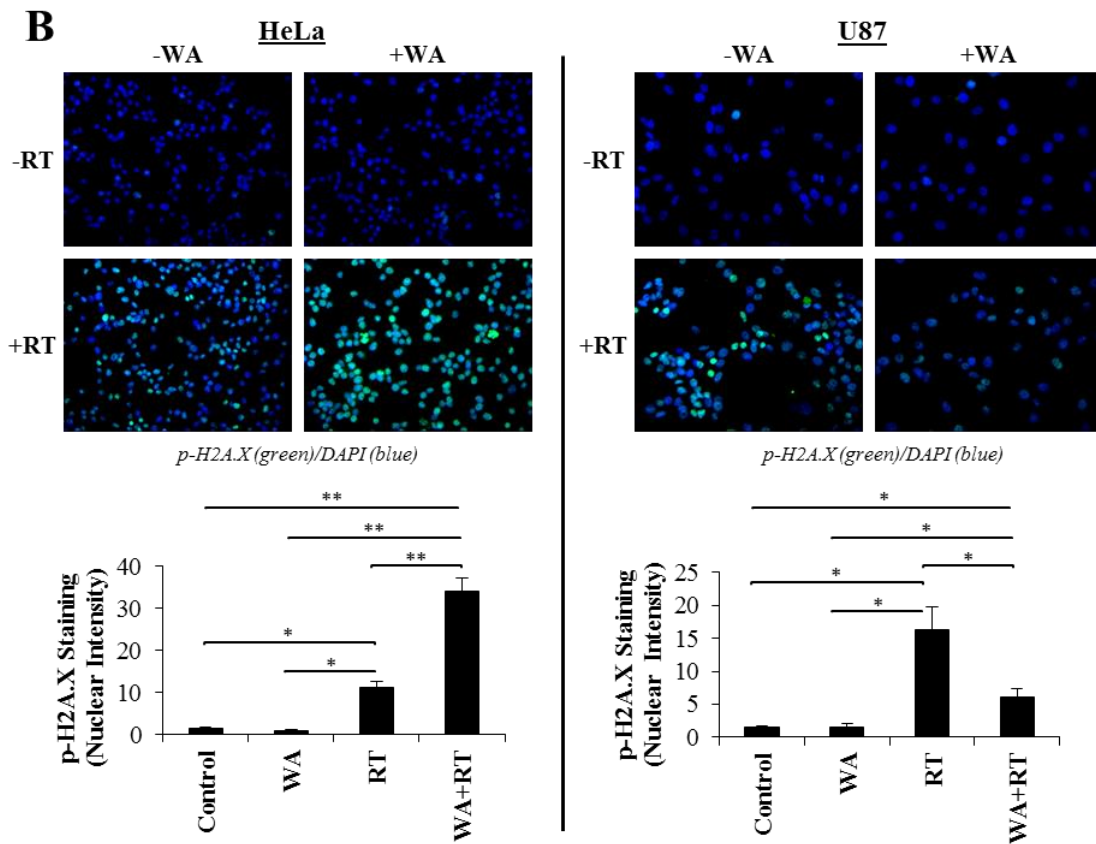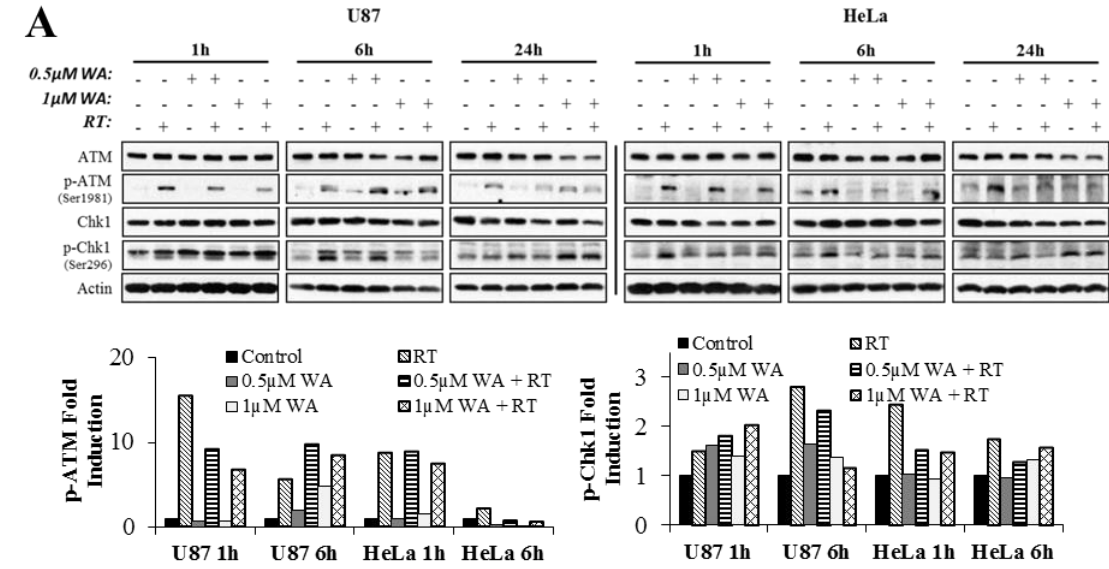
Figure 6-4. A) WA pretreatment disrupted the normal signal transduction response following RT. RT (5 Gy in U87; 10 Gy in HeLa) initiated phosphorylation of ATM (Ser1981) and downstream Chk1 (Ser296) at 1-6 h post-irradiation. Pretreatment with WA altered the normal signaling response with reduction in ATM and Chk1 phosphorylation in a dose- and time-dependent manner. Total levels of ATM and Chk1 remained largely unchanged at 1-6 h post-RT. Bar graphs represent quantified densitometry of the Western blots. B) Recognition of DNA damage was evaluated by ICC for p-H2A.X (Ser139) and quantified by intensity of the nuclear staining. Both HeLa and U87 demonstrated significant induction of p-H2A.X 1 h post-10 Gy RT, but 2.5 μM WA yielded no effect. WA differentially modulated normal the normal recognition response to RT-mediated DNA damage with combination therapy showing enhanced p-H2A.X in HeLa but reduction in U87. C) These immunocytochemistry findings were supported by Western blotting for p-H2A.X which demonstrated comparable patterns of treatment-mediated modulation. $*p < 0.05$, $**p < 0.01$, $***p < 0.001$

for p-H2A.X and quantified by intensity of the nuclear staining (Figure 6-4B). HeLa and U87 cells displayed 8.1-fold ($p = 0.017$) and 11.1-fold ($p = 0.021$) increases in p-H2A.X 1 h post-10 Gy RT compared to controls, respectively. Pretreatment with 2.5 µM WA for 2 h, which alone produced no deviation from control in either line, resulted in diverging effects when followed by RT. In HeLa cells, combination therapy further induced expression of p-H2A.X 3.0-fold greater than RT alone ($p = 0.006$) and 24.7-fold above control ($p = 0.007$). In contrast, the addition of WA to RT in U87 cells resulted in a 62.5% decrease in the phosphorylation of H2A.X compare to RT alone ($p = 0.049$) but was still significantly greater than control ($p = 0.048$). These results were supported by Western blotting for p-H2A.X which demonstrated comparable patterns of treatment-mediated modulation (Figure 6-4C). Modulation of H2A.X phosphorylation was consistent with the large early impairment of ATM activation in U87 but not HeLa, suggesting that the effects of WA are manifest at different signaling levels in various cells, such that diminished ability to recognize DNA damage is observed in U87 whereas a failure to response to and repair the damage is observed and in HeLa despite enhanced phosphorylation of H2A.X.

6.4.5 WA blocks dsDNA damage repair

Direct measurement of dsDNA damage was evaluated through the neural comet assay, measuring the movement of the DNA content of single cells through electrophoresis (Figure 6-5A and 5B). U87 cells were pretreated with WA for 12 h, irradiated, and collected after a 4 h incubation. Enhanced DNA damage was associated with a higher percentage of total DNA shifted and a greater distance traveled, quantified as the tail moment. Control cells displayed a baseline tail moment of 1.1 which was increased 2.3-fold to 2.6 with 0.5 µM WA ($p = 0.028$),

228
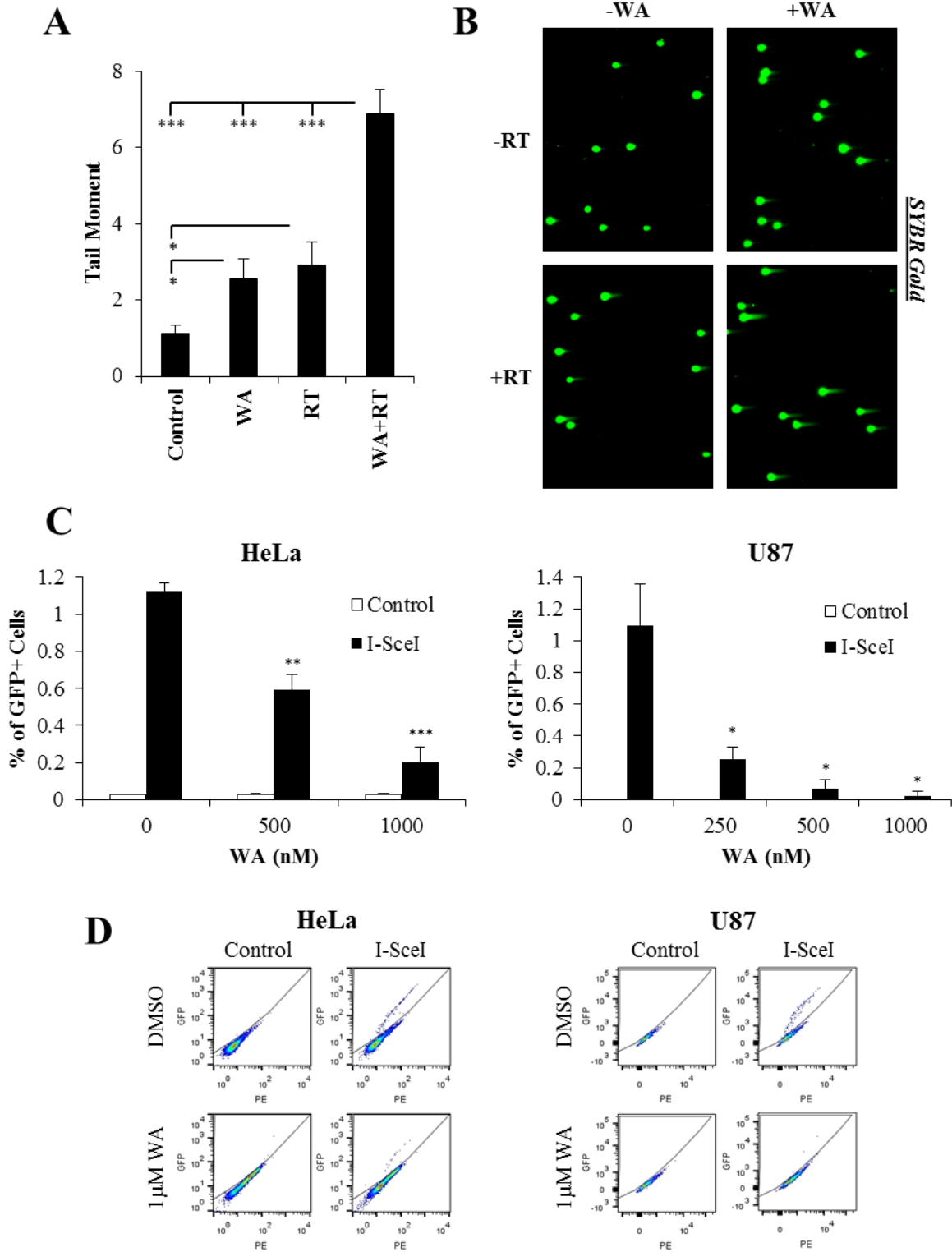
Figure 6-5.

Figure 6-5. A) Direct measurement of dsDNA damage was evaluated through the neural comet assay, measuring the movement of the DNA content of single cells through electrophoresis followed by nucleic acid staining with SYBR Gold. U87 cells were pretreated with WA for 12 h, irradiated with 5 Gy, and collected after a 4 h incubation. Mildly increased DNA damage was observed with treatment of either WA or RT, but combination of the agents significantly enhanced the average comet tail moment, demonstrating enhanced DNA damage. B) Representative examples of comets from each treatment group. SYBR Gold = green. C) HeLa and U87 cells stably expressing the DR-GFP reporter were transfected with an empty vector control or an I-SceI construct, plated, and treated immediately with multiple concentrations of WA for 72 h before analysis of GFP expression, a marker of successful HR, by flow cytometry. WA demonstrated significant dose-dependent reduction in HR function through decreases in GFP+ cells in both lines. Cells transfected with the control empty vector demonstrated no or minimal GFP at all concentrations. D) Representative examples of the flow cytometry results for HeLa and U87. $*p < 0.05$, $**p < 0.01$, $***p < 0.001$

likely a result of minor DNA fragmentation characteristic of intrinsically cytotoxic compounds, and 2.6-fold to 2.9 with 5Gy RT (p = 0.023). Combination of these two agents resulted in a tail moment of 6.9, a 6.1-fold increase over baseline (p < 0.001) and statistically greater than either agent alone (p < 0.001). These findings demonstrate that reduced phosphorylation of H2A.X resulting from WA+RT compared to RT alone in U87 cells is the result of reduced DDR signaling rather than enhanced repair.

These findings were supported functionally by the WA-mediated inhibition of HR as evaluated through the DR-GFP reporter assay (Figure 6-5C and 6-5D; Supplemental Figure 6-2). U87 and HeLa cells stably expressing the reporter following clonal selection were transfected with a vector for the restriction enzyme I-SceI or a control vector. Expression of I-SceI in the cell functioned to cut the reporter assay at a specific site, mimicking a dsDNA break with functional HR repair that could be monitored through ultimate expression of GFP by flow cytometry and microscopy. HR-mediated repair was shown to occur in 1.10% of U87 and 1.12% of HeLa control cells after 72 h. This was significantly reduced by treatment with WA. At 0.5 μM, U87 and HeLa cell repair of the break through HR was reduced to 0.07% (p = 0.017) and 0.59% (p = 0.003), respectively which was further reduced by 1 μM WA to 0.02% (p = 0.018) and 0.20% (p < 0.001), respectively. Cells transfected with the control empty vector demonstrated no GFP+ cells at all concentrations in U87 and 0.03% at all concentrations in HeLa. Preliminary data in the murine GBM cell line GL26 demonstrated the same pattern of HR reduction with WA treatment. These findings support the results demonstrating enhanced dsDNA damage with combination of WA and RT as well as reductions in DNA damage repair proteins following WA treatment. This suggests that WA-mediated radiosensitization functions in-part through inhibition of these repair pathways.

231

6.5 Discussion

WA is a promising novel anti-cancer therapeutic agent that has shown both *in vitro* and *in vivo* promise in a variety of models by targeting a multitude of proliferation, survival, and growth progression pathways (Vanden Berghe et al., 2012; Vyas and Singh, 2014). While monotherapy with WA in animal models has yielded impressive results, single agent therapy in the treatment of human cancer often demonstrates disappointing outcomes and the rapid development of resistance. Treatment of many cancers now relies on the utilization of several adjuvant therapies to target multiple cellular susceptibilities simultaneously, often through production of DNA damage or alterations of DNA/cellular replication (Kamal and Burrows, 2004). Here, we demonstrated that WA inhibits normal pathways of DSB repair through depletion of total proteins involved in HR and NHEJ as well as alterations and delays in DDR signaling in two highly aggressive cancer cell lines, HeLa and U87. Combining WA and RT potentiated the efficacy of both agents leading to enhanced DNA damage and diminished viability through failure of cells to synthesize DNA and progress through the cell cycle.

Several early studies on WA identified it as a possible radiosensitizer, including its potential *in vivo* utility as such (Devi et al., 1995; Devi et al., 1996; Devi et al., 2000; Devi and Kamath, 2003; Devi et al., 2008). This research group then demonstrated that knockout of Rad54, but not Ku70 or both Ku70 and Rad54, could sensitize cells to radiation and concluded that WA may alter normal homologous recombination repair (Devi et al., 2008). Since then, several additional studies further evaluated the merit of combination therapy and suggested that it increases efficacy through enhanced oxidation and modulation of the MAPK and Akt

pathways (Yang et al., 2011b; Yang et al., 2011a). A lack of adequate controls and data quantification limits the overall interpretation of the data in these studies, but each demonstrated the promise of co-treatment with both agents.

Ionizing RT is a frequently utilized treatment modality against many primary cancer types and some metastatic disease. While certain cancers are quite responsive to the DNA damaging effects of RT, others show only modest sensitivity or even radio-resistance (Begg et al., 2011). Given the widespread importance of RT for cancer patients, efforts have been made to identify means by which to enhance its effect, frequently through the additional of specific adjuvant chemotherapies. For example, the addition of TMZ to RT in the treatment of GBM patients extended average post-diagnosis survival by approximately two months, although the specific mechanism for this radiosensitization is unclear (Chakravarti et al., 2006; Stupp et al., 2009; Bobola et al., 2010). Other agents have been developed to specifically target mechanisms of the DDR such as direct inhibitors of ATM and Chk1 (Dent et al., 2011; Nadkarni et al., 2012).

In the present study, WA demonstrated the ability to reduce expression of multiple proteins in the HR, NHEJ, and MMR DDR pathways. Such findings suggest that WA may sensitize cancer cells to radiotherapy and/or other DNA-altering chemotherapeutic agents through induction of instability and promotion of degradation of proteins critical in the recognition and response to such an insult. WA has previously shown the ability to disrupt the interaction between HSP90 and Cdc37 with direct binding to the C-terminus of HSP90, a chaperone protein that functions to fold, refold, and stabilize a specific set of client proteins (Yu et al., 2010). This disruption corresponds with subsequent degradation of various client proteins despite no direct inhibition of HSP90 function through its mediation of GR steroid binding (unpublished data). However, total GR and levels of proteins not previously described to be

233

associated with Cdc37 were depleted, suggesting that WA may also directly inhibit HSP90 activity through a separate mechanism or induce protein depletion through an alternative means. While Cdc37 is thought to have minor intrinsic protein chaperone properties, it has traditionally been considered a co-chaperone of HSP90 that promotes localization of the HSP90 chaperone complex to various protein targets, largely kinases. Such a binding effect of WA to HSP90 appears to be specific to a small subset of proteins such as HSP90 and vimentin (Bargagna-Mohan et al., 2007), demonstrating the specificity of WA targeting. We hypothesize that the depletion of a large number proteins globally, including those involved in the DDR, is not due to direct interaction with the compound but rather the secondary effect of HSP90 axis modulation.

Indeed, WA-mediated depletion of DDR proteins patterned HSP90 inhibition with enhanced decreases in known HSP90 clients BRCA1 (Stecklein et al., 2012), Chk1 (Arlander et al., 2003), and DNA-PK (Solier et al., 2012) compared to other proteins at 1-2.5 μM after 24 h. Other HSP90 client or interacting proteins such as BRCA2 (Noguchi et al., 2006), members of the MRN complex (Dote et al., 2006), and Rad51 (Ko et al., 2012) demonstrated enhanced depletion upon WA exposure or responded in a cell line-dependent manner. This suggests either diminished cellular importance on the HSP90 axis for stability as frequently confirmed with 17-AAG treatment such as for BRCA2, Cdc37-independent protein targeting, or alternate WA-induced effects. The importance of the roles of HSP90 and Cdc37 for the stability and function of proteins involved in the DNA damage recognition and repair pathway is incompletely defined, and these findings suggest that it may be more significant than currently understood. Consistent with these findings, direct inhibition of HSP90 has been shown to result in radiosensitization with inhibition or depletion of proteins in the DDR such as Akt, BRCA1, and Rad51 (Dote et al., 2006; Kabakov et al., 2010; Ko et al., 2012; Stecklein et al., 2012). To date, no studies have been

completed to identify a role for Cdc37 in the interaction with the altered DDR proteins either directly or indirectly. Further study is also necessary to identify why ATM is significantly depleted with both WA and 17-AAG treatment but has previously been shown to not interact with HSP90 (Dote et al., 2006). Importantly, WA modulates proteins from all pathways of the DDR, including both HR and NHEJ, demonstrating its potential broad-spectrum effectiveness as a radiosensitizer against various malignancies regardless of the favored repair pathway(s).

Additionally, our group has demonstrated the ability of WA to elevate the oxidative potential in cancer cells which suggests an alternative mechanism by which DDR proteins can be degraded (Grogan et al., 2013; Grogan et al., 2014). O^6-methylguanine-DNA methyltransferase (MGMT), a protein involved in the removal of TMZ-mediated DNA alkylation, was depleted by WA in a dose-dependent manner. While MGMT has not been described as a client of HSP90 or Cdc37 and was not significantly decreased with 17-AAG exposure, it had previously shown sensitivity to compounds inducing oxidative stress such as valproic acid (Fu et al., 2010; Ryu et al., 2012). Further studies are necessary to identify whether the pro-oxidant capacity of WA results in protein misfolding and/or depletion and if it is a direct consequence of reactive oxygen species (ROS) production through its epoxide group or an indirect shift in background potential resulting from thiol sequestering of the compound. Regardless, such a dual mechanism of oxidation and HSP90 axis inhibition provides great potential for enhanced efficacy while minimizing the development of resistance. In addition, oxygen is a known radiosensitizer (Teicher, 1995; Okunieff et al., 1996), and the known oxidizing effects of WA may play an indirect role in further enhancing the efficacy of RT through increased formation of DNA-damaging free radicals, although it is unclear if introduction of oxygen in this form will indeed be beneficial. While WA elevates cellular oxidative potential and increases p-H2A.X at high

concentrations after 24 h (Grogan et al., 2014), this p-H2A.X induction could be completely eliminated with pretreatment of a global caspase inhibitor in a breast cancer model, suggesting the effect was an apoptosis-related phenomenon rather than direct damage to the DNA (data not published).

Interestingly, the results of this study suggest that WA not only functions to deplete total levels of proteins critical to the DDR but can also alter normal signaling at concentrations below those that alter protein levels. In the evaluation of ATM and Chk1 activation and signaling, total levels of each protein at low-dose WA remain largely unchanged while phosphorylation is altered. If these findings are related to inhibition of the HSP90 chaperone axis induced by WA, this may suggest general mild destabilization of some fraction of ATM and its upstream kinases that alters function but remains detectable in total level analysis. Consistent with this observation, disruption of Cdc37 has previously been demonstrated in prostate cancer to inhibit cellular kinase activity without significantly depleting certain HSP90 client proteins (Gray et al., 2007).

Despite the WA-mediated modulation of ATM and Chk1 signaling following RT, each cell line showed an enhanced the ability to undergo cell cycle arrest at 24-72 h with a notably reduced fraction of DNA synthesis phase cells. Diminished phosphorylation of Chk1 after combination therapy was observed between 1-6 h post-RT but not after 24 h, suggesting delayed but not eliminated cell cycle checkpoint signaling which may perpetuate error generation or lack of timely repair early post-RT as the cell continues to cycle. Further, additional signaling proteins such as ataxia telangiectasia and Rad3-related protein (ATR) and Chk2 may compensate for this effect, and it is unclear if the mild reduction in p-Chk1 was functionally significant. It is hypothesized that the maintained low dose WA-mediated reduction of p-ATM after RT favors

reduction in DNA damage recognition and ultimately repair, both effects demonstrated in this study, compared to inhibited checkpoint modulation and may eventually overcome any diminished regulation of the checkpoints. Higher dose WA, which leads to significant direct depletion of Chk1 and/or Chk2 but manifests notable cytotoxicity independent of RT, may eventually limit the functional execution of these checkpoints.

Interestingly, the data suggest that combination of WA and RT results in a reduction of cells entering the DNA synthesis phase of the cell cycle with cells existing in the S-phase shifting to a non-mitotic population containing 4N DNA. The notable accumulation of cyclin B_1 in U87 cells treated with WA for 24-48 h is nearly completely reduced to baseline when simultaneously treated with RT. This suggests that the 4N DNA cells are not appropriately progressing in the G2/M phase as has previously been demonstrated with the flavoprotein-specific inhibitor diphenyl eneiodonium (Scaife, 2004). While p21, which is increased in this study with WA treatment and further with combination therapy, has traditionally been regarded as a regulator of the G1/S transition, it has also been demonstrated to play a role during the G2/M phase (Sherr and Roberts, 1995; Dulic et al., 1998; Cazzalini et al., 2010). Indeed, knockout of p21 prevented cells from appropriately arresting at the G2/M checkpoint following the induction of DNA damage. This was similarly identified in p27 which has also been traditionally regarded as an inhibitor of the G1/S transition and is increased in the present study (Sgambato et al., 2000; Payne et al., 2008). Further, this induction of p21 and repression of cyclin B_1 to maintain G2 arrest has been demonstrated to be a p53-mediated effect (Levesque et al., 2008), a protein that of wild-type status in both U87 and HeLa albeit of low expression in the latter. In addition to functioning as a transient inhibitor of the cell cycle, p21 elevation is also a marker of cellular senescence. While further studies are necessary to address this, the enhanced

237

retention of cell cycle arrest and elevated p21 with combination WA and RT supports this idea. A previous study has demonstrated that WA alone is capable of inducing senescence with induction of marker β-galactosidase (Vaishnavi et al., 2012).

Previous reports from Yang, et al. showed that combination of WA and RT in U937 and Caki cells resulted in enhanced markers of apoptosis without cell cycle radiosensitization contributions from p21 (Yang et al., 2011b). In contrast, we demonstrated in HeLa and U87 cells that cleavage of PARP as an apoptotic marker was either not enhanced or otherwise reduced with combination therapy compared to either agent alone in favor of increased expression of p21 and p27 and diminished progression of the cell cycle. These differences may represent intrinsic difference among cells or variability in dosing timepoints and concentration as analysis was only completed up to 24 h in the previous evaluation, however, both studies demonstrate the therapeutic value of combining WA and RT. Of note, U937 cell are a known p53-mutant cell line (Sugimoto et al., 1992), suggesting one potential intrinsic explanation for the difference. Caki cells contain wild-type p53 comparable to the cells used in the present study which was indeed shown to be activated through phosphorylation in the Yang, et al. study, indicating the potential role of an alternative mechanism not yet identified (Warburton et al., 2005). The Caki study did not evaluate changes in cell cycle distribution resulting from combination therapy, so it is possible that p53/p21 may still demonstrate comparable effects at later timepoints.

Future studies will be necessary to further define the dosing schedule that will yield optimal potentiation or synergy in the combination of WA and RT, particularly *in vivo*. Our *in vitro* studies determined that 2 h pretreatment was sufficient to all for this enhanced efficacy. Depending on the tissue levels achieved and the time necessary to manifest effects in the DDR pathways, a build-up period may be necessary in translational studies. WA dosing prior to rounds

of RT appear to be necessary to fully take advantage of the blockage of DNA damage repair. Studies are also necessary to identify the ability of WA to penetrate the blood-brain barrier (BBB) to evaluate its potential utility against brain tumors such as GBM which is indicated based on these studies, although tumors such as these are frequently described to disrupt the normal architecture of the BBB (Zhang et al., 1992). One preliminary study of WA in a murine orthotopic GBM model demonstrated a survival advantage with treatment, indicating that WA was reaching its target (Santagata et al., 2012). Further, evaluation of WA against the Lipinski Rule of Five, typically utilized for predicting favorability of drug absorption oral but often applied to the BBB, demonstrates that it does not violate any rule (Banks, 2009; Vaishnavi et al., 2012).

In this study, WA was determined for the first time to be a highly effective radiosensitizer through modulation of the normal DDR. Following WA treatment, proteins involved in DNA damage recognition and repair through HR and NHEJ were depleted, resulting in altered recognition and functionally inhibited repair of RT-induced DNA damage. Our previous findings show that WA acts as a potent cytotoxic monotherapy against GBM and re-sensitizes resistant cells to TMZ, the standard chemotherapeutic along with RT against GBM (Grogan et al., 2013; Grogan et al., 2014). Other groups have demonstrated WA efficacy other non-central nervous system (CNS) cancers and identified that WA enhances the efficacy of the broad-spectrum agent cisplatin, an agent often used against cervical cancer (Kakar et al., 2012; Vanden Berghe et al., 2012; Vyas and Singh, 2014). Taken together with WA-mediated enhancement of RT, these findings suggest the great clinical potential of WA as an adjuvant agent for brain tumors and non-CNS solid tumors like cervical cancer that warrant further translational exploration.

Supplemental Figure 6-1.
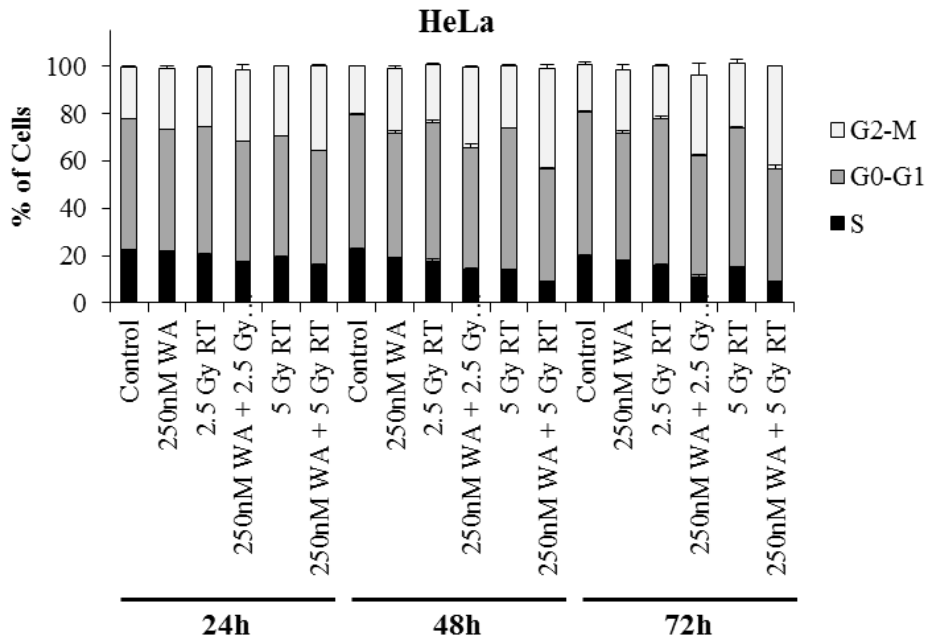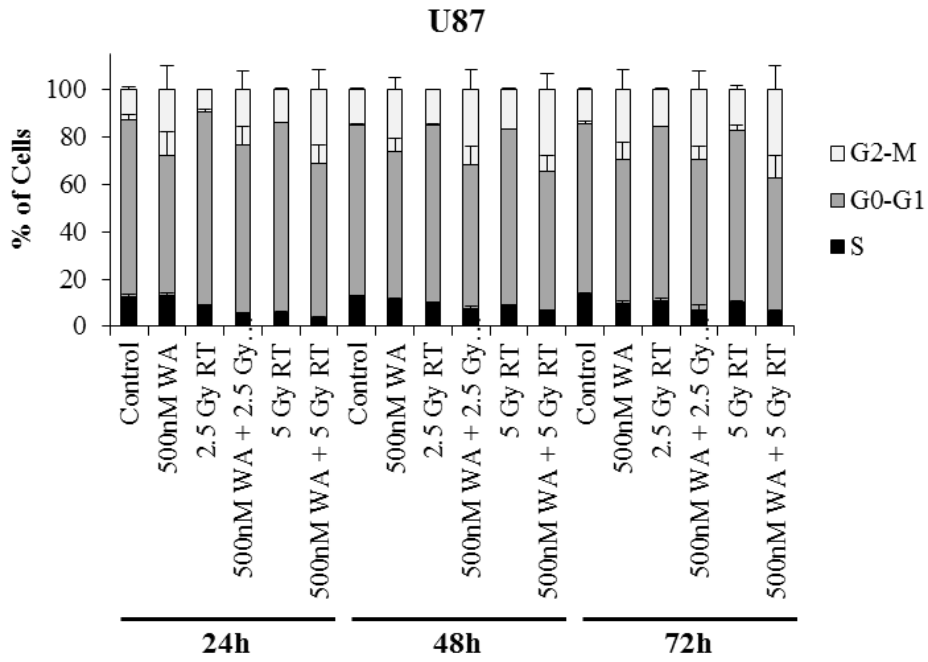
Supplemental Figure 6-1. Complete cell cycle analysis of the percentages of cells in the G0/G1 (2N DNA), S, and G2/M (4N DNA) phases with WA and RT treatment. WA treatment results in an increased percentage of cells in the G2/M-phase of the cell cycle with minimal changes in S-phase percentage. RT-treated U87 and HeLa cells both demonstrated small reductions in S-phase percentage, maximally at 24 h or 48 h, but showed variable shifts with cell predominantly moving to G0/G1 in U87 and G2/M in HeLa. Combination of WA and RT produced enhanced depletion of S-phase cells at 24 h and maintained the depletion at 72 h despite normalizing levels in the RT-only groups in both U87 and HeLa cells. Depletion of S-phase cells was primarily associated with maintained or minimally decreased levels of G0/G1-phase cells compared to WA-only with displacement to G2/M after 24 h. U87 cells demonstrated maintained elevation of G0/G1-phase cells at 24 h only with combination therapy.

Supplemental Figure 6-2.

HeLa

(GFP)
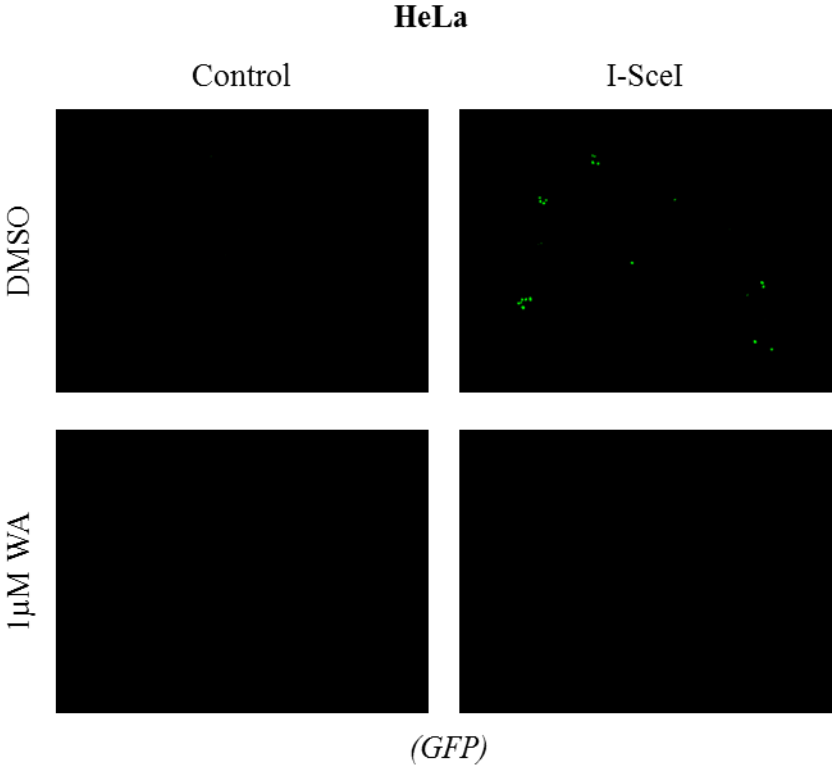
Supplemental Figure 6-2. HeLa cells stably expressing the DR-GFP reporter were transfected with an empty vector control or an I-SceI construct, plated, and treated immediately with 1 μM WA for 72 h before analysis of GFP expression, a marker of successful HR. WA demonstrated significant reduction in HR function with undetectable GFP+ cells as assessed by microscopy. Cells transfected with the control empty vector demonstrated no detected GFP by microscopy. GFP = green.

Chapter 7

Summary, Significance, and Future Directions

7.1 Summary and significance

7.1.1 Introduction

The treatment of brain tumors, particularly high grade malignancies like glioblastoma multiforme (GBM) and medulloblastoma (MB), continues to remain a tremendous clinical challenge. While surgical resection followed by radiation therapy (RT) and temozolomide (TMZ) in GBM patients limits disease progression, the average post-diagnosis survival time is still only approximately 14 months with rapid and frequent development of TMZ resistance (Stupp et al., 2002; DeAngelis, 2005; Stupp et al., 2005; Taphoorn et al., 2005; Chamberlain et al., 2007). TMZ was approved for use in GBM patients in 2004, but little therapeutic progress has been achieved since that time. Avastin® (bevacizumab), an angiogenesis inhibitor, was approved after TMZ but is largely utilized to reduce disease progression during the management phase rather than to provide a long-term disease response (Friedman et al., 2009; Zhang et al., 2012a). MB, largely but not exclusively a pediatric disease, demonstrates a greater response to currently available chemotherapies and RT, but patients are shown to frequently develop short-term and chronic quality of life issues that manifest from the off-target effects of the treatment in a young patient population (Khatua et al., 2012; Smoll, 2012). The research of the present study demonstrates the potent *in vitro* utility of WA as a therapeutic agent against the high-grade malignant brain tumors GBM and MB. The following briefly summarizes relevant finds in each of the chapters and identifies key significance and utility of the data. Further detailed interpretation and discussion can be found in each chapter.

7.1.2 Chapter 2: Cytotoxicity of withaferin A in glioblastomas involves induction of an oxidative stress-mediated heat shock response while altering Akt/mTOR and MAPK signaling pathways

Given the promising efficacy of WA in several non-brain tumor models and the identified need for novel therapeutic approaches in these cancers, the effects of WA were evaluated in a GBM model. The aim of this chapter was to determine if these previously observed cytotoxic effects could be translated to GBM with subsequent analysis of the nature of these effects. In this study, WA was indeed described to have an anti-proliferative effect on GBM cells with induction of G2/M cell cycle arrest at correspondingly low-to-moderate concentrations with a transition to cell death through apoptotic mechanisms at moderate-to-high doses. These findings were associated with changes in expression of Akt/mTOR and MAPK pathway proteins and upstream tyrosine kinase receptors. Notably, WA reduced activation of oncoproteins in the Akt/mTOR pathway but enhanced phosphorylation in MAPK proteins despite a reduction of total Raf-1. Simultaneously, WA produced significant cellular oxidation with induction of biomarkers HSP27, HSP32, and HSP70. All effects could be completely abrogated with N-acetyl-L-cysteine (NAC) pretreatment.

These findings demonstrated the *in vitro* utility of WA against GBM and provided a broad and general evaluation of its utility. Notably it also expanded on the limited data available addressing the effects of WA on the Akt/mTOR pathway. Here, WA not only decreased total and phosphorylated Akt as previously described but also diminished activation of downstream mTOR and p70 S6K. The α-subunit of the stress-response protein AMPK and its downstream tumor suppressor TSC2 that ultimately signal to mTOR were also activated via phosphorylation. This demonstrates that WA functions, in part, to inhibit the the Akt/mTOR pathway in the

manifestation of its effects. This study also showed the potential utility of thiol-reactive oxidative agents against GBM, further enhancing the altered redox state that has been described in cancer cells.

7.1.3 Chapter 3: Oxidative cytotoxic agent withaferin A resensitizes temozolomide-resistant glioblastomas via MGMT depletion and induces apoptosis through Akt/mTOR pathway inhibitory modulation

Intrinsic or acquired therapeutic resistance to TMZ has been shown to represent a major problem in the treatment of GBM patients (Hansen et al., 2007; Kitange et al., 2009). With a poor system of pre-therapy tumor screening methods currently in place, patients frequently receive TMZ when it would be contraindicated either early in the treatment process or after multiple cycles of chemotherapy (Chamberlain, 2010; Quick et al., 2010; Zhang et al., 2012c). Given the *in vitro* success of WA in known TMZ-sensitive GBM cell lines, the aim of this chapter was to evaluate the potential use of WA in developed TMZ-resistant GBM as a monotherapy and as a potential re-sensitizer to TMZ. As a monotherapy, WA demonstrated the same pattern of efficacy in resistant cells as was seen in the sensitive lines but with enhanced potency. This was expanded to demonstrate that phosphorylation of components of the MAPK cascade was a compensatory activation of the pathway in response to the cytotoxicity of WA, identifying a potentially effective target for the use of WA in synergistic combination therapy. Additionally, inhibition of both the intrinsic and extrinsic apoptotic pathways resulted in reduced downstream cleavage of PARP and effector caspases, demonstrating the role of both pathways in WA-mediated apoptosis.

Most importantly, WA demonstrated the ability to deplete cells of O^6-methylguanine-DNA-methyltransferase (MGMT) which confers resistance to TMZ. This effect was associated with re-sensitization to TMZ and was potentiated with TMZ combination therapy. Re-sensitization was not observed in a TMZ-resistant line with resistance through mismatch repair (MMR) alterations, and TMZ-sensitive lines were inconsistently further sensitized to TMZ by WA but never desensitized. These results demonstrate that WA, in addition to functioning as an effective monotherapy in a model of TMZ resistance, can be utilized to enhance the utility of WA in a setting where it would otherwise be contraindicated. Given that around 50% of patients are thought to display intrinsic characteristics for poor response to TMZ but receive TMZ regardless (Chamberlain, 2010; Quick et al., 2010; Zhang et al., 2012c), addition of WA to GBM treatment has the potential to function as 1) a cytotoxic therapeutic addition in a system that would otherwise be using an ineffective chemotherapeutic agent, and 2) as an agent to establish value with for the inclusion of TMZ. Of note, while MMR-driven resistance may not be re-sensitized to TMZ with WA, the presence of WA potentially provides a valuable cytotoxic component in a system with otherwise limited efficacy beyond RT. In cases where tumors display TMZ sensitivity, despite the inconsistent synergistic benefit of combination therapy, the additive presence of two agents may still be beneficial. Overall, the addition of WA, if tolerated, would appear to be universally beneficial.

7.1.4 Chapter 4: Withaferin A is a novel inhibitor of the Wnt/β-catenin signaling pathway in medulloblasoma through proteasome-mediated degradation of TCF/LEF

With the effective *in vitro* utilization of WA against GBM and its observed inhibition of Akt/mTOR pathway signaling, the use of WA was expanded to a model of MB. The aim of this chapter was to confirm the known cytotoxicity of WA in MB and evaluate the effects of WA in the Wnt/β-catenin signaling pathway. Indeed, WA demonstrated the anti-proliferative, pro-apoptotic, G2/M cell cycle arresting, and oxidative effects identified previously in GBM. Given the well-described cross-talk between the Akt/mTOR and Wnt/β-catenin pathways through GSK-3β and the overactivation of Wnt signaling in a subgroup of MBs (Baryawno et al., 2010; Northcott et al., 2012), inhibition of Akt as previously described in GBM was expected to result in inhibition of Wnt signaling through diminished phosphorylation of GSK-3β and subsequent degradation of β-catenin. WA did in fact reduce Wnt signaling through a reporter assay. However, in contrast to this original expectation, WA induced significant phosphorylation of GSK-3β and failed to significantly alter β-catenin levels or nuclear translocation in the cells. Rather, WA promoted proteasomal degradation of the TCF/LEF transcription factors that associate with β-catenin for the transcription of Wnt target genes.

These findings not only demonstrate the general efficacy of WA against MB but also identify it as a novel inhibitor of the Wnt/β-catenin signaling pathway through a unique mechanism. Further, WA was shown to disrupt the interaction between HSP90 and co-chaperone Cdc37 in MB, and inhibition of HSP90 with the established small molecule 17-AAG resulted in depletion of TCF/LEF proteins. Previous studies have identified the interaction of HSP90 with upstream components of the pathway like β-catenin and GSK-3β but have failed to conclusively demonstrate the role of HSP90 in their stability (inhibition of HSP90 did not consistently reduce levels of these proteins) (Cooper et al., 2011; Liu et al., 2012). Despite our inability to co-IP TCF/LEF members with HSP90 or Cdc37, these findings demonstrate a previous undescribed

role for HSP90 in the function of the Wnt signaling pathway which will require further exploration but suggests a novel role for HSP90 inhibitors against Wnt-driven malignancies like MB and colorectal cancer (Polakis, 2012). While WA targets this important signaling pathway overactivated in a subset of MB, it is also intrinsically cytotoxic through alternative pathways suggesting that it can be utilized against all MB subgroups without pathological pre-identification of subgroup. Its known selectivity for cancer cells with minimal off-target toxicity in murine models, as currently described, could reduce quality of life issues plaguing pediatric MB patients with current treatments while maintaining efficacy, although more studies are required in regard to translational toxicity and efficacy.

7.1.5 Chapter 5: Withaferin A promotes global proteasome-mediated protein degradation through oxidation and inhibition of the HSP90 chaperone axis and is cytotoxically potentiated by inhibition of the proteasome

WA has demonstrated the ability to yield diverse effects throughout the cell, frequently with protein depletion and modulation of multiple oncogenic signaling pathways (Vanden Berghe et al., 2012; Vyas and Singh, 2014). Several studies have suggested that WA alters the HSP90 chaperone axis and promotes cellular oxidation to promote the broad effects that are observed (Samadi et al., 2009; Yu et al., 2010; Wang et al., 2012). The aim of this chapter was to identify and explore the role of WA on cellular proteotoxicity through these mechanisms in GBM and the well-established HeLa cervical cancer line. WA favored a shift to HSP70 in the HSP90/HSP70 balance, promoting enhanced global protein ubiquitination. This was associated with degradation of HSP90 client proteins via the proteasome with inhibition of the HSP90 axis

through disruption of the HSP90/Cdc37 interaction but not direct reduction in intrinsic HSP90 function. Cytotoxicity and oxidation events following WA exposure could be completely abrogated with thiol antioxidant NAC pretreatment and enhanced with reduction in cellular glutathione. Non-thiol antioxidant ascorbic acid reduced oxidation but failed to alter cytotoxicity.

These findings further define the novel mechanism by which WA manifests its cytotoxic effects and provide details regarding both the oxidative and HSP90 inhibitory components which are likely not mutually exclusive. Such an effect on the HSP90 axis may predict WA utility in altering additional proteins and pathways critical to cancer progression subsequently revealing appropriate clinical uses. Future studies identifying other HSP90 inhibitory aspects given the depletion of non-Cdc37 proteins will be necessary. Additional experiments were completed to evaluate WA in combination with a proteasome inhibitor. Given that WA promotes widespread protein degradation via the proteasome, simultaneous inhibition of the proteasome promoted accumulation of ubiquitinated aberrant proteins, induced cytotoxicity with reduced cell viability, and ultimately potentiated the induction of apoptosis compared to either agent as a monotherapy. Proteasome inhibitors are currently approved for clinical use in some cancer types including multiple myeloma (Chauhan et al., 2005), identifying an opportunity for rapid WA translation to human use and establishment of proof-of-concept. This enhanced efficacy of combination with a proteasome inhibitor has been supported with the use of traditional HSP90 inhibitors (Minnnaugh et al., 2004). These data support translational utility derived from the identified mechanisms of WA.

7.1.6 Chapter 6: Withaferin A disrupts the cellular DNA-damage response to promote radiosensitization

251

RT represents a key therapeutic component in the treatment of a significant percentage of primary tumors including GBM and MB (Delaney et al., 2005). Therefore, efforts to enhance RT-induced DNA damage and limit the repair of this damage by cancer cells has been seen as means by which to effectively enhance cytotoxicity and efficacy of clinical RT in patients (Begg et al., 2011). Given that inhibition of HSP90, among other targets, can radiosensitize (Dote et al., 2006; Kabakov et al., 2010; Ko et al., 2012; Stecklein et al., 2012), the aim of this chapter was to evaluate the radiosensitization properties of WA against GBM cells and the homologous recombination (HR)-competent HeLa cervical cancer line. Indeed, low-dose WA potentiated the efficacy of RT in both lines. This was associated with a reduction in cells synthesizing new DNA and elevation of the checkpoint inhibitors p21 and p27. Functionally, WA reduced total levels of key proteins involved in the recognition and repair of DNA damage through HR and non-homologous end-joining (NHEJ) and modulated normal signaling in response to RT. This lead to altered recognition of the damage assessed by p-H2A.X, enhanced and sustained DNA damage with combination therapy, and a functional block of HR.

These findings further demonstrate the potential clinical application of WA. Given that RT is used in the treatment of an estimated 50% of cancer patients (Delaney et al., 2005), enhancing the efficacy of this therapeutic modality is an extremely important translational prospect and has been a consideration in the selection of adjuvant chemotherapy previously, including the addition of TMZ to RT (Chakravarti et al., 2006). The data suggests that WA is likely to enhance DNA damage induced by other agents and repaired through a range of modalities including HR, NHEJ, and MMR which identifies a potential for broad spectrum combination use clinically alone with the intrinsic cytotoxicity of WA as a monotherapy.

Because augmented DNA damage response mechanisms are known to play a key role in chemo- and radio-resistance, we believe that modulation and depletion of these pathways with WA may provide enhanced efficacy of therapeutics in refractory or resistant GBM or other cancer types. Indeed, we demonstrated WA's ability to re-sensitize resistant GBM cells to TMZ through depletion of MGMT, showing proof-of-concept (Grogan et al., 2014).

7.2 Future directions

The conducted research identified, defined, and utilized the cytotoxic anti-cancer properties of WA in a model of high-grade brain tumors. Among the results, WA induced inhibitory modulation of the PI3K/Akt/mTOR and Wnt/β-catenin oncogenic signaling pathways. These are the first studies to thoroughly evaluate the influence of WA on both pathways in any cancer model and potentially define several therapeutic roles for the compound. Given the broad effects of WA on multiple oncogenic or otherwise cancer-promoting pathways in our studies and those published by others (Vanden Berghe et al., 2012; Vyas and Singh, 2014), particularly with noted activity against the HSP90 chaperone axis with over 400 known client or interacting proteins, future experiments are necessary to further expand on the effects of WA against other proteins that have yet to be explored and the resulting changes in signal transduction efficiency. Notably, there are currently no published reports on the effect of WA on the SHH pathway, important in a subgroup of MB. Similarly, the inhibition of the pathways identified with this research can be expanded to other relevant cancer models. For example, the Wnt/β-catenin pathway is overactivated in a significant percentage of colorectal cancers (Polakis, 2012). Targeting this pathway with WA along with the general cytotoxicity of the compound through

additional mechanisms would be thought to have great therapeutic benefits clinically by blocking a key driving oncogenic pathway and inducing additional anti-cancer manifestations.

The efficacy of WA was also demonstrated to be enhanced in combination with both RT and a proteasome inhibitor and functioned to re-sensitize resistant GBM cells to TMZ. Previous studies have identified that WA synergizes with other chemotherapeutic agents such as sorafenib and cisplatin (Cohen et al., 2012; Kakar et al., 2012). HSP90 inhibition, a described function of WA, has also been shown to potentiate, enhance, or re-sensitize the activity of numerous agents (Lu et al., 2012). These observations suggest that WA may function well in combination with other therapeutic agents, particularly those inducing DNA damage, generating a large expansion in the potential for studying and ultimately using this compound. Additionally, because WA was demonstrated to promote activation of the MAPK pathway through phosphorylation of Raf-1 and ERK1/2, relevant inhibitors of these proteins would be expected to yield favorable efficacy in combination with WA. Given the apparent protective effect of GSH against WA, selective depletion of GSH in redox susceptible cancer cells, perhaps through inhibition of γ-glutamylcysteine synthetase, could serve to enhance the cellular cytotoxicity to WA, although the potential for off-target toxicity would need to be evaluated if similar reduction in GSH was observed in normal tissue. These combinations also establish greater therapeutic relevance for WA given the problems of ineffectiveness and resistance frequently associated with monotherapy. Interestingly, however, our *in vitro* attempts to develop cell line resistance to WA have been largely unsuccessful and warrant further exploration.

These findings open some additional questions regarding the role of WA in the inhibition of the HSP90 axis. While these results clearly indicate that WA eliminates the interaction between HSP90 and the co-chaperone Cdc37 at high enough concentrations and does not appear

to alter the intrinsic activity of HSP90 at least in regard to steroid receptor association, protein depletion mirrors total inhibition of HSP90 (and perhaps more) rather than a prevention of Cdc37 function. Cdc37 primarily functions as a kinase-specific co-chaperone to promote the folding and maturation of these proteins through localization with HSP90 with enhanced client loading though modulation of HSP90 ATPase activity (Siligardi et al., 2002; Roe et al., 2004). However, proteins not previously known to associate with Cdc37 and non-kinase proteins such as c-myc and the glucocorticoid receptor were dose-dependently degraded with WA exposure. Such findings suggest that while the disruption of the HSP90/Cdc37 interaction was real, the effects of WA extend beyond that observation or the role of Cdc37 is greater than currently thought. Cdc37 has also been shown to interact with other co-chaperone proteins, suggesting another way by which it can still join the HSP90 chaperone complex (Abbas-Terki et al., 2002). Given that WA interacts with the C-terminus of HSP90 in the location that other co-chaperones are known to associate, this represents a potential explanation of these expanded findings (Yu et al., 2010). Interestingly p23 and Hop were not dissociated from HSP90 in the presence of WA (Yu et al., 2010), but their maintained functionality directly with HSP90 was not addressed. Clearly, further study of this system is required to better understand the variations observed whether due to additional modulation of the HSP90 axis or indirect effect from associated observations like cellular oxidation.

Additionally, while alterations in the HSP90 chaperone axis have been clearly demonstrated to play a role in the cytotoxicity of WA, there have been arguments regarding the specificity of this effect. In order to determine whether the cytotoxic manifestations are primarily driven by its association with HSP90, it is proposed that future studies be conducted with cells in which endogenous HSP90 has been replaced or supplemented with HSP90 mutants retaining

function but lacking the appropriate WA binding site, likely through mutation of an existing C-terminal cysteine. As such, the HSP90-independent effects of WA could be studied. Further, enrichment or depletion of GSH in the context of non-thiol antioxidants could further help define the nature of the effect as it relates to general oxidation and redox alterations. To date, few proteins have been shown to directly associate with WA, including via a broad spectrum analysis of biotinylated-WA binding, suggesting some specificity of is binding (Bargagna-Mohan et al., 2007; Yu et al., 2010). Such studies could further demonstrate the importance of the HSP90 target with WA treatment.

Studies from our group and others have evaluated novel natural and semi-synthetic withanolides beyond WA (Zhang et al., 2011a; Santagata et al., 2012; Zhang et al., 2012b; Wijeratne et al., 2014). Notably, significant cytotoxicity is lost with the elimination of the A-ring enone and/or the epoxide group. Our preliminary studies in triple negative breast cancer and several other models demonstrate that acetylation of one or more of the hydroxide groups enhance cytotoxic activity and anti-tumor efficacy *in vivo*. A recent study also identified that synthetic acetylation or other modifications of functional groups on WA or the withanolide structure can differentially alter biological cytotoxicity and/or heat shock-inducing activity (Wijeratne et al., 2014). It is unclear if this heat shock response is a function of HSP90 inhibition, general oxidation, or perhaps more likely, both. Such structure-activity relationship (SAR) studies will be necessary going forward to identify improved therapeutic withanolides with better anti-cancer efficacy, more favorable pharmacokinetics for a particular malignancy [especially for crossing the blood-brain-barrier (BBB)], and diminished off-target toxicity. To date, SAR studies with withanolides have primarily been assessed *in vitro*. While these studies have yield valuable information, they have failed to address the pharmacokinetic aspect for

translational use. Withanolides, primarily WA, have demonstrated *in vivo* efficacy against a number of murine cancer models (Vyas and Singh, 2014) but drug absorption, distribution, and elimination have remained largely unexplored.

Pharmacokinetic studies, particularly those involving the metabolism of WA and these other novel withanolides, will shed light on the body's ability to activate and/or detoxify these compounds, thereby suggesting potential benefits or limitations to various dosing schemes. To date, very few studies have evaluated the metabolism of WA with the last studies emerging from the 1980s. Those studies, conducted in *Cunninghamella elegans* and *Arthrobacter simplex*, revealed that WA can be metabolized via hydroxylation, hydrogenation, and hydrolysis (Rosazza et al., 1978; Fuska et al., 1982; Proksa et al., 1986; Fuska et al., 1987). Because WA shares many structural similarities with endogenous steroids given its steroidal lactone classification, the study of its metabolism remains a critical element necessary for its potential use in the clinic as steroids are often metabolized in oxidative reactions by cytochrome P450 (CYP450) enzymes (Gonzalez, 1990). On top of that, an estimated minimum of 75-90% of the reactions in the metabolism of pharmaceutical drugs are by CYP450s, demonstrating an integral role for their study in the development of any compound (Guengerich, 2008; Sun and Scott, 2010). An overlap in the metabolic processes serving WA with other chemotherapeutic agents whose metabolism has been previously well-characterized could suggest successful pairing schemes on the basis of toxicokinetics or generating more favorable pharmacokinetic parameters (Cheng et al., 2010).

Additionally, studies on the distribution of WA and its metabolites, particularly to the brain and more specifically during the diseased state of a brain tumor, have remained largely unpublished, although one preliminary study utilizing a murine orthotopic glioma model demonstrated a survival benefit with WA (Santagata et al., 2012). Given this survival benefit, it

257

is evident that the compound or an active metabolite likely reaches the site of the tumor lesion regardless of whether the BBB lacks integrity. What is less clear is whether WA is capable of crossing an intact BBB peritumorally where tumor invasion has occurred or in healthy brain tissue with relatively normal and maintained architecture. A recent bioinformatics study suggested that WA's structure fails to violate Lipinski's Rule of Five and has a favorable blood/brain partition coefficient (Vaishnavi et al., 2012), but translation to a biological system still needs to be examined. Other active withanolides in which polar functional groups are masked or simply absence may yield more favorable results if not ultimately achieved with WA, and indeed, preliminary studies in several non-brain tumor murine models show this. Encouragingly, multiple additional non-brain tumor murine models have demonstrated promising responses to WA treatment with multiple dosing schedules and levels (Vyas and Singh, 2014). One report identified a maximum plasma concentration of WA following a single intraperitoneal injection of the moderate dose of 4 mg/kg to be 1.8 µM, well-above typical *in vitro* IC$_{50}$ values for cancer cells, with a plasma half-life of 1.3 h. Tissue distribution has not yet been reported. Overall, further translational studies with WA and other withanolides, particularly in an orthotopic brain tumor model, are necessary to evaluate both the pharmacokinetics and pharmacodynamics of the compound and establish maximally effective and minimally toxic dosing levels and schedules. Such studies can be followed up with efficacy and toxicity studies for combination therapy as previously discussed and utilization of NAC as a rescue agent in cases of toxicity or attempted high-dose regimens.

References

Abbas-Terki T, Briand PA, Donze O and Picard D (2002) The Hsp90 co-chaperones Cdc37 and Sti1 interact physically and genetically. *Biol Chem* **383**:1335-1342.

ACS (2013) Cancer Facts and Figures 2013, in *Atlanta, GA: American Cancer Society*, American Cancer Society, Atlanta, GA.

Agarwal S, Sane R, Oberoi R, Ohlfest JR and Elmquist WF (2011) Delivery of molecularly targeted therapy to malignant glioma, a disease of the whole brain. *Expert Rev Mol Med* **13**:e17.

Ahles TA and Saykin A (2001) Cognitive effects of standard-dose chemotherapy in patients with cancer. *Cancer Invest* **19**:812-820.

Alam MI, Beg S, Samad A, Baboota S, Kohli K, Ali J, Ahuja A and Akbar M (2010) Strategy for effective brain drug delivery. *Eur J Pharm Sci* **40**:385-403.

Ansari N, Khodagholi F and Amini M (2011) 2-Ethoxy-4,5-diphenyl-1,3-oxazine-6-one activates the Nrf2/HO-1 axis and protects against oxidative stress-induced neuronal death. *Eur J Pharmacol* **658**:84-90.

Antosiewicz J, Ziolkowski W, Kar S, Powolny AA and Singh SV (2008) Role of reactive oxygen intermediates in cellular responses to dietary cancer chemopreventive agents. *Planta Med* **74**:1570-1579.

Arce L, Yokoyama NN and Waterman ML (2006) Diversity of LEF/TCF action in development and disease. *Oncogene* **25**:7492-7504.

Arlander SJH, Eapen AK, Vroman BT, McDonald RJ, Toft DO and Karnitz LM (2003) Hsp90 inhibition depletes Chk1 and sensitizes tumor cells to replication stress. *J Biol Chem* **278**:52572-52577.

Au Q, Zhang Y, Barber JR, Ng SC and Zhang B (2009) Identification of inhibitors of HSF1 functional activity by high-content target-based screening. *J Biomol Screen* **14**:1165-1175.

Avruch J, Khokhlatchev A, Kyriakis JM, Luo Z, Tzivion G, Vavvas D and Zhang XF (2001) Ras activation of the Raf kinase: tyrosine kinase recruitment of the MAP kinase cascade. *Recent Prog Horm Res* **56**:127-155.

Baer JC, Freeman AA, Newlands ES, Watson AJ, Rafferty JA and Margison GP (1993) Depletion of O6-alkylguanine-DNA alkyltransferase correlates with potentiation of temozolomide and CCNU toxicity in human tumour cells. *Br J Cancer* **67**:1299-1302.

Bailey CK, Andriola IF, Kampinga HH and Merry DE (2002) Molecular chaperones enhance the degradation of expanded polyglutamine repeat androgen receptor in a cellular model of spinal and bulbar muscular atrophy. *Hum Mol Genet* **11**:515-523.

Baka S, Clamp AR and Jayson GC (2006) A review of the latest clinical compounds to inhibit VEGF in pathological angiogenesis. *Expert Opin Ther Targets* **10**:867-876.

Banks WA (2009) Characteristics of compounds that cross the blood-brain barrier. *BMC Neurol* **9 Suppl 1**.

Bargagna-Mohan P, Hamza A, Kim YE, Khuan Abby Ho Y, Mor-Vaknin N, Wendschlag N, Liu J, Evans RM, Markovitz DM, Zhan CG, Kim KB and Mohan R (2007) The tumor inhibitor and antiangiogenic agent withaferin A targets the intermediate filament protein vimentin. *Chem Biol* **14**:623-634.

Bargagna-Mohan P, Ravindranath PP and Mohan R (2006) Small molecule anti-angiogenic probes of the ubiquitin proteasome pathway: potential application to choroidal neovascularization. *Invest Ophthalmol Vis Sci* **47**:4138-4145.

Barrott JJ and Haystead TA (2013) Hsp90, an unlikely ally in the war on cancer. *FEBS J* **280**:1381-1396.

Baryawno N, Sveinbjornsson B, Eksborg S, Chen CS, Kogner P and Johnsen JI (2010) Small-Molecule Inhibitors of Phosphatidylinositol 3-Kinase/Akt Signaling Inhibit Wnt/beta-Catenin Pathway Cross-Talk and Suppress Medulloblastoma Growth. *Cancer Res* **70**:266-276.

Baskar R, Lee KA, Yeo R and Yeoh KW (2012) Cancer and radiation therapy: current advances and future directions. *Int J Med Sci* **9**:193-199.

Begg AC, Stewart FA and Vens C (2011) Strategies to improve radiotherapy with targeted drugs. *Nat Rev Cancer* **11**:239-253.

Berezowska S and Schlegel J (2011) Targeting ErbB receptors in high-grade glioma. *Curr Pharm Des* **17**:2468-2487.

Bobola MS, Kolstoe DD, Blank A and Silber JR (2010) Minimally cytotoxic doses of temozolomide produce radiosensitization in human glioblastoma cells regardless of MGMT expression. *Mol Cancer Ther* **9**:1208-1218.

Boman KK, Hoven E, Anclair M, Lannering B and Gustafsson G (2009) Health and persistent functional late effects in adult survivors of childhood CNS tumours: a population-based cohort study. *Eur J Cancer* **45**:2552-2561.

Buonerba C, Di Lorenzo G, Marinelli A, Federico P, Palmieri G, Imbimbo M, Conti P, Peluso G, De Placido S and Sampson JH (2011) A comprehensive outlook on intracerebral therapy of malignant gliomas. *Crit Rev Oncol Hematol* **80**:54-68.

Butler JM, Rapp SR and Shaw EG (2006) Managing the cognitive effects of brain tumor radiation therapy. *Curr Treat Options Oncol* **7**:517-523.

Byfield JE (1989) 5-Fluorouracil radiation sensitization--a brief review. *Invest New Drugs* **7**:111-116.

Cabello CM, Bair WB, 3rd and Wondrak GT (2007) Experimental therapeutics: targeting the redox Achilles heel of cancer. *Curr Opin Investig Drugs* **8**:1022-1037.

Carter EL and Ragsdale SW (2014) Modulation of nuclear receptor function by cellular redox poise. *J Inorg Biochem* **133**:92-103.

Carter RE and Sorkin A (1998) Endocytosis of functional epidermal growth factor receptor-green fluorescent protein chimera. *J Biol Chem* **273**:35000-35007.

Cazzalini O, Scovassi AI, Savio M, Stivala LA and Prosperi E (2010) Multiple roles of the cell cycle inhibitor p21(CDKN1A) in the DNA damage response. *Mutat Res* **704**:12-20.

Chakravarti A, Erkkinen MG, Nestler U, Stupp R, Mehta M, Aldape K, Gilbert MR, Black PM and Loeffler JS (2006) Temozolomide-mediated radiation enhancement in glioblastoma: a report on underlying mechanisms. *Clin Cancer Res* **12**:4738-4746.

Chamberlain MC (2010) Temozolomide: therapeutic limitations in the treatment of adult high-grade gliomas. *Expert Rev Neurother* **10**:1537-1544.

Chamberlain MC, Glantz MJ, Chalmers L, Van Horn A and Sloan AE (2007) Early necrosis following concurrent Temodar and radiotherapy in patients with glioblastoma. *J Neurooncol* **82**:81-83.

Chang L and Karin M (2001) Mammalian MAP kinase signalling cascades. *Nature* **410**:37-40.

Chauhan D, Hideshima T, Mitsiades C, Richardson P and Anderson KC (2005) Proteasome inhibitor therapy in multiple myeloma. *Mol Cancer Ther* **4**:686-692.

Chen WY, Chang FR, Huang ZY, Chen JH, Wu YC and Wu CC (2008) Tubocapsenolide A, a novel withanolide, inhibits proliferation and induces apoptosis in MDA-MB-231 cells by thiol oxidation of heat shock proteins. *J Biol Chem* **283**:17184-17193.

Cheng JW, Frishman WH and Aronow WS (2010) Updates on cytochrome p450-mediated cardiovascular drug interactions. *Dis Mon* **56**:163-179.

Citti L, Boldrini L, Preuss I, Kaina B, Mariani L and Rainaldi G (1996) Targeting of O6-methylguanine-DNA methyltransferase (MGMT) activity by antimessenger oligonucleotide sensitizes CHO/Mex+ transfected cells to mitozolomide. *Carcinogenesis* **17**:25-29.

Cohen SM, Mukerji R, Timmermann BN, Samadi AK and Cohen MS (2012) A novel combination of withaferin A and sorafenib shows synergistic efficacy against both papillary and anaplastic thyroid cancers. *Am J Surg* **204**:895-900.

Cooper LC, Prinsloo E, Edkins AL and Blatch GL (2011) Hsp90alpha/beta associates with the GSK3beta/axin1/phospho-beta-catenin complex in the human MCF-7 epithelial breast cancer model. *Biochem Biophys Res Commun* **413**:550-554.

Cumming RC, Andon NL, Haynes PA, Park M, Fischer WH and Schubert D (2004) Protein disulfide bond formation in the cytoplasm during oxidative stress. *J Biol Chem* **279**:21749-21758.

D'Atri S, Graziani G, Lacal PM, Nistico V, Gilberti S, Faraoni I, Watson AJ, Bonmassar E and Margison GP (2000) Attenuation of O(6)-methylguanine-DNA methyltransferase activity and mRNA levels by cisplatin and temozolomide in jurkat cells. *J Pharmacol Exp Ther* **294**:664-671.

Dai K, Kobayashi R and Beach D (1996) Physical interaction of mammalian CDC37 with CDK4. *J Biol Chem* **271**:22030-22034.

DeAngelis LM (2005) Chemotherapy for brain tumors--a new beginning. *N Engl J Med* **352**:1036-1038.

Delaney G, Jacob S, Featherstone C and Barton M (2005) The role of radiotherapy in cancer treatment: estimating optimal utilization from a review of evidence-based clinical guidelines. *Cancer* **104**:1129-1137.

Deneke SM (2000) Thiol-based antioxidants. *Curr Top Cell Regul* **36**:151-180.

Dent P, Tang Y, Yacoub A, Dai Y, Fisher PB and Grant S (2011) CHK1 inhibitors in combination chemotherapy: thinking beyond the cell cycle. *Mol Interv* **11**:133-140.

Desjardins A, Reardon DA, Herndon JE, 2nd, Marcello J, Quinn JA, Rich JN, Sathornsumetee S, Gururangan S, Sampson J, Bailey L, Bigner DD, Friedman AH, Friedman HS and Vredenburgh JJ (2008) Bevacizumab plus irinotecan in recurrent WHO grade 3 malignant gliomas. *Clin Cancer Res* **14**:7068-7073.

Devi PU, Akagi K, Ostapenko V, Tanaka Y and Sugahara T (1996) Withaferin A: a new radiosensitizer from the Indian medicinal plant Withania somnifera. *Int J Radiat Biol* **69**:193-197.

Devi PU and Kamath R (2003) Radiosensitizing effect of withaferin A combined with hyperthermia on mouse fibrosarcoma and melanoma. *J Radiat Res* **44**:1-6.

Devi PU, Kamath R and Rao BS (2000) Radiosensitization of a mouse melanoma by withaferin A: in vivo studies. *Indian J Exp Biol* **38**:432-437.

Devi PU, Sharada AC and Solomon FE (1995) In vivo growth inhibitory and radiosensitizing effects of withaferin A on mouse Ehrlich ascites carcinoma. *Cancer Lett* **95**:189-193.

Devi PU, Utsumi H, Takata M and Takeda S (2008) Enhancement of radiation induced cell death in chicken B lymphocytes by withaferin A. *Indian J Exp Biol* **46**:437-442.

Dhillon AS, Hagan S, Rath O and Kolch W (2007) MAP kinase signalling pathways in cancer. *Oncogene* **26**:3279-3290.

Dote H, Burgan WE, Camphausen K and Tofilon PJ (2006) Inhibition of hsp90 compromises the DNA damage response to radiation. *Cancer Res* **66**:9211-9220.

Dulic V, Stein GH, Far DF and Reed SI (1998) Nuclear accumulation of p21(Cip1) the onset of mitosis: a role at the G(2)/M-phase transition. *Mol Cell Biol* **18**:546-557.

Eckl JM, Rutz DA, Haslbeck V, Zierer BK, Reinstein J and Richter K (2013) Cdc37 (cell division cycle 37) restricts Hsp90 (heat shock protein 90) motility by interaction with N-terminal and middle domain binding sites. *J Biol Chem* **288**:16032-16042.

Ellis LM and Hicklin DJ (2008) Pathways mediating resistance to vascular endothelial growth factor-targeted therapy. *Clin Cancer Res* **14**:6371-6375.

Ellison DW, Kocak M, Dalton J, Megahed H, Lusher ME, Ryan SL, Zhao W, Nicholson SL, Taylor RE, Bailey S and Clifford SC (2011) Definition of disease-risk stratification groups in childhood

medulloblastoma using combined clinical, pathologic, and molecular variables. *J Clin Oncol* **29**:1400-1407.

Erdfelder F, Hertweck M, Filipovich A, Uhrmacher S and Kreuzer KA (2010a) High lymphoid enhancer-binding factor-1 expression is associated with disease progression and poor prognosis in chronic lymphocytic leukemia. *Hematol Rep* **2**:e3.

Erdfelder F, Poll-Wolbeck SJ, Gehrke I, Hallek M and Kreuzer KA (2010b) High Lymphoid Enhancer-Binding Factor-1 (LEF1) Expression Is Associated with ZAP70 Positivity, Requirement of Treatment, and Fibromodulin (FMOD) Expression In Chronic Lymphocytic Leukemia (CLL). *Blood* **116**:718-718.

Eriksson D, Lofroth PO, Johansson L, Riklund K and Stigbrand T (2009) Apoptotic signalling in HeLa Hep2 cells following 5 Gy of cobalt-60 gamma radiation. *Anticancer Res* **29**:4361-4366.

Evans SM, Judy KD, Dunphy I, Jenkins WT, Hwang WT, Nelson PT, Lustig RA, Jenkins K, Magarelli DP, Hahn SM, Collins RA, Grady MS and Koch CJ (2004a) Hypoxia is important in the biology and aggression of human glial brain tumors. *Clin Cancer Res* **10**:8177-8184.

Evans SM, Judy KD, Dunphy I, Jenkins WT, Nelson PT, Collins R, Wileyto EP, Jenkins K, Hahn SM, Stevens CW, Judkins AR, Phillips P, Geoerger B and Koch CJ (2004b) Comparative measurements of hypoxia in human brain tumors using needle electrodes and EF5 binding. *Cancer Res* **64**:1886-1892.

Evron A, Goldman S and Shalev E (2012) Human amniotic epithelial cells differentiate into cells expressing germ cell specific markers when cultured in medium containing serum substitute supplement. *Reprod Biol Endocrinol* **10**.

Frange P, Alapetite C, Gaboriaud G, Bours D, Zucker JM, Zerah M, Brisse H, Chevignard M, Mosseri V, Bouffet E and Doz F (2009) From childhood to adulthood: long-term outcome of medulloblastoma patients. The Institut Curie experience (1980-2000). *J Neurooncol* **95**:271-279.

Friedman HS, Prados MD, Wen PY, Mikkelsen T, Schiff D, Abrey LE, Yung WK, Paleologos N, Nicholas MK, Jensen R, Vredenburgh J, Huang J, Zheng M and Cloughesy T (2009) Bevacizumab alone and in combination with irinotecan in recurrent glioblastoma. *J Clin Oncol* **27**:4733-4740.

Fu J, Shao CJ, Chen FR, Ng HK and Chen ZP (2010) Autophagy induced by valproic acid is associated with oxidative stress in glioma cell lines. *Neuro Oncol* **12**:328-340.

Furgason JM and Bahassi EM (2012) Targeting DNA repair mechanisms in cancer. *Pharmacol Ther*.

Fuska J, Proska B, Williamson J and Rosazza JP (1987) Microbiological and chemical dehydrogenation of withaferin A. *Folia Microbiol (Praha)* **32**:112-115.

Fuska J, Prousek J, Rosazza J and Budesinsky M (1982) Microbial transformations of natural antitumor agents. 23. Conversion of withaferin-A to 12 beta- and 15 beta-hydroxy derivatives of withaferin-A. *Steroids* **40**:157-169.

Giese A, Bjerkvig R, Berens ME and Westphal M (2003) Cost of migration: invasion of malignant gliomas and implications for treatment. *J Clin Oncol* **21**:1624-1636.

Gilbertson RJ and Ellison DW (2008) The origins of medulloblastoma subtypes. *Annu Rev Pathol* **3**:341-365.

Gilbertson RJ, Langdon JA, Hollander A, Hernan R, Hogg TL, Gajjar A, Fuller C and Clifford SC (2006) Mutational analysis of PDGFR-RAS/MAPK pathway activation in childhood medulloblastoma. *Eur J Cancer* **42**:646-649.

Gillingham FJ and Yamashita J (1975) [The effect of radiotherapy for glioblastoma: a review of 516 cases (author's transl)]. *No Shinkei Geka* **3**:329-336.

Golding SE, Rosenberg E, Khalil A, McEwen A, Holmes M, Neill S, Povirk LF and Valerie K (2004) Double strand break repair by homologous recombination is regulated by cell cycle-independent signaling via ATM in human glioma cells. *J Biol Chem* **279**:15402-15410.

Gonzalez FJ (1990) Molecular genetics of the P-450 superfamily. *Pharmacol Ther* **45**:1-38.

Grammatikakis N, Lin JH, Grammatikakis A, Tsichlis PN and Cochran BH (1999) p50(cdc37) acting in concert with Hsp90 is required for Raf-1 function. *Mol Cell Biol* **19**:1661-1672.

Gray PJ, Jr., Stevenson MA and Calderwood SK (2007) Targeting Cdc37 inhibits multiple signaling pathways and induces growth arrest in prostate cancer cells. *Cancer Res* **67**:11942-11950.

Gregory MA and Hann SR (2000) c-Myc proteolysis by the ubiquitin-proteasome pathway: stabilization of c-Myc in Burkitt's lymphoma cells. *Mol Cell Biol* **20**:2423-2435.

Grogan PT, Samadi AK and Cohen MS (2010) A novel cytotoxic agent induced apoptosis in malignant gliomas in vitro, in *Academic Surgical Congress* pp 341-342, Journal of Surgical Research, San Antonio, TX.

Grogan PT, Sarkaria JN, Timmermann BN and Cohen MS (2014) Oxidative cytotoxic agent withaferin A resensitizes temozolomide-resistant glioblastomas via MGMT depletion and induces apoptosis through Akt/mTOR pathway inhibitory modulation. *Invest New Drugs* **[Epub ahead of print]**.

Grogan PT, Sleder KD, Samadi AK, Zhang H, Timmermann BN and Cohen MS (2013) Cytotoxicity of withaferin A in glioblastomas involves induction of an oxidative stress-mediated heat shock response while altering Akt/mTOR and MAPK signaling pathways. *Invest New Drugs* **31**:545-557.

Grogan PT, Sleder KD, Stecklein SR and Cohen MS (2011) Vassobia Breviflora Root-Extract Withaferin A As A Novel Cytotoxic And Synergistic Agent Against Malignant Gliomas, in *Academic Surgical Congress* p 311, Journal of Surgical Research, Huntington Beach, CA.

Grover A, Shandilya A, Agrawal V, Pratik P, Bhasme D, Bisaria VS and Sundar D (2011) Hsp90/Cdc37 chaperone/co-chaperone complex, a novel junction anticancer target elucidated by the mode of action of herbal drug Withaferin A. *BMC Bioinformatics* **12 Suppl 1**.

Gu M, Yu Y, Gunaherath GM, Gunatilaka AA, Li D and Sun D (2014) Structure-activity relationship (SAR) of withanolides to inhibit Hsp90 for its activity in pancreatic cancer cells. *Invest New Drugs* **32**:68-74.

Guengerich FP (2008) Cytochrome p450 and chemical toxicology. *Chem Res Toxicol* **21**:70-83.

Guessous F, Zhang Y, diPierro C, Marcinkiewicz L, Sarkaria J, Schiff D, Buchanan S and Abounader R (2010) An orally bioavailable c-Met kinase inhibitor potently inhibits brain tumor malignancy and growth. *Anticancer Agents Med Chem* **10**:28-35.

Gyori BM, Venkatachalam G, Thiagarajan PS, Hsu D and Clement MV (2014) OpenComet: An automated tool for comet assay image analysis. *Redox Biol* **2**:457-465.

Hahm ER, Moura MB, Kelley EE, Van Houten B, Shiva S and Singh SV (2011) Withaferin A-Induced Apoptosis in Human Breast Cancer Cells Is Mediated by Reactive Oxygen Species. *PLoS One* **6**.

Hamilton A and Sibson NR (2013) Role of the systemic immune system in brain metastasis. *Mol Cell Neurosci* **53**:42-51.

Hansen RJ, Nagasubramanian R, Delaney SM, Samson LD and Dolan ME (2007) Role of O6-methylguanine-DNA methyltransferase in protecting from alkylating agent-induced toxicity and mutations in mice. *Carcinogenesis* **28**:1111-1116.

Harper JW and Elledge SJ (2007) The DNA damage response: ten years after. *Mol Cell* **28**:739-745.

Hartmann W, Digon-Sontgerath B, Koch A, Waha A, Endl E, Dani I, Denkhaus D, Goodyer CG, Sorensen N, Wiestler OD and Pietsch T (2006) Phosphatidylinositol 3'-kinase/AKT signaling is activated in medulloblastoma cell proliferation and is associated with reduced expression of PTEN. *Clin Cancer Res* **12**:3019-3027.

He J, Niu X, Hu C, Zhang H, Guo Y, Ge Y, Wang G and Jiang Y (2013) Expression and purification of recombinant NRL-Hsp90alpha and Cdc37-CRL proteins for in vitro Hsp90/Cdc37 inhibitors screening. *Protein Expr Purif* **92**:119-127.

Heath EI, Gaskins M, Pitot HC, Pili R, Tan W, Marschke R, Liu G, Hillman D, Sarkar F, Sheng S, Erlichman C and Ivy P (2005) A phase II trial of 17-allylamino-17- demethoxygeldanamycin in patients with hormone-refractory metastatic prostate cancer. *Clin Prostate Cancer* **4**:138-141.

263

Heath EI, Hillman DW, Vaishampayan U, Sheng S, Sarkar F, Harper F, Gaskins M, Pitot HC, Tan W, Ivy SP, Pili R, Carducci MA, Erlichman C and Liu G (2008) A phase II trial of 17-allylamino-17-demethoxygeldanamycin in patients with hormone-refractory metastatic prostate cancer. *Clin Cancer Res* **14**:7940-7946.

Hegi ME, Diserens AC, Gorlia T, Hamou MF, de Tribolet N, Weller M, Kros JM, Hainfellner JA, Mason W, Mariani L, Bromberg JE, Hau P, Mirimanoff RO, Cairncross JG, Janzer RC and Stupp R (2005) MGMT gene silencing and benefit from temozolomide in glioblastoma. *N Engl J Med* **352**:997-1003.

Herbst RS (2004) Review of epidermal growth factor receptor biology. *Int J Radiat Oncol Biol Phys* **59**:21-26.

Hirose Y, Kreklau EL, Erickson LC, Berger MS and Pieper RO (2003) Delayed repletion of O6-methylguanine-DNA methyltransferase resulting in failure to protect the human glioblastoma cell line SF767 from temozolomide-induced cytotoxicity. *J Neurosurg* **98**:591-598.

Hu Y and Mivechi NF (2011) Promotion of heat shock factor Hsf1 degradation via adaptor protein filamin A-interacting protein 1-like (FILIP-1L). *J Biol Chem* **286**:31397-31408.

Huang M, Shen AJ, Ding J and Geng MY (2014) Molecularly targeted cancer therapy: some lessons from the past decade. *Trends Pharmacol Sci* **35**:41-50.

Ikeguchi M, Ueta T, Yamane Y, Hirooka Y and Kaibara N (2002) Inducible nitric oxide synthase and survivin messenger RNA expression in hepatocellular carcinoma. *Clin Cancer Res* **8**:3131-3136.

Jakopovic M, Thomas A and Lopez-Chavez A (2014) From platinum compounds to targeted therapies in advanced thoracic malignancies. *Anticancer Res* **34**:477-482.

Jana NR, Tanaka M, Wang G and Nukina N (2000) Polyglutamine length-dependent interaction of Hsp40 and Hsp70 family chaperones with truncated N-terminal huntingtin: their role in suppression of aggregation and cellular toxicity. *Hum Mol Genet* **9**:2009-2018.

Jayaprakasam B, Zhang YJ, Seeram NP and Nair MG (2003) Growth inhibition of human tumor cell lines by withanolides from Withania somnifera leaves. *Life Sci* **74**:125-132.

Jiang YW and Uhrbom L (2012) On the origin of glioma. *Ups J Med Sci* **117**:113-121.

Jinwal UK, Trotter JH, Abisambra JF, Koren J, Lawson LY, Vestal GD, O'Leary JC, Johnson AG, Jin Y, Jones JR, Li QY, Weeber EJ and Dickey CA (2011) The Hsp90 Kinase Co-chaperone Cdc37 Regulates Tau Stability and Phosphorylation Dynamics. *J Biol Chem* **286**:16976-16983.

Kabakov AE, Kudryavtsev VA and Gabai VL (2010) Hsp90 inhibitors as promising agents for radiotherapy. *J Mol Med (Berl)* **88**:241-247.

Kachhap SK, Vetale SP, Dange P and Ghosh SN (2001) Reduced expression of the BRCA1 gene and increased chromosomal instability in MCF-7 cell line. *Cell Biol Int* **25**:547-551.

Kaina B, Margison GP and Christmann M (2010) Targeting O(6)-methylguanine-DNA methyltransferase with specific inhibitors as a strategy in cancer therapy. *Cell Mol Life Sci* **67**:3663-3681.

Kakar SS, Jala VR and Fong MY (2012) Synergistic cytotoxic action of cisplatin and withaferin A on ovarian cancer cell lines. *Biochem Biophys Res Commun* **423**:819-825.

Kamal A and Burrows FJ (2004) Hsp90 inhibitors as selective anticancer drugs. *Discov Med* **4**:277-280.

Kamemura K, Hayes BK, Comer FI and Hart GW (2002) Dynamic interplay between O-glycosylation and O-phosphorylation of nucleocytoplasmic proteins - Alternative glycosylation/phosphorylation of Thr-58, a known mutational hot spot of c-Myc in lymphomas, is regulated by mitogens. *J Biol Chem* **277**:19229-19235.

Karnitz LM and Felts SJ (2007) Cdc37 regulation of the kinome: when to hold 'em and when to fold 'em. *Sci STKE* **2007**:pe22.

Kawahara K, Hashimoto M, Bar-On P, Ho GJ, Crews L, Mizuno H, Rockenstein E, Imam SZ and Masliah E (2008) alpha-Synuclein aggregates interfere with Parkin solubility and distribution: role in the pathogenesis of Parkinson disease. *J Biol Chem* **283**:6979-6987.

Kekatpure VD, Dannenberg AJ and Subbaramaiah K (2009) HDAC6 Modulates Hsp90 Chaperone Activity and Regulates Activation of Aryl Hydrocarbon Receptor Signaling. *J Biol Chem* **284**:7436-7445.

Khan S, Rammeloo AW and Heikkila JJ (2012) Withaferin A induces proteasome inhibition, endoplasmic reticulum stress, the heat shock response and acquisition of thermotolerance. *PLoS One* **7**:e50547.

Khatua S, Sadighi ZS, Pearlman ML, Bochare S and Vats TS (2012) Brain Tumors in Children- Current Therapies and Newer Directions. *Indian J Pediatr* **79**:922-927.

Kim W, Choy W, Dye J, Nagasawa D, Safaee M, Fong B and Yang I (2011) The tumor biology and molecular characteristics of medulloblastoma identifying prognostic factors associated with survival outcomes and prognosis. *J Clin Neurosci* **18**:886-890.

Kitange GJ, Carlson BL, Schroeder MA, Grogan PT, Lamont JD, Decker PA, Wu W, James CD and Sarkaria JN (2009) Induction of MGMT expression is associated with temozolomide resistance in glioblastoma xenografts. *Neuro Oncol* **11**:281-291.

Klucken J, Shin Y, Masliah E, Hyman BT and McLean PJ (2004) Hsp70 Reduces alpha-Synuclein Aggregation and Toxicity. *J Biol Chem* **279**:25497-25502.

Ko JC, Chen HJ, Huang YC, Tseng SC, Weng SH, Wo TY, Huang YJ, Chiu HC, Tsai MS, Chiou RYY and Lin YW (2012) HSP90 inhibition induces cytotoxicity via down-regulation of Rad51 expression and DNA repair capacity in non-small cell lung cancer cells. *Regul Toxicol Pharm* **64**:415-424.

Koduru S, Kumar R, Srinivasan S, Evers MB and Damodaran C (2010) Notch-1 inhibition by Withaferin-A: a therapeutic target against colon carcinogenesis. *Mol Cancer Ther* **9**:202-210.

Kolligs FT, Hu G, Dang CV and Fearon ER (1999) Neoplastic transformation of RK3E by mutant beta-catenin requires deregulation of Tcf/Lef transcription but not activation of c-myc expression. *Mol Cell Biol* **19**:5696-5706.

Koul D (2008) PTEN signaling pathways in glioblastoma. *Cancer Biol Ther* **7**:1321-1325.

Krakstad C and Chekenya M (2010) Survival signalling and apoptosis resistance in glioblastomas: opportunities for targeted therapeutics. *Mol Cancer* **9**.

Krejci L, Altmannova V, Spirek M and Zhao X (2012) Homologous recombination and its regulation. *Nucleic Acids Res* **40**:5795-5818.

Kreth S, Limbeck E, Hinske LC, Schutz SV, Thon N, Hoefig K, Egensperger R and Kreth FW (2013) In human glioblastomas transcript elongation by alternative polyadenylation and miRNA targeting is a potent mechanism of MGMT silencing. *Acta Neuropathol* **125**:671-681.

Lamarche BJ, Orazio NI and Weitzman MD (2010) The MRN complex in double-strand break repair and telomere maintenance. *FEBS Lett* **584**:3682-3695.

Lamphere L, Fiore F, Xu X, Brizuela L, Keezer S, Sardet C, Draetta GF and Gyuris J (1997) Interaction between Cdc37 and Cdk4 in human cells. *Oncogene* **14**:1999-2004.

Laurent A, Nicco C, Chereau C, Goulvestre C, Alexandre J, Alves A, Levy E, Goldwasser F, Panis Y, Soubrane O, Weill B and Batteux F (2005) Controlling tumor growth by modulating endogenous production of reactive oxygen species. *Cancer Res* **65**:948-956.

Lee JJ, Kim BC, Park MJ, Lee YS, Kim YN, Lee BL and Lee JS (2011) PTEN status switches cell fate between premature senescence and apoptosis in glioma exposed to ionizing radiation. *Cell Death Differ* **18**:666-677.

Levesque AA, Fanous AA, Poh A and Eastman A (2008) Defective p53 signaling in p53 wild-type tumors attenuates p21(waf1) induction and cyclin B repression rendering them sensitive to Chk1 inhibitors that abrogate DNA damage-induced S and G(2) arrest. *Mol Cancer Ther* **7**:252-262.

Lim YC, Roberts TL, Day BW, Harding A, Kozlov S, Kijas AW, Ensbey KS, Walker DG and Lavin MF (2012) A Role for Homologous Recombination and Abnormal Cell-Cycle Progression in Radioresistance of Glioma-Initiating Cells. *Mol Cancer Ther* **11**:1863-1872.

Linabery AM and Ross JA (2008) Trends in childhood cancer incidence in the U.S. (1992-2004). *Cancer* **112**:416-432.

Lino MM and Merlo A (2011) PI3Kinase signaling in glioblastoma. *J Neurooncol* **103**:417-427.

Liu KS, Ding WC, Wang SX, Liu Z, Xing GW, Wang Y and Wang YF (2012) The heat shock protein 90 inhibitor SNX-2112 inhibits B16 melanoma cell growth in vitro and in vivo. *Oncol Rep* **27**:1904-1910.

Lu D, Liu JX, Endo T, Zhou H, Yao S, Willert K, Schmidt-Wolf IG, Kipps TJ and Carson DA (2009) Ethacrynic acid exhibits selective toxicity to chronic lymphocytic leukemia cells by inhibition of the Wnt/beta-catenin pathway. *PLoS One* **4**:e8294.

Lu XY, Xiao L, Wang L and Ruden DM (2012) Hsp90 inhibitors and drug resistance in cancer: The potential benefits of combination therapies of Hsp90 inhibitors and other anti-cancer drugs. *Biochem Pharmacol* **83**:995-1004.

Luo J, Solimini NL and Elledge SJ (2009) Principles of cancer therapy: oncogene and non-oncogene addiction. *Cell* **136**:823-837.

Ma L, Sato F, Sato R, Matsubara T, Hirai K, Yamasaki M, Shin T, Shimada T, Nomura T, Mori K, Sumino Y and Mimata H (2014) Dual targeting of heat shock proteins 90 and 70 promotes cell death and enhances the anticancer effect of chemotherapeutic agents in bladder cancer. *Oncol Rep*.

MacDonald TJ, Aguilera D and Castellino RC (2014) The rationale for targeted therapies in medulloblastoma. *Neuro Oncol* **16**:9-20.

MacLean M and Picard D (2003) Cdc37 goes beyond Hsp90 and kinases. *Cell Stress Chaperones* **8**:114-119.

Malik F, Kumar A, Bhushan S, Khan S, Bhatia A, Suri KA, Qazi GN and Singh J (2007) Reactive oxygen species generation and mitochondrial dysfunction in the apoptotic cell death of human myeloid leukemia HL-60 cells by a dietary compound withaferin A with concomitant protection by N-acetyl cysteine. *Apoptosis* **12**:2115-2133.

Mandal C, Dutta A, Mallick A, Chandra S, Misra L and Sangwan RS (2008) Withaferin A induces apoptosis by activating p38 mitogen-activated protein kinase signaling cascade in leukemic cells of lymphoid and myeloid origin through mitochondrial death cascade. *Apoptosis* **13**:1450-1464.

Markman M (2013) Chemoradiation in the management of cervix cancer: current status and future directions. *Oncology* **84**:246-250.

Mayola E, Gallerne C, Esposti DD, Martel C, Pervaiz S, Larue L, Debuire B, Lemoine A, Brenner C and Lemaire C (2011) Withaferin A induces apoptosis in human melanoma cells through generation of reactive oxygen species and down-regulation of Bcl-2. *Apoptosis* **16**:1014-1027.

McCarthy N (2011) Medulloblastoma Origins. *Nature Reviews Cancer* **11**:80-80.

Mihaylova MM and Shaw RJ (2011) The AMPK signalling pathway coordinates cell growth, autophagy and metabolism. *Nat Cell Biol* **13**:1016-1023.

Minnnaugh EG, Xu WP, Vos M, Yuan XT, Isaacs JS, Bisht KS, Gius D and Neckers L (2004) Simultaneous inhibition of hsp 90 and the proteasome promotes protein ubiquitination, causes endoplasmic reticulum-derived cytosolic vacuolization, and enhances antitumor activity. *Mol Cancer Ther* **3**:551-566.

Mladenov E, Magin S, Soni A and Iliakis G (2013) DNA double-strand break repair as determinant of cellular radiosensitivity to killing and target in radiation therapy. *Front Oncol* **3**:113.

Modi S, Stopeck A, Linden H, Solit D, Chandarlapaty S, Rosen N, D'Andrea G, Dickler M, Moynahan ME, Sugarman S, Ma WN, Patil S, Norton L, Hannah AL and Hudis C (2011) HSP90 Inhibition Is Effective in Breast Cancer: A Phase II Trial of Tanespimycin (17-AAG) Plus Trastuzumab in Patients with HER2-Positive Metastatic Breast Cancer Progressing on Trastuzumab. *Clin Cancer Res* **17**:5132-5139.

Modi S, Stopeck AT, Gordon MS, Mendelson D, Solit DB, Bagatell R, Ma W, Wheler J, Rosen N, Norton L, Cropp GF, Johnson RG, Hannah AL and Hudis CA (2007) Combination of trastuzumab and tanespimycin (17-AAG, KOS-953) is safe and active in trastuzumab-refractory HER-2-overexpressing breast cancer: A phase I Dose-Escalation study. *J Clin Oncol* **25**:5410-5417.

Mohan AL, Friedman MD, Ormond DR, Tobias M, Murali R and Jhanwar-Uniyal M (2012) PI3K/mTOR signaling pathways in medulloblastoma. *Anticancer Res* **32**:3141-3146.

Mohan R, Hammers HJ, Bargagna-Mohan P, Zhan XH, Herbstritt CJ, Ruiz A, Zhang L, Hanson AD, Conner BP, Rougas J and Pribluda VS (2004) Withaferin A is a potent inhibitor of angiogenesis. *Angiogenesis* **7**:115-122.

Morishima Y, Kanelakis KC, Murphy PJM, Lowe ER, Jenkins GJ, Osawa Y, Sunahara RK and Pratt WB (2003) The Hsp90 cochaperone p23 is the limiting component of the multiprotein Hsp90/Hsp70-based chaperone system in vivo where it acts to stabilize the client protein center dot Hsp90 complex. *J Biol Chem* **278**:48754-48763.

Moulick K, Ahn JH, Zong H, Rodina A, Cerchietti L, Gomes DaGama EM, Caldas-Lopes E, Beebe K, Perna F, Hatzi K, Vu LP, Zhao X, Zatorska D, Taldone T, Smith-Jones P, Alpaugh M, Gross SS, Pillarsetty N, Ku T, Lewis JS, Larson SM, Levine R, Erdjument-Bromage H, Guzman ML, Nimer SD, Melnick A, Neckers L and Chiosis G (2011) Affinity-based proteomics reveal cancer-specific networks coordinated by Hsp90. *Nat Chem Biol* **7**:818-826.

Murphy PJ, Franklin HR and Furukawa NW (2011) Biochemical reconstitution of steroid receptor*Hsp90 protein complexes and reactivation of ligand binding. *J Vis Exp*.

Nadkarni A, Shrivastav M, Mladek AC, Schwingler PM, Grogan PT, Chen J and Sarkaria JN (2012) ATM inhibitor KU-55933 increases the TMZ responsiveness of only inherently TMZ sensitive GBM cells. *J Neurooncol* **110**:349-357.

Neckers L (2002) Hsp90 inhibitors as novel cancer chemotherapeutic agents. *Trends Mol Med* **8**:S55-S61.

Noguchi M, Yu D, Hirayama R, Ninomiya Y, Sekine E, Kubota N, Ando K and Okayasu R (2006) Inhibition of homologous recombination repair in irradiated tumor cells pretreated with Hsp90 inhibitor 17-allylamino-17-demethoxygeldanamycin. *Biochem Biophys Res Commun* **351**:658-663.

Nogueira V, Park Y, Chen CC, Xu PZ, Chen ML, Tonic I, Unterman T and Hay N (2008) Akt determines replicative senescence and oxidative or oncogenic premature senescence and sensitizes cells to oxidative apoptosis. *Cancer Cell* **14**:458-470.

Nokia MS, Anderson ML and Shors TJ (2012) Chemotherapy disrupts learning, neurogenesis and theta activity in the adult brain. *Eur J Neurosci* **36**:3521-3530.

Northcott PA, Jones DT, Kool M, Robinson GW, Gilbertson RJ, Cho YJ, Pomeroy SL, Korshunov A, Lichter P, Taylor MD and Pfister SM (2012) Medulloblastomics: the end of the beginning. *Nat Rev Cancer* **12**:818-834.

Oh JH and Kwon TK (2009) Withaferin A inhibits tumor necrosis factor-alpha-induced expression of cell adhesion molecules by inactivation of Akt and NF-kappaB in human pulmonary epithelial cells. *Int Immunopharmacol* **9**:614-619.

Oh JH, Lee TJ, Kim SH, Choi YH, Lee SH, Lee JM, Kim YH, Park JW and Kwon TK (2008) Induction of apoptosis by withaferin A in human leukemia U937 cells through down-regulation of Akt phosphorylation. *Apoptosis* **13**:1494-1504.

Okayama S, Kopelovich L, Balmus G, Weiss RS, Herbert BS, Dannenberg AJ and Subbaramaiah K (2014) p53 Regulates Hsp90 ATPase Activity and Thereby Wnt Signaling by Modulating Aha1 Expression. *J Biol Chem* **289**:6513-6525.

Okita N, Minato S, Ohmi E, Tanuma S and Higami Y (2012) DNA damage-induced CHK1 autophosphorylation at Ser296 is regulated by an intramolecular mechanism. *FEBS Lett* **586**:3974-3979.

Okunieff P, de Bie J, Dunphy EP, Terris DJ and Hockel M (1996) Oxygen distributions partly explain the radiation response of human squamous cell carcinomas. *Br J Cancer Suppl* **27**:S185-190.

Onoyama Y, Abe M, Yabumoto E, Sakamoto T and Nishidai T (1976) Radiation therapy in the treatment of glioblastoma. *AJR Am J Roentgenol* **126**:481-492.

Orr MS, Watson NC, Sundaram S, Randolph JK, Jain PT and Gewirtz DA (1997) Ionizing radiation and teniposide increase p21(waf1/cip1) and promote Rb dephosphorylation but fail to suppress E2F activity in MCF-7 breast tumor cells. *Mol Pharmacol* **52**:373-379.

Pacey S, Gore M, Chao D, Banerji U, Larkin J, Sarker S, Owen K, Asad Y, Raynaud F, Walton M, Judson I, Workman P and Eisen T (2012) A Phase II trial of 17-allylamino, 17-demethoxygeldanamycin (17-AAG, tanespimycin) in patients with metastatic melanoma. *Invest New Drugs* **30**:341-349.

Patel M, McCully C, Godwin K and Balis FM (2003) Plasma and cerebrospinal fluid pharmacokinetics of intravenous temozolomide in non-human primates. *J Neurooncol* **61**:203-207.

Payne SR, Zhang S, Tsuchiya K, Moser R, Gurley KE, Longton G, deBoer J and Kemp CJ (2008) p27kip1 deficiency impairs G2/M arrest in response to DNA damage, leading to an increase in genetic instability. *Mol Cell Biol* **28**:258-268.

Paz MF, Yaya-Tur R, Rojas-Marcos I, Reynes G, Pollan M, Aguirre-Cruz L, Garcia-Lopez JL, Piquer J, Safont MJ, Balana C, Sanchez-Cespedes M, Garcia-Villanueva M, Arribas L and Esteller M (2004) CpG island hypermethylation of the DNA repair enzyme methyltransferase predicts response to temozolomide in primary gliomas. *Clin Cancer Res* **10**:4933-4938.

Pearl LH, Prodromou C and Workman P (2008) The Hsp90 molecular chaperone: an open and shut case for treatment. *Biochem J* **410**:439-453.

Petrelli F, Coinu A, Borgonovo K, Cabiddu M, Ghilardi M, Lonati V and Barni S (2014) The value of platinum agents as neoadjuvant chemotherapy in triple-negative breast cancers: a systematic review and meta-analysis. *Breast Cancer Res Treat* **144**:223-232.

Polakis P (2012) Wnt Signaling in Cancer. *Cold Spring Harb Perspect Biol* **4**.

Potti A, Forseen SE, Koka VK, Pervez H, Koch M, Fraiman G, Mehdi SA and Levitt R (2004) Determination of HER-2/neu overexpression and clinical predictors of survival in a cohort of 347 patients with primary malignant brain tumors. *Cancer Invest* **22**:537-544.

Pouratian N, Crowley RW, Sherman JH, Jagannathan J and Sheehan JP (2009) Gamma Knife radiosurgery after radiation therapy as an adjunctive treatment for glioblastoma. *J Neurooncol* **94**:409-418.

Powers MV and Workman P (2006) Targeting of multiple signalling pathways by heat shock protein 90 molecular chaperone inhibitors. *Endocr Relat Cancer* **13**:S125-S135.

Pratt WB, Morishima Y, Peng HM and Osawa Y (2010) Proposal for a role of the Hsp90/Hsp70-based chaperone machinery in making triage decisions when proteins undergo oxidative and toxic damage. *Exp Biol Med* **235**:278-289.

Proksa B, Uhrin D and Fuska J (1986) Hydrolysis of withaferin A-4,27-diacetate. *Pharmazie* **41**:282.

Puputti M, Tynninen O, Sihto H, Blom T, Maenpaa H, Isola J, Paetau A, Joensuu H and Nupponen NN (2006) Amplification of KIT, PDGFRA, VEGFR2, and EGFR in gliomas. *Mol Cancer Res* **4**:927-934.

Qiao SX, Lamore SD, Cabello CM, Lesson JL, Munoz-Rodriguez JL and Wondrak GT (2012) Thiostrepton is an inducer of oxidative and proteotoxic stress that impairs viability of human melanoma cells but not primary melanocytes. *Biochem Pharmacol* **83**:1229-1240.

Quick A, Patel D, Hadziahmetovic M, Chakravarti A and Mehta M (2010) Current therapeutic paradigms in glioblastoma. *Rev Recent Clin Trials* **5**:14-27.

Quiros S, Roos WP and Kaina B (2011) Rad51 and BRCA2--New molecular targets for sensitizing glioma cells to alkylating anticancer drugs. *PLoS One* **6**:e27183.

Ransburgh DJR, Chiba N, Ishioka C, Toland AE and Parvin JD (2010) Identification of Breast Tumor Mutations in BRCA1 That Abolish Its Function in Homologous DNA Recombination. *Cancer Res* **70**:988-995.

Rao J, Lee P, Benzeno S, Cardozo C, Albertus J, Robins DM and Caplan AJ (2001) Functional interaction of human Cdc37 with the androgen receptor but not with the glucocorticoid receptor. *J Biol Chem* **276**:5814-5820.

Remke M, Ramaswamy V and Taylor MD (2013) Medulloblastoma molecular dissection: the way toward targeted therapy. *Curr Opin Oncol* **25**:674-681.

Richardson PG, Chanan-Khan AA, Lonial S, Krishnan AY, Carroll MP, Alsina M, Albitar M, Berman D, Messina M and Anderson KC (2011) Tanespimycin and bortezomib combination treatment in patients with relapsed or relapsed and refractory multiple myeloma: results of a phase 1/2 study. *Br J Haematol* **153**:729-740.

Robinson KE, Fraley CE, Pearson MM, Kuttesch JF and Compas BE (2012) Neurocognitive Late Effects of Pediatric Brain Tumors of the Posterior Fossa: A Quantitative Review. *J Int Neuropsychol Soc*:1-10.

Roe SM, Ali MM, Meyer P, Vaughan CK, Panaretou B, Piper PW, Prodromou C and Pearl LH (2004) The Mechanism of Hsp90 regulation by the protein kinase-specific cochaperone p50(cdc37). *Cell* **116**:87-98.

Rogakou EP, Nieves-Neira W, Boon C, Pommier Y and Bonner WM (2000) Initiation of DNA fragmentation during apoptosis induces phosphorylation of H2AX histone at serine 139. *J Biol Chem* **275**:9390-9395.

Rosazza JP, Nicholas AW and Gustafson ME (1978) Microbial transformations of natural antitumor agents. 7. 14-alpha-Hydroxylation of withaferin-A by Cunninghamella elegans (NRRL 1393). *Steroids* **31**:671-679.

Ryu CH, Yoon WS, Park KY, Kim SM, Lim JY, Woo JS, Jeong CH, Hou Y and Jeun SS (2012) Valproic acid downregulates the expression of MGMT and sensitizes temozolomide-resistant glioma cells. *J Biomed Biotechnol* **2012**:987495.

Samadi A, Loo P, Mukerji R, O'Donnell G, Tong X, Timmermann BN and Cohen MS (2009) A novel HSP90 modulator with selective activity against thyroid cancers in vitro. *Surgery* **146**:1196-1207.

Samadi AK, Mukerji R, Shah A, Timmermann BN and Cohen MS (2010a) A novel RET inhibitor with potent efficacy against medullary thyroid cancer in vivo. *Surgery* **148**:1228-1236; discussion 1236.

Samadi AK, Tong X, Mukerji R, Zhang H, Timmermann BN and Cohen MS (2010b) Withaferin A, a cytotoxic steroid from Vassobia breviflora, induces apoptosis in human head and neck squamous cell carcinoma. *J Nat Prod* **73**:1476-1481.

Samadi AK, Zhang X, Mukerji R, Donnelly AC, Blagg BS and Cohen MS (2011) A novel C-terminal HSP90 inhibitor KU135 induces apoptosis and cell cycle arrest in melanoma cells. *Cancer Lett* **312**:158-167.

Santagata S, Xu YM, Wijeratne EM, Kontnik R, Rooney C, Perley CC, Kwon H, Clardy J, Kesari S, Whitesell L, Lindquist S and Gunatilaka AA (2012) Using the heat-shock response to discover anticancer compounds that target protein homeostasis. *ACS Chem Biol* **7**:340-349.

Scaife RM (2004) G2 cell cycle arrest, down-regulation of cyclin B, and induction of mitotic catastrophe by the flavoprotein inhibitor diphenyleneiodonium. *Mol Cancer Ther* **3**:1229-1237.

Sears R, Nuckolls F, Haura E, Taya Y, Tamai K and Nevins JR (2000) Multiple Ras-dependent phosphorylation pathways regulate Myc protein stability. *Genes Dev* **14**:2501-2514.

Seki Y, Yamamoto H, Ngan CY, Yasui M, Tomita N, Kitani K, Takemasa I, Ikeda M, Sekimoto M, Matsuura N, Albanese C, Kaneda Y, Pestell RG and Monden M (2006) Construction of a novel DNA decoy that inhibits the oncogenic beta-catenin/T-cell factor pathway. *Mol Cancer Ther* **5**:985-994.

Sepp-Lorenzino L, Ma Z, Lebwohl DE, Vinitsky A and Rosen N (1995) Herbimycin A induces the 20 S proteasome- and ubiquitin-dependent degradation of receptor tyrosine kinases. *J Biol Chem* **270**:16580-16587.

Serwer LP and James CD (2012) Challenges in drug delivery to tumors of the central nervous system: an overview of pharmacological and surgical considerations. *Adv Drug Deliv Rev* **64**:590-597.

Sgambato A, Cittadini A, Faraglia B and Weinstein IB (2000) Multiple functions of p27(Kip1) and its alterations in tumor cells: a review. *J Cell Physiol* **183**:18-27.

Shah N, Kataria H, Kaul SC, Ishii T, Kaur G and Wadhwa R (2009) Effect of the alcoholic extract of Ashwagandha leaves and its components on proliferation, migration, and differentiation of glioblastoma cells: combinational approach for enhanced differentiation. *Cancer Sci* **100**:1740-1747.

Sheline GE (1977) Radiation therapy of brain tumors. *Cancer* **39**:873-881.

Shen DW, Pouliot LM, Hall MD and Gottesman MM (2012) Cisplatin Resistance: A Cellular Self-Defense Mechanism Resulting from Multiple Epigenetic and Genetic Changes. *Pharmacol Rev* **64**:706-721.

Sherr CJ and Roberts JM (1995) Inhibitors of mammalian G1 cyclin-dependent kinases. *Genes Dev* **9**:1149-1163.

Shin SY, Kim CG, Jho EH, Rho MS, Kim YS, Kim YH and Lee YH (2004) Hydrogen peroxide negatively modulates Wnt signaling through downregulation of beta-catenin. *Cancer Lett* **212**:225-231.

Sidera K and Patsavoudi E (2014) HSP90 Inhibitors: Current Development and Potential in Cancer Therapy. *Recent Pat Anticancer Drug Discov* **9**:1-20.

Siligardi G, Panaretou B, Meyer P, Singh S, Woolfson DN, Piper PW, Pearl LH and Prodromou C (2002) Regulation of Hsp90 ATPase activity by the co-chaperone Cdc37p/p50cdc37. *J Biol Chem* **277**:20151-20159.

Singh D, Aggarwal A, Maurya R and Naik S (2007) Withania somnifera inhibits NF-kappaB and AP-1 transcription factors in human peripheral blood and synovial fluid mononuclear cells. *Phytother Res* **21**:905-913.

Smith JR, de Billy E, Hobbs S, Powers M, Prodromou C, Pearl L, Clarke PA and Workman P (2013) Restricting direct interaction of CDC37 with HSP90 does not compromise chaperoning of client proteins. *Oncogene* **{Epub ahead of print}**.

Smoll NR (2012) Relative survival of childhood and adult medulloblastomas and primitive neuroectodermal tumors (PNETs). *Cancer* **118**:1313-1322.

Solier S, Kohn KW, Scroggins B, Xu W, Trepel J, Neckers L and Pommier Y (2012) Heat shock protein 90alpha (HSP90alpha), a substrate and chaperone of DNA-PK necessary for the apoptotic response. *Proc Natl Acad Sci U S A* **109**:12866-12872.

Solit DB, Osman I, Polsky D, Panageas KS, Daud A, Goydos JS, Teitcher J, Wolchok JD, Germino FJ, Krown SE, Coit D, Rosen N and Chapman PB (2008) Phase II trial of 17-allylamino-17-demethoxygeldanamycin in patients with metastatic melanoma. *Clin Cancer Res* **14**:8302-8307.

Stadtman ER (1986) Oxidation of Proteins by Mixed-Function Oxidation Systems - Implication in Protein-Turnover, Aging and Neutrophil Function. *Trends Biochem Sci* **11**:11-12.

Stan SD, Zeng Y and Singh SV (2008) Ayurvedic medicine constituent withaferin a causes G2 and M phase cell cycle arrest in human breast cancer cells. *Nutr Cancer* **60 Suppl 1**:51-60.

Stebbing J, Copson E and O'Reilly S (2000) Herceptin (trastuzamab) in advanced breast cancer. *Cancer Treat Rev* **26**:287-290.

Stecklein SR, Kumaraswamy E, Behbod F, Wang W, Chaguturu V, Harlan-Williams LM and Jensen RA (2012) BRCA1 and HSP90 cooperate in homologous and non-homologous DNA double-strand-break repair and G2/M checkpoint activation. *Proc Natl Acad Sci U S A* **109**:13650-13655.

Stordal B and Davey M (2007) Understanding cisplatin resistance using cellular models. *IUBMB Life* **59**:696-699.

Strik HM, Marosi C, Kaina B and Neyns B (2012) Temozolomide dosing regimens for glioma patients. *Curr Neurol Neurosci Rep* **12**:286-293.

Stupp R, Dietrich PY, Ostermann Kraljevic S, Pica A, Maillard I, Maeder P, Meuli R, Janzer R, Pizzolato G, Miralbell R, Porchet F, Regli L, de Tribolet N, Mirimanoff RO and Leyvraz S (2002) Promising survival for patients with newly diagnosed glioblastoma multiforme treated with concomitant radiation plus temozolomide followed by adjuvant temozolomide. *J Clin Oncol* **20**:1375-1382.

Stupp R, Hegi ME, Mason WP, van den Bent MJ, Taphoorn MJ, Janzer RC, Ludwin SK, Allgeier A, Fisher B, Belanger K, Hau P, Brandes AA, Gijtenbeek J, Marosi C, Vecht CJ, Mokhtari K, Wesseling P, Villa S, Eisenhauer E, Gorlia T, Weller M, Lacombe D, Cairncross JG, Mirimanoff RO, European Organisation for R, Treatment of Cancer Brain T, Radiation Oncology G and National Cancer Institute of Canada Clinical Trials G (2009) Effects of radiotherapy with concomitant and adjuvant temozolomide versus radiotherapy alone on survival in glioblastoma in a randomised phase III study: 5-year analysis of the EORTC-NCIC trial. *Lancet Oncol* **10**:459-466.

Stupp R, Mason WP, van den Bent MJ, Weller M, Fisher B, Taphoorn MJ, Belanger K, Brandes AA, Marosi C, Bogdahn U, Curschmann J, Janzer RC, Ludwin SK, Gorlia T, Allgeier A, Lacombe D, Cairncross JG, Eisenhauer E, Mirimanoff RO, European Organisation for R, Treatment of Cancer Brain T, Radiotherapy G and National Cancer Institute of Canada Clinical Trials G (2005) Radiotherapy plus concomitant and adjuvant temozolomide for glioblastoma. *N Engl J Med* **352**:987-996.

Sugimoto K, Toyoshima H, Sakai R, Miyagawa K, Hagiwara K, Ishikawa F, Takaku F, Yazaki Y and Hirai H (1992) Frequent mutations in the p53 gene in human myeloid leukemia cell lines. *Blood* **79**:2378-2383.

Sun H and Scott DO (2010) Structure-based drug metabolism predictions for drug design. *Chem Biol Drug Des* **75**:3-17.

Sundberg TB, Ney GM, Subramanian C, Opipari AW and Glick GD (2006) The immunomodulatory benzodiazepine Bz-423 inhibits B-cell proliferation by targeting c-Myc protein for rapid and specific degradation. *Cancer Res* **66**:1775-1782.

Sztajnkrycer MD (2002) Valproic acid toxicity: Overview and management. *J Toxicol Clin Toxicol* **40**:789-801.

Taipale M, Jarosz DF and Lindquist S (2010) HSP90 at the hub of protein homeostasis: emerging mechanistic insights. *Nat Rev Mol Cell Bio* **11**:515-528.

Taphoorn MJ, Stupp R, Coens C, Osoba D, Kortmann R, van den Bent MJ, Mason W, Mirimanoff RO, Baumert BG, Eisenhauer E, Forsyth P, Bottomley A, European Organisation for R, Treatment of Cancer Brain Tumour G, Group ER and National Cancer Institute of Canada Clinical Trials G (2005) Health-related quality of life in patients with glioblastoma: a randomised controlled trial. *Lancet Oncol* **6**:937-944.

Taylor MD, Northcott PA, Korshunov A, Remke M, Cho YJ, Clifford SC, Eberhart CG, Parsons DW, Rutkowski S, Gajjar A, Ellison DW, Lichter P, Gilbertson RJ, Pomeroy SL, Kool M and Pfister SM (2012) Molecular subgroups of medulloblastoma: the current consensus. *Acta Neuropathol* **123**:465-472.

Teicher BA (1995) Physiologic mechanisms of therapeutic resistance. Blood flow and hypoxia. *Hematol Oncol Clin North Am* **9**:475-506.

Tew KD and Townsend DM (2011) Redox platforms in cancer drug discovery and development. *Curr Opin Chem Biol* **15**:156-161.

Thaiparambil JT, Bender L, Ganesh T, Kline E, Patel P, Liu Y, Tighiouart M, Vertino PM, Harvey RD, Garcia A and Marcus AI (2011) Withaferin A inhibits breast cancer invasion and metastasis at sub-cytotoxic doses by inducing vimentin disassembly and serine 56 phosphorylation. *Int J Cancer* **129**:2744-2755.

Vaishnavi K, Saxena N, Shah N, Singh R, Manjunath K, Uthayakumar M, Kanaujia SP, Kaul SC, Sekar K and Wadhwa R (2012) Differential activities of the two closely related withanolides, Withaferin A and Withanone: bioinformatics and experimental evidences. *PLoS One* **7**:e44419.

271

Vanden Berghe W, Sabbe L, Kaileh M, Haegeman G and Heyninck K (2012) Molecular insight in the multifunctional activities of Withaferin A. *Biochem Pharmacol* **84**:1282-1291.

Voronkov A and Krauss S (2013) Wnt/beta-Catenin Signaling and Small Molecule Inhibitors. *Curr Pharm Des* **19**:634-664.

Vyas AR and Singh SV (2014) Molecular targets and mechanisms of cancer prevention and treatment by withaferin a, a naturally occurring steroidal lactone. *AAPS J* **16**:1-10.

Waaler J, Machon O, Tumova L, Dinh H, Korinek V, Wilson SR, Paulsen JE, Pedersen NM, Eide TJ, Machonova O, Gradl D, Voronkov A, von Kries JP and Krauss S (2012) A Novel Tankyrase Inhibitor Decreases Canonical Wnt Signaling in Colon Carcinoma Cells and Reduces Tumor Growth in Conditional APC Mutant Mice. *Cancer Res* **72**:2822-2832.

Wachters FM, van Putten JW, Maring JG, Zdzienicka MZ, Groen HJ and Kampinga HH (2003) Selective targeting of homologous DNA recombination repair by gemcitabine. *Int J Radiat Oncol Biol Phys* **57**:553-562.

Wang HC, Tsai YL, Wu YC, Chang FR, Liu MH, Chen WY and Wu CC (2012) Withanolides-Induced Breast Cancer Cell Death Is Correlated with Their Ability to Inhibit Heat Protein 90. *PLoS One* **7**.

Warburton HE, Brady M, Vlatkovic N, Linehan WM, Parsons K and Boyd MT (2005) p53 regulation and function in renal cell carcinoma. *Cancer Res* **65**:6498-6503.

Welch WJ and Feramisco JR (1982) Purification of the major mammalian heat shock proteins. *J Biol Chem* **257**:14949-14959.

Weller M, Gorlia T, Cairncross JG, van den Bent MJ, Mason W, Belanger K, Brandes AA, Bogdahn U, Macdonald DR, Forsyth P, Rossetti AO, Lacombe D, Mirimanoff RO, Vecht CJ and Stupp R (2011) Prolonged survival with valproic acid use in the EORTC/NCIC temozolomide trial for glioblastoma. *Neurology* **77**:1156-1164.

Wen PY and Kesari S (2008) Malignant gliomas in adults. *N Engl J Med* **359**:492-507.

Wensing KU and Ciarimboli G (2013) Saving Ears and Kidneys from Cisplatin. *Anticancer Res* **33**:4183-4188.

Westphal M, Hilt DC, Bortey E, Delavault P, Olivares R, Warnke PC, Whittle IR, Jaaskelainen J and Ram Z (2003) A phase 3 trial of local chemotherapy with biodegradable carmustine (BCNU) wafers (Gliadel wafers) in patients with primary malignant glioma. *Neuro Oncol* **5**:79-88.

Weterings E and Chen DJ (2008) The endless tale of non-homologous end-joining. *Cell Res* **18**:114-124.

Wheeler DL, Dunn EF and Harari PM (2010) Understanding resistance to EGFR inhibitors-impact on future treatment strategies. *Nat Rev Clin Oncol* **7**:493-507.

Whitesell L, Mimnaugh EG, De Costa B, Myers CE and Neckers LM (1994) Inhibition of heat shock protein HSP90-pp60v-src heteroprotein complex formation by benzoquinone ansamycins: essential role for stress proteins in oncogenic transformation. *Proc Natl Acad Sci U S A* **91**:8324-8328.

Widodo N, Priyandoko D, Shah N, Wadhwa R and Kaul SC (2010) Selective Killing of Cancer Cells by Ashwagandha Leaf Extract and Its Component Withanone Involves ROS Signaling. *PLoS One* **5**.

Wijeratne EM, Xu YM, Scherz-Shouval R, Marron MT, Rocha DD, Liu MX, Costa-Lotufo LV, Santagata S, Lindquist S, Whitesell L and Gunatilaka AA (2014) Structure-Activity Relationships for Withanolides as Inducers of the Cellular Heat-Shock Response. *J Med Chem* **[Epub ahead of print]**.

Wondrak GT (2009) Redox-directed cancer therapeutics: molecular mechanisms and opportunities. *Antioxid Redox Signal* **11**:3013-3069.

Wong AL and Lee SC (2012) Mechanisms of Resistance to Trastuzumab and Novel Therapeutic Strategies in HER2-Positive Breast Cancer. *Int J Breast Cancer* **2012**:415170.

Workman P (2003) Auditing the pharmacological accounts for Hsp90 molecular chaperone inhibitors: unfolding the relationship between pharmacokinetics and pharmacodynamics. *Mol Cancer Ther* **2**:131-138.

Workman P, Burrows F, Neckers L and Rosen N (2007) Drugging the cancer chaperone HSP90: combinatorial therapeutic exploitation of oncogene addiction and tumor stress. *Ann N Y Acad Sci* **1113**:202-216.

Wu J, Chien CC, Yang LY, Huang GC, Cheng MC, Lin CT, Shen SC and Chen YC (2011) Vitamin K3-2,3-epoxide induction of apoptosis with activation of ROS-dependent ERK and JNK protein phosphorylation in human glioma cells. *Chem Biol Interact* **193**:3-11.

Wu W, Zhu HY, Fu Y, Xu JD, Shen WY, Xu W, Liu P and Li JY (2012) High Expression of Lymphoid Enhancer-Binding Factor 1 (LEF1) Is Related to Ummutated Status of Igvh and Is an Unfavorable Prognostic Marker for Aggressive CLL Patients. *Blood* **120**.

Wullich B, Muller HW, Fischer U, Zang KD and Meese E (1993) Amplified met gene linked to double minutes in human glioblastoma. *Eur J Cancer* **29A**:1991-1995.

Xie SM, Fang M, Guo H and Zhong XY (2011) Silencing of MGMT with small interference RNA reversed resistance in human BCUN-resistant glioma cell lines. *Chin Med J (Engl)* **124**:2605-2610.

Xu W, Trepel J and Neckers L (2011) Ras, ROS and proteotoxic stress: a delicate balance. *Cancer Cell* **20**:281-282.

Yang ES, Choi MJ, Kim JH, Choi KS and Kwon TK (2011a) Combination of withaferin A and X-ray irradiation enhances apoptosis in U937 cells. *Toxicol In Vitro* **25**:1803-1810.

Yang ES, Choi MJ, Kim JH, Choi KS and Kwon TK (2011b) Withaferin A enhances radiation-induced apoptosis in Caki cells through induction of reactive oxygen species, Bcl-2 downregulation and Akt inhibition. *Chem Biol Interact* **190**:9-15.

Yang H, Shi G and Dou QP (2007) The tumor proteasome is a primary target for the natural anticancer compound Withaferin A isolated from "Indian winter cherry". *Mol Pharmacol* **71**:426-437.

Yang H, Wang Y, Cheryan VT, Wu W, Cui CQ, Polin LA, Pass HI, Dou QP, Rishi AK and Wali A (2012) Withaferin a inhibits the proteasome activity in mesothelioma in vitro and in vivo. *PLoS One* **7**:e41214.

Young JC, Obermann WM and Hartl FU (1998) Specific binding of tetratricopeptide repeat proteins to the C-terminal 12-kDa domain of hsp90. *J Biol Chem* **273**:18007-18010.

Yu Y, Hamza A, Zhang T, Gu M, Zou P, Newman B, Li Y, Gunatilaka AA, Zhan CG and Sun D (2010) Withaferin A targets heat shock protein 90 in pancreatic cancer cells. *Biochem Pharmacol* **79**:542-551.

Yun BG, Huang W, Leach N, Hartson SD and Matts RL (2004) Novobiocin induces a distinct conformation of Hsp90 and alters Hsp90-cochaperone-client interactions. *Biochemistry* **43**:8217-8229.

Zhang G, Huang S and Wang Z (2012a) A meta-analysis of bevacizumab alone and in combination with irinotecan in the treatment of patients with recurrent glioblastoma multiforme. *J Clin Neurosci* **19**:1636-1640.

Zhang H, Bazzill J, Gallagher RJ, Subramanian C, Grogan PT, Day VW, Kindscher K, Cohen MS and Timmermann BN (2013) Antiproliferative withanolides from Datura wrightii. *J Nat Prod* **76**:445-449.

Zhang H and Burrows F (2004) Targeting multiple signal transduction pathways through inhibition of Hsp90. *J Mol Med (Berl)* **82**:488-499.

Zhang H, Chung D, Yang YC, Neely L, Tsurumoto S, Fan J, Zhang L, Biamonte M, Brekken J, Lundgren K and Burrows F (2006) Identification of new biomarkers for clinical trials of Hsp90 inhibitors. *Mol Cancer Ther* **5**:1256-1264.

Zhang H, Samadi AK, Cohen MS and Timmermann BN (2012b) Anti-proliferative withanolides from the Solanaceae: a structure-activity study. *Pure Appl Chem* **84**:1353-1367.

Zhang H, Samadi AK, Gallagher RJ, Araya JJ, Tong X, Day VW, Cohen MS, Kindscher K, Gollapudi R and Timmermann BN (2011a) Cytotoxic withanolide constituents of Physalis longifolia. *J Nat Prod* **74**:2532-2544.

Zhang J, Stevens MF and Bradshaw TD (2012c) Temozolomide: mechanisms of action, repair and resistance. *Curr Mol Pharmacol* **5**:102-114.

Zhang RD, Price JE, Fujimaki T, Bucana CD and Fidler IJ (1992) Differential permeability of the blood-brain barrier in experimental brain metastases produced by human neoplasms implanted into nude mice. *Am J Pathol* **141**:1115-1124.

Zhang T, Hamza A, Cao X, Wang B, Yu S, Zhan CG and Sun D (2008) A novel Hsp90 inhibitor to disrupt Hsp90/Cdc37 complex against pancreatic cancer cells. *Mol Cancer Ther* **7**:162-170.

Zhang T, Li Y, Yu Y, Zou P, Jiang Y and Sun D (2009) Characterization of celastrol to inhibit hsp90 and cdc37 interaction. *J Biol Chem* **284**:35381-35389.

Zhang WB, Wang Z, Shu F, Jin YH, Liu HY, Wang QJ and Yang Y (2010) Activation of AMP-activated protein kinase by temozolomide contributes to apoptosis in glioblastoma cells via p53 activation and mTORC1 inhibition. *J Biol Chem* **285**:40461-40471.

Zhang X, Mukerji R, Samadi AK and Cohen MS (2011b) Down-regulation of estrogen receptor-alpha and rearranged during transfection tyrosine kinase is associated with withaferin a-induced apoptosis in MCF-7 breast cancer cells. *BMC Complement Altern Med* **11**:84.

Zheng M, Bocangel D, Ramesh R, Ekmekcioglu S, Poindexter N, Grimm EA and Chada S (2008) Interleukin-24 overcomes temozolomide resistance and enhances cell death by down-regulation of O6-methylguanine-DNA methyltransferase in human melanoma cells. *Mol Cancer Ther* **7**:3842-3851.

Appendix I: List of Publications during Graduate Training

(In chronological order; June 2009-May 2014)

Carlson BL, **Grogan PT**, Mladek AC, Schroeder MA, Kitange GJ, Decker PA, Giannini C, Wu W, Ballman KA, James CD and Sarkaria JN (2009) Radiosensitizing effects of temozolomide observed in vivo only in a subset of O6-methylguanine-DNA methyltransferase methylated glioblastoma multiforme xenografts. *Int J Radiat Oncol Biol Phys* **75**:212-219.

Pluhar GE, **Grogan PT**, Seiler C, Goulart M, Santacruz KS, Carlson C, Chen W, Olin MR, Lowenstein PR, Castro MG, Haines SJ and Ohlfest JR (2010) Anti-tumor immune response correlates with neurological symptoms in a dog with spontaneous astrocytoma treated by gene and vaccine therapy. *Vaccine* **28**:3371-3378.

Staley J, **Grogan P**, Samadi AK, Cui H, Cohen MS and Yang X (2010) Growth of melanoma brain tumors monitored by photoacoustic microscopy. *J Biomed Opt* **15**:040510.

Olin MR, Andersen BM, Zellmer DM, **Grogan PT**, Popescu FE, Xiong Z, Forster CL, Seiler C, SantaCruz KS, Chen W, Blazar BR and Ohlfest JR (2010) Superior efficacy of tumor cell vaccines grown in physiologic oxygen. *Clin Cancer Res* **16**:4800-4808.

Olin MR, Andersen BM, Litterman AJ, **Grogan PT**, Sarver AL, Robertson PT, Liang X, Chen W, Parney IF, Hunt MA, Blazar BR and Ohlfest JR (2011) Oxygen is a master regulator of the immunogenicity of primary human glioma cells. *Cancer Res* **71**:6583-6589.

Nadkarni A, Shrivastav M, Mladek AC, Schwingler PM, **Grogan PT**, Chen J and Sarkaria JN (2012) ATM inhibitor KU-55933 increases the TMZ responsiveness of only inherently TMZ sensitive GBM cells. *J Neurooncol* **110**:349-357.

Grogan PT, Sleder KD, Samadi AK, Zhang H, Timmermann BN and Cohen MS (2013) Cytotoxicity of withaferin A in glioblastomas involves induction of an oxidative stress-mediated heat shock response while altering Akt/mTOR and MAPK signaling pathways. *Invest New Drugs* **31**:545-557.

Zhang H, Bazzill J, Gallagher RJ, Subramanian C, **Grogan PT**, Day VW, Kindscher K, Cohen MS and Timmermann BN (2013) Antiproliferative withanolides from Datura wrightii. *J Nat Prod* **76**:445-449.

Cen L, Carlson BL, Pokorny JL, Mladek AC, **Grogan PT**, Schroeder MA, Decker PA, Anderson SK, Giannini C, Wu W, Ballman KV, Kitange GJ and Sarkaria JN (2013) Efficacy of protracted temozolomide dosing is limited in MGMT unmethylated GBM xenograft models. *Neuro Oncol* **15**:735-746.

Cao CM, Zhang H, Gallagher RJ, Day VW, Kindscher K, **Grogan P**, Cohen MS and Timmermann BN (2014) Withanolides from Physalis hispida. *J Nat Prod* [Epub ahead of print].

Grogan PT, Sarkaria JN, Timmermann BN and Cohen MS (2014) Oxidative cytotoxic agent withaferin A resensitizes temozolomide-resistant glioblastomas via MGMT depletion and

induces apoptosis through Akt/mTOR pathway inhibitory modulation. *Invest New Drugs* [Epub ahead of print].

Appendix II: License agreements for published papers and copyrighted materials

**SPRINGER LICENSE
TERMS AND CONDITIONS**

Apr 28, 2014

This is a License Agreement between Patrick Grogan ("You") and Springer ("Springer") provided by Copyright Clearance Center ("CCC"). The license consists of your order details, the terms and conditions provided by Springer, and the payment terms and conditions.

All payments must be made in full to CCC. For payment instructions, please see information listed at the bottom of this form.

License Number	3377640530802
License date	Apr 28, 2014
Licensed content publisher	Springer
Licensed content publication	Investigational New Drugs
Licensed content title	Cytotoxicity of withaferin A in glioblastomas involves induction of an oxidative stress-mediated heat shock response while altering Akt/mTOR and MAPK signaling pathways
Licensed content author	Patrick T. Grogan
Licensed content date	Jan 1, 2012
Volume number	31
Issue number	3
Type of Use	Thesis/Dissertation
Portion	Full text
Number of copies	1
Author of this Springer article	Yes and you are a contributor of the new work
Order reference number	None
Title of your thesis / dissertation	Withaferin A: a novel therapeutic approach for malignant brain tumors
Expected completion date	May 2014
Estimated size(pages)	200
Total	0.00 USD
Terms and Conditions	

Introduction

The publisher for this copyrighted material is Springer Science + Business Media. By clicking "accept" in connection with completing this licensing transaction, you agree that the following terms and conditions apply to this transaction (along with the Billing and Payment terms and conditions established by Copyright Clearance Center, Inc. ("CCC"), at the time that you opened your Rightslink account and that are available at any time at http://myaccount.copyright.com).

Limited License

With reference to your request to reprint in your thesis material on which Springer Science and Business Media control the copyright, permission is granted, free of charge, for the use indicated in your enquiry.

Licenses are for one-time use only with a maximum distribution equal to the number that you identified in the licensing process.

This License includes use in an electronic form, provided its password protected or on the university's intranet or repository, including UMI (according to the definition at the Sherpa website: http://www.sherpa.ac.uk/romeo/). For any other electronic use, please contact Springer at (permissions.dordrecht@springer.com or permissions.heidelberg@springer.com).

The material can only be used for the purpose of defending your thesis limited to university-use only. If the thesis is going to be published, permission needs to be re-obtained (selecting "book/textbook" as the type of use).

Although Springer holds copyright to the material and is entitled to negotiate on rights, this license is only valid, subject to a courtesy information to the author (address is given with the article/chapter) and provided it concerns original material which does not carry references to other sources (if material in question appears with credit to another source, authorization from that source is required as well).

Permission free of charge on this occasion does not prejudice any rights we might have to charge for reproduction of our copyrighted material in the future.

Altering/Modifying Material: Not Permitted

You may not alter or modify the material in any manner. Abbreviations, additions, deletions and/or any other alterations shall be made only with prior written authorization of the author(s) and/or Springer Science + Business Media. (Please contact Springer at (permissions.dordrecht@springer.com or permissions.heidelberg@springer.com)

Reservation of Rights

Springer Science + Business Media reserves all rights not specifically granted in the combination of (i) the license details provided by you and accepted in the course of this licensing transaction, (ii) these terms and conditions and (iii) CCC's Billing and Payment terms and conditions.

Copyright Notice:Disclaimer

You must include the following copyright and permission notice in connection with any reproduction of the licensed material: "Springer and the original publisher /journal title, volume, year of publication, page, chapter/article title, name(s) of author(s), figure number(s), original copyright notice) is given to the publication in which the material was originally published, by adding; with kind permission from Springer Science and Business Media"

Warranties: None

Example 1: Springer Science + Business Media makes no representations or warranties with

279

respect to the licensed material.

Example 2: Springer Science + Business Media makes no representations or warranties with respect to the licensed material and adopts on its own behalf the limitations and disclaimers established by CCC on its behalf in its Billing and Payment terms and conditions for this licensing transaction.

Indemnity
You hereby indemnify and agree to hold harmless Springer Science + Business Media and CCC, and their respective officers, directors, employees and agents, from and against any and all claims arising out of your use of the licensed material other than as specifically authorized pursuant to this license.

No Transfer of License
This license is personal to you and may not be sublicensed, assigned, or transferred by you to any other person without Springer Science + Business Media's written permission.

No Amendment Except in Writing
This license may not be amended except in a writing signed by both parties (or, in the case of Springer Science + Business Media, by CCC on Springer Science + Business Media's behalf).

Objection to Contrary Terms
Springer Science + Business Media hereby objects to any terms contained in any purchase order, acknowledgment, check endorsement or other writing prepared by you, which terms are inconsistent with these terms and conditions or CCC's Billing and Payment terms and conditions. These terms and conditions, together with CCC's Billing and Payment terms and conditions (which are incorporated herein), comprise the entire agreement between you and Springer Science + Business Media (and CCC) concerning this licensing transaction. In the event of any conflict between your obligations established by these terms and conditions and those established by CCC's Billing and Payment terms and conditions, these terms and conditions shall control.

Jurisdiction
All disputes that may arise in connection with this present License, or the breach thereof, shall be settled exclusively by arbitration, to be held in The Netherlands, in accordance with Dutch law, and to be conducted under the Rules of the 'Netherlands Arbitrage Instituut' (Netherlands Institute of Arbitration).*OR:*

All disputes that may arise in connection with this present License, or the breach thereof, shall be settled exclusively by arbitration, to be held in the Federal Republic of Germany, in accordance with German law.

Other terms and conditions:

v1.3

If you would like to pay for this license now, please remit this license along with your payment made payable to "COPYRIGHT CLEARANCE CENTER" otherwise you will be

invoiced within 48 hours of the license date. Payment should be in the form of a check or money order referencing your account number and this invoice number 501288935. Once you receive your invoice for this order, you may pay your invoice by credit card. Please follow instructions provided at that time.

Make Payment To:
Copyright Clearance Center
Dept 001
P.O. Box 843006
Boston, MA 02284-3006

For suggestions or comments regarding this order, contact RightsLink Customer Support: customercare@copyright.com or +1-877-622-5543 (toll free in the US) or +1-978-646-2777.

Gratis licenses (referencing $0 in the Total field) are free. Please retain this printable license for your reference. No payment is required.

SPRINGER LICENSE
TERMS AND CONDITIONS

Apr 28, 2014

This is a License Agreement between Patrick Grogan ("You") and Springer ("Springer") provided by Copyright Clearance Center ("CCC"). The license consists of your order details, the terms and conditions provided by Springer, and the payment terms and conditions.

All payments must be made in full to CCC. For payment instructions, please see information listed at the bottom of this form.

License Number	3377640798848
License date	Apr 28, 2014
Licensed content publisher	Springer
Licensed content publication	Investigational New Drugs
Licensed content title	Oxidative cytotoxic agent withaferin A resensitizes temozolomide-resistant glioblastomas via MGMT depletion and induces apoptosis through Akt/mTOR pathway inhibitory modulation
Licensed content author	Patrick T. Grogan
Licensed content date	Jan 1, 2014
Type of Use	Thesis/Dissertation
Portion	Full text
Number of copies	1
Author of this Springer article	Yes and you are a contributor of the new work
Order reference number	None
Title of your thesis / dissertation	Withaferin A: a novel therapeutic approach for malignant brain tumors
Expected completion date	May 2014
Estimated size(pages)	200
Total	0.00 USD

Terms and Conditions

Introduction

The publisher for this copyrighted material is Springer Science + Business Media. By clicking "accept" in connection with completing this licensing transaction, you agree that the following terms and conditions apply to this transaction (along with the Billing and Payment terms and conditions established by Copyright Clearance Center, Inc. ("CCC"), at the time that you opened your Rightslink account and that are available at any time at http://myaccount.copyright.com).

Limited License

282

With reference to your request to reprint in your thesis material on which Springer Science and Business Media control the copyright, permission is granted, free of charge, for the use indicated in your enquiry.

Licenses are for one-time use only with a maximum distribution equal to the number that you identified in the licensing process.

This License includes use in an electronic form, provided its password protected or on the university's intranet or repository, including UMI (according to the definition at the Sherpa website: http://www.sherpa.ac.uk/romeo/). For any other electronic use, please contact Springer at (permissions.dordrecht@springer.com or permissions.heidelberg@springer.com).

The material can only be used for the purpose of defending your thesis limited to university-use only. If the thesis is going to be published, permission needs to be re-obtained (selecting "book/textbook" as the type of use).

Although Springer holds copyright to the material and is entitled to negotiate on rights, this license is only valid, subject to a courtesy information to the author (address is given with the article/chapter) and provided it concerns original material which does not carry references to other sources (if material in question appears with credit to another source, authorization from that source is required as well).

Permission free of charge on this occasion does not prejudice any rights we might have to charge for reproduction of our copyrighted material in the future.

Altering/Modifying Material: Not Permitted
You may not alter or modify the material in any manner. Abbreviations, additions, deletions and/or any other alterations shall be made only with prior written authorization of the author(s) and/or Springer Science + Business Media. (Please contact Springer at (permissions.dordrecht@springer.com or permissions.heidelberg@springer.com)

Reservation of Rights
Springer Science + Business Media reserves all rights not specifically granted in the combination of (i) the license details provided by you and accepted in the course of this licensing transaction, (ii) these terms and conditions and (iii) CCC's Billing and Payment terms and conditions.

Copyright Notice:Disclaimer
You must include the following copyright and permission notice in connection with any reproduction of the licensed material: "Springer and the original publisher /journal title, volume, year of publication, page, chapter/article title, name(s) of author(s), figure number(s), original copyright notice) is given to the publication in which the material was originally published, by adding; with kind permission from Springer Science and Business Media"

Warranties: None

Example 1: Springer Science + Business Media makes no representations or warranties with respect to the licensed material.

283

Example 2: Springer Science + Business Media makes no representations or warranties with respect to the licensed material and adopts on its own behalf the limitations and disclaimers established by CCC on its behalf in its Billing and Payment terms and conditions for this licensing transaction.

Indemnity
You hereby indemnify and agree to hold harmless Springer Science + Business Media and CCC, and their respective officers, directors, employees and agents, from and against any and all claims arising out of your use of the licensed material other than as specifically authorized pursuant to this license.

No Transfer of License
This license is personal to you and may not be sublicensed, assigned, or transferred by you to any other person without Springer Science + Business Media's written permission.

No Amendment Except in Writing
This license may not be amended except in a writing signed by both parties (or, in the case of Springer Science + Business Media, by CCC on Springer Science + Business Media's behalf).

Objection to Contrary Terms
Springer Science + Business Media hereby objects to any terms contained in any purchase order, acknowledgment, check endorsement or other writing prepared by you, which terms are inconsistent with these terms and conditions or CCC's Billing and Payment terms and conditions. These terms and conditions, together with CCC's Billing and Payment terms and conditions (which are incorporated herein), comprise the entire agreement between you and Springer Science + Business Media (and CCC) concerning this licensing transaction. In the event of any conflict between your obligations established by these terms and conditions and those established by CCC's Billing and Payment terms and conditions, these terms and conditions shall control.

Jurisdiction
All disputes that may arise in connection with this present License, or the breach thereof, shall be settled exclusively by arbitration, to be held in The Netherlands, in accordance with Dutch law, and to be conducted under the Rules of the 'Netherlands Arbitrage Instituut' (Netherlands Institute of Arbitration).*OR:*

All disputes that may arise in connection with this present License, or the breach thereof, shall be settled exclusively by arbitration, to be held in the Federal Republic of Germany, in accordance with German law.

Other terms and conditions:

v1.3

If you would like to pay for this license now, please remit this license along with your payment made payable to "COPYRIGHT CLEARANCE CENTER" otherwise you will be invoiced within 48 hours of the license date. Payment should be in the form of a check or money order referencing your account number and this invoice number 501288940. Once you receive your invoice for this order, you may pay your invoice by credit card. Please follow instructions provided at that time.

284

Make Payment To:
Copyright Clearance Center
Dept 001
P.O. Box 843006
Boston, MA 02284-3006

For suggestions or comments regarding this order, contact RightsLink Customer Support: customercare@copyright.com or +1-877-622-5543 (toll free in the US) or +1-978-646-2777.

Gratis licenses (referencing $0 in the Total field) are free. Please retain this printable license for your reference. No payment is required.

**NATURE PUBLISHING GROUP LICENSE
TERMS AND CONDITIONS**

May 02, 2014

This is a License Agreement between Patrick Grogan ("You") and Nature Publishing Group ("Nature Publishing Group") provided by Copyright Clearance Center ("CCC"). The license consists of your order details, the terms and conditions provided by Nature Publishing Group, and the payment terms and conditions.

All payments must be made in full to CCC. For payment instructions, please see information listed at the bottom of this form.

License Number	3380891014826
License date	May 02, 2014
Licensed content publisher	Nature Publishing Group
Licensed content publication	Nature Reviews Molecular Cell Biology
Licensed content title	Coordinating ERK/MAPK signalling through scaffolds and inhibitors
Licensed content author	Walter Kolch
Licensed content date	Nov 1, 2005
Volume number	6
Issue number	11
Type of Use	reuse in a dissertation / thesis
Requestor type	academic/educational
Format	print and electronic
Portion	figures/tables/illustrations
Number of figures/tables/illustrations	2
High-res required	no
Figures	Box 1 and Figure 2
Author of this NPG article	no
Your reference number	None
Title of your thesis / dissertation	Withaferin A: a novel therapeutic approach for malignant brain tumors
Expected completion date	May 2014
Estimated size (number of pages)	200
Total	0.00 USD
Terms and Conditions	

Terms and Conditions for Permissions

286

Nature Publishing Group hereby grants you a non-exclusive license to reproduce this material for this purpose, and for no other use, subject to the conditions below:

1. NPG warrants that it has, to the best of its knowledge, the rights to license reuse of this material. However, you should ensure that the material you are requesting is original to Nature Publishing Group and does not carry the copyright of another entity (as credited in the published version). If the credit line on any part of the material you have requested indicates that it was reprinted or adapted by NPG with permission from another source, then you should also seek permission from that source to reuse the material.

2. Permission granted free of charge for material in print is also usually granted for any electronic version of that work, provided that the material is incidental to the work as a whole and that the electronic version is essentially equivalent to, or substitutes for, the print version. Where print permission has been granted for a fee, separate permission must be obtained for any additional, electronic re-use (unless, as in the case of a full paper, this has already been accounted for during your initial request in the calculation of a print run).NB: In all cases, web-based use of full-text articles must be authorized separately through the 'Use on a Web Site' option when requesting permission.

3. Permission granted for a first edition does not apply to second and subsequent editions and for editions in other languages (except for signatories to the STM Permissions Guidelines, or where the first edition permission was granted for free).

4. Nature Publishing Group's permission must be acknowledged next to the figure, table or abstract in print. In electronic form, this acknowledgement must be visible at the same time as the figure/table/abstract, and must be hyperlinked to the journal's homepage.

5. The credit line should read:
Reprinted by permission from Macmillan Publishers Ltd: [JOURNAL NAME] (reference citation), copyright (year of publication)
For AOP papers, the credit line should read:
Reprinted by permission from Macmillan Publishers Ltd: [JOURNAL NAME], advance online publication, day month year (doi: 10.1038/sj.[JOURNAL ACRONYM].XXXXX)

Note: For republication from the *British Journal of Cancer*, the following credit lines apply.
Reprinted by permission from Macmillan Publishers Ltd on behalf of Cancer Research UK: [JOURNAL NAME] (reference citation), copyright (year of publication)For AOP papers, the credit line should read:
Reprinted by permission from Macmillan Publishers Ltd on behalf of Cancer Research UK: [JOURNAL NAME], advance online publication, day month year (doi: 10.1038/sj.[JOURNAL ACRONYM].XXXXX)

6. Adaptations of single figures do not require NPG approval. However, the adaptation should be credited as follows:

Adapted by permission from Macmillan Publishers Ltd: [JOURNAL NAME] (reference citation), copyright (year of publication)

Note: For adaptation from the *British Journal of Cancer*, the following credit line applies.
Adapted by permission from Macmillan Publishers Ltd on behalf of Cancer Research UK: [JOURNAL NAME] (reference citation), copyright (year of publication)

7. Translations of 401 words up to a whole article require NPG approval. Please visit http://www.macmillanmedicalcommunications.com for more information.Translations of up to a 400 words do not require NPG approval. The translation should be credited as follows:

Translated by permission from Macmillan Publishers Ltd: [JOURNAL NAME] (reference citation), copyright (year of publication).

<u>**Note: For translation from the** *British Journal of Cancer,* **the following credit line applies.**</u>
Translated by permission from Macmillan Publishers Ltd on behalf of Cancer Research UK: [JOURNAL NAME] (reference citation), copyright (year of publication)

We are certain that all parties will benefit from this agreement and wish you the best in the use of this material. Thank you.

Special Terms:

v1.1

288

NATURE PUBLISHING GROUP LICENSE
TERMS AND CONDITIONS

May 02, 2014

This is a License Agreement between Patrick Grogan ("You") and Nature Publishing Group ("Nature Publishing Group") provided by Copyright Clearance Center ("CCC"). The license consists of your order details, the terms and conditions provided by Nature Publishing Group, and the payment terms and conditions.

All payments must be made in full to CCC. For payment instructions, please see information listed at the bottom of this form.

License Number	3380900309259
License date	May 02, 2014
Licensed content publisher	Nature Publishing Group
Licensed content publication	Nature Reviews Drug Discovery
Licensed content title	Current development of mTOR inhibitors as anticancer agents
Licensed content author	Sandrine Faivre,Guido KroemerandEric Raymond
Licensed content date	Aug 1, 2006
Volume number	5
Issue number	8
Type of Use	reuse in a dissertation / thesis
Requestor type	academic/educational
Format	print and electronic
Portion	figures/tables/illustrations
Number of figures/tables/illustrations	2
High-res required	no
Figures	Figure 1 and Figure 6
Author of this NPG article	no
Your reference number	None
Title of your thesis / dissertation	Withaferin A: a novel therapeutic approach for malignant brain tumors
Expected completion date	May 2014
Estimated size (number of pages)	200
Total	0.00 USD
Terms and Conditions	

Terms and Conditions for Permissions

289

Nature Publishing Group hereby grants you a non-exclusive license to reproduce this material for this purpose, and for no other use, subject to the conditions below:

1. NPG warrants that it has, to the best of its knowledge, the rights to license reuse of this material. However, you should ensure that the material you are requesting is original to Nature Publishing Group and does not carry the copyright of another entity (as credited in the published version). If the credit line on any part of the material you have requested indicates that it was reprinted or adapted by NPG with permission from another source, then you should also seek permission from that source to reuse the material.

2. Permission granted free of charge for material in print is also usually granted for any electronic version of that work, provided that the material is incidental to the work as a whole and that the electronic version is essentially equivalent to, or substitutes for, the print version.Where print permission has been granted for a fee, separate permission must be obtained for any additional, electronic re-use (unless, as in the case of a full paper, this has already been accounted for during your initial request in the calculation of a print run).NB: In all cases, web-based use of full-text articles must be authorized separately through the 'Use on a Web Site' option when requesting permission.

3. Permission granted for a first edition does not apply to second and subsequent editions and for editions in other languages (except for signatories to the STM Permissions Guidelines, or where the first edition permission was granted for free).

4. Nature Publishing Group's permission must be acknowledged next to the figure, table or abstract in print. In electronic form, this acknowledgement must be visible at the same time as the figure/table/abstract, and must be hyperlinked to the journal's homepage.

5. The credit line should read:
   Reprinted by permission from Macmillan Publishers Ltd: [JOURNAL NAME] (reference citation), copyright (year of publication)
   For AOP papers, the credit line should read:
   Reprinted by permission from Macmillan Publishers Ltd: [JOURNAL NAME], advance online publication, day month year (doi: 10.1038/sj.[JOURNAL ACRONYM].XXXXX)

   Note: For republication from the *British Journal of Cancer*, the following credit lines apply.
   Reprinted by permission from Macmillan Publishers Ltd on behalf of Cancer Research UK: [JOURNAL NAME] (reference citation), copyright (year of publication)For AOP papers, the credit line should read:
   Reprinted by permission from Macmillan Publishers Ltd on behalf of Cancer Research UK: [JOURNAL NAME], advance online publication, day month year (doi: 10.1038/sj.[JOURNAL ACRONYM].XXXXX)

6. Adaptations of single figures do not require NPG approval. However, the adaptation should be credited as follows:

   Adapted by permission from Macmillan Publishers Ltd: [JOURNAL NAME] (reference citation), copyright (year of publication)

   Note: For adaptation from the *British Journal of Cancer*, the following credit line applies.
   Adapted by permission from Macmillan Publishers Ltd on behalf of Cancer Research UK: [JOURNAL NAME] (reference citation), copyright (year of publication)

7. Translations of 401 words up to a whole article require NPG approval. Please visit http://www.macmillanmedicalcommunications.com for more information.Translations of up to a 400 words do not require NPG approval. The translation should be credited as follows:

   Translated by permission from Macmillan Publishers Ltd: [JOURNAL NAME] (reference citation), copyright (year of publication).

290

Note: For translation from the *British Journal of Cancer,* the following credit line applies.
Translated by permission from Macmillan Publishers Ltd on behalf of Cancer Research UK: [JOURNAL NAME] (reference citation), copyright (year of publication)

We are certain that all parties will benefit from this agreement and wish you the best in the use of this material. Thank you.

Special Terms:

v1.1

NATURE PUBLISHING GROUP LICENSE
TERMS AND CONDITIONS

May 02, 2014

This is a License Agreement between Patrick Grogan ("You") and Nature Publishing Group ("Nature Publishing Group") provided by Copyright Clearance Center ("CCC"). The license consists of your order details, the terms and conditions provided by Nature Publishing Group, and the payment terms and conditions.

All payments must be made in full to CCC. For payment instructions, please see information listed at the bottom of this form.

License Number	3380890115648
License date	May 02, 2014
Licensed content publisher	Nature Publishing Group
Licensed content publication	Nature Reviews Drug Discovery
Licensed content title	Mining the Wnt pathway for cancer therapeutics
Licensed content author	Nick BarkerandHans Clevers
Licensed content date	Dec 1, 2006
Volume number	5
Issue number	12
Type of Use	reuse in a dissertation / thesis
Requestor type	academic/educational
Format	print and electronic
Portion	figures/tables/illustrations
Number of figures/tables/illustrations	1
High-res required	no
Figures	Figure 1
Author of this NPG article	no
Your reference number	None
Title of your thesis / dissertation	Withaferin A: a novel therapeutic approach for malignant brain tumors
Expected completion date	May 2014
Estimated size (number of pages)	200
Total	0.00 USD
Terms and Conditions	

Terms and Conditions for Permissions

Nature Publishing Group hereby grants you a non-exclusive license to reproduce this material for this purpose, and for no other use, subject to the conditions below:

1. NPG warrants that it has, to the best of its knowledge, the rights to license reuse of this material. However, you should ensure that the material you are requesting is original to Nature Publishing Group and does not carry the copyright of another entity (as credited in the published version). If the credit line on any part of the material you have requested indicates that it was reprinted or adapted by NPG with permission from another source, then you should also seek permission from that source to reuse the material.

2. Permission granted free of charge for material in print is also usually granted for any electronic version of that work, provided that the material is incidental to the work as a whole and that the electronic version is essentially equivalent to, or substitutes for, the print version.Where print permission has been granted for a fee, separate permission must be obtained for any additional, electronic re-use (unless, as in the case of a full paper, this has already been accounted for during your initial request in the calculation of a print run).NB: In all cases, web-based use of full-text articles must be authorized separately through the 'Use on a Web Site' option when requesting permission.

3. Permission granted for a first edition does not apply to second and subsequent editions and for editions in other languages (except for signatories to the STM Permissions Guidelines, or where the first edition permission was granted for free).

4. Nature Publishing Group's permission must be acknowledged next to the figure, table or abstract in print. In electronic form, this acknowledgement must be visible at the same time as the figure/table/abstract, and must be hyperlinked to the journal's homepage.

5. The credit line should read:
Reprinted by permission from Macmillan Publishers Ltd: [JOURNAL NAME] (reference citation), copyright (year of publication)
For AOP papers, the credit line should read:
Reprinted by permission from Macmillan Publishers Ltd: [JOURNAL NAME], advance online publication, day month year (doi: 10.1038/sj.[JOURNAL ACRONYM].XXXXX)

Note: For republication from the *British Journal of Cancer*, the following credit lines apply.
Reprinted by permission from Macmillan Publishers Ltd on behalf of Cancer Research UK: [JOURNAL NAME] (reference citation), copyright (year of publication)For AOP papers, the credit line should read:
Reprinted by permission from Macmillan Publishers Ltd on behalf of Cancer Research UK: [JOURNAL NAME], advance online publication, day month year (doi: 10.1038/sj.[JOURNAL ACRONYM].XXXXX)

6. Adaptations of single figures do not require NPG approval. However, the adaptation should be credited as follows:

Adapted by permission from Macmillan Publishers Ltd: [JOURNAL NAME] (reference citation), copyright (year of publication)

Note: For adaptation from the *British Journal of Cancer*, the following credit line applies.
Adapted by permission from Macmillan Publishers Ltd on behalf of Cancer Research UK: [JOURNAL NAME] (reference citation), copyright (year of publication)

7. Translations of 401 words up to a whole article require NPG approval. Please visit http://www.macmillanmedicalcommunications.com for more information.Translations of up to a 400 words do not require NPG approval. The translation should be credited as follows:

Translated by permission from Macmillan Publishers Ltd: [JOURNAL NAME] (reference citation), copyright (year of publication).

293

Note: For translation from the *British Journal of Cancer,* the following credit line applies.
Translated by permission from Macmillan Publishers Ltd on behalf of Cancer Research UK: [JOURNAL NAME] (reference citation), copyright (year of publication)

We are certain that all parties will benefit from this agreement and wish you the best in the use of this material. Thank you.

Special Terms:

v1.1

If you would like to pay for this license now, please remit this license along with your payment made payable to "COPYRIGHT CLEARANCE CENTER" otherwise you will be invoiced within 48 hours of the license date. Payment should be in the form of a check or money order referencing your account number and this invoice number 501293451. Once you receive your invoice for this order, you may pay your invoice by credit card. Please follow instructions provided at that time.

Make Payment To:
Copyright Clearance Center
Dept 001
P.O. Box 843006
Boston, MA 02284-3006

For suggestions or comments regarding this order, contact RightsLink Customer Support: customercare@copyright.com or +1-877-622-5543 (toll free in the US) or +1-978-646-2777.

Gratis licenses (referencing $0 in the Total field) are free. Please retain this printable license for your reference. No payment is required.

**NATURE PUBLISHING GROUP LICENSE
TERMS AND CONDITIONS**

May 02, 2014

This is a License Agreement between Patrick Grogan ("You") and Nature Publishing Group ("Nature Publishing Group") provided by Copyright Clearance Center ("CCC"). The license consists of your order details, the terms and conditions provided by Nature Publishing Group, and the payment terms and conditions.

All payments must be made in full to CCC. For payment instructions, please see information listed at the bottom of this form.

License Number	3380900824583
License date	May 02, 2014
Licensed content publisher	Nature Publishing Group
Licensed content publication	Nature Reviews Molecular Cell Biology
Licensed content title	The emerging role of nuclear architecture in DNA repair and genome maintenance
Licensed content author	Tom Misteli and Evi Soutoglou
Licensed content date	Apr 1, 2009
Volume number	10
Issue number	4
Type of Use	reuse in a dissertation / thesis
Requestor type	academic/educational
Format	print and electronic
Portion	figures/tables/illustrations
Number of figures/tables/illustrations	1
High-res required	no
Figures	Box 1
Author of this NPG article	no
Your reference number	None
Title of your thesis / dissertation	Withaferin A: a novel therapeutic approach for malignant brain tumors
Expected completion date	May 2014
Estimated size (number of pages)	200
Total	0.00 USD
Terms and Conditions	

295

Terms and Conditions for Permissions

Nature Publishing Group hereby grants you a non-exclusive license to reproduce this material for this purpose, and for no other use, subject to the conditions below:

1. NPG warrants that it has, to the best of its knowledge, the rights to license reuse of this material. However, you should ensure that the material you are requesting is original to Nature Publishing Group and does not carry the copyright of another entity (as credited in the published version). If the credit line on any part of the material you have requested indicates that it was reprinted or adapted by NPG with permission from another source, then you should also seek permission from that source to reuse the material.

2. Permission granted free of charge for material in print is also usually granted for any electronic version of that work, provided that the material is incidental to the work as a whole and that the electronic version is essentially equivalent to, or substitutes for, the print version.Where print permission has been granted for a fee, separate permission must be obtained for any additional, electronic re-use (unless, as in the case of a full paper, this has already been accounted for during your initial request in the calculation of a print run).NB: In all cases, web-based use of full-text articles must be authorized separately through the 'Use on a Web Site' option when requesting permission.

3. Permission granted for a first edition does not apply to second and subsequent editions and for editions in other languages (except for signatories to the STM Permissions Guidelines, or where the first edition permission was granted for free).

4. Nature Publishing Group's permission must be acknowledged next to the figure, table or abstract in print. In electronic form, this acknowledgement must be visible at the same time as the figure/table/abstract, and must be hyperlinked to the journal's homepage.

5. The credit line should read:
   Reprinted by permission from Macmillan Publishers Ltd: [JOURNAL NAME] (reference citation), copyright (year of publication)
   For AOP papers, the credit line should read:
   Reprinted by permission from Macmillan Publishers Ltd: [JOURNAL NAME], advance online publication, day month year (doi: 10.1038/sj.[JOURNAL ACRONYM].XXXXX)

   Note: For republication from the *British Journal of Cancer*, the following credit lines apply.
   Reprinted by permission from Macmillan Publishers Ltd on behalf of Cancer Research UK: [JOURNAL NAME] (reference citation), copyright (year of publication)For AOP papers, the credit line should read:
   Reprinted by permission from Macmillan Publishers Ltd on behalf of Cancer Research UK: [JOURNAL NAME], advance online publication, day month year (doi: 10.1038/sj.[JOURNAL ACRONYM].XXXXX)

6. Adaptations of single figures do not require NPG approval. However, the adaptation should be credited as follows:

   Adapted by permission from Macmillan Publishers Ltd: [JOURNAL NAME] (reference citation), copyright (year of publication)

   Note: For adaptation from the *British Journal of Cancer*, the following credit line applies.
   Adapted by permission from Macmillan Publishers Ltd on behalf of Cancer Research UK: [JOURNAL NAME] (reference citation), copyright (year of publication)

7. Translations of 401 words up to a whole article require NPG approval. Please visit http://www.macmillanmedicalcommunications.com for more information.Translations of up to a 400 words do not require NPG approval. The translation should be credited as follows:

Translated by permission from Macmillan Publishers Ltd: [JOURNAL NAME] (reference citation), copyright (year of publication).

Note: For translation from the *British Journal of Cancer,* the following credit line applies.
Translated by permission from Macmillan Publishers Ltd on behalf of Cancer Research UK: [JOURNAL NAME] (reference citation), copyright (year of publication)

We are certain that all parties will benefit from this agreement and wish you the best in the use of this material. Thank you.

Special Terms:

v1.1

If you would like to pay for this license now, please remit this license along with your payment made payable to "COPYRIGHT CLEARANCE CENTER" otherwise you will be invoiced within 48 hours of the license date. Payment should be in the form of a check or money order referencing your account number and this invoice number 501293476. Once you receive your invoice for this order, you may pay your invoice by credit card. Please follow instructions provided at that time.

Make Payment To:
Copyright Clearance Center
Dept 001
P.O. Box 843006
Boston, MA 02284-3006

For suggestions or comments regarding this order, contact RightsLink Customer Support: customercare@copyright.com or +1-877-622-5543 (toll free in the US) or +1-978-646-2777.

Gratis licenses (referencing $0 in the Total field) are free. Please retain this printable license for your reference. No payment is required.

NATURE PUBLISHING GROUP LICENSE
TERMS AND CONDITIONS

Apr 23, 2014

This is a License Agreement between Patrick Grogan ("You") and Nature Publishing Group ("Nature Publishing Group") provided by Copyright Clearance Center ("CCC"). The license consists of your order details, the terms and conditions provided by Nature Publishing Group, and the payment terms and conditions.

All payments must be made in full to CCC. For payment instructions, please see information listed at the bottom of this form.

License Number	3374891410148
License date	Apr 23, 2014
Licensed content publisher	Nature Publishing Group
Licensed content publication	Nature Reviews Cancer
Licensed content title	Strategies to improve radiotherapy with targeted drugs
Licensed content author	Adrian C. Begg, Fiona A. Stewart, Conchita Vens
Licensed content date	Mar 24, 2011
Volume number	11
Issue number	4
Type of Use	reuse in a dissertation / thesis
Requestor type	academic/educational
Format	print and electronic
Portion	figures/tables/illustrations
Number of figures/tables/illustrations	2
High-res required	no
Figures	Figure 1 and Figure 2
Author of this NPG article	no
Your reference number	
Title of your thesis / dissertation	Withaferin A: a novel therapeutic approach for malignant brain tumors
Expected completion date	May 2014
Estimated size (number of pages)	200
Total	0.00 USD
Terms and Conditions	

Terms and Conditions for Permissions

298

Nature Publishing Group hereby grants you a non-exclusive license to reproduce this material for this purpose, and for no other use, subject to the conditions below:

1. NPG warrants that it has, to the best of its knowledge, the rights to license reuse of this material. However, you should ensure that the material you are requesting is original to Nature Publishing Group and does not carry the copyright of another entity (as credited in the published version). If the credit line on any part of the material you have requested indicates that it was reprinted or adapted by NPG with permission from another source, then you should also seek permission from that source to reuse the material.

2. Permission granted free of charge for material in print is also usually granted for any electronic version of that work, provided that the material is incidental to the work as a whole and that the electronic version is essentially equivalent to, or substitutes for, the print version.Where print permission has been granted for a fee, separate permission must be obtained for any additional, electronic re-use (unless, as in the case of a full paper, this has already been accounted for during your initial request in the calculation of a print run).NB: In all cases, web-based use of full-text articles must be authorized separately through the 'Use on a Web Site' option when requesting permission.

3. Permission granted for a first edition does not apply to second and subsequent editions and for editions in other languages (except for signatories to the STM Permissions Guidelines, or where the first edition permission was granted for free).

4. Nature Publishing Group's permission must be acknowledged next to the figure, table or abstract in print. In electronic form, this acknowledgement must be visible at the same time as the figure/table/abstract, and must be hyperlinked to the journal's homepage.

5. The credit line should read:
Reprinted by permission from Macmillan Publishers Ltd: [JOURNAL NAME] (reference citation), copyright (year of publication)
For AOP papers, the credit line should read:
Reprinted by permission from Macmillan Publishers Ltd: [JOURNAL NAME], advance online publication, day month year (doi: 10.1038/sj.[JOURNAL ACRONYM].XXXXX)

Note: For republication from the *British Journal of Cancer*, the following credit lines apply.
Reprinted by permission from Macmillan Publishers Ltd on behalf of Cancer Research UK: [JOURNAL NAME] (reference citation), copyright (year of publication)For AOP papers, the credit line should read:
Reprinted by permission from Macmillan Publishers Ltd on behalf of Cancer Research UK: [JOURNAL NAME], advance online publication, day month year (doi: 10.1038/sj.[JOURNAL ACRONYM].XXXXX)

6. Adaptations of single figures do not require NPG approval. However, the adaptation should be credited as follows:

   Adapted by permission from Macmillan Publishers Ltd: [JOURNAL NAME] (reference citation), copyright (year of publication)

   Note: For adaptation from the *British Journal of Cancer*, the following credit line applies.
   Adapted by permission from Macmillan Publishers Ltd on behalf of Cancer Research UK: [JOURNAL NAME] (reference citation), copyright (year of publication)

7. Translations of 401 words up to a whole article require NPG approval. Please visit http://www.macmillanmedicalcommunications.com for more information.Translations of up to a 400 words do not require NPG approval. The translation should be credited as follows:

   Translated by permission from Macmillan Publishers Ltd: [JOURNAL NAME] (reference

citation), copyright (year of publication).

Note: For translation from the _British Journal of Cancer_, the following credit line applies.
Translated by permission from Macmillan Publishers Ltd on behalf of Cancer Research UK: [JOURNAL NAME] (reference citation), copyright (year of publication)

We are certain that all parties will benefit from this agreement and wish you the best in the use of this material. Thank you.

Special Terms:

v1.1

If you would like to pay for this license now, please remit this license along with your payment made payable to "COPYRIGHT CLEARANCE CENTER" otherwise you will be invoiced within 48 hours of the license date. Payment should be in the form of a check or money order referencing your account number and this invoice number RLNK501285502. Once you receive your invoice for this order, you may pay your invoice by credit card. Please follow instructions provided at that time.

Make Payment To:
Copyright Clearance Center
Dept 001
P.O. Box 843006
Boston, MA 02284-3006

For suggestions or comments regarding this order, contact RightsLink Customer Support: customercare@copyright.com or +1-877-622-5543 (toll free in the US) or +1-978-646-2777.

Gratis licenses (referencing $0 in the Total field) are free. Please retain this printable license for your reference. No payment is required.